NUREG/CR-5535
EGG-2596
(Draft)
Volume III
June 1990

RELAP5/MOD3 Code Manual Volume III: Developmental Assessment Problems (DRAFT)

K. E. Carlson
R. A. Riemke
S. Z. Rouhani
R. W. Shumway
W. L. Weaver

Editors:
C. M. Allison
C. S. Miller
N. L. Wade

for the U.S. Nuclear Regulatory Commission

NUREG/CR-5535
EGG-2596
(Draft)
Volume III
Distribution Category: R4

RELAP5/MOD3 CODE MANUAL VOLUME III: DEVELOPMENTAL ASSESSMENT PROBLEMS (DRAFT)

Contributing Authors:
K. E. Carlson
R. A. Riemke
S. Z. Rouhani
R. W. Shumway
W. L. Weaver

Editors:
C. M. Allison
C. S. Miller
N. L. Wade

Manuscript Completed: June 1990

EG&G Idaho, Inc.
Idaho Falls, Idaho 83415

Prepared for the
Division of Systems Research
Office of Nuclear Regulatory Research
U.S. Nuclear Regulatory Commission
Washington, D.C. 20555
Under DOE Contract No. DE-AC07-76ID01570
FIN No. A6052

ABSTRACT

The RELAP5 code has been developed for best-estimate transient simulation of light-water-reactor coolant systems during a severe accident. The code models the coupled behavior of the reactor coolant system and the core during a severe accident transient, as well as large- and small-break loss-of-coolant accidents, and operational transients, such as anticipated transient without scram, loss of offsite power, loss of feedwater, and loss of flow. A generic modeling approach is used that permits as much of a particular system to be modeled as necessary. Control system and secondary system components are included to permit modeling of plant controls, turbines, condensers, and secondary feedwater conditioning systems.

RELAP5/MOD3 code documentation is divided into five volumes: Volume I provides modeling theory and associated numerical schemes; Volume II contains detailed instructions for code application and input data preparation; Volume III provides the results of developmental assessment cases that demonstrate and verify the models used in the code; Volume IV presents a detailed discussion of RELAP5 models and correlations; and Volume V contains guidelines that have evolved over the past several years through use of the RELAP5 code.

FIN No. A6052--RELAP5 Code Development

EXECUTIVE SUMMARY

The light water reactor (LWR) transient analysis code, RELAP5, was developed at the Idaho National Engineering Laboratory (INEL) for the U. S. Nuclear Regulatory Commission (NRC). Code uses include analysis required to support rulemaking, licensing audit calculations, evaluation of accident mitigation strategies, evaluation of operator guidelines, and experiment planning and analysis. RELAP5 has also been used as the basis for a nuclear plant analyzer. Specific applications of this capability have included simulations of transients in LWR systems that lead to severe accidents, such as loss of coolant, anticipated transients without scram (ATWS), and operational transients such as loss of feedwater, loss of offsite power, station blackout, and turbine trip. RELAP5 is a highly generic code that, in addition to calculating the behavior of a reactor coolant system during a transient, can be used for simulation of a wide variety of hydraulic and thermal transients in both nuclear and nonnuclear systems involving steam-water noncondensable solute fluid mixtures.

The MOD3 version of RELAP5 has been developed jointly by the NRC and a consortium consisting of several of the countries and domestic organizations that are members of the International Code Assessment and Applications Program (ICAP). The mission of the RELAP5/MOD3 development program was to develop a code version suitable for the analysis of all transients and postulated accidents in PWR systems, including both large- and small-break loss-of-coolant accidents (LOCAs) as well as the full range of operational transients. Although the emphasis of the RELAP5/MOD3 development was on large-break LOCAs, improvements to existing code models, based on the results of assessments against small-break LOCAs and operational transient test data, were also made.

The RELAP5/MOD3 code is based on a nonhomogeneous and nonequilibrium model for the two-phase system that is solved by a fast, partially implicit numerical scheme to permit economical calculation of system transients. The objective of the RELAP5 development effort from the outset was to produce a code that includes important first-order effects necessary for accurate

prediction of system transients but is sufficiently simple and cost-effective such that parametric or sensitivity studies are possible.

The code includes many generic component models from which general systems can be simulated. The component models include pumps, valves, pipes, heat structures, reactor point kinetics, electric heaters, jet pumps, turbines, separators, accumulators, and control system components. In addition, special process models are included for effects such as form loss, flow at an abrupt area change, branching, choke flow, boron tracking, and noncondensable gas transport.

The system mathematical models are coupled into an efficient code structure. The code includes extensive input checking capability to help the user discover input errors and inconsistencies. Also included are free-format input, internal plot capability, restart, renodalization, and variable output edit features. These user conveniences were developed in recognition that generally the major cost associated with the use of a system transient code is in the engineering labor and time involved in accumulating system data and developing system models, while the computer cost associated with generation of the final result is usually small.

The development of the models and codes that constitute RELAP5 has spanned approximately 12 years from the early stages of RELAP5 numerical scheme development to the present. RELAP5 represents the aggregate accumulation of experience in modeling core behavior during severe accidents, two-phase flow process, and LWR systems. The code development has benefitted from extensive application and comparison to experimental data in the LOFT, PBF, Semiscale, ACRR, NRU, and other experimental programs.

As noted earlier, several new models, improvements to existing models, and user conveniences have been added to RELAP5/MOD3. The new models include:

- the Bankoff counter-current flow limiting correlation, which is based on actual geometry and can be activated by the user at each junction in the system model

- the ECCMIX component for modeling of the mixing of subcooled emergency core cooling system (ECCS) liquid and the resulting interfacial condensation

- a zirconium-water reaction model to model the exothermic energy production on the surface of zirconium cladding material at high temperature

- a radiation heat transfer model with multiple radiation enclosures defined through user input

Improvements to existing models include:

- new correlations for interfacial friction for all types of geometry in the bubbly-slug flow regime in vertical flow passages

- an improved model for vapor pullthrough and liquid entrainment in horizontal pipes to obtain correct computation of the fluid state convected through the break

- a new critical heat flux correlation for rod bundles based on tabular data

- an improved horizontal stratification inception criterion for predicting the flow regime transition between horizontally stratified and dispersed flow

- a modified reflood heat transfer model

- improved vertical stratification inception logic to avoid excessive activation of the water packing model

- the extension of water packing logic to horizontal volumes
- the addition of a simple plastic strain model with clad burst criterion to the fuel mechanical model
- the addition of a radiation heat transfer term to the gap conductance model
- modifications to the noncondensable gas model to eliminate erratic code behavior and failure
- improvements to the downcomer penetration, ECCS bypass, and upper plenum deentrainment capabilities
- modifications that place both the vertical stratification and water packing models under user control so they can be deactivated

Additional user conveniences include:

- code speedup through vectorization for the CRAY X-MP computer
- code portability through the conversion of the FORTRAN coding to adhere to the FORTRAN 77 standard
- code execution and validation on a variety of systems (CRAY X-MP; CYBER (NOS/VE); IBM 3090 (MVS); and VAX (ULTRIX)

The RELAP5/MOD3 code manual consists of five separate volumes. The modeling theory and associated numerical schemes are described in Volume I, to acquaint the user with the modeling base and thus aid in effective use of the code. Volume II contains more detailed instructions for code application and specific instructions for input data preparation. Both

Volumes I and II are expanded and revised versions of the RELAP5/MOD2 code manual[a] and Volumes I and III of the SCDAP/RELAP5/MOD2 code manual.[b]

Volume III provides the results of developmental assessment cases run with RELAP5/MOD3 to demonstrate and verify the models used in the code. The assessment matrix contains phenomenological problems, separate-effects tests, and integral systems tests. Results of the RELAP5/MOD3 calculations have been compared to those produced with previous versions of the code and documented in the RELAP5/MOD2 developmental assessment report.[c]

Volume IV contains a detailed discussion of the models and correlations used in RELAP5/MOD3 and is an expanded and revised version of the RELAP5/MOD2 models and correlations document.[d] It provides the user with the underlying assumptions and simplifications used to generate and implement the base equations into the code so that an intelligent assessment of the applicability and accuracy of the resulting calculations can be made. Thus, the user can determine whether RELAP5/MOD3 is capable of modeling his or her particular application, whether the calculated results will be directly comparable to measurement or whether they must be interpreted in an average sense, and whether the results can be used to make quantitative decisions.

Volume V provides guidelines for users that have evolved over the past several years from application of the RELAP5 code at the Idaho National Engineering Laboratory, at other national laboratories, and by users throughout the world.

---

a. V. H. Ransom et al., *RELAP5/MOD2 Code Manual*, Volumes I and II, NUREG/CR-4312, EGG-2396, August and December, 1985; revised April 1987.

b. C. M. Allison and E. C. Johnson, Eds., *SCDAP/RELAP5/MOD2 Code Manual*, Volume I: RELAP5 Code Structure, System Models, and Solution Methods, and Volume III: User's Guide and Input Requirements.

c. V. H. Ransom et al., *RELAP5/MOD2 Code Manual*, Volume III: Developmental Assessment Problems, EGG-TFM-7952, December 1987.

d. R. A. Dimenna et al., *RELAP5/MOD2 Models and Correlations*, NUREG/CR-5194, EGG-2531, August 1988.

ACKNOWLEDGMENT

Development of a complex computer code such as RELAP5 is the result of a team effort. Acknowledgment is made of those who made significant contributions to the earlier versions of RELAP5, in particular, V. H. Ransom, J. A. Trapp, R. J. Wagner, Dr. H. H. Kuo, Dr. J. C. Lin, Dr. H. Chow, Dr. C. C. Tsai, L. R. Feinauer, and Dr. W. Bryce (UKAEA). Acknowledgment is also made to E. C. Johnson, N. S. Larson, and C. S. Miller, for their work in RELAP5 configuration control and user services.

The RELAP5 Program is indebted to the technical monitors responsible for directing the overall program; Drs. R. Lee, Y. Chen, and R. Landry, of the U. S. Nuclear Regulatory Commission, and Dr. D. Majumdar, Mr. N. Bonicelli, and Mr. C. Noble, of the Department of Energy-Idaho Operations Office. Finally, acknowledgment is made of all the code users who have been very helpful in stimulating timely correction of code deficiencies.

CONTENTS

ABSTRACT iii

SUMMARY iv

ACKNOWLEDGMENTS ix

1. INTRODUCTION 1-1

1.1 Added Capability of RELAP5/MOD2 1-2

1.2 Intended Application of RELAP5/MOD3 1-4

1.3 Known Limitations of RELAP5/MOD3 1-4

2. DEVELOPMENTAL ASSESSMENT PROBLEMS 2.1-1

2.1 Phenomenological Problems 2.1-1

2.1.1 Nine-Volume Water Over Steam 2.1-1
2.1.2 Air-Water Manometer Problem 2.1-9
2.1.3 Branch Tee Problem 2.1-9
2.1.4 Crossflow Tee Problem 2.1-13
2.1.5 Three-Stage Turbine 2.1-16
2.1.6 Workshop Problem 2 ..... 2.1-20
2.1.7 Workshop Problem 3 ..... 2.1-24
2.1.8 Horizontally Stratified Countercurrent Flow 2.1-38
2.1.9 Edwards Pipe Problem with Extras 2.1-44
2.1.10 Pryor's Pipe Problem 2.1-44
2.1.11 References 2.1-49

2.2 Separate-Effects Problems 2.2-1

2.2.1 LOFT-Wyle Blowdown Test WSB03R 2.2-1
2.2.2 One-Foot General Electric Level Swell Test 1004-3 ..... 2.2-4
2.2.3 Four-Foot General Electric Level Swell Test 5801-15 ..... 2.2-10
2.2.4 Dukler Air-Water Flooding Tests 2.2-26
2.2.5 Marviken Test 24 ..... 2.2-35
2.2.6 Marviken Test 22 ..... 2.2-42
2.2.7 LOFT Test L3-1 Accumulator Blowdown 2.2-46
2.2.8 Bennett's Heated Tube Experiments 2.2-56
2.2.9 Royal Institute of Technology Tube Test 261 ..... 2.2-56
2.2.10 ORNL Bundle CHF Tests 2.2-63
2.2.11 ORNL Void Profile Test 2.2-63
2.2.12 Christensen Subcooled Boiling Test 15 ..... 2.2-70
2.2.13 MIT Pressurizer Test 2.2-70
2.2.14 FLECHT-SEASET Forced Reflood Tests 2.2-73
2.2.15 UCSB Reflux Condensation and Natural Circulation Tests 101 and 309 ..... 2.2-98

2.2.16 UPTF Downcomer Countercurrent Flow Test 6 .....2.2-110
2.2-17 References 2.2-113

2.3 Integral Test Problems 2.3-1

2.3.1 LOFT Small-Break Test L3-7 ..... 2.3-1
2.3.2 LOFT Large-Break Test L2-5 ..... 2.3-15
2.3.3 Semiscale Natural Circulation Tests S-NC-1, S-NC-2, S-NC-3, AND S-NC-10 ..... 2.3-38
2.3.4 LOBI Large Break Test A1-04R 2.3-48
2.3.5 Zion-1 PWR Small Break 2.3-65
2.3.6 References 2.3-70

3. CONCLUSIONS .....

FIGURES

2.1-1. RELAP5 nodalization diagram of the nine-volume water over steam problem 2.1-5

2.1-2. The history of void distribution for the nine-volume problem (volumes 1-3) 2.1-6

2.1-3. The history of void distribution for the nine-volume problem (volumes 4-6) 2.1-7

2.1-4. The history of void distribution for the nine-volume problem (volumes 7-9) 2.1-8

2.1-5. Air-water manometer nodalization 2.1-10

2.1-6. Vapor fraction oscillation in volume 1050000 of manometer .. 2.1-11

2.1-7. Vapor fraction oscillation in volume 1060000 of manometer .. 2.1-12

2.1-8. Nodalization of the branch tee problem using two non-sink junctions 2.1-14

2.1-9. Nodalization of the crossflow tee problem using a left-right square for the tee 2.1-17

2.1-10. Nodalization used for three-stage group turbine problem 2.1-19

2.1-11. RELAP5 nodalization diagram for Workshop Problems 2 and 3 .. 2.1-22

2.1-12. Pressurizer pressure history of Workshop Problem 2 ..... 2.1-25

2.1-13. Core outlet pressure history of Workshop Problem 2 ..... 2.1-26

2.1-14. Steam generator steam dome pressure history of Workshop Problem 2 ..... 2.1-27

2.1-15. Steam generator secondary side liquid level for Workshop Problem 2 ..... 2.1-28

2.1-16. Mass flow in the primary loop hot leg for Workshop Problem 2 ..... 2.1-29

2.1-17. Mass flow in the primary side of steam generator for Workshop Problem 2 ..... 2.1-30

2.1-18. Volume pressure of the reactor core for Workshop Problem 3 ..... 2.1-33

2.1-19. Volume pressure of the pressurizer for Workshop Problem 3 .. 2.1-34

2.1-20. Volume pressure of the steam generator steam dome for Workshop Problem 3 ..... 2.1-35

2.1-21. Mass flow in the reactor core for Workshop Problem 3 ..... 2.1-36

2.1-22. Mass flow in the pressurizer for Workshop Problem 3 ..... 2.1-37

2.1-23. Mass flow in the steam generator secondary side (riser) for Workshop Problem 3 ..... 2.1-39

2.1-24. Mass flow in the steam discharge line for Workship Problem 3 ..... 2.1-40

2.1-25. RELAP5 nodalization diagram for a horizontally stratified countercurrent flow problem 2.1-41

2.1-26 RELAP5-calculated junction liquid velocities at three locations 2.1-42

2.1-27. RELAP5-calculated junction vapor velocities at three locations..... 2.1-43

2.1-28. RELAP5 nodalization for Edwards' pipe experiment 2.1-45

2.1-29. Comparison of measured and calculated history of midsection void fraction (Edwards' pipe with extras) 2.1-46

2.1-30. Comparison of measured and calculated history of midsection pressure (Edwards' pipe with extras) 2.1-47

2.1-31. RELAP5 nodalization diagram for Pryor's pipe problem 2.1-48

2.1-32. The history of void fraction distribution for Pryor's pipe problem 2.1-50

2.1-33. The history of pressure distribution for Pryor's pipe problem for RELAP5/MOD2 ..... 2.1-51

2.1-34. The history of pressure distribution for Pryor's pipe problem for RELAP5/MOD3 ..... 2.1-52

2.2-1. Schematic and nodalization for Wyle Test WSB03R 2.2-3

2.2-2. Measured and calculated (RELAP5/MOD1, MOD2, MOD3) mass flow rate at the break orifice for Wyle Test WSB03R 2.2-5

2.2-3. Measured and calculated (RELAP5/MOD1, MOD2, MOD3) pressure upstream of the break orifice for Wyle Test WSB03R 2.2-6

2.2-4. Measured and calculated (RELAP5/MOD1, MOD2, MOD3) density upstream of the break orifice for Wyle Test WSB03R 2.2-7

2.2-5. Schematic and nodalization for GE level swell Test 1004-3 .. 2.2-8

2.2-6. Measured and calculated (RELAP5/MOD1, MOD2, MOD3) pressure in the top of the vessel for GE level swell Test 1004-3 .... 2.2-11

2.2-7. Measured and calculated (RELAP5/MOD1, MOD2, MOD3) void fraction at 1.83 m (6 ft) above the bottom of the vessel for GE level swell Test 1004-3 ..... 2.2-12

2.2-8. Measured and calculated (RELAP5/MOD1, MOD2, MOD3) void fraction at 3.66 m (12 ft) above the bottom of the vessel for GE level swell Test 1004-3 ..... 2.2-13

2.2-9. Measured and calculated (RELAP5/MOD1, MOD2, MOD3) void fraction profile in the vessel at 10 s for GE level swell Test 1004-3 ..... 2.2-14

2.2-10. Measured and calculated (RELAP5/MOD1, MOD2, MOD3) void fraction profile in the vessel at 40 s for GE level swell Test 1004-3 ..... 2.2-15

2.2-11. Measured and calculated (RELAP5/MOD1, MOD2, MOD3) void fraction profile in the vessel at 100 s for GE level swell Test 1004-3 ..... 2.2-16

2.2-12. Measured and calculated (RELAP5/MOD1, MOD2, MOD3) void fraction profile in the vessel at 160 s for GE level swell Test 1004-3 ..... 2.2-17

2.2-13. Schematic for GE level swell Test 5801-15 ..... 2.2-19

2.2-14. Nodalization for GE level swell Test 5801-15 ..... 2.2-20

2.2-15. Measured and calculated (RELAP5/MOD1, MOD2, MOD3) pressure in the top of the vessel for GE level swell Test 5801-15 ... 2.2-21

2.2-16. Measured and calculated (RELAP5/MOD1, MOD2, MOD3) void fraction profile in the vessel at 2 s for GE level swell Test 5801-15 ..... 2.2-22

2.2-17. Measured and calculated (RELAP5/MOD1, MOD2, MOD3) void fraction profile in the vessel at 5 s for GE level swell Test 5801-15 ..... 2.2-23

2.2-18. Measured and calculated (RELAP5/MOD1, MOD2, MOD3) void fraction profile in the vessel at 10 s for GE level swell Test 5801-15 ..... 2.2-24

2.2-19. Measured and calculated (RELAP5/MOD1, MOD2, MOD3) void fraction profile in the vessel at 20 s for GE level swell Test 5801-15 ..... 2.2-25

2.2-20. Flooding/upflow test loop schematic diagram 2.2-27

2.2-21. Nodalization for Dukler's air-water test problem 2.2-28

2.2-22. RELAP5/MOD3 calculation of instantaneous liquid downflow rate in junction 101020000 for Dukler's air-water problem (air injection rate = 250 lb/h; liquid injection rate = 100 lb/h) 2.2-30

2.2-23. RELAP5/MOD3 calculation of instantaneous pressure in volume 104020000 for Dukler's air-water problem (air injection rate = 250 lb/h; liquid injection rate = 100 lb/h) 2.2-31

2.2-24. Data for liquid downflow rate for Dukler's air-water problem 2.2-32

2.2-25. RELAP5/MOD3 calculation without using the CCFL correlation flag for liquid downflow rate for Dukler's air-water problem 2.2-33

2.2-26. RELAP5/MOD3 calculation using the CCFL correlation flag for liquid downflow rate for Dukler's air-water problem 2.2-34

2.2-27. Schematic, nodalization, and initial temperature profile for Marviken Test 24 ..... 2.2-37

2.2-28. Measured and calculated (RELAP5/MOD2, MOD3) pressure in the top of the vessel for Marviken Test 24 ..... 2.2-39

2.2-29. Measured and calculated (RELAP5/MOD2, MOD3) density in the middle of the discharge pipe for Marviken Test 24 ..... 2.2-40

2.2-30. Measured and calculated (RELAP5/MOD2, MOD3) mass flow rate at the nozzle for Marviken Test 24 ..... 2.2-41

2.2-31. Schematic, nodalization, and initial temperature profile for Marviken Test 22 ..... 2.2-43

2.2-32. Measured and calculated (RELAP5/MOD2, MOD3) pressure in the top of the vessel for Marviken Test 22 ..... 2.2-44

2.2-33. Measured and calculated (RELAP5/MOD2, MOD3) mass flow rate at the nozzle for Marviken Test 22 ..... 2.2-45

2.2-34. LOFT L3-1 Accumulator A and surgeline schematic 2.2-47

2.2-35. LOFT L3-1 accumulator model schematic 2.2-49

2.2-36. Calculated accumulator gas dome pressure versus volume 2.2-50

2.2-37. Calculated accumulator gas dome pressure 2.2-51

2.2-38. Calculated accumulator surge line liquid velocity 2.2-52

2.2-39. (figure deleted) 2.2-53

2.2-40. Calculated accumulator combined heat and mass transfer energy 2.2-54

2.2-41. RELAP5 nodalization diagram for Bennett's heated tube experiment 2.2-57

2.2-42. Measured and RELAP5/MOD3-calculated axial wall temperature profiles for Bennett's heated tube low mass flux experiment 2.2-60

2.2-43. Measured and RELAP5/MOD3-calculated axial wall temperature profiles for Bennett's heated tube intermediate mass flux experiment 2.2-61

2.2-44. Measured and RELAP5/MOD3-calculated axial wall temperature profiles for Bennett's heated tube high mass flux experiment 2.2-62

2.2-45. RELAP5/MOD3-predicted critical heat flux position 2.2-64

2.2-46. Measured and RELAP5/MOD3-calculated surface temperature for ORNL bundle CHF test 3.07.9B 2.2-65

2.2-47. Measured and RELAP5/MOD3-calculated surface temperature for ORNL bundle CHF test 3.07.9N 2.2-66

2.2-48. Measured and RELAP5/MOD3-calculated surface temperature for ORNL bundle CHF test 3.07.9W 2.2-68

2.2-49. Measured and RELAP5/MOD3-calculated wall temperature for the ORNL void profile test 2.2-68

2.2-50. Measured and RELAP5/MOD3-calculated steam temperature for the ORNL void profile test 2.2-69

2.2-51. Measured and RELAP5/MOD3-calculated axial void fractions for the ORNL void profile test 2.2-71

2.2-52. Measured and RELAP5/MOD3-calculated axial void fractions for the Christensen subcooled boiling test 15 ..... 2.2-72

2.2-53. Schematic of the experimental apparatus for the MIT pressurizer test 2.2-74

2.2-54. Measured and RELAP5/MOD3-calculated rate of pressure rise for the MIT pressurizer test 2.2-75

2.2-55. Tank fluid and inside wall temperature at 35 s into the transient during the MIT pressurizer test 2.2-76

2.2-56. RELAP5 nodalization for the FLECHT-SEASET forced reflood tests 2.2-77

2.2-57. Measured and RELAP5/MOD3-calculated rod surface temperature histories for the FLECHT-SEASET forced reflood tests at the 0.62- (24-) and 1.23-m (48-in.) elevations 2.2-79

2.2-58. Measured and RELAP5/MOD3-calculated rod surface temperature histories for the FLECHT-SEASET forced reflood tests at the 1.85-m (72-in.) elevation 2.2-80

2.2-59. Measured and RELAP5/MOD3-calculated rod surface temperature histories for the FLECHT-SEASET forced reflood tests at the 2.46- (96-) and 2.85-m (111-in.) elevations 2.2-81

2.2-60. Measured and RELAP5/MOD3-calculated rod surface temperature histories for the FLECHT-SEASET forced reflood tests at the 3.08- (120-) and 3.38-m (132-in.) elevations 2.2-82

2.2-61. Measured and RELAP5/MOD3-calculated steam temperatures for the FLECHT-SEASET forced reflood tests at 1.23- (4-) and 1.85-m (6-ft) elevations 2.2-83

2.2-62. Measured and RELAP5/MOD3-calculated steam temperatures for the FLECHT-SEASET forced reflood tests at 2.46- (8-) and 2.85-m (9.5-ft) elevations 2.2-84

2.2-63. Measured and RELAP5/MOD3-calculated steam temperatures for the FLECHT-SEASET forced reflood tests at 3.08- (10-) and 3.54-m (11.5-ft) elevations 2.2-85

2.2-64. Measured and RELAP5/MOD3-calculated total bundle mass inventory for the FLECHT-SEASET forced reflood tests 2.2-86

2.2-65. Measured and RELAP5/MOD3-calculated void fractions at 0.92 to 1.23 m (3 to 4 ft) for the FLECHT-SEASET forced reflood tests 2.2-88

2.2-66. Measured and RELAP5/MOD3-calculated void fractions at 1.23 to 1.54 m (4 to 5 ft) for the FLECHT-SEASET forced reflood tests 2.2-89

2.2-67. Measured and RELAP5/MOD3-calculated void fractions at 1.54 to 1.85 m (5 to 6 ft) for the FLECHT-SEASET forced reflood tests 2.2-90

2.2-68. Measured and RELAP5/MOD3-calculated void fractions at 1.85 to 2.15 m (6 to 7 ft) for the FLECHT-SEASET forced reflood tests 2.2-91

2.2-69. Measured and RELAP5/MOD3-calculated void fractions at 2.15 to 2.46 m (7 to 8 ft) for the FLECHT-SEASET forced reflood tests 2.2-92

2.2-70. Measured and RELAP5/MOD3-calculated axial void profile at 300 s for the FLECHT-SEASET forced reflood tests 2.2-93

2.2-71. Measured and RELAP5/MOD3-calculated rod surface temperatures for the FLECHT-SEASET forced reflood test run 31701 at the 0.62- (24-), 1.0- (39-), and 2.85-m (111-in.) elevations 2.2-94

2.2-72. Measured and RELAP5/MOD3-calculated rod surface temperatures for the FLECHT-SEASET forced reflood test run 31701 at the 1.85- (72-) and 2.0-m (78-in.) elevations 2.2-95

2.2-73. Measured and RELAP5/MOD3-calculated rod surface temperatures for the FLECHT-SEASET forced reflood test run 31701 at the 2.46- (96-), 3.08- (120-), and 3.38-m (132-in.) elevations 2.2-96

2.2-74. Measured and RELAP5/MOD3-calculated void fraction profiles for the FLECHT-SEASET forced reflood test run 31701 ..... 2.2-97

2.2-75. Schematic diagram for UCSB reflux condensation and natural circulation tests 101 and 309 ..... 2.2-99

2.2-76. RELAP5 nodalization diagram for UCSB reflux condensation and and natural circulation tests 101 and 309 .....2.2-101

2.2-77. Measured and calculated (RELAP5/MOD2, MOD3) pressure in the top of the boiler for the UCSB reflux condensation and natural circulation test 101 .....2.2-104

2.2-78. Measured and calculated (RELAP5/MOD2, MOD3) pressure drop between the top of the boiler and the top of the riser for the UCSB reflux condensation and natural circulation test 101 .....2.2-105

2.2-79. Measured and calculated (RELAP5/MOD2, MOD3) temperature in the top of the riser water jacket for the UCSB reflux condensation and natural circulation test 101 .....2.2-106

2.2-80. Measured and calculated (RELAP5/MOD2, MOD3) pressure in the top of the boiler for the UCSB reflux condensation and natural circulation test 309 .....2.2-107

2.2-81. Measured and calculated (RELAP5/MOD2, MOD3) pressure drop between the top of the boiler and the top of the riser for the UCSB reflux condensation and natural circulation test 309 .....2.2-108

2.2-82. Measured and calculated (RELAP5/MOD2, MOD3) temperature in the top of the riser water jacket for the UCSB reflux condensation and natural circulation test 309 .....2.2-109

2.2-83. Schematic of the Upper Plenum Test Facility (UPTF) 2.2-111

2.2-84. RELAP5 nodalization for UPTF downcomer countercurrent flow test 6 (UPTF-6) 2.2-112

2.2-85. RELAP5/MOD3 void fraction in the lower plenum for UPTF-6 ...2.2-114

2.3-1. Schematic of LOFT test facility 2.3-2

2.3-2. Nodalization for LOFT Test L3-7 ..... 2.3-5

2.3-3. CPU time versus simulated time for LOFT Test L3-7 ..... 2.3-7

2.3-4. Measured and calculated (RELAP5/MOD2, MOD3) primary system pressure for LOFT Test L3-7 ..... 2.3-8

2.3-5. Measured and calculated (RELAP5/MOD2, MOD3) secondary system pressure for LOFT Test L3-7 ..... 2.3-9

2.3-6. Measured and calculated (RELAP5/MOD2, MOD3) liquid velocity in the intact loop hot leg for LOFT Test L3-7 ..... 2.3-10

2.3-7. Measured and calculated (RELAP5/MOD2, MOD3) vapor velocity in the intact loop hot leg for LOFT Test L3-7 ..... 2.3-11

2.3-8. Measured and calculated (RELAP5/MOD2, MOD3) core temperature difference for LOFT Test L3-7 ..... 2.3-12

2.3-9. Measured and calculated (RELAP5/MOD2, MOD3) mass flow rate at the break for LOFT Test L3-7 ..... 2.3-13

2.3-10. Measured and calculated (RELAP5/MOD2, MOD3) density in the intact loop hot leg for LOFT Test L3-7 ..... 2.3-14

2.3-11. Nodalization for LOFT Test L2-5 ..... 2.3-16

2.3-12. Measured and calculated (RELAP5/MOD2, MOD3) primary system pressure for LOFT Test L2-5 ..... 2.3-18

2.3-13. Measured and calculated (RELAP5/MOD2, MOD3) secondary system pressure for LOFT Test L2-5 ..... 2.3-19

2.3-14. Measured and calculated (RELAP5/MOD2, MOD3) mass flow rate in the broken loop cold leg for LOFT Test L2-5 ..... 2.3-20

2.3-15. Measured and calculated (RELAP5/MOD2, MOD3) mass flow rate in the broken loop hot leg for LOFT Test L2-5 ..... 2.3-21

2.3-16. Measured and calculated (RELAP5/MOD2, MOD3) mass flow rate in the intact loop cold leg for LOFT Test L2-5 ..... 2.3-22

2.3-17. Measured and calculated (RELAP5/MOD2, MOD3) mass flow rate in the intact loop hot leg for LOFT Test L2-5 ..... 2.3-23

2.3-18. Measured and calculated (RELAP5/MOD2, MOD3) density in the intact loop hot leg for LOFT Test L2-5 ..... 2.3-24

2.3-19. Measured and calculated (RELAP5/MOD2, MOD3) mass flow rate from the accumulator for LOFT Test L2-5 ..... 2.3-26

2.3-20. Measured and calculated (RELAP5/MOD2, MOD3) accumulator level for LOFT Test L2-5 ..... 2.3-27

2.3-21. Measured and calculated (RELAP5/MOD2, MOD3) pump speed for primary coolant pump 2 (hydrodynamic volume 165) for LOFT Test L2-5 ..... 2.3-28

2.3-22. Measured and calculated (RELAP5/MOD2, MOD3) upper plenum temperature below the nozzle for LOFT Test L2-5 ..... 2.3-29

2.3-23. Measured and calculated (RELAP5/MOD2, MOD3) lower plenum temperature for LOFT Test L2-5 ..... 2.3-30

2.3-24. Measured and calculated (RELAP5/MOD2, MOD3) fuel centerline temperature 0.69 m (27 in.) above the bottom of the core for LOFT Test L2-5 ..... 2.3-31

2.3-25. Measured and calculated (RELAP5/MOD2, MOD3) fuel cladding temperature 0.13 m (5 in.) above the bottom of the core for LOFT Test L2-5 ..... 2.3-32

2.3-26. Measured and calculated (RELAP5/MOD2, MOD3) fuel cladding temperature 0.53 m (21 in.) above the bottom of the core for LOFT Test L2-5 ..... 2.3-33

2.3-27. Measured and calculated (RELAP5/MOD2, MOD3) fuel cladding temperature 0.69 m (27 in.) above the bottom of the core for LOFT Test L2-5 ..... 2.3-34

2.3-28. Measured and calculated (RELAP5/MOD2, MOD3) fuel cladding temperature 0.99 m (39 in.) above the bottom of the core for LOFT Test L2-5 ..... 2.3-35

2.3-29. Measured and calculated (RELAP5/MOD2, MOD3) fuel cladding temperature 1.37 m (54 in.) above the bottom of the core for LOFT Test L2-5 ..... 2.3-36

2.3-30. Measured and calculated (RELAP5/MOD2, MOD3) fuel cladding temperature 1.47 m (58 in.) above the bottom of the core for LOFT Test L2-5 ..... 2.3-37

2.3-31. Semiscale Mod-2A single-loop configuration 2.3-39

2.3-32. Schematic of RELAP5/MOD3 natural circulation test model 2.3-41

2.3-33. Measured and calculated (RELAP5/MOD3) mass flow rate at 60-kW core power for Semiscale natural circulation tests ... 2.3-43

2.3-34. Measured and calculated (RELAP5/MOD3) core Δt at 60-kW core power for Semiscale natural circulation tests 2.3-44

2.3-35. Measured and calculated (RELAP5/MOD3) primary pressure at 60-kW core power for Semiscale natural circulation tests ... 2.3-45

2.3-36. Measured and calculated (RELAP5/MOD3) mass flow rate versus steam generator secondary side heat transfer area for Semiscale natural circulation test S-NC-3 ..... 2.3-47

2.3-37. LOBI test facility 2.3-49

2.3-38. LOBI test facility nodalization 2.3-51

2.3-39. LOBI vessel nodalization 2.3-52

2.3-40. LOBI steam generator nodalization 2.3-53

2.3-41. Measured and calculated (RELAP5/MOD3) intact and broken loop pressure for LOBI Test A1-04R 2.3-56

2.3-42. Measured and calculated (RELAP5/MOD3) pump-side and vessel-side break mass flow for LOBI Test A1-04 ..... 2.3-57

2.3-43. Measured and calculated core differential pressure for LOBI Test A1-04R 2.3-59

2.3-44. Measured and calculated accumulator injection flow rate for LOBI Test A1-04R 2.3-60

2.3-45. Measured and calculated fluid density at accumulator injection point for LOBI Test A1-04R 2.3-61

2.3-46. Measured and calculated fluid temperature at accumulator injection for LOBI Test A1-04R 2.3-62

2.3-47. Measured and calculated lower core rod temperature for LOBI Test A1-04R 2.3-63

2.3-48. Measured and calculated mid-core rod temperatures for LOBI Test A1-04R 2.3-64

2.3-49. Measured and calculated upper core rod temperature for LOBI Test A1-04R 2.3-65

2.3-50. Measured and calculated core inlet density for LOBI Test A1-04R 2.3-67

2.3-51. Measured and calculated intact loops steam generator temperature for LOBI Test A1-04R 2.3-68

2.3-52. Measured and calculated broken loop steam generator temperature for LOBI Test A1-04R 2.3-69

2.3-53. RELAP5 nodalization for the Zion-1 PWR 2.3-70

2.3-54. Calculated (RELAP5/MOD3, MOD2) primary system pressure for the Zion-1 small break 2.3-72

2.3-55. Calculated (RELAP5/MOD3, MOD2) intact loop secondary pressure for the Zion-1 small break 2.3-73

2.3-56. Calculated (RELAP5/MOD3, MOD2) break mass flow rate for the Zion-1 small break 2.3-74

TABLES

2.1-1. Developmental assessment matrix 2.1-2

2.1-2. Results for the branch tee problem 2.1-15

2.1-3. Results for the crossflow tee problem 2.1-18

2.1-4. Turbine parameters for the assessment problem 2.1-21

2.1-5. Workshop problem 2 initial conditions 2.1-23

2.1-6. Transient sequence for workshop problem 3 ..... 2.1-31

2.2-1. RELAP5/MOD3 nonequilibrium model developmental assessment matrix 2.2-58

2.3-1. Steady-state conditions for LOBI Test A1-04R 2.3-54

RELAP5/MOD3 CODE MANUAL
VOLUME III:
DEVELOPMENTAL ASSESSMENT PROBLEMS

1. INTRODUCTION

The RELAP5 computer code is a light water reactor transient analysis code developed for the U.S. Nuclear Regulatory Commission (NRC) for use in rulemaking, licensing audit calculations, evaluation of operator guidelines, and as a basis for a nuclear plant analyzer. Specific applications of this capability have included simulations of transients in LWR systems, such as loss of coolant, anticipated transients without scram (ATWS), and operational transients such as loss of feedwater, loss of offsite power, station blackout, and turbine trip. RELAP5 is a highly generic code that, in addition to calculating the behavior of a reactor coolant system during a transient, can be used for simulation of a wide variety of hydraulic and thermal transients in both nuclear and nonnuclear systems involving steam-water noncondensable solute fluid mixtures.

The MOD3 version of RELAP5 has been developed jointly by the NRC and a consortium consisting of several of the countries and domestic organizations that are members of the International Code Assessment and Applications Program (ICAP). The mission of the RELAP5/MOD3 development program was to develop a code version suitable for the analysis of all transients and postulated accidents in PWR systems, including both large- and small-break loss-of-coolant accidents (LOCAs) as well as the full range of operational transients. Although the emphasis of the RELAP5/MOD3 development was on large-break LOCAs, improvements to existing code models, based on the results of assessments against small-break LOCAs and operational transient test data, were also made.

RELAP5/MOD3 contains new and improved modeling capability as well as additional user conveniences compared to RELAP5/MOD2. The purpose of this volume is to document the developmental assessment problems performed using

RELAP5/MOD3. The remainder of this section briefly describes the newly developed features and improvements in RELAP5/MOD3, the intended application of the code, and its known limitations. Section 2 presents the developmental assessment problems. Within this section, the problems are divided into three categories: phenomenological problems (Section 2.1); separate effects-problems (Section 2.2); and integral test problems (Section 2.3). Finally, Section 3 presents conclusions drawn from the assessment.

1.1 Added Capability of RELAP5/MOD3

The added capability in RELAP5/MOD3 include new modeling, improvements to existing models, and new user conveniences. A detailed description of these capabilities can be found in Volumes I and II of the RELAP5/MOD3 code manual. The new models include:

- the Bankoff counter-current flow limiting correlation, which is based on actual geometry and can be activated by the user at each junction in the system model

- the ECCMIX component for modeling of the mixing of subcooled emergency core cooling system (ECCS) liquid and the resulting interfacial condensation

- a zirconium-water reaction model to model the exothermic energy production on the surface of zirconium cladding material at high temperature

- a radiation heat transfer model with multiple radiation enclosures defined through user input

Improvements to existing models include:

- new correlations for interfacial friction for all types of geometry in the bubbly-slug flow regime in vertical flow passages

- an improved model for vapor pullthrough and liquid entrainment in horizontal pipes to obtain correct computation of the fluid state convected through the break

- a new critical heat flux correlation for rod bundles based on tabular data

- an improved horizontal stratification inception criterion for predicting the flow regime transition between horizontally stratified and dispersed flow

- a modified reflood heat transfer model

- improved vertical stratification inception logic to avoid excessive activation of the water packing model

- the extension of water packing logic to horizontal volumes

- the addition of a simple plastic strain model with clad burst criterion to the fuel mechanical model

- the addition of a radiation heat transfer term to the gap conductance model

- modifications to the noncondensable gas model to eliminate erratic code behavior and failure

- improvements to the downcomer penetration, ECCS bypass, and upper plenum deentrainment capabilities

- modifications that place both the vertical stratification and water packing models under user control so they can be deactivated

Additional user conveniences include:

- code speedup through vectorization for the CRAY X-MP computer

- code portability through the conversion of the FORTRAN coding to adhere to the FORTRAN 77 standard

- code execution and validation on a variety of systems (CRAY X-MP; CYBER (NOS/VE); IBM 3090 (MVS); and VAX (ULTRIX)

1.2 Intended Application of RELAP5/MOD3

RELAP5/MOD3 is designed for use in the analysis of pressurized water reactor transients resulting from large- and small-break loss-of-coolant accidents and operational transients such as anticipated transients without scram, loss of feedwater, and turbine trip. Both primary and secondary systems, including balance of plant components, can be modeled. The code has generic modeling capability so that separate effects experiments can also be modeled for use in the assessment of code capability and for extrapolation of separate effects results to integral system behavior.

The modeling philosophy to be followed in using RELAP5/MOD3 is the same as for MOD2 except where new modeling capability requires special treatment. In general, all modeling capability present in the MOD2 version of the code has been retained in the MOD3 version, and it has been an objective to keep input decks which have been developed for MOD2 compatible with MOD3. With a few exceptions, this has been achieved.

1.3 Known Limitations of RELAP5/MOD3

The discussion of known limitations of RELAP5/MOD3 is based on experiences with the MOD3 version, the developmental assessment work reported herein, and known or suspected limitations of the models used in the code.

While there are no known limitations of the stratification models for horizontal components, the user should be cautioned that only the LOFT-Wyle

blowdown orifice calibration experiment was used for the developmental assessment. The main objective of this test was orifice calibration; and, as such, the stratification data are limited. More specialized separate-effects calculations are needed for an accurate assessment. The code does not contain a critical open channel flow limit (hydraulic jump) model for horizontal stratified flow. The omission of this model results in limited agreement with the TPTF experiments at JAERI.

The reflood model developed for RELAP5/MOD3 has shown good agreement with nonuniformly heated rod bundle data with respect to time to maximum temperature, but use of the Chen transition boiling correlation results in a quench temperature that is too low. The liquid entrainment appears to be about right, since the liquid inventory in the core is predicted well. However, the axial drag distribution is not correct because an inverted void profile develops at low reflood rates. This results in quench front velocity stalling at about core midplane.

The pump model does not have an internal model to represent cavitation. The pump model does allow the user the option of accounting for the cavitation or two-phase degradation effects on pump performance through the input of homologous, two-phase curves for heat and torque, curves that are in the form of difference curves. This approach is not generally acceptable, particularly when correlations for a given pump are available for determining the cavitating pump head as a function of required and available net positive suction head. Users have resorted to using the RELAP5 control system or hardwired updates for a particular pump in order to base the pump head on the net positive suction head.

The code has limited two- and three-dimensional capability, which can be invoked by using cross-flow junctions. The results appear to be adequate for friction-dominated cases. This approach is simplified in that one or both of the momentum flux terms from the connecting volumes are neglected. In addition, the momentum equations are only coded for the primary flow direction. Also, there are no cross product terms.

For horizontal flow, the plug flow regime is not generally available in the code. It is only present in the ECC mixer volume.

The reactor kinetics model uses point kinetics. There may be some situations where one- and three-dimensional capability is required but is not available in the code.

2. DEVELOPMENTAL ASSESSMENT PROBLEMS

A total of 31 developmental assessment calculations were performed using RELAP5/MOD3. Table 2.1-1 shows the developmental assessment matrix, which includes a brief description of the objective of each problem. The matrix contains 10 phenomenological problems, 16 separate-effects problems, and 5 integral test problems.

2.1 PHENOMENOLOGICAL PROBLEMS

2.1.1 Nine-Volume Water Over Steam

The 9-volume water-over-steam problem is simply a vertical pipe with the upper one-third of the pipe initially filled with water and the bottom two-thirds of the pipe filled with steam. The problem was developed to check the gravitational head effect in the RELAP5/MOD3 code.

Figure 2.1-1 shows the RELAP5/MOD3 nodalization diagram. The vertical pipe (total pipe length = 4.16448 m, pipe area = 1.0 m^2) was modeled using nine volumes and eight junctions. The upper three volumes are initially filled with saturated water at a pressure of 413 kPa, and the bottom six volumes are filled with saturated steam at a pressure of 413 kPa. During the transient, the liquid falls and displaces the vapor.

The local void fraction history of the nine volumes, as calculated by both RELAP5/MOD2 and RELAP5/MOD3, is shown in Figures 2.1-2, 2.1-3, and 2.1-4. The water in the upper three volumes depletes quickly and drops into the lower volumes. The upper three volumes become empty, and the bottom three volumes become full. Note that the water falls slower in MOD3 than in MOD2, possibly because the interphase drag is different. Also, the inversed void profile (which lowers the interphase drag) present in MOD2 has been removed from MOD3. The results show that the gravitational head in RELAP5/MOD3 is properly modeled.

Table 2.1-1. Developmental assessment matrix

Problem Type	Assessment Objective
Phenomenological Problems:	
1. Nine-volume water over steam	Gravitation head effect
2. Air-water manometer problem	Noncondensable state Oscillatory flow
3. Branch tee problem	Tee model using branch component
4. Crossflow tee problem	Tee model using crossflow feature
5. Three stage turbine	Turbine component
6. Workshop Problem 2	Hypothetical two-loop PWR System modeling Control system Steady-state option
7. Workshop Problem 3	Hypothetical two-loop PWR System modeling Control system Transient option
8. Horizontal stratified countercurrent flow	Countercurrent flow model
9. Edwards pipe problem with extras	Vapor generation model
10. Pryor's pipe problem	Water packing
Separate-Effects Problems:	
1. LOFT-Wyle Blowdown Test WSB03R	Horizontal stratified flow model Choked flow model
2. One-foot General Electric level swell test 1004-3	Interphase drag model
3. Four-foot General Electric level swell Test 5801-15	Interphase drag model
4. Dukler air-water flooding tests	Noncondensables Interphase drag model Countercurrent flow model

Table 2.1-1. (continued)

Problem Type	Assessment Objective
Separate-Effects Problems continued:	
5. Marviken Test 24	Subcooled choking model
6. Marviken Test 22	Subcooled choking model
7. LOFT Test L3-1 accumulator blowdown	Accumulator model
8. Bennett's heated tube experiments	Nonequilibrium heat transfer Vapor generation model CHF correlation
9. Royal Institute of Technology tube test 261	Nonequilibrium heat transfer Vapor generation model CHF correlation
10. ORNL bundle CHF tests	Nonequilibrium heat transfer Vapor generation model CHF correlation
11. ORNL void profile test	Nonequilibrium heat transfer Vapor generation model
12. Christensen subcooled boiling test 15	Subcooled boiling model
13. MIT pressurizer test	Wall condensation model Stratified interfacial heat transfer
14. FLECHT-SEASET forced reflood tests	Reflood model
15. UCSB reflux condensation and natural circulation Tests 101 and 309	Reflux condensation Natural circulation Countercurrent flow
16. UPTF downcomer countercurrent flow test 6	Pressurizer modeling
Integral-Effects Problems:	
1. LOFT small-break Test L3-7	Small-break LOCA
2. LOFT large-break Test L2-5	Large-break LOCA

Table 2.1-1. (continued)

Problem Type	Assessment Objective
Integral-Effects Problems continued:	
3. Semiscale natural circulation Tests S-NC-1, S-NC-2, S-NC-3, and S-NC-10	Natural circulation
4. LOBI large-break test A1-04R	Large-break LOCA
5. Zion-1 PWR small break	Small-break LOCA Loss of offsite power Instrument tube rupture

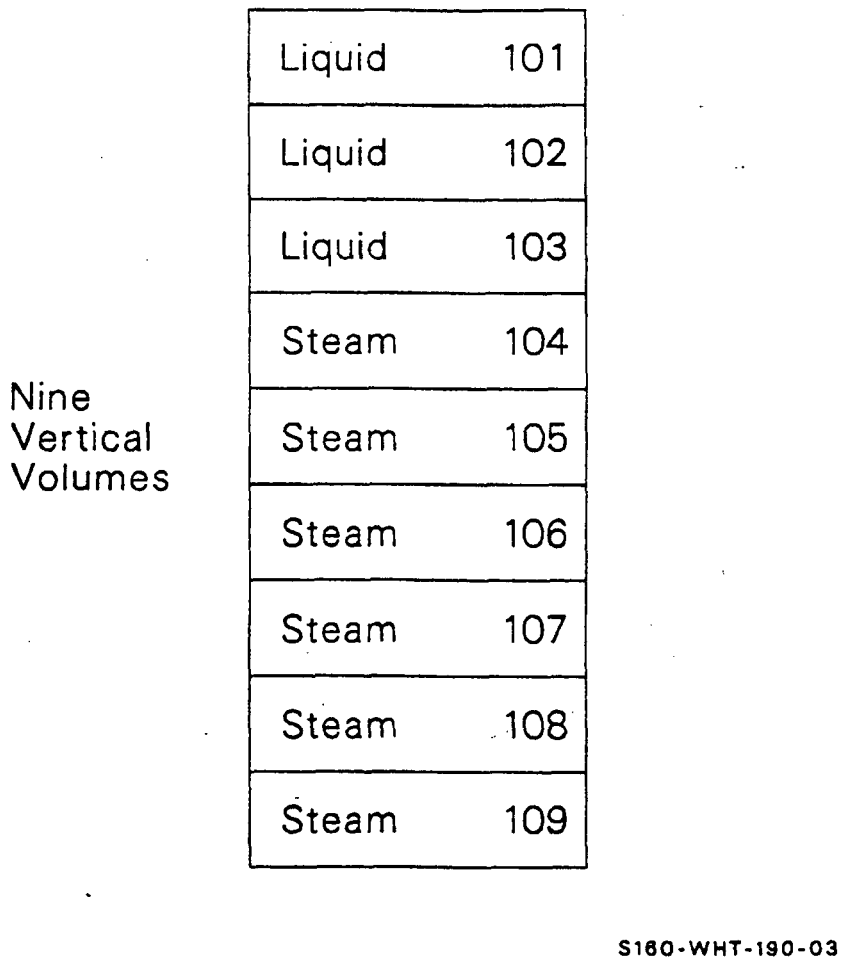

Figure 2.1-1. RELAP5 nodalization diagram of the nine-volume water over steam problem.

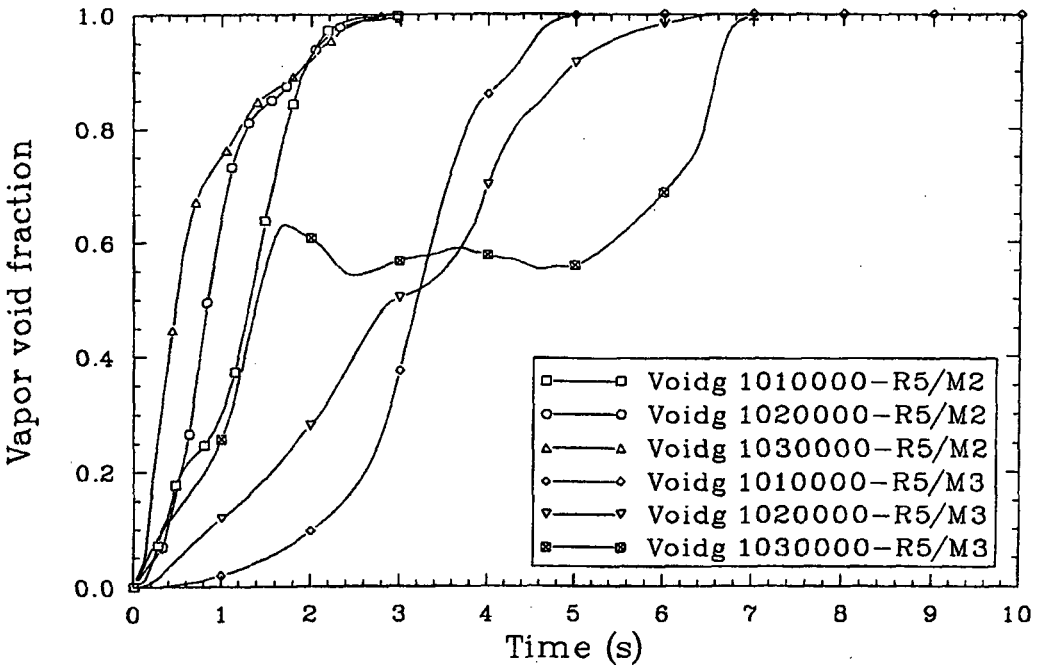

Figure 2.1-2. The history of void distribution for the nine-volume problem (volumes 1-3).

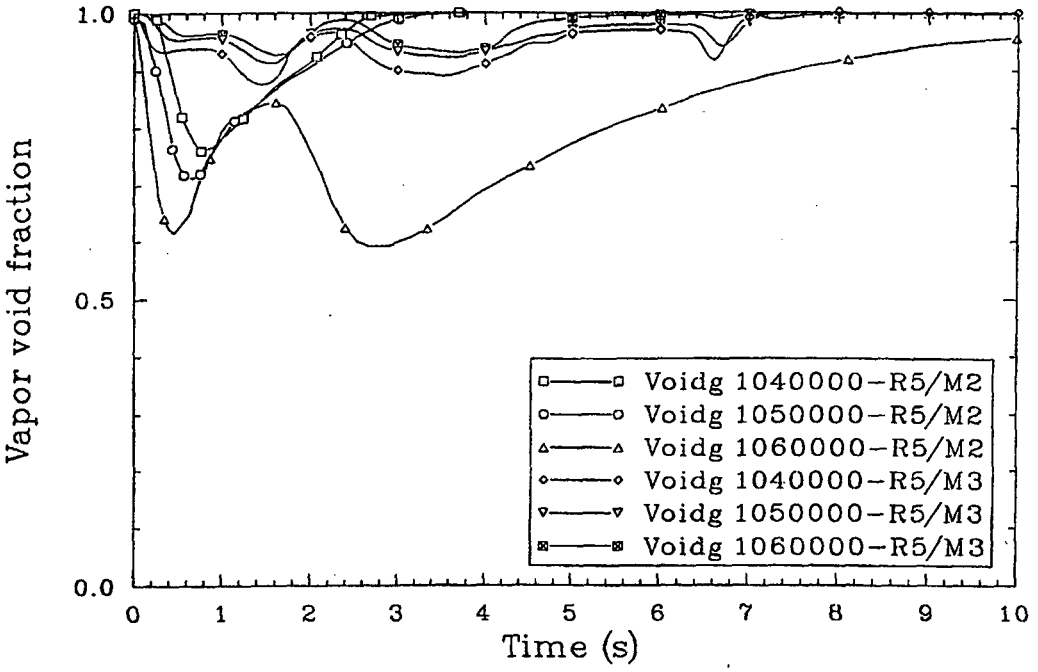

jan-rar21

Figure 2.1-3. The history of void distribution for the nine-volume problem (volumes 4-6).

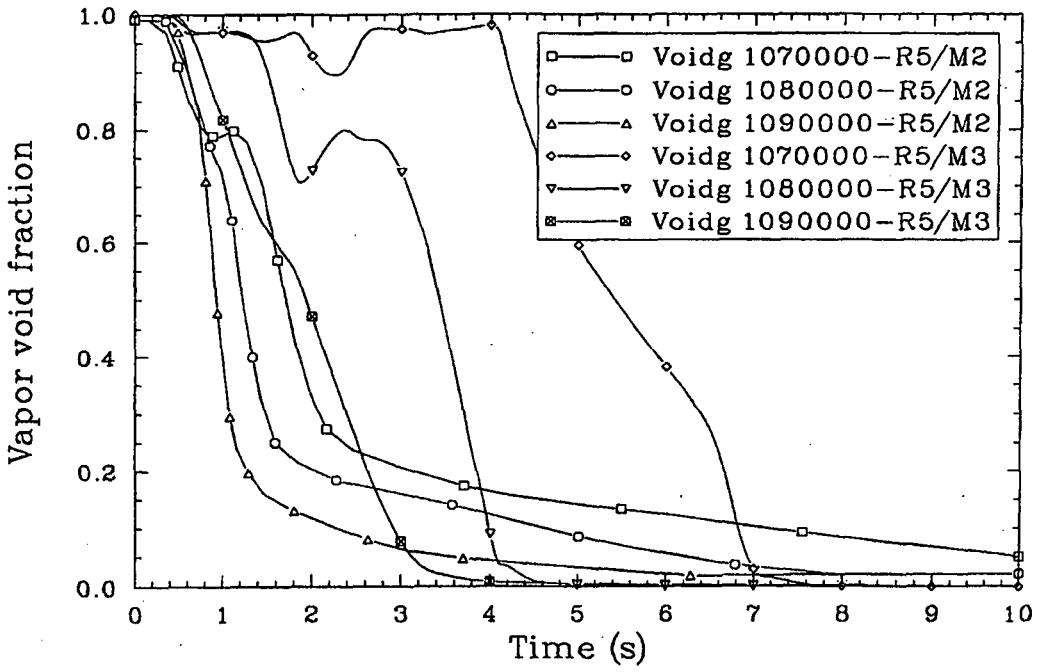

jan-rer31

Figure 2.1-4. The history of void distribution for the nine-volume problem (volumes 7-9).

The MOD3 calculation was run to 10 s on Version 5g2, using the Cray, and required 1000 attempted advancements and 3.91 cpu seconds.

2.1.2 Air-Water Manometer Problem

A 20-volume air-water manometer, as shown in Figure 2.1-5, was set up to check the noncondensable state calculation and code capability to handle oscillatory flows. Each volume has an area of 0.733 m^2 (8 ft^2) and a length of 0.305 m (1 ft). Four volumes (107-110) on the left side and 6 volumes (111-116) on the right side were filled initially with saturated water at 101.4 kPa (14.7 psi) and 294.2 K (70°F). The remaining volumes were initialized with saturated air at the same pressure and temperature.

Plots of void fractions to demonstrate the behavior of the manometer are shown in Figures 2.1-6 and 2.1-7. The period of oscillation obtained from the RELAP5/MOD3 plots is 2.92 s, compared to 2.5 s from RELAP5/MOD2. The MOD3 period is larger than the MOD2 period or the theoretical period, perhaps due to the MOD3 interphase drag changes. The large decrease in oscillation amplitude in the first 10 s is due to incorrectly setting all initial pressures equal. The MOD3 void fraction amplitude is smaller than the MOD2 void fraction amplitude, perhaps due to the different interphase drag model, which results in better phase separation in MOD3 for this problem.

The MOD3 calculation was run to 40 s on Version 5g2, using the Cray, and required 1289 attempted advancements and 17.24 cpu seconds.

2.1.3 Branch Tee Problem

The branch tee problem is a conceptual problem that was set up during the development of RELAP5/MOD1 to test the ability of the branch component to accurately model a tee. At that time, it illuminated some of the code's problems in modeling a tee, and it was rerun on RELAP5/MOD3 to ascertain its status on this latest code.

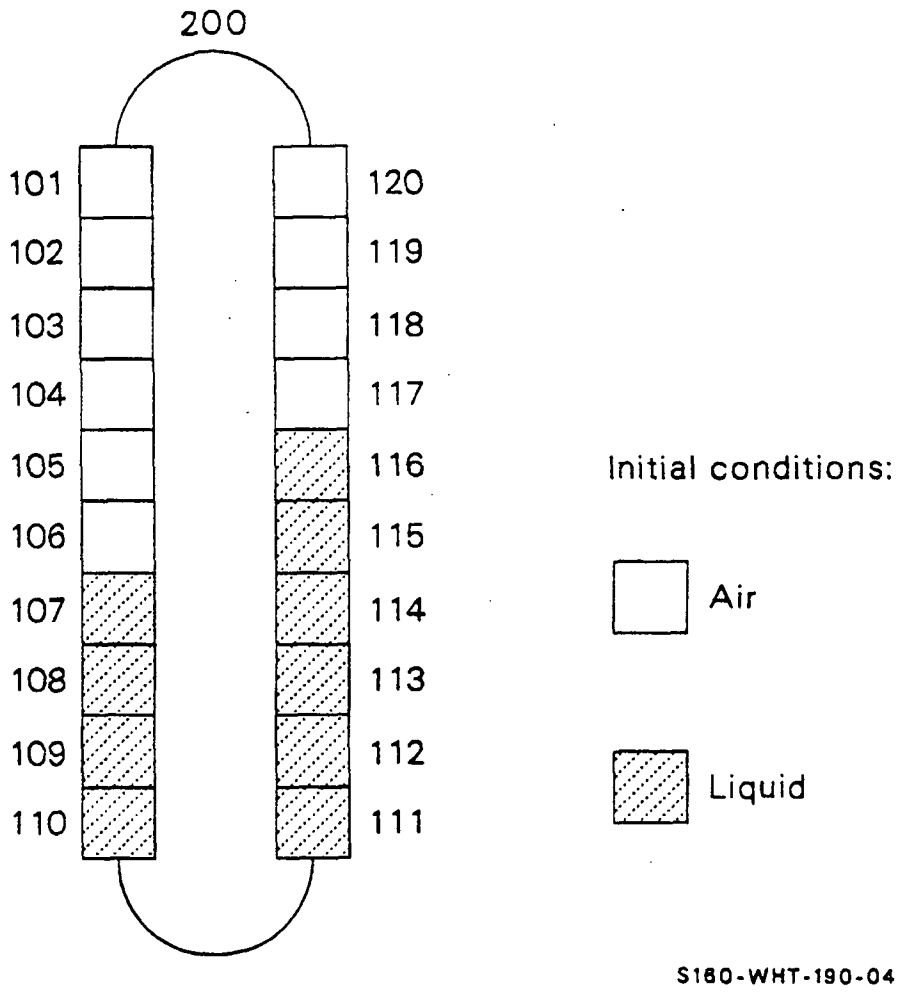

Figure 2.1-5. Air-water manometer nodalization.

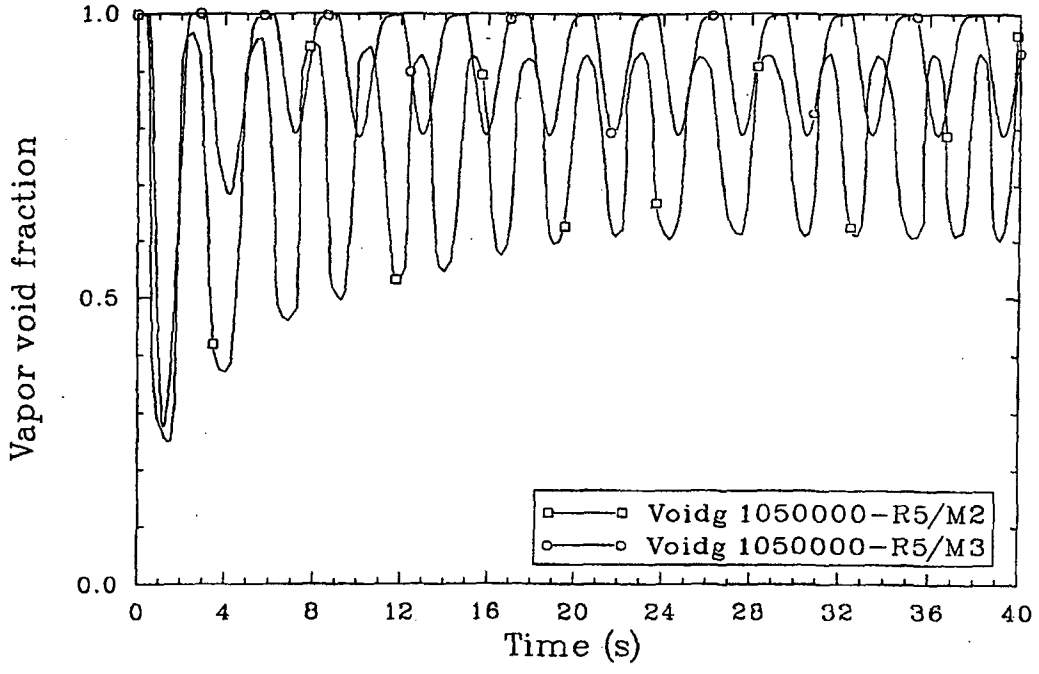

Figure 2.1-6. Vapor fraction oscillation in volume 1050000 of manometer.

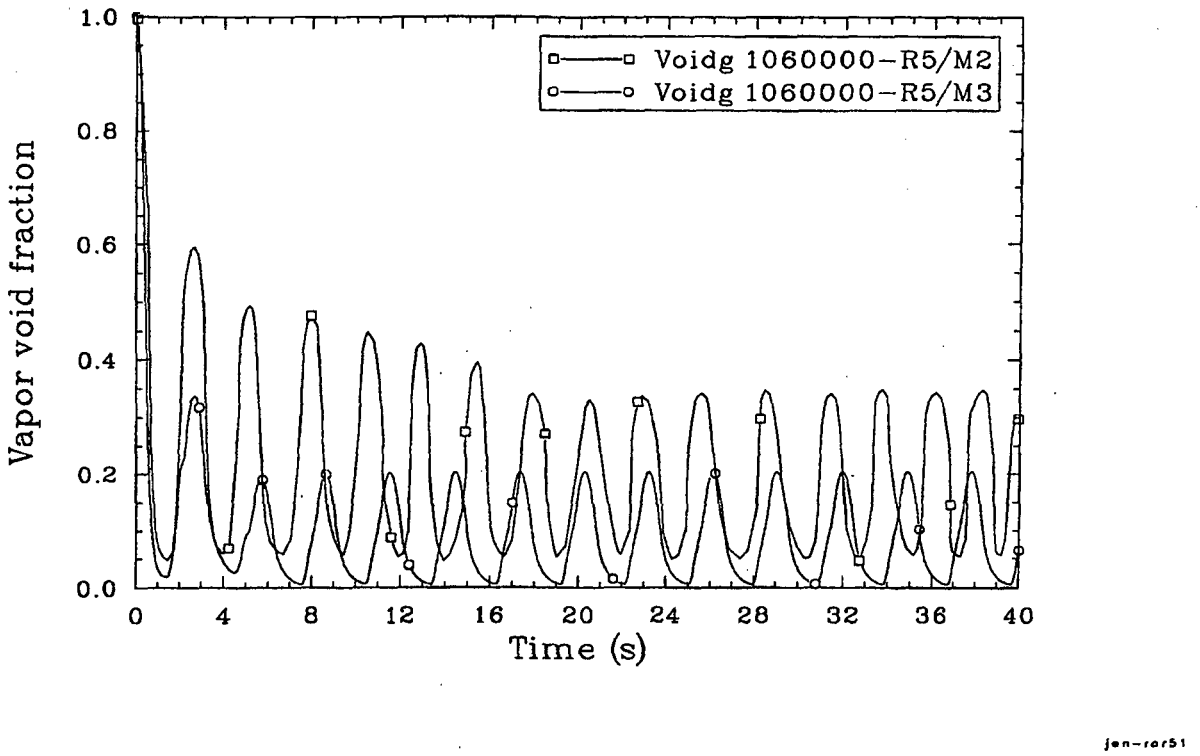

Figure 2.1-7. Vapor fraction oscillation in volume 1060000 of manometer.

The problem is in the horizontal plane. Single-phase, saturated water, at 2.63962 MPa and 500 K in two side pipes and a tee, is connected to a sink volume containing single-phase saturated water at 2.5 MPa and 497.09 K. Fluid flows from the pipes through the tee and into the sink volume. One of the calculations that showed symmetrical flows in the two side pipes in RELAP5/MOD2 was rerun on RELAP5/MOD3 to check that symmetrical flow still existed. The nodalization diagram for this case is shown in Figure 2.1-8. The tee is represented by two junctions from the two pipes to the branch component on the non-sink side, and the sink volume is time-dependent volume 401. The run was made with a large, time-dependent volume area (100 times larger than the pipe area) for volumes 201 and 301. This is called the "two non-sink junctions, big area" case in the RELAP5/MOD2 developmental assessment.[2.1-1] The problem is run to 20 s with two-phase conditions developing in the pipes and branches.

The results of the RELAP5/MOD2 and MOD3 calculations are shown in Table 2.1-2. The top five numbers are taken from the time step summary at the top of the last major edit. The bottom three numbers are the mass flow rates in the two pipes and the junction to the sink junction. There is symmetrical flow in the two pipe mass flow rates in MOD3 as there was in MOD2, and the mass flow rates between the two calculations are fairly close. MOD3 required more attempted advancements than MOD2, with the MOD3 calculation being Courant limited.

The MOD3 calculation was run to 20 s on Version 461, using the Masscomp, and required 1920 attempted advancements and 755.30 cpu seconds. The MOD2 calculation was run to 20 s on Cycle 2, using the Cyber, and required 1543 attempted advancements and 17.63 cpu seconds.

2.1.4 Cross-Flow Tee Problem

The cross-flow tee problem is a conceptual problem that was set up for RELAP5/MOD2 to test how the new cross-flow junction feature in RELAP5/MOD2 handled the tee problem presented in the previous section. It was rerun on RELAP5/MOD3 to ascertain its status with this latest code.

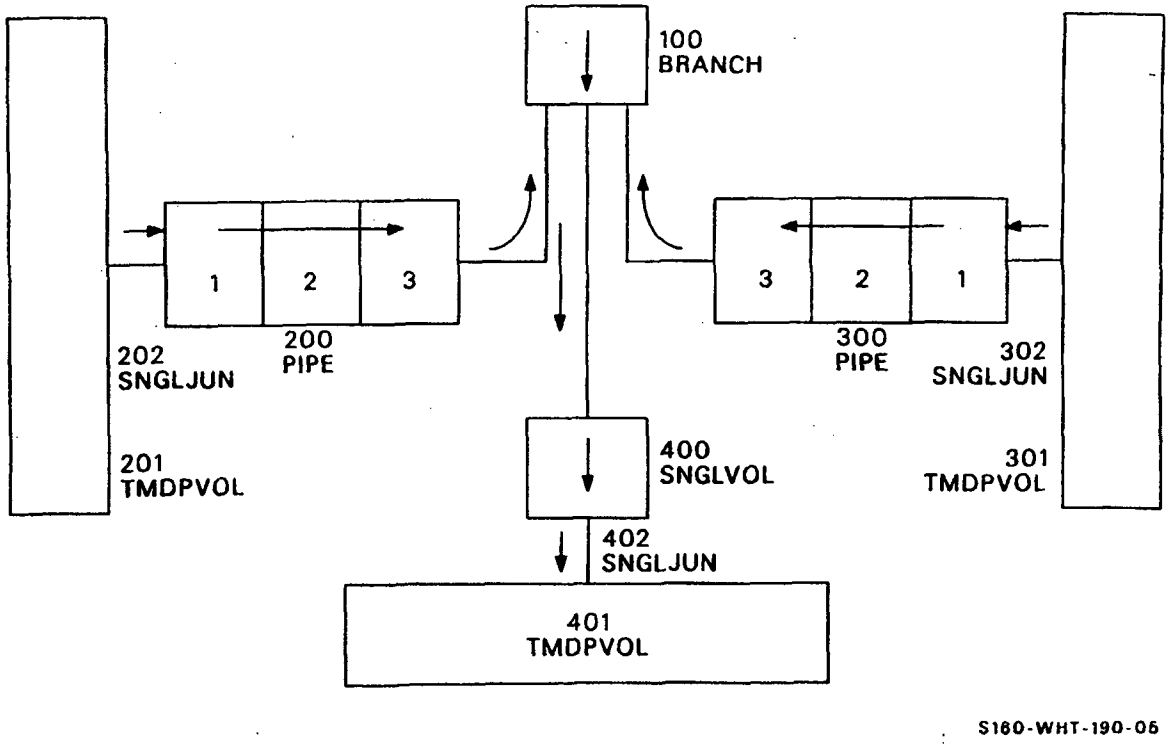

Figure 2.1-8. Nodalization of the branch tee problem using two non-sink junctions.

Table 2.1-2. Results for the branch tee problem

	RELAP5/MOD2	RELAP5/MOD3
Attempted advancements	1543	1920
Repeated advancements	9	10
Successful advancements	1534	1920
CPU time (s)	17.63 (Cyber)	755.30 (Masscomp)
End time (s)	20	20
Mass flow rate in pipe 200 (kg/s)	885.09	899.78
Mass flow rate in pipe 300 (kg/s)	885.09	899.78
Mass flow rate in single junction 402 (kg/s)	1770.2	1799.6

The problem was first set up using the nodalization diagram in Figure 2.1-9. The tee volume (single-volume component 250) was obtained by combining parts of each of the two pipe components. The volume is square and oriented left to right. The perpendicular junctions 251 and 254 were made cross flow. Large, time-dependent volumes (100 times) were used for volumes 201 and 301. Forward and reverse loss coefficients of 1.0 were used for the crossflow junctions. This is called the "Left-Right Square, Big Area, K=1" case in the RELAP5/MOD2 developmental assessment.[2.1-1]

The results of the RELAP5/MOD2 and MOD3 calculations are shown in Table 2.1-3. The same items listed in Table 2.1-2 for the branch tee problem are also listed in Table 2.1-3. There is symmetrical flow in the two pipe mass flow rates in MOD3 as there was in MOD2. The mass flow rates between the two calculations are fairly close. MOD3 required fewer attempted advancements than MOD2, with the MOD3 calculation being Courant limited.

The MOD3 calculation was run to 20 s on Version 461, using the Masscomp, and required 1388 attempted advancements and 349.45 cpu seconds. The MOD2 calculation was run to 20 s on Cycle 2, using the Cyber, and required 1388 attempted advancements and 15.69 cpu seconds.

2.1.5 Three-Stage Turbine

A steam turbine is a device that converts thermal energy contained in high-pressure and high-temperature steam to mechanical work. A turbine can be modeled using a single stage, i.e., a single volume and junction, or several stage groups, depending upon the resolution required.

The three-stage turbine problem is a conceptual problem and is shown in Figure 2.1-10. It is presented here to check out the turbine component in RELAP5/MOD3. Single-phase, superheated vapor was supplied to the turbine from the upper steam volume and exhausted into a downstream volume of the turbine. The pressure and temperature in the upstream volume and the downstream volume are 6 MPa, 748 K, and 0.5 MPa, 430 K, respectively.

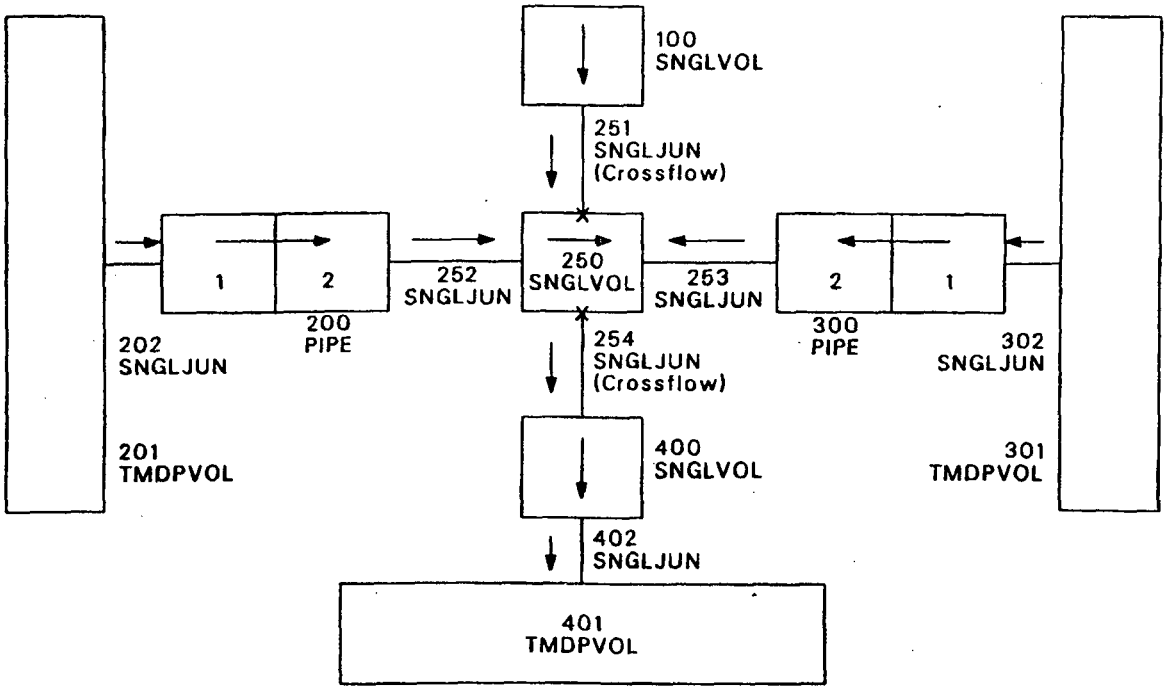

Figure 2.1-9. Nodalization of the crossflow tee problem using a left-right square for the tee.

Table 2.1-3. Results for the crossflow tee problem

	RELAP5/MOD2	RELAP5/MOD3
Attempted advancements	1388	987
Repeated advancements	268	21
Successful advancements	1120	966
CPU time (s)	15.69 (Cyber)	349.45 (Masscomp)
End time (s)	20	20
Mass flow rate in pipe 200 (kg/s)	646.73	656.81
Mass flow rate in pipe 300 (kg/s)	646.73	656.81
Mass flow rate in single junction 402 (kg/s)	1293.7	1313.7

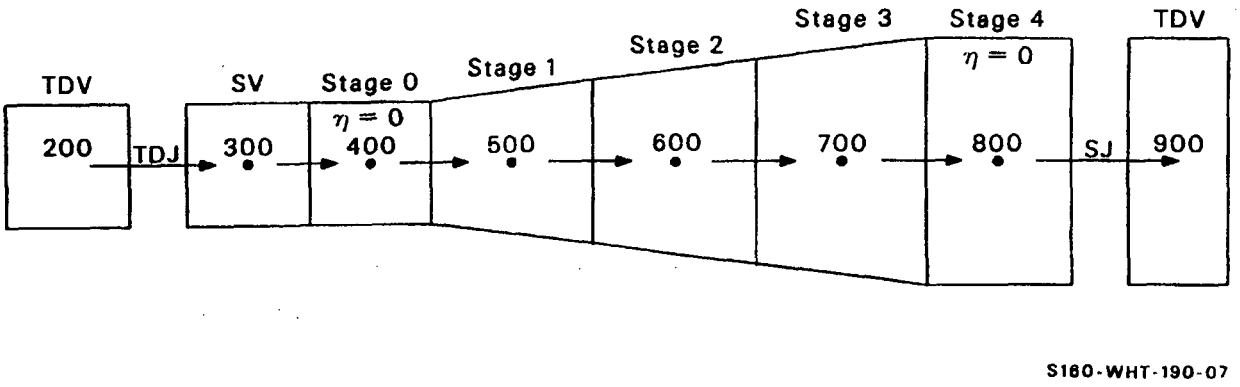

Figure 2.1-10. Nodalization used for three-stage group turbine problem.

The RELAP5/MOD3 nodalization diagram is also shown in Figure 2.1-10. Two time-dependent volumes were used to model the upstream and downstream volumes of the turbine. Three turbine components were used to simulate each stage of the three stages in the turbine. Artificial turbines (n=0) were placed before (stage 0) and after (stage 4) the three normal turbines (stages 1, 2, and 3). No loss coefficient was used for the exit junction.

The RELAP5/MOD3-calculated stage pressures, torques, and efficiencies for each stage are shown in Table 2.1-4. There is a pressure drop through the turbines and a slight pressure rise from stage 3 to the exit time. The RELAP5/MOD2 calculation was performed with a deck that did not contain single volume 300, and thus it is hard to compare the results.

The MOD3 calculation was run to 1 s on Version 552, using the Cray, with an update to correct some initialization problems; it required 104 attempted advancements and 0.64 cpu seconds.

2.1.6 Workshop Problem 2

This problem was named Workshop Problem 2 as it was used as the second demonstration problem during the RELAP5/MOD1[2.1-2] workshop held in April 1982. It was set up to simulate one loop of a two-loop pressurized water reactor (PWR) and to assess the system modeling capability of the RELAP5 computer code and the control features in the code for steady-state operation. The system consists of a primary loop and a secondary loop. The primary loop contains a reactor vessel, including an electrically heated reactor core, a pressurizer, a steam generator, and a coolant pump. The secondary loop consists of a steam discharge line with a control valve and the secondary side of the steam generator.

The RELAP5/MOD3 nodalization diagram for the system is shown in Figure 2.1-11. The model consists of four time-dependent volumes, 26 regular volumes, 21 junctions, and six heat structures, including one pump and two valves. In the model, the built-in, homologous curves for the Westinghouse pump were used. The initial conditions are shown in Table 2.1-5.

Table 2.1-4. Turbine parameters for the assessment problem

Volume Number	Pressure (Pa)	Torque (n•m)	Efficiency
TPV--200010000	6.000×10^6	--	--
SV--300010000	2.816×10^6	--	--
Artificial turbine--400010000 (Stage 0)	2.312×10^6	0	0
Turbine--500010000 (Stage 1)	1.312×10^6	4.30×10^5	0.800
Turbine--600010000 (Stage 2)	0.422×10^6	6.87×10^5	0.800
Turbine--700010000 (Stage 3)	0.398×10^6	3.435×10^4	0.800
Artificial turbine--800010000	0.449×10^6	0	0
TPV--900010000	0.500×10^6	--	--

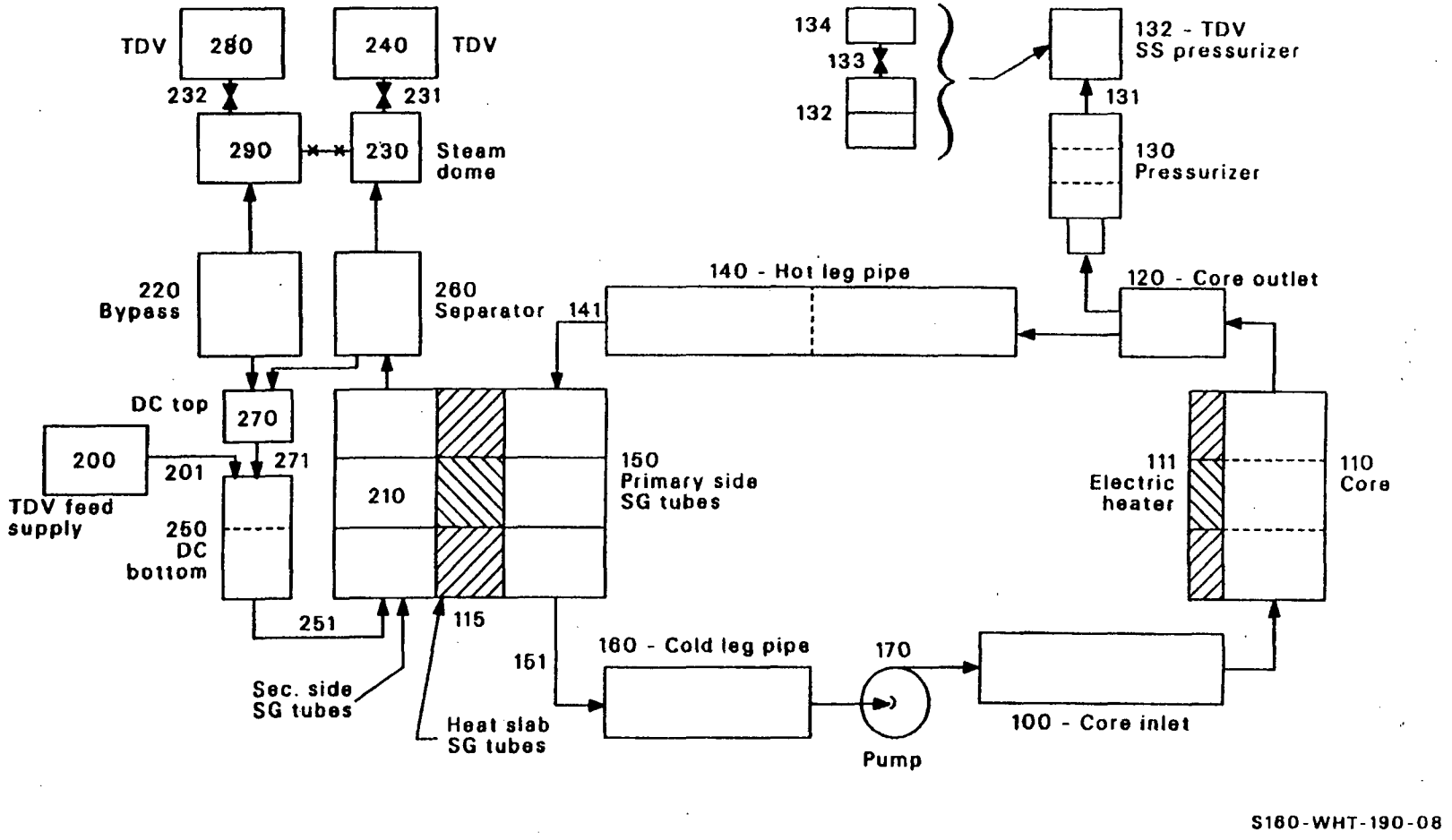

Figure 2.1-11. RELAP5 nodalization diagram for Workshop Problems 2 and 3.

Table 2.1-5. Workshop Problem 2 initial conditions

Primary System		Secondary System	
Pressure	= 1.5×10^7 Pa	Pressure	= 2×10^6 Pa
Average temperature	= 550 K	Feedwater flow	= 26.1 kg/s
Flow	= 131 kg/s	Feedwater temperature	= 478 K
Core power	= 50 MW		

The following figures show comparisons for RELAP5/MOD3 (Version 5g2), RELAP5/MOD2 (Cycle 7), and RELAP5/MOD1 (Cycle 23) for selected parameters. The MOD3 calculation was performed with the steady-state option, whereas the MOD2 and MOD1 calculations were performed with the transient option. Figures 2.1-12, 2.1-13, and 2.1-14 show the RELAP5/MOD3, MOD2, and MOD1 calculated volume pressure in the pressurizer, core outlet, and steam dome of the secondary side of steam generator, respectively. The three results are similar except that the final steam dome pressure is different. This difference is caused by the difference in the interfacial drag calculation of the three codes. The lower mass flow rate exhausting from the steam dome results in a higher secondary pressure. This evidence can be found from the steam generator secondary liquid level comparison, as shown in Figure 2.1-15. The MOD3 steam dome pressure oscillates, whereas MOD2 and MOD1 do not. In addition, the MOD3 secondary liquid level is quite different from MOD2 and MOD1 in the first 50 s. These two differences did not occur in Version 461 of MOD3, using the steady-state option; and this will need to be examined in the future.

Figures 2.1-16 and 2.1-17 show the mass flow rate in the hot leg to the pressurizer and in the primary side of steam generator. The RELAP5/MOD3, MOD2, and MOD1 results are similar, which implies that the heat transfer from the primary side to the secondary side is similar in the two codes.

The MOD3 calculation was run to 110.7 s (stopped by steady-state checks) on Version 5g2, using the Cray, and required 1129 attempted advancements and 16.54 cpu seconds. The MOD2 calculation was run to 120 s (stopped due to end of time step cards) on Cycle 36.06, using the Cray, and required 1209 attempted advancements and 21.46 cpu seconds.

2.1.7 Workshop Problem 3

Workshop Problem 3 simulates a modified station blackout transient for the system described in Workshop Problem 2. The transient scenario is specified in Table 2.1-6. The same model of Workshop Problem 2 was used for the transient analysis except that time-dependent volume 132 is replaced by

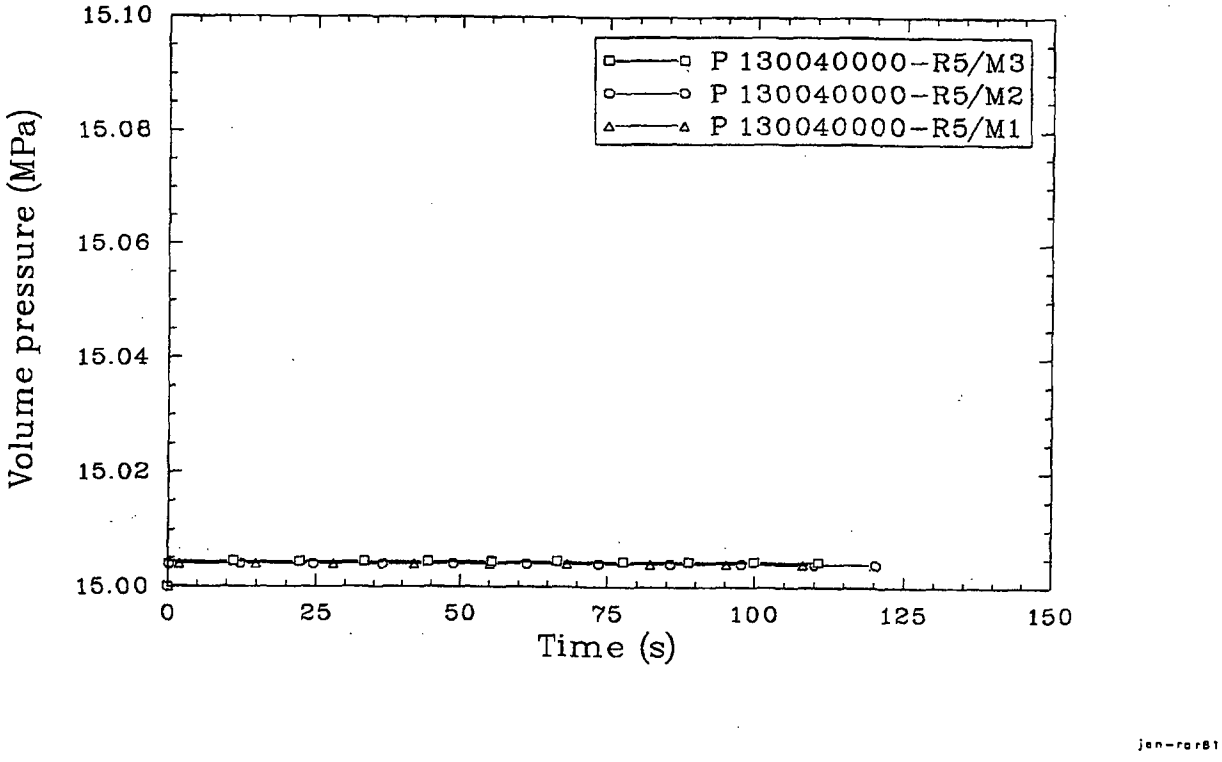

Figure 2.1-12. Pressurizer pressure history of Workshop Problem 2.

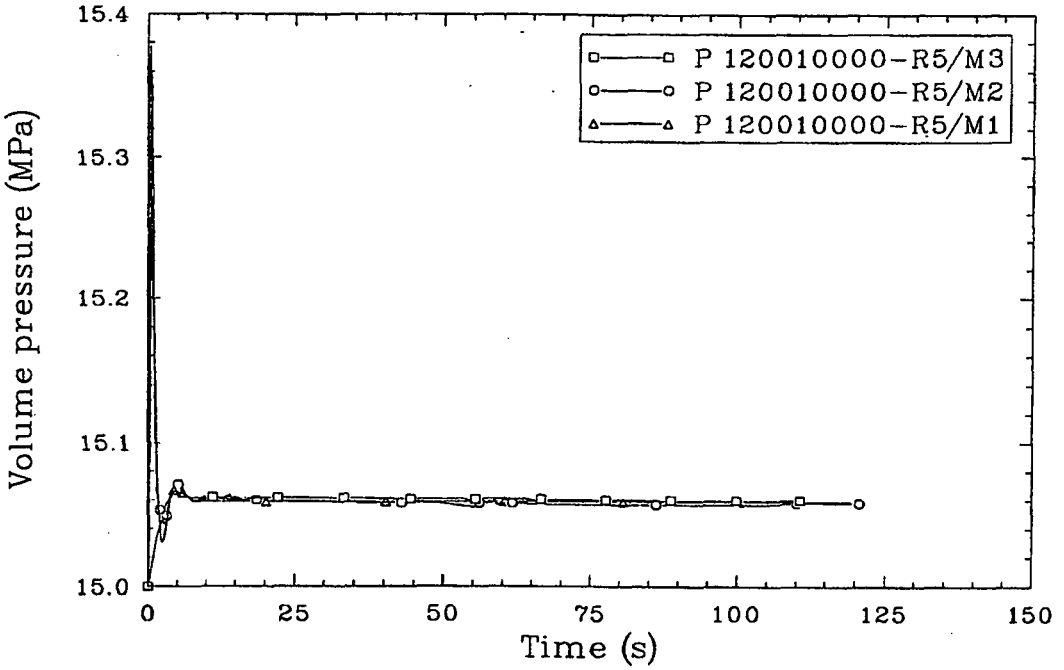

Figure 2.1-13. Core outlet pressure history of Workshop Problem 2.

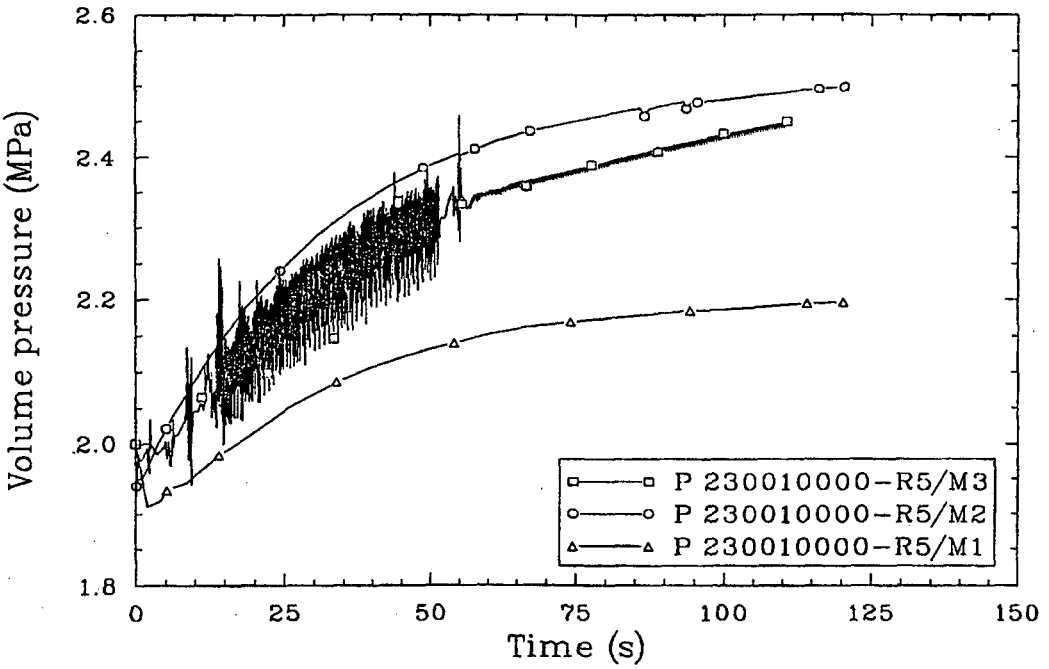

Figure 2.1-14. Steam generator steam dome pressure history of Workshop Problem 2.

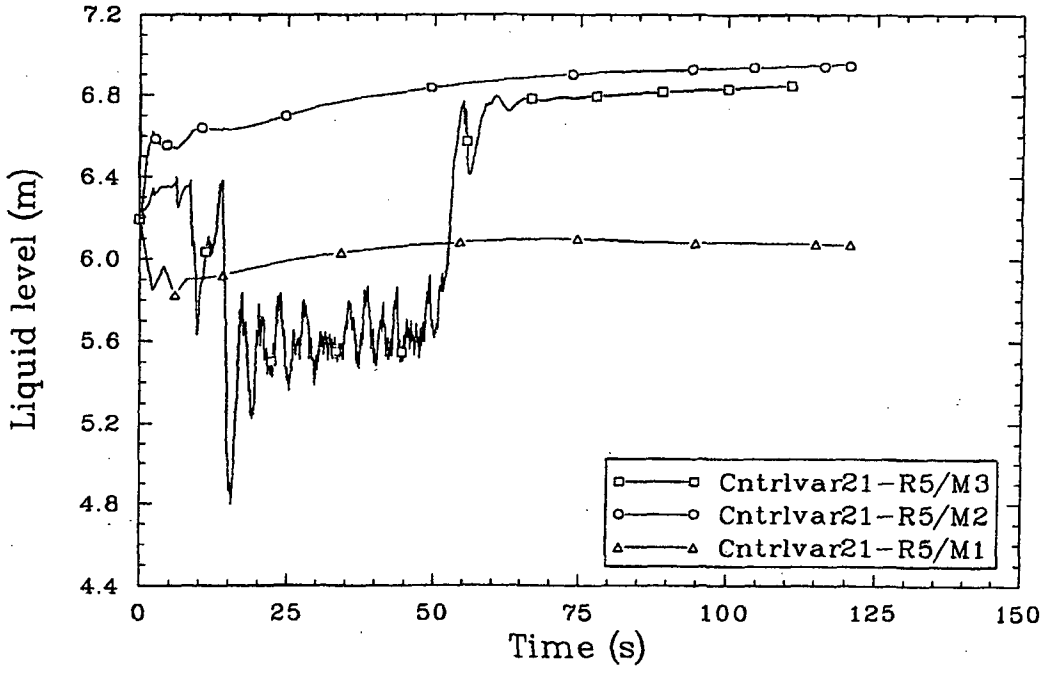

Figure 2.1-15. Steam generator secondary side liquid level for Workshop Problem 2.

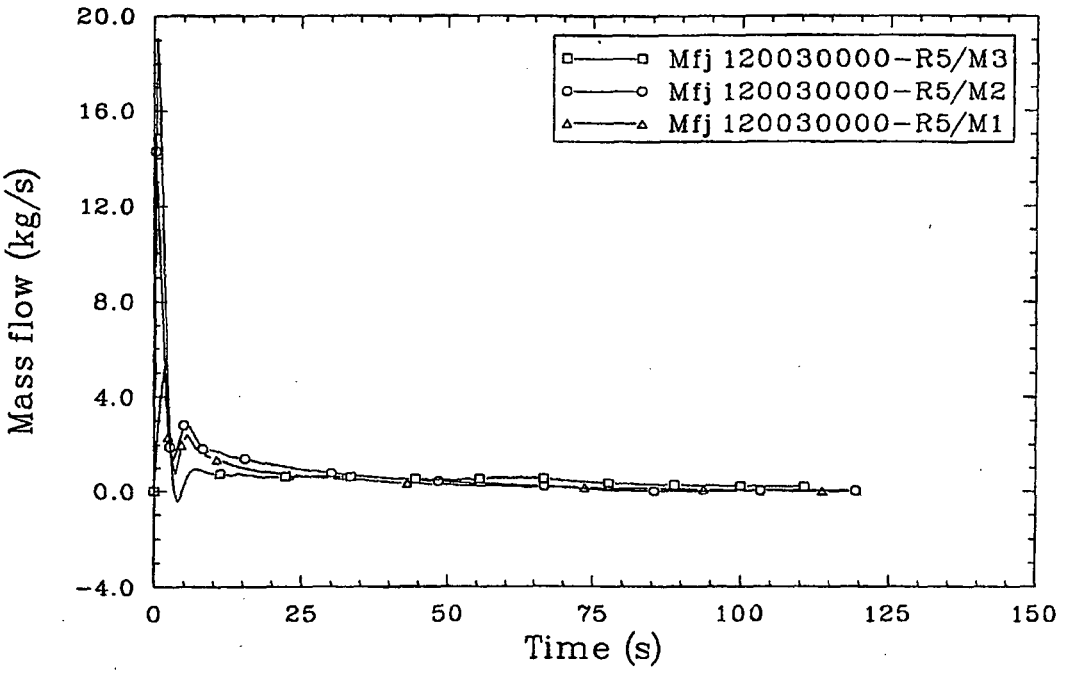

jen-rar101

Figure 2.1-16. Mass flow in the primary loop hot leg for Workshop Problem 2.

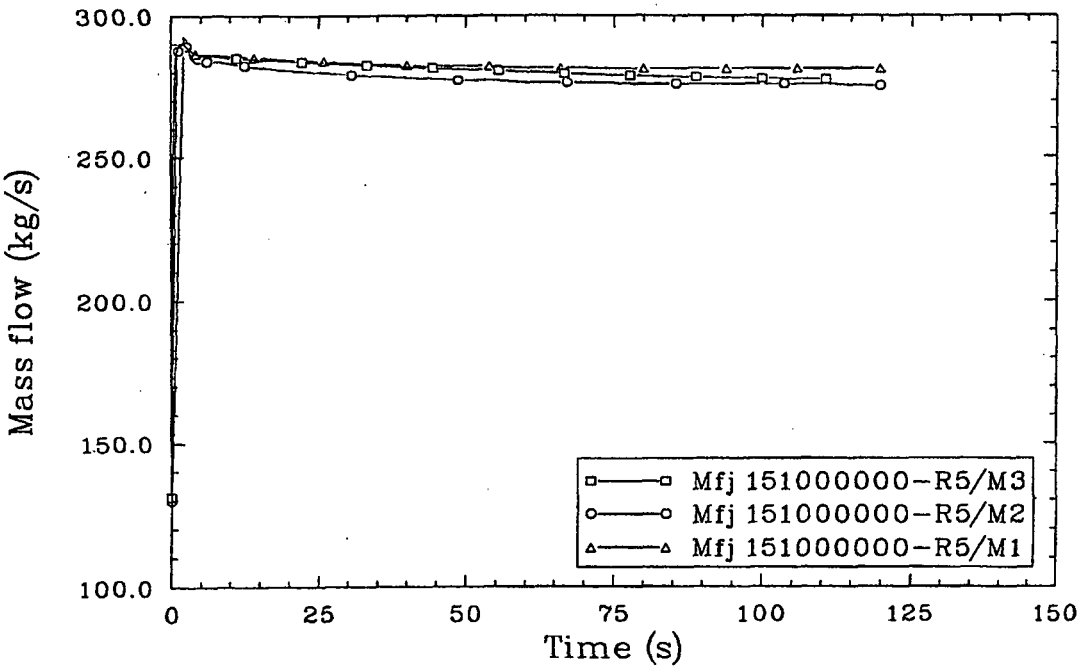

Figure 2.1-17. Mass flow in the primary side of steam generator for Workshop Problem 2.

Table 2.1-6. Transient sequence for Workshop Problem 3

1. Relief valve opens when the pressurizer pressure is higher than 15.05 MPa.
2. Reactor shutdown occurs after 5 s continuous actuation of the pressurizer relief valve.

a vertical, two-volume pipe component 132, a pressurizer trip valve 133 (pressurizer relief valve), and a time-dependent volume 134 (see Figure 2.1-11). In the model, the steady-state conditions calculated from Workshop Problem 2 were used as initial conditions; and the transient sequence shown in Table 2.1-6 was used as a boundary condition.

The Workshop Problem 3 deck has changed from one code version to another due to various requirements. The original deck (transient option) used for RELAP5/MOD1 was a restart/renodalization of Workshop Problem 2 (transient option) at 120 s, with another 30 s of steady state before the actual transient was initiated at 150 s (shut off steam generator feedwater and pump trip). The deck (transient option) used for RELAP5/MOD2 again was a restart/renodalization of Workshop Problem 2 (transient option) at 120 s; however, the 30 s of steady state were removed and thus the actual transient was initiated at 120 s. The deck (transient option) used for RELAP5/MOD3 again is a restart/renodalization of Workshop Problem 2 (steady-state option) at 120 s; however the 30 s of steady state were added back in. As a result, because of the option switch (steady state to transient), time is reset to zero when Problem 3 begins; thus, the actual transient begins at 30 s. In comparison plots, MOD2 and MOD1 will show the Workshop Problem 2 calculation to 120 s, with the Workshop Problem 3 calculation continuing on from 120 s; MOD3 will show Workshop Problem 3 beginning at 0 s.

In addition, the upper set point for the pressurizer relief valves was 18 MPa for MOD1 and MOD2 but was changed to 15.05 MPa for MOD3.

Figures 2.1-18, 2.1-19, and 2.1-20 show the volume pressure in the core, in the pressurizer, and in the steam dome of the secondary side of the steam generator. The RELAP5/MOD3, MOD2, and MOD1 results are similar except for the starting of the transient at 30, 120, and 150 s. The pressure depression at 20 s in the MOD3 plots is because the pressurizer relief valve opened (hit 150-MPa limit), whereas MOD2 and MOD1 had a higher limit (18 MPa). In Figure 2.1-19, since volume 132020000 was added on the renodalization, its pressure shows zero from 0 to 120 s for MOD2 and MOD1. Figures 2.1-21 and 2.1-22 show the core mass flow and pressurizer flow. The

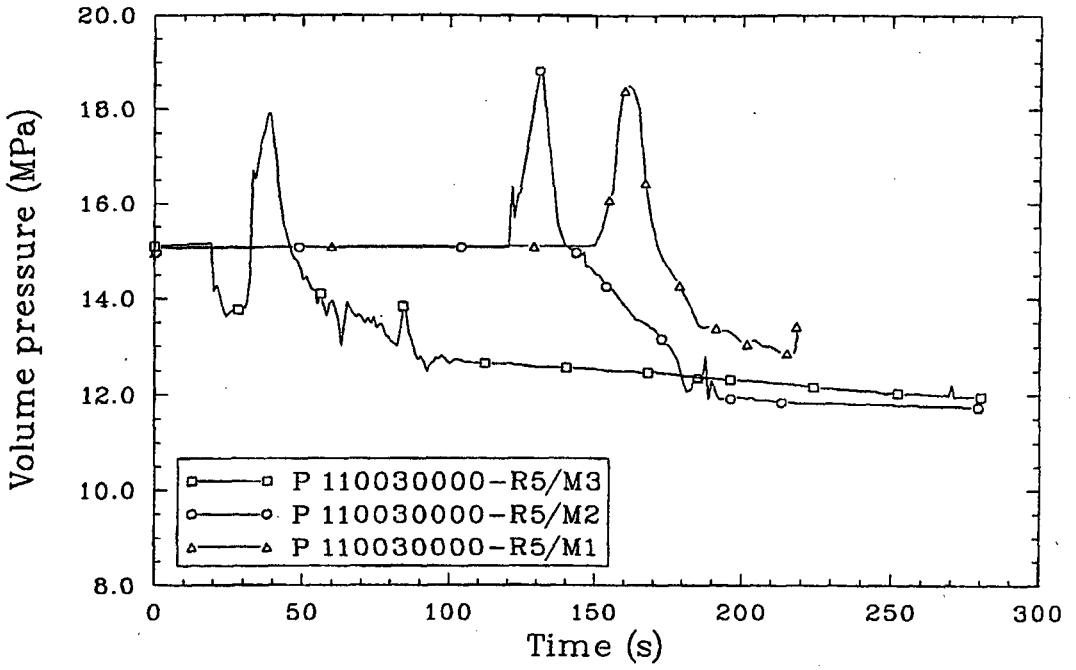

Figure 2.1-18. Volume pressure of the reactor core for Workshop Problem 3.

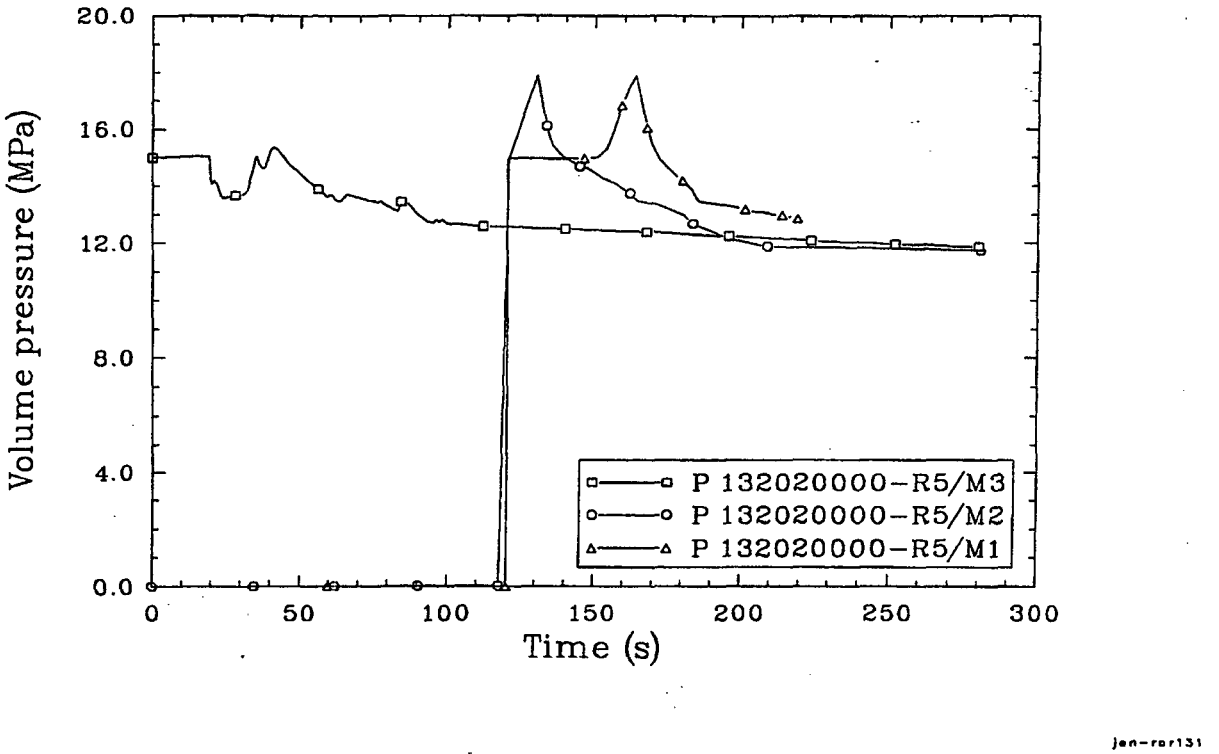

Figure 2.1-19. Volume pressure of the pressurizer for Workshop Problem 3.

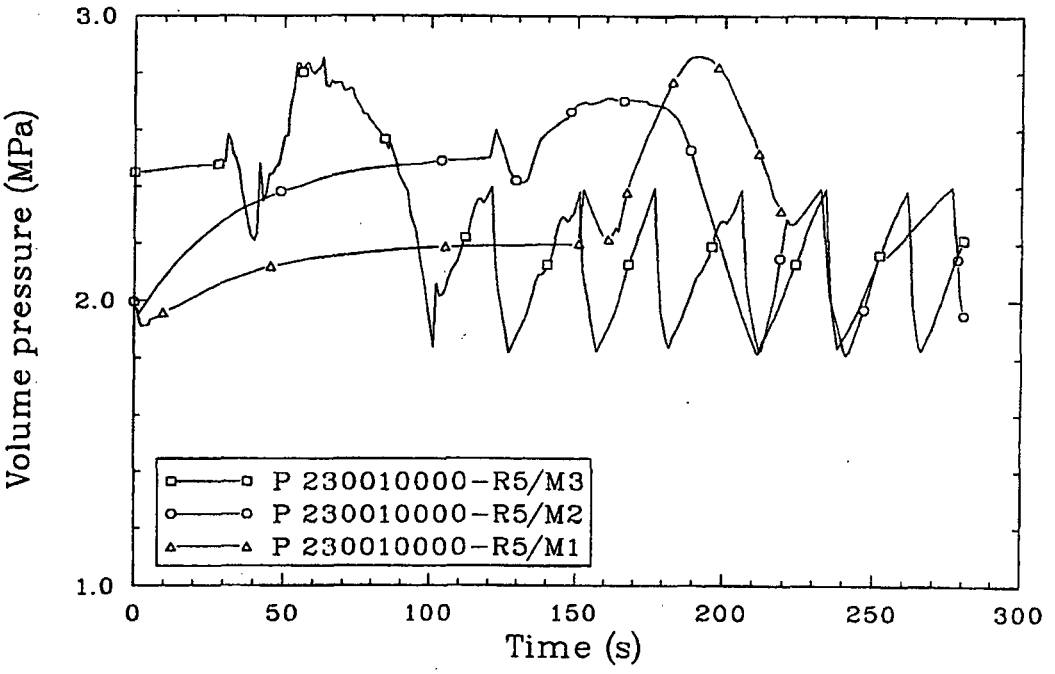

jan-rer141

Figure 2.1-20. Volume pressure of the steam generator steam dome for Workshop Problem 3.

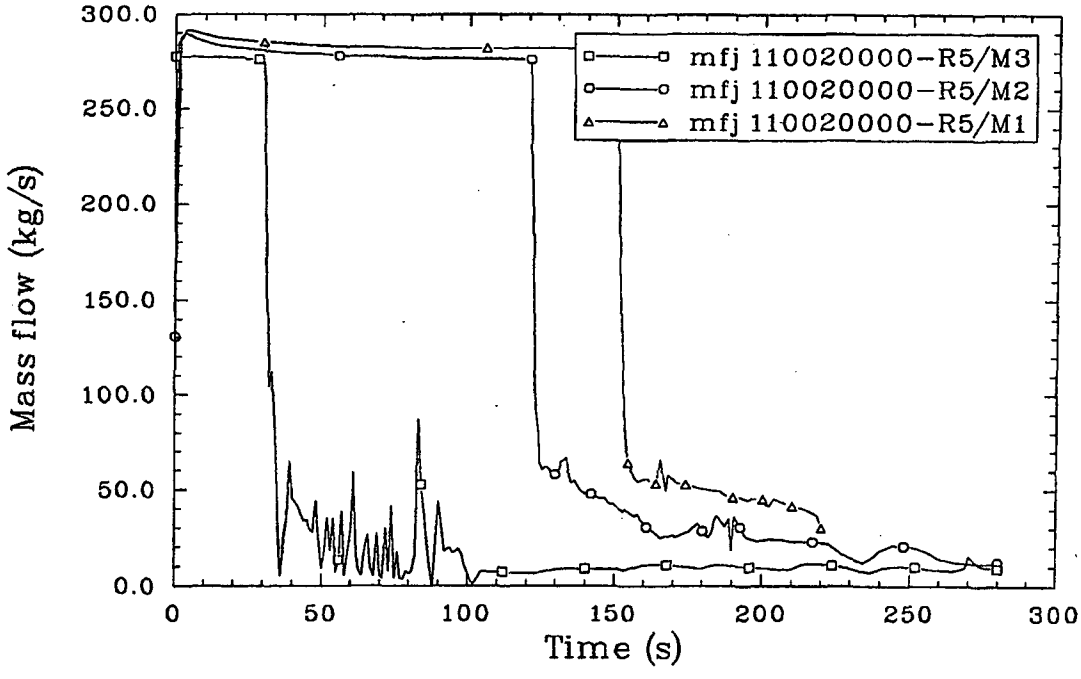

Figure 2.1-21. Mass flow in the reactor core for Workshop Problem 3.

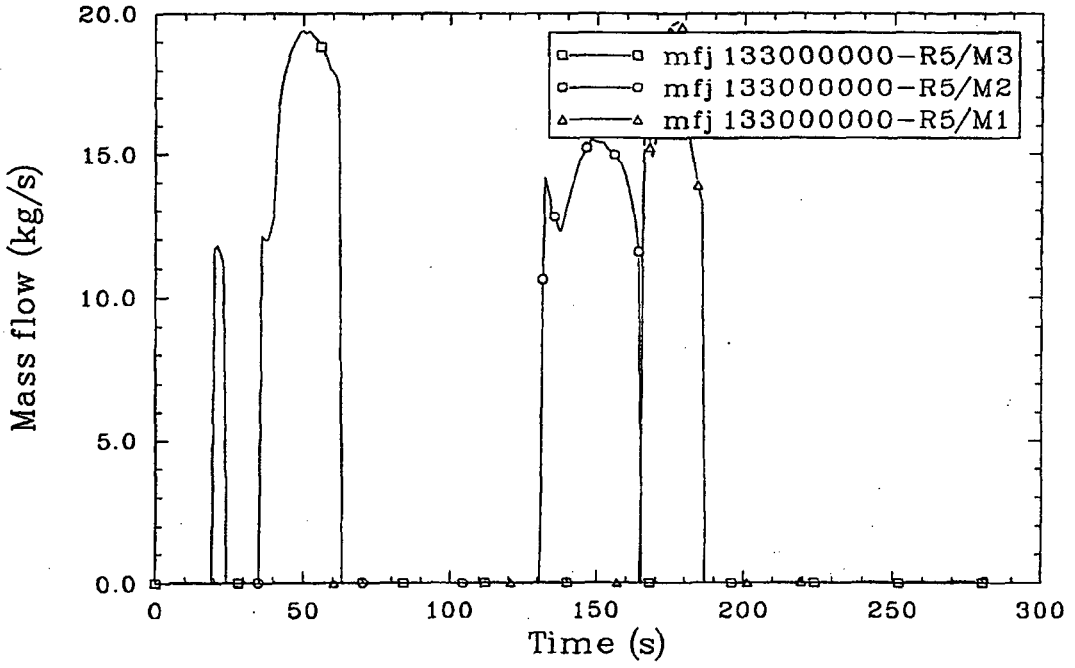

Figure 2.1-22. Mass flow in the pressurizer for Workshop Problem 3.

results are similar except for the timing and the MOD3 different pressure valve set point. Figures 2.1-23 and 2.1-24 show the secondary loop mass flow in the steam generator riser and steam exit line. The results are again similar except for the timing.

The MOD3 calculation was run to 280 s on Version 562, using the Cray, with an update to modify the water packer (pclec2); it required 5643 attempted advancements and 80.86 cpu seconds. The MOD2 calculation was run to 280 s on Cycle 36.06, using the Cray, and required 5661 attempted advancements and 92.86 cpu seconds.

2.1.8 Horizontally Stratified Countercurrent Flow

The horizontally stratified countercurrent flow problem is a conceptual problem involving a horizontal pipe closed at both ends with a linearly graduated liquid level. Due to the gravitational head difference, the liquid tends to flow from the higher-level side to the lower-level side. The vapor is forced to flow in the opposite direction from the liquid. A countercurrent flow is developed. The problem was designed to check the RELAP5 countercurrent flow model.

Figure 2.1-25 shows the RELAP5 nodalization diagram. The pipe was modeled using 20 volumes and 19 junctions (total pipe length = 10 m, pipe flow area = 0.19635 m^2). The pipe is initially filled with a linearly distributed, two-phase, saturated, liquid/vapor mixture at a pressure of 10^7 Pa; and the quality varies from 0.083 to 0.067.

The predicted history of the liquid and vapor junction velocities at three locations (left, middle, and right) are shown in Figures 2.1-26 and 2.1-27. The liquid flows in the opposite direction as the vapor and propagates as a wave. These results show qualitatively that the countercurrent flow model in RELAP5/MOD3 is functioning properly.

The MOD3 calculation was run to 30 s on Version 4b1, using the Cray, and required 1185 attempted advancements and 8.12 cpu seconds.

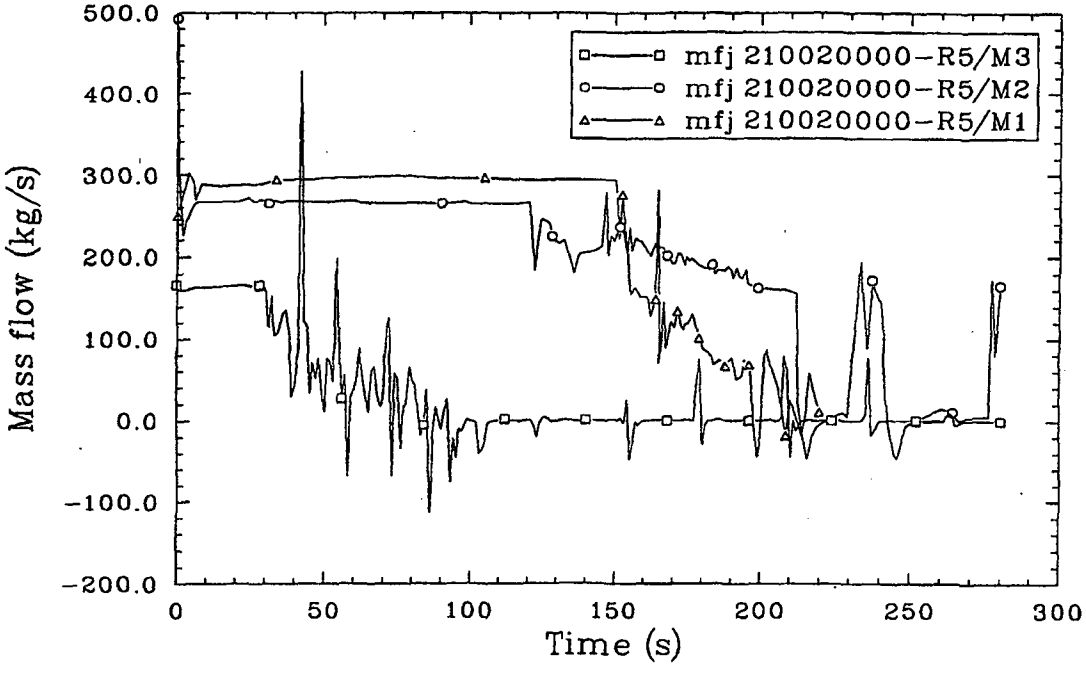

jan-ci71

Figure 2.1-23. Mass flow in the steam generator secondary side (riser) for Workshop Problem 3.

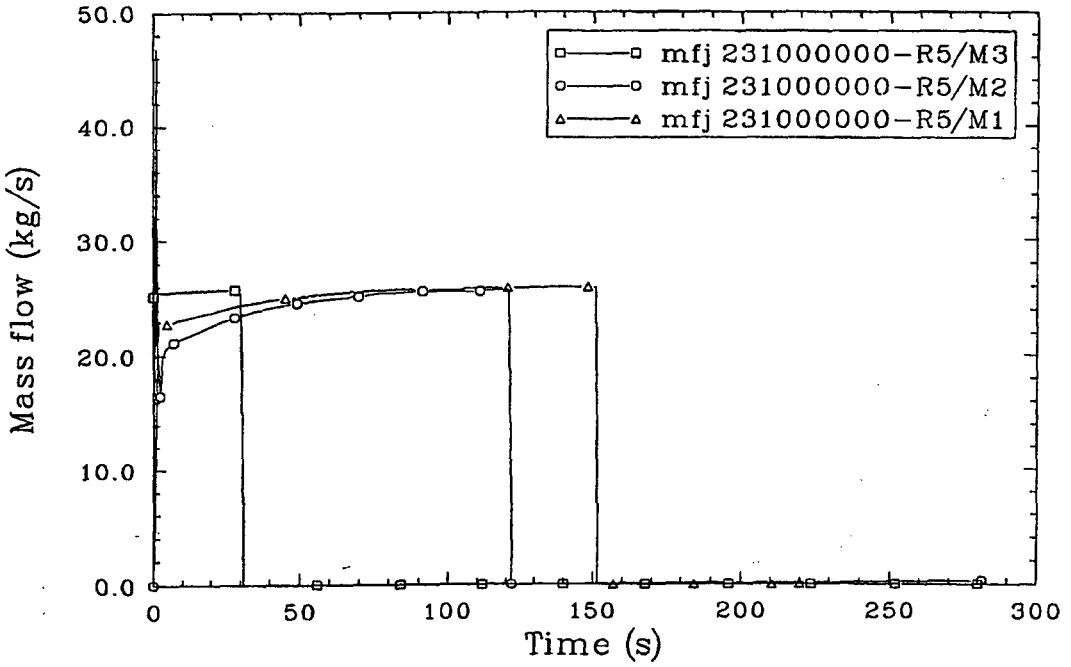

Figure 2.1-24. Mass flow in the steam discharge line for Workshop Problem 3.

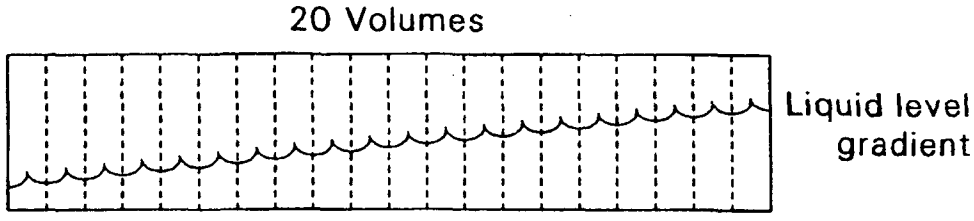

Figure 2.1-25. RELAP5 nodalization diagram for a horizontally stratified countercurrent flow problem.

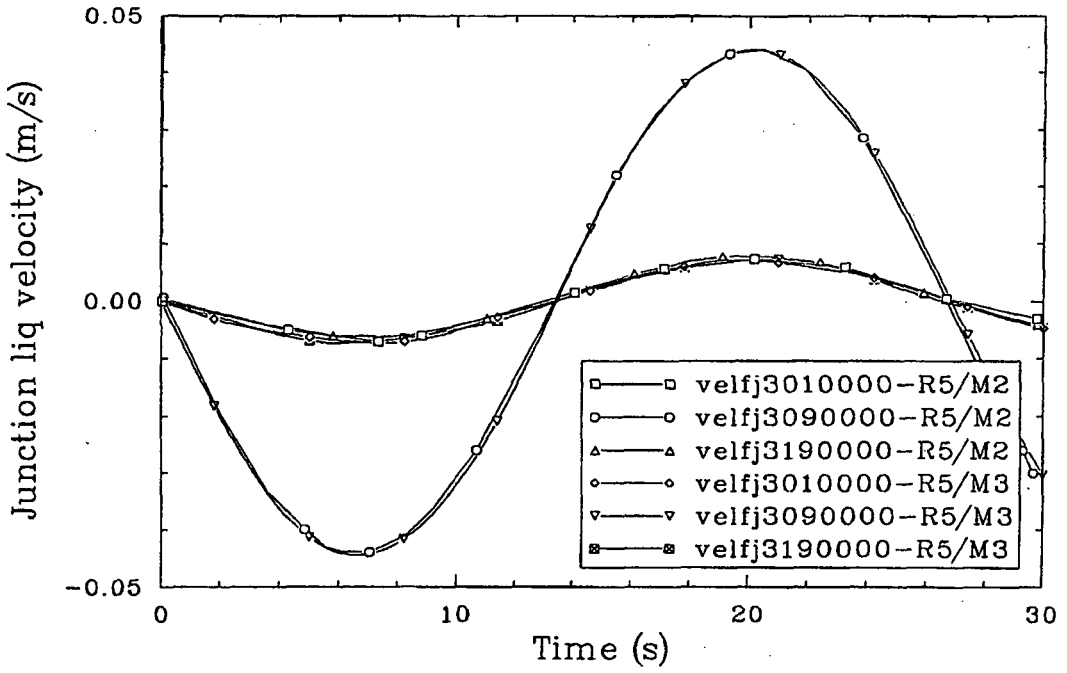

Figure 2.1-26. RELAP5-calculated junction liquid velocities at three locations.

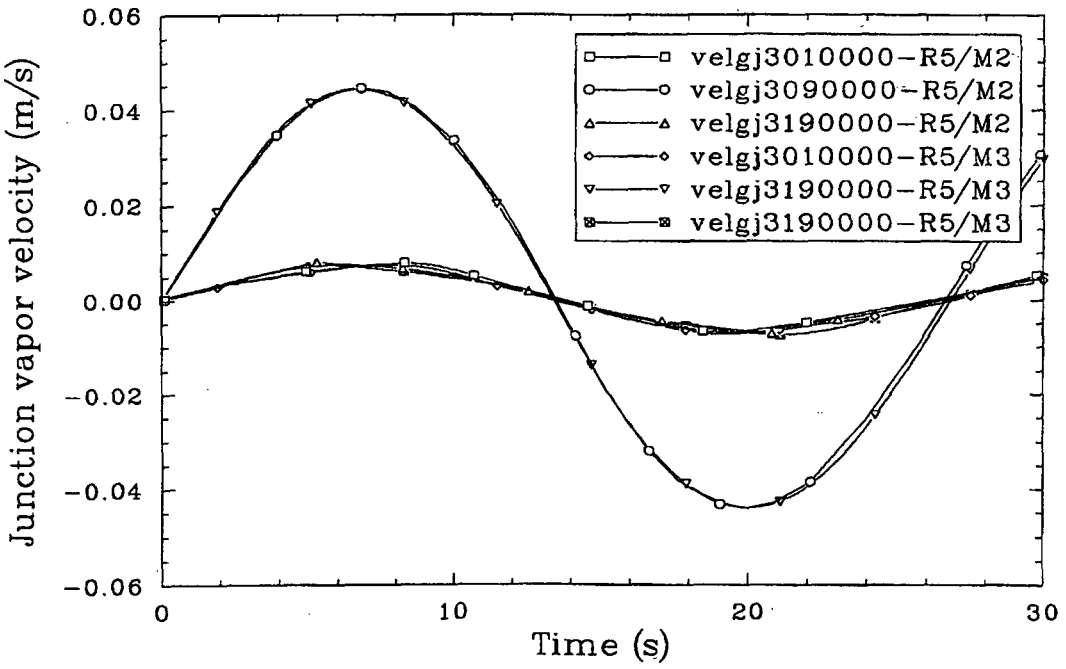

jan-r201

Figure 2.1-27. RELAP5-calculated junction vapor velocities at three locations.

2.1.9 Edwards Pipe Problem with Extras

The problem is similar to the Edwards[2.1-3] pipe experiment except that a few artificial boundary conditions were added. These included heat loss at the pipe wall, a couple of control components, a few trips, and a reactor kinetics model. These are added so that more components are exercised, since this problem is run whenever a new version is made. The problem was originally used to verify the vapor generation model in the RELAP5/MOD1 code after a program modification was made. The same hydrodynamic nodalization diagram as the Edwards pipe problem was used and is shown in Figure 2.1-28.

A comparison of measured and calculated void fraction by RELAP5/MOD3 and MOD2 at the middle location of the test section is shown in Figure 2.1-29. A similar comparison for pressure at the same location is shown in Figure 2.1-30. The RELAP5/MOD3 and MOD2 results are in good agreement with the data. The additional components added have little effect on these key parameters.

The MOD3 calculation was run to 0.5 s on Version 511, using the Cray, and required 519 attempted advancements and 7.04 cpu seconds. The MOD2 calculation was run to 0.5 s on Cycle 36.06, using the Cray, and required 538 attempted advancements and 9.96 cpu seconds.

2.1.10 Pryor's Pipe Problem

The Pryor's pipe problem was developed to check the water packing problem that occurs in the finite difference scheme. The problem consists of a pipe section, a water injection system, and a two-phase exit system. Initially, the pipe is filled with slightly superheated vapor, at a pressure of 0.4 MPa and a temperature of 418.2 K. The problem was modeled using RELAP5/MOD3, and the nodalization diagram is shown in Figure 2.1-31. The model consisted of 20 volumes for the pipe section, 19 junctions, two time-dependent volumes for the water injection and discharge systems, a time-dependent junction for the injection junction, and a single volume for the exit junction.

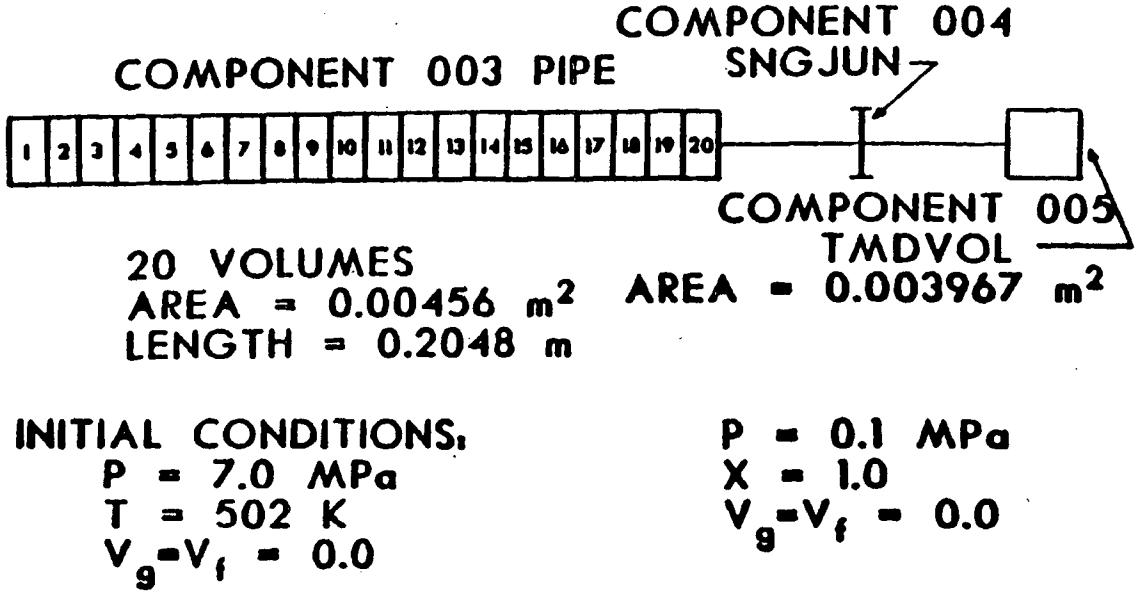

Figure 2.1-28. RELAP5 nodalization for Edwards' pipe experiment.

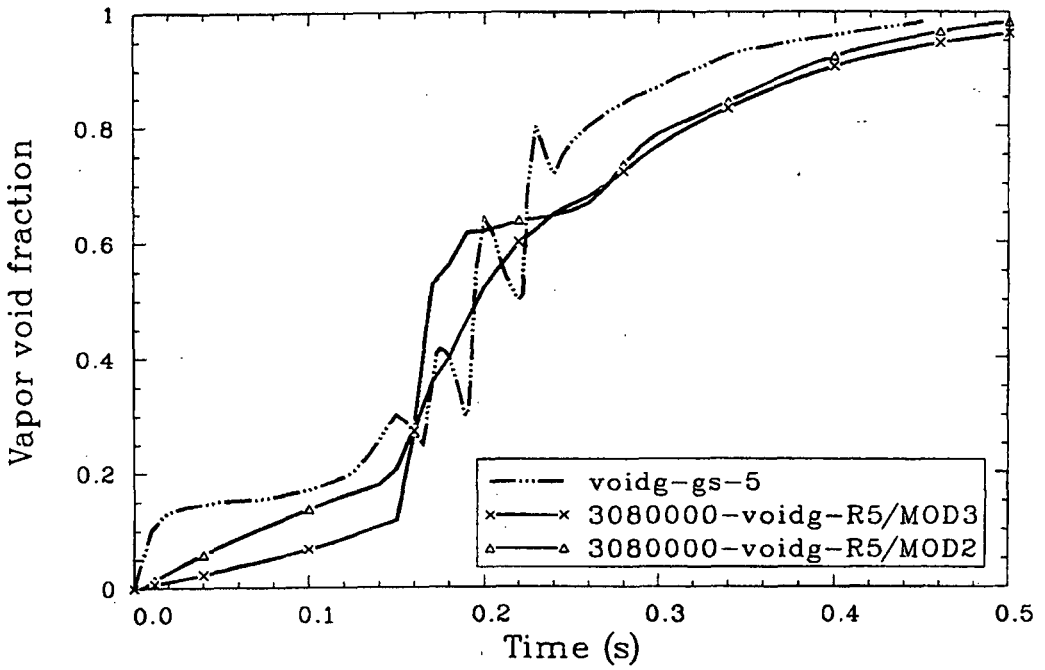

Figure 2.1-29. Comparison of measured and calculated history of midsection void fraction (Edwards' pipe with extras).

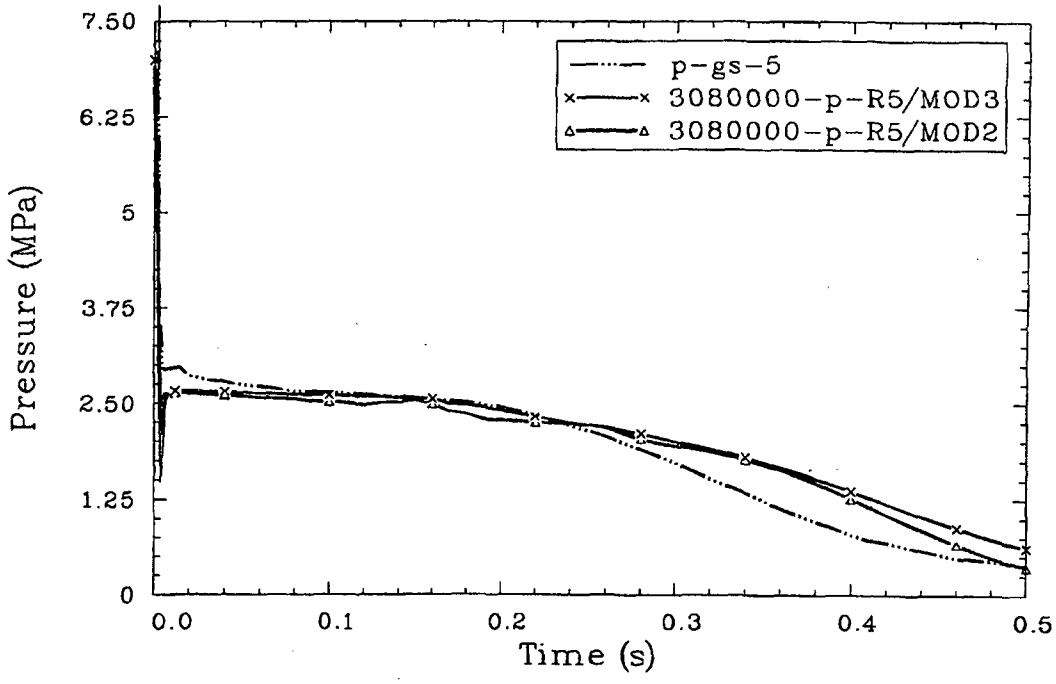

Figure 2.1-30. Comparison of measured and calculated history of midsection pressure (Edwards' pipe with extras).

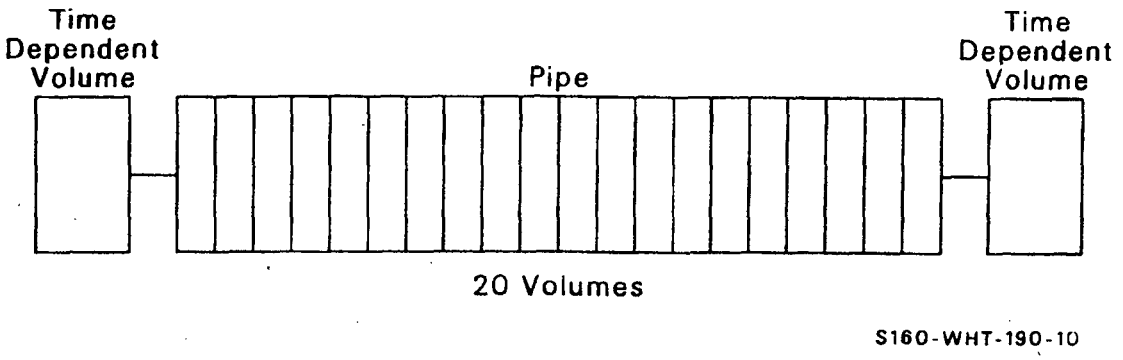

Figure 2.1-31. RELAP5 nodalization diagram for Pryor's pipe problem.

RELAP5/MOD3 and MOD2 calculated local void fraction and pressure in the even numbered volumes are shown in Figures 2.1-32, 2.1-33, and 2.1-34. The RELAP5/MOD3 calculation was run with the water packer turned on, and the RELAP5/MOD2 calculation was run without the water packer. For MOD3, it was necessary to include a 0.5-s velocity ramp on the injection junction. When the volume is filled with water, the RELAP5/MOD2 code (without water packer) calculated volume pressure increases (about 0.4 MPa maximum). This pressure spike is caused by water packing. The RELAP5/MOD3 calculation (with water packer on) does not show these pressure increases.

The MOD3 calculation was run to 1 s on Version 5i1, using the Cray, and required 100 attempted advancements and 1.27 cpu seconds.

2.1.11 References

2.1-1. V. H. Ransom et al., *RELAP5/MOD2 Code Manual, Volume 3: Developmental Assessment Problems*, EGG-TFM-7952, December 1987.

2.1-2. V. H. Ransom et al., *RELAP5/MOD1 Code Manual, Volumes 1 and 2*, NUREG/CR-1826, EGG-2070, March 1982.

2.1-3. A. R. Edwards and F. P. O'Brien, "Studies of Phenomena Connected with the Depressurization of Water Reactors," *Journal of the British Nuclear Energy Society, 9*, 1970, pp. 125-135.

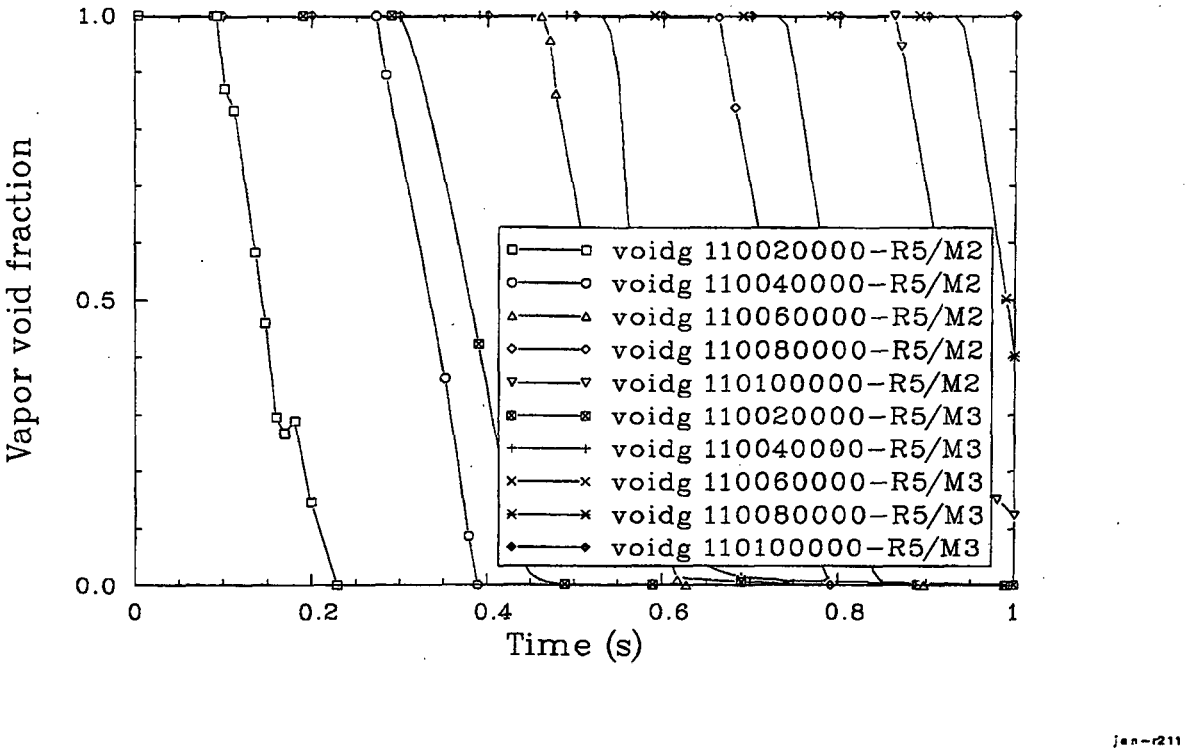

Figure 2.1-32. The history of void fraction distribution for Pryor's pipe problem.

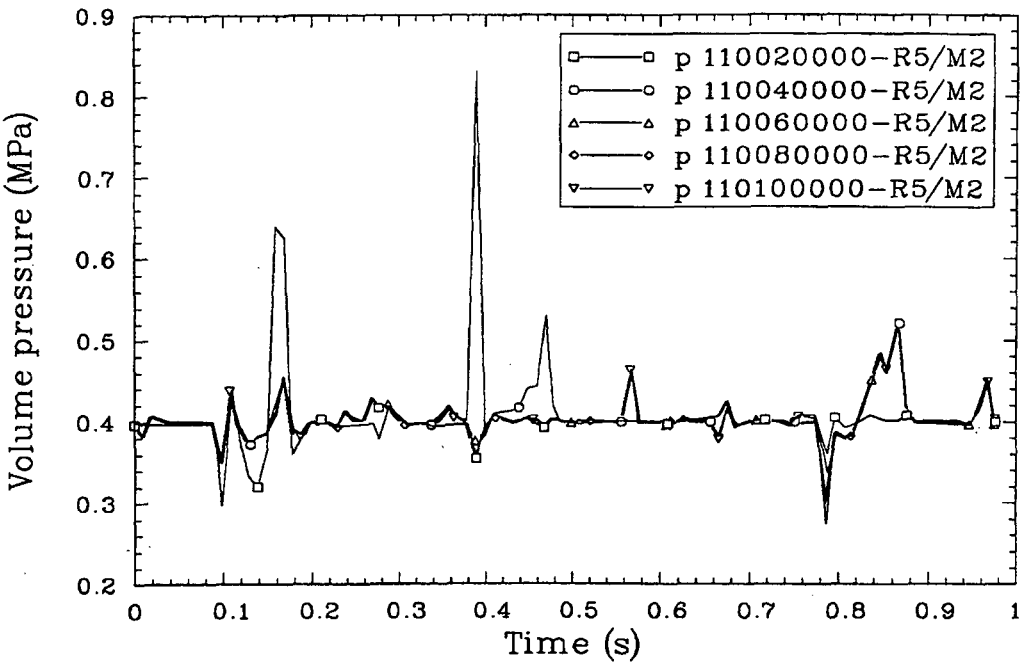

jen-r221

Figure 2.1-33. The history of pressure distribution for Pryor's pipe problem for RELAP5/MOD2.

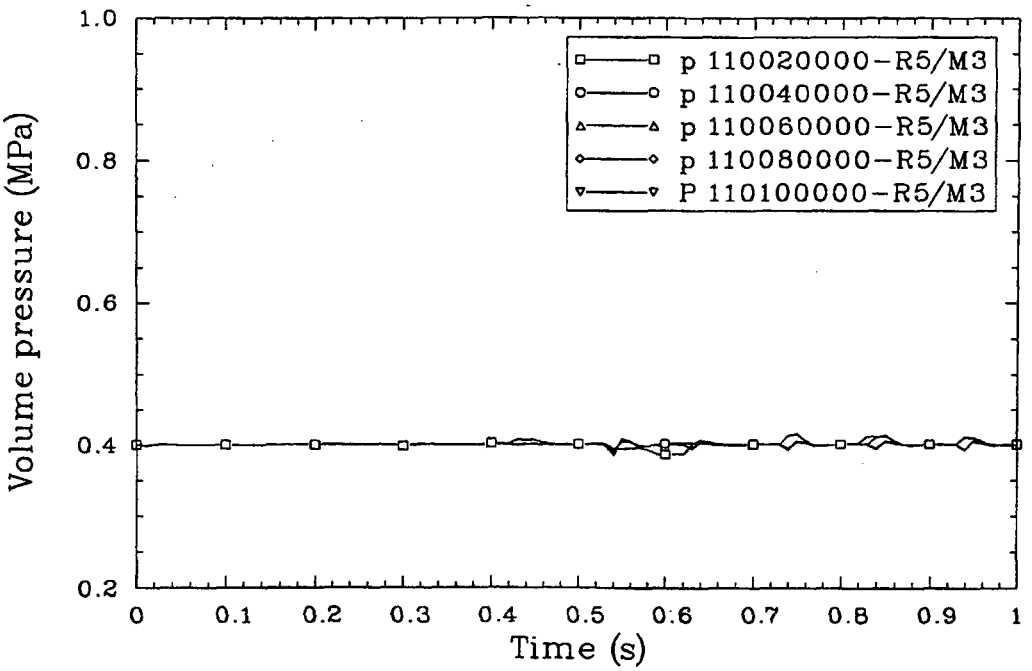

Figure 2.1-34. The history of pressure distribution for Pryor's pipe problem for RELAP5/MOD3.

2.2 SEPARATE-EFFECTS PROBLEMS

2.2.1 LOFT-Wyle Blowdown Test WSB03R

In order to test the RELAP5 horizontal stratified flow model and its coupling to the choked flow model, a simulation of the Wyle small break test WSB03R[2.2-1] was performed. Wyle Laboratories, in Norco, California, conducted transient tests of the LOFT break orifice using the LOFT Transient Fluid Calibration Facility. The objectives of the test were to obtain orifice calibration data at fluid conditions typical of small break loss-of-coolant accidents (LOCAs) and to provide a data base for critical flow model development.

A schematic of the Wyle Test Facility is shown in Figure 2.2-1. The facility hardware consisted of a pressure vessel and a blowdown leg, which are similar to the LOFT reactor vessel and broken loop cold leg. The pressure vessel was made from carbon steel, with a volume of approximately 5.4 m^3 (190 ft^3). The pressure vessel contained a carbon steel flow skirt to simulate the LOFT downcomer. The blowdown leg was connected to the vessel outlet flange. The flow skirt extended 0.8382 m (33 in.) above the connection. The blowdown leg consisted of a vessel outlet nozzle, an instrumentation test section, the break orifice, a shutoff gate valve, a burst disc assembly, and a discharge pipe. The test section was made from 0.36-m (14-in.) Schedule 160 stainless steel pipe. The break orifice was centered inside the test section.

Four load cells supported the vessel and blowdown leg. The pressure vessel was supported from three equally spaced, cantilevered, mounting lugs located at the outlet nozzle centerline, which supported the full weight of the vessel through the load cells. The fourth load cell supported the blowdown leg above a concrete mass on air springs. The primary transducers for determining the system weight were the system load cells. The mass flow rate was calculated by differentiating the vessel weight measurement from the four load cells. A second reference vessel mass inventory measurement was provided by the top-to-bottom vessel differential pressure measurement.

A six-beam gamma densitometer, comprised of two three-beam densitometers mounted on opposite sides of the pipe, was used to determine the density upstream of the small break orifice. The fluid temperature upstream of the small break orifice and near the bottom of the vessel were measured by ISA Type K function thermocouples. The pressure upstream of the small break orifice was measured by a pressure transducer.

The test WSB03R was performed at an initial pressure of 15.0 MPa. The diameter of the break orifice was 16 mm (0.6374 in). This test was performed for the 16-mm diameter nozzle installed in the LOFT facility to control break flow during the LOFT small-break loss-of-coolant Experiment L3-1. The test duration was 1500 s.

The RELAP5 model nodalization for the Wyle transient system is also presented in Figure 2.2-1. The system configuration was nodalized so that system area changes and significant changes of piping are located at junctions. The pressure vessel, with core barrel in place, was modeled by 10 volumes, using a 7-volume pipe, a branch, and two single volumes. All junctions were smooth, except for two abrupt junctions in the branch that connects to the 7-volume pipe and the downcomer. The downcomer was modeled by a 4-volume pipe. The flow skirt extension above the blowdown pipe connection was modeled by a single volume. All other junctions were modeled using the smooth option. A single volume was connected to the blowdown pipe using a cross flow junction, which was modeled as a 4-volume horizontal pipe. The length of this single volume was made equal to the diameter of the blowdown pipe. The orifice was modeled as an abrupt single junction with the area equal to the actual orifice area. In the calculation, unity subcooled, two-phase, and superheated break flow multipliers were used. The unity multipliers were chosen because the measured values of density, pressure, and temperature were not consistent. This suggested that density was not known accurately; thus, it was felt to be of little value to use any value other than the default values. There were insufficient data to determine the actual initial conditions for the whole system. Thus, some discrepancies in the comparisons of data and calculation may be due to the assumed initial conditions differing from the actual values. The MOD3 and

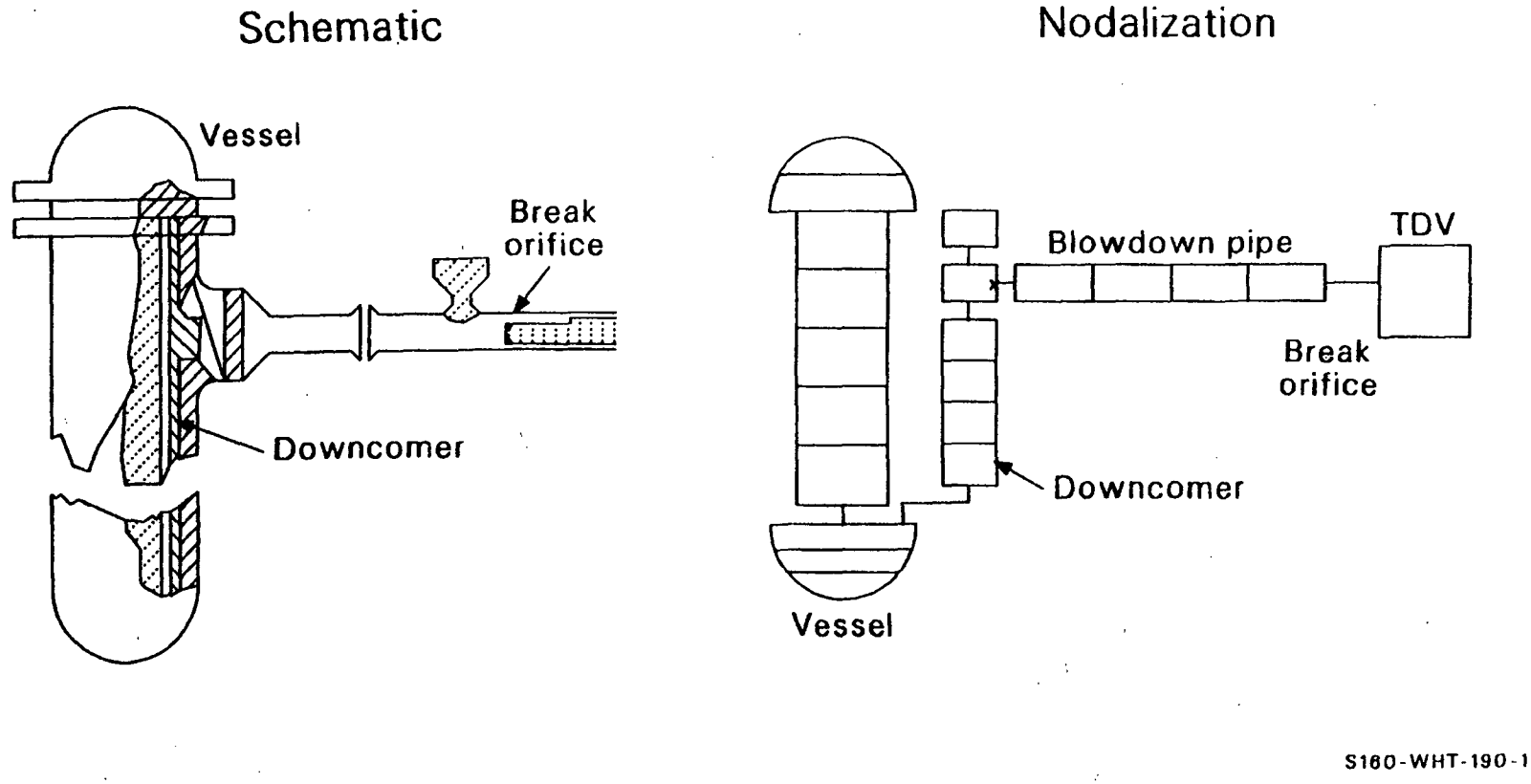

Figure 2.2-1. Schematic and nodalization for Wyle Test WSB03R.

MOD2 maximum requested time steps were the same; however, for MOD1 it was necessary to reduce this in order to remove oscillations.

Figure 2.2-2 shows a comparison of the RELAP5/MOD3, MOD2, and MOD1 predicted and measured mass flow rate at the break. The results agree well with the data. Figure 2.2-3 shows the pressure upstream of the break. Here, RELAP5/MOD2 calculates a somewhat higher pressure for the first two-thirds of the run, while RELAP5/MOD1 calculates a higher pressure for the first one-third of the run. RELAP5/MOD3 falls in between. Figure 2.2-4 shows the density upstream of the break. The RELAP5/MOD2 calculated density is higher than MOD3 and MOD1 from 500 to 1500 s; however, it is smoother.

The MOD3 calculation was run to 1500 s on Version 5il, using the Cray, and required 6324 attempted advancements and 48.48 cpu seconds. The MOD2 calculation was run to 1500 s on Cycle 4, using the Cyber, with a horizontal stratification update (HXCX004); it required 5760 attempted advancements and 139.50 cpu seconds. The MOD1 calculation was run to 1500 s on Cycle 17, using the Cyber, with a momentum equation update;[2.2-2] it required 28665 attempted advancements and 450 cpu seconds.

2.2.2 One-Foot General Electric Level Swell Test 1004-3

The GE level swell Test 1004-3[2.2-3] involves a vertical vessel that is initially pressurized and partially filled with saturated water. The test is initiated by opening a simulated break near the top of the vessel. As the vessel depressurizes, a two-phase mixture is formed in the vessel; and the transient void distribution is measured to provide a test of two-phase interphase momentum interaction. The data are useful for testing the interphase drag formulation of two-phase mathematical descriptions.

The GE level swell test facility consists of a 0.3048-m (1-ft) diameter, 4.2672.2-m (14-ft) long, vertically oriented cylindrical pressure vessel; a blowdown line containing an orifice; and a suppression pool at atmospheric conditions. A schematic of the vessel and the portion of the blowdown line containing the orifice is shown in Figure 2.2-5. The vessel,

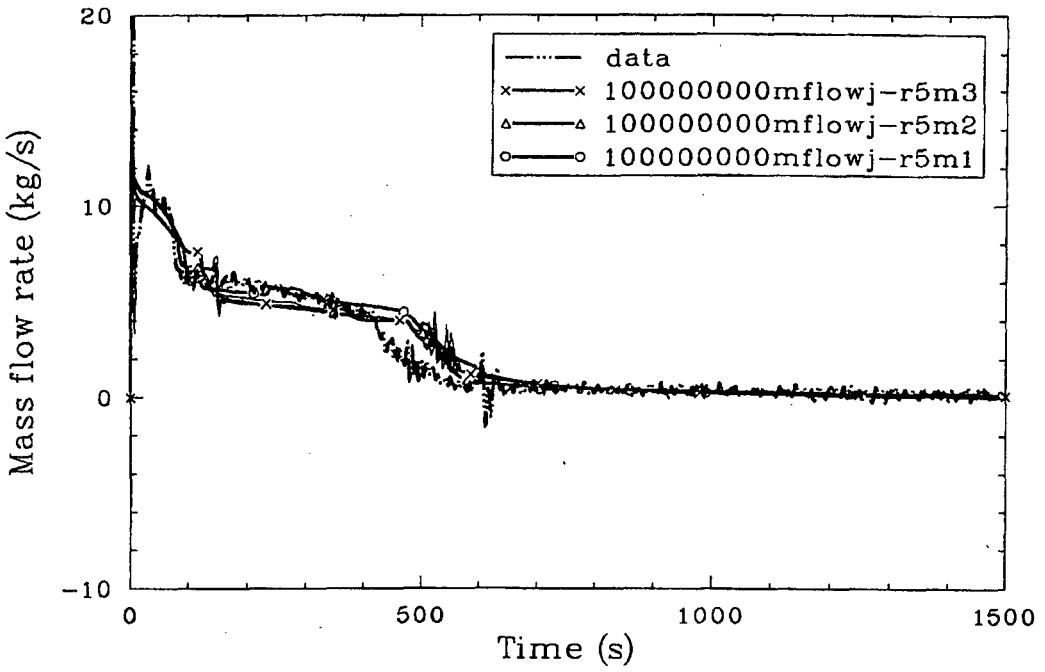

Figure 2.2-2. Measured and calculated (RELAP5/MOD1, MOD2, MOD3) mass flow rate at the break orifice for Wyle Test WSB03R.

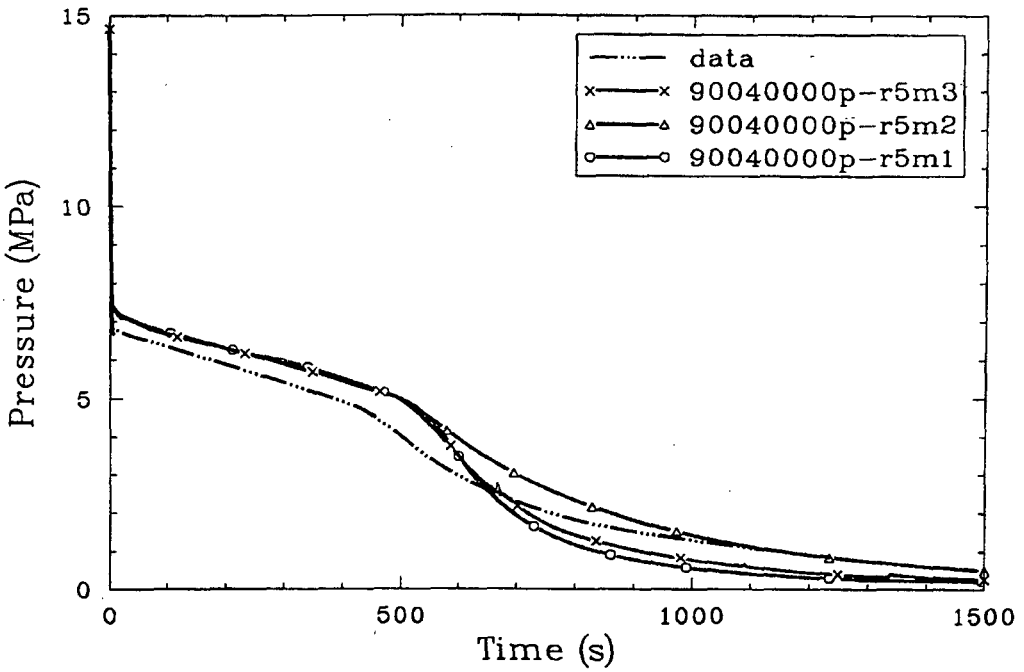

Figure 2.2-3. Measured and calculated (RELAP5/MOD1, MOD2, MOD3) pressure upstream of the break orifice for Wyle Test WSB03R.

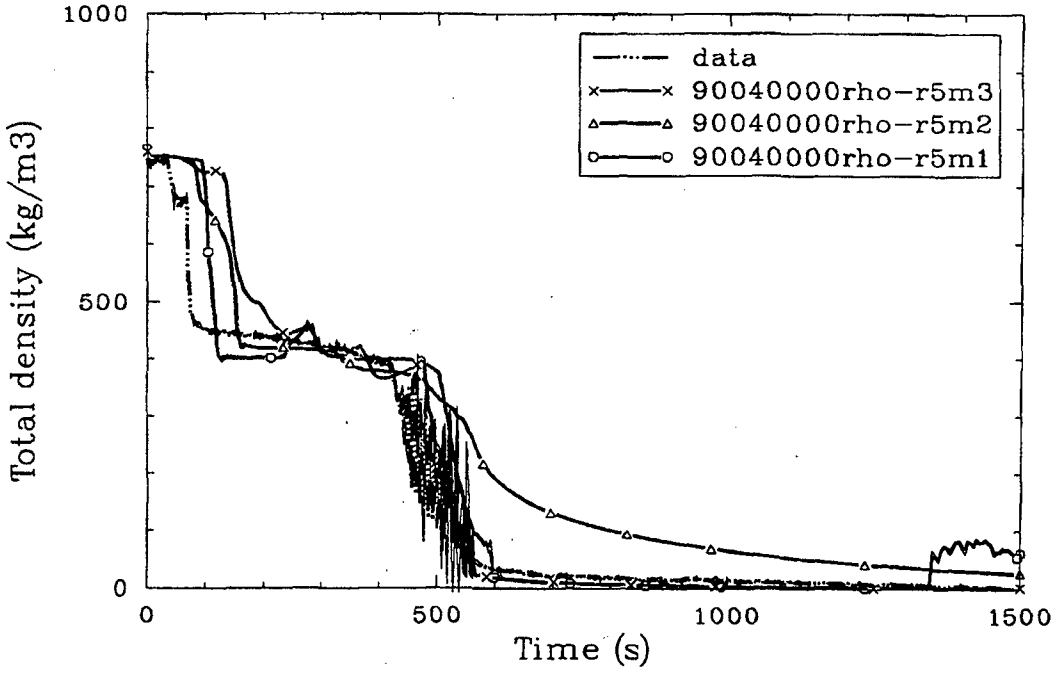

Figure 2.2-4. Measured and calculated (RELAP5/MOD1, MOD2, MOD3) density upstream of the break orifice for Wyle Test WSB03R.

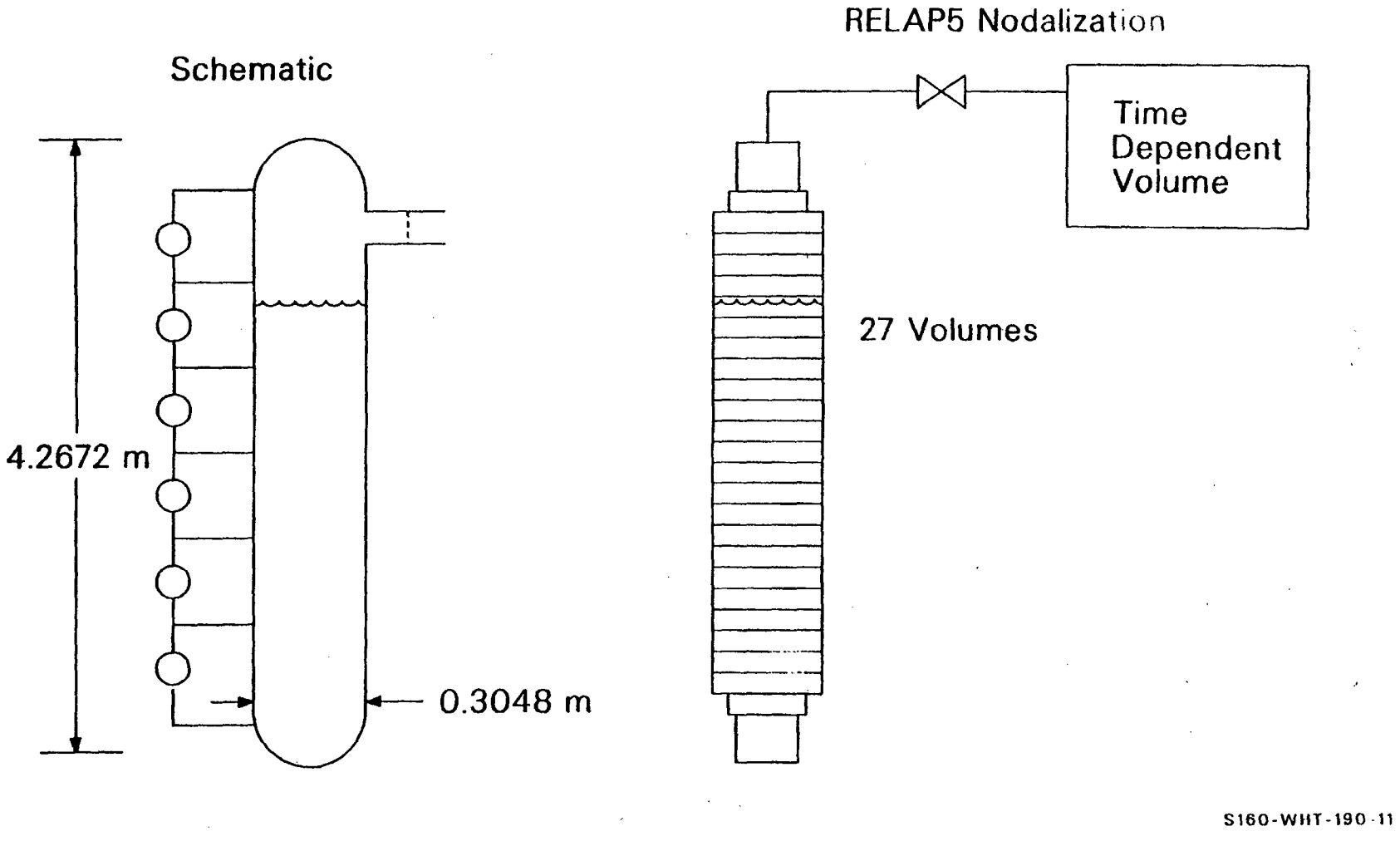

Figure 2.2-5. Schematic and nodalization for GE level swell Test 1004-3.

which initially contains both liquid water and steam at saturation conditions, discharges to the atmosphere through the break orifice [0.009525 m (3/8 in.) I.D.] located within the 0.0508-m (2.2-in.) diameter Schedule 80 blowdown pipe at the top of the vessel. Measurements made during the test transient included system pressure obtained by means of a pressure transducer at the top of the vessel and differential pressure measurements over 0.6096-m (2.2-ft) vertical intervals along the vessel. The differential pressure measurements were converted to mean void fraction at each level by assuming hydrostatic conditions to exist at all times. Further information on the data reduction method can be obtained from Reference 2.2-3.

The RELAP5 model of the One-Foot GE Test Facility is also shown in Figure 2.2-5. The vessel was approximated as a cylinder that had the same height as the vessel. It was modeled using a vertical, 27-volume pipe component. The volumes in the pipe were 0.1524 m (0.5 ft) high, except for the volumes at the top and bottom. These volumes were 0.2286 m (0.75 ft) high in order that the 0.6096-m (2.2-ft) vertical intervals used for the void fraction comparisons would coincide with the volume centers. This nodalization was used for the RELAP5/MOD2 and MOD3 calculations. ForRELAP5/MOD1, 29 volumes were used, with the middle 27 volumes being 0.1524 m (0.5 ft) high and the top and bottom volumes being 0.0762 m (0.25 ft) high.

The orifice in the blowdown pipe was modeled as a trip valve, which was open for times greater than 0.07 s. The abrupt area change option in the code was used to model this orifice. In the MOD3 calculation of this level swell problem, the two-phase and superheated discharge coefficients for the valve were both taken to be 0.65. This value corresponds to that typically reported for orifices.[2.2-4]

The blowdown pipe was not modeled for this simulation, since the discharge orifice is choked throughout the experiment. A time-dependent volume component at atmospheric conditions was connected to the valve to represent the suppression pool at atmospheric conditions.

For MOD3, it was necessary to turn off the vertical stratification and water packing; otherwise, the code ran slower. The time step cards were the same for MOD3 and MOD2 (maximum requested time step of 0.2 s for most of the transient). For MOD1, a maximum requested time step of 0.02 s was required in order to remove void oscillations.)

Comparisons of RELAP5/MOD3, MOD2, and MOD1 predictions and data for pressure and void fraction are shown in Figures 2.2-6 through 2.2-12. Figure 2.2-6 shows the pressure versus time in the top of the vessel, and Figures 2.2-7 and 2.2-8 show the void fraction versus time at 1.83 and 3.65 m (6 and 12 ft) above the bottom of the vessel. Figures 2.2-9 through 2.2-12 show the void fraction versus length in the vessel at 10, 40, 100, and 160 s. The agreement to the data is similar for all three codes. Most of the MOD3 void-fraction-versus-length plots show a void depression before rising to a value of one, whereas the MOD2 plots do not. This is probably due to the removal of the inverted profile logic from MOD3 that was present in MOD2. The void depression is more severe in MOD1, including more oscillations versus length.

The MOD3 calculation was run to 200 s on Version 5i1, using the Cray, and required 1142 attempted advancements and 12.80 cpu seconds. The MOD2 calculation was run to 200 s on Cycle 4, using the Cyber, and required 1142 attempted advancements and 35.94 cpu seconds. The MOD1 calculation was run to 200 s on Cycle 17, using the Cray, with a momentum equation update; it required 10060 attempted advancements and 223 cpu seconds.

2.2.3 Four-Foot General Electric Level Swell Test 5801-15

The GE level swell Test 5801-15[2.2-3] also involves a vertical vessel that is initially pressurized and partially filled with saturated water. In this test, the vessel is considerably larger [1.22.2-m (4 ft) diameter] than that used for Test 1004-3 [0.305 m (1-ft) diameter]; and the test is initiated by opening a simulated break near the bottom of the vessel. As with the 0.305-m (1-ft) vessel, the data from this test are useful for testing the interphase drag formulation.

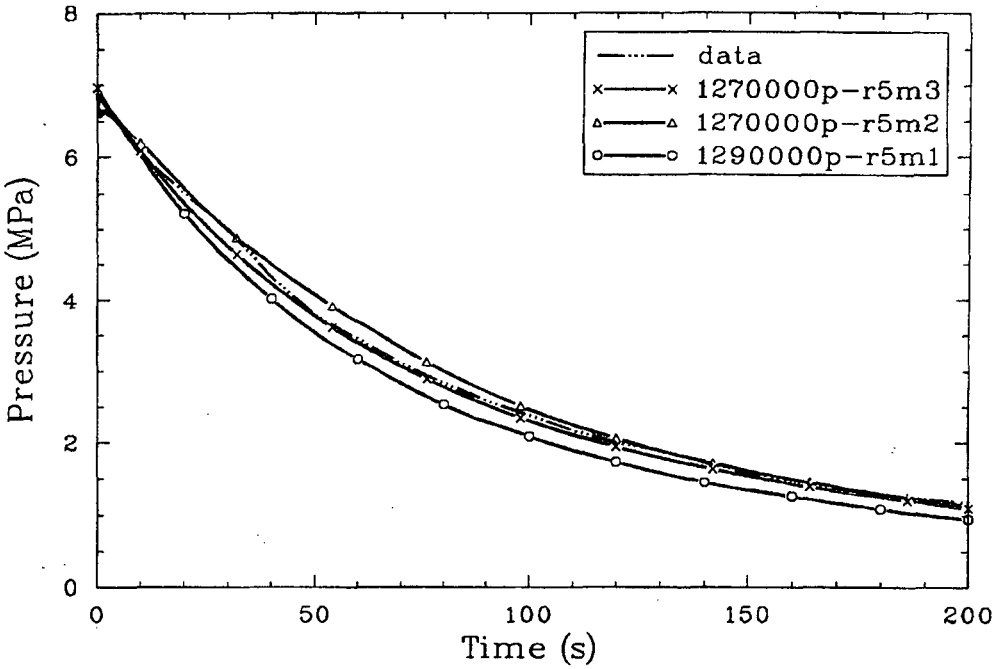

Figure 2.2-6. Measured and calculated (RELAP5/MOD1, MOD2, MOD3) pressure in the top of the vessel for GE level swell Test 1004-3.

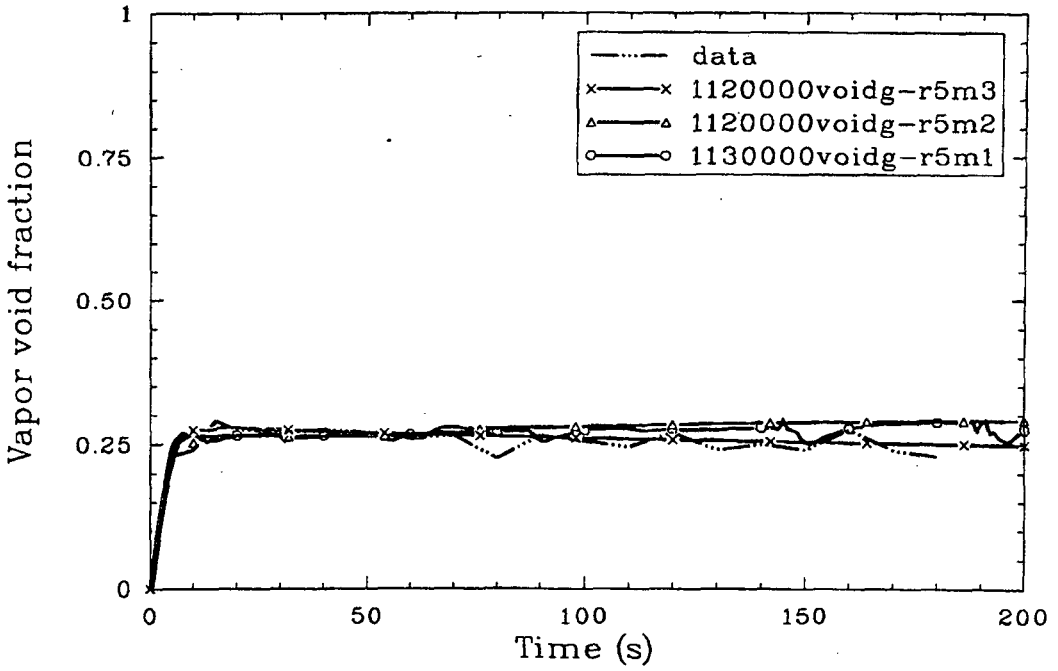

Figure 2.2-7. Measured and calculated (RELAP5/MOD1, MOD2, MOD3) void fraction at 1.83 m (6 ft) above the bottom of the vessel for GE level swell Test 1004-3.

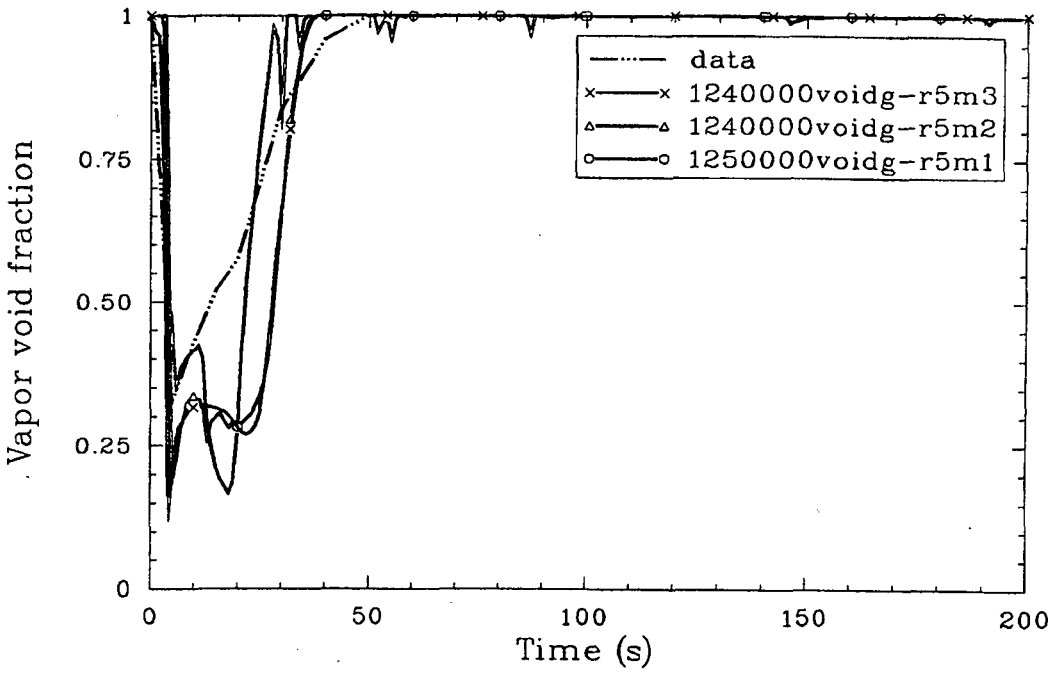

Figure 2.2-8. Measured and calculated (RELAP5/MOD1, MOD2, MOD3) void fraction at 3.66 m (12 ft) above the bottom of the vessel for GE level swell Test 1004-3.

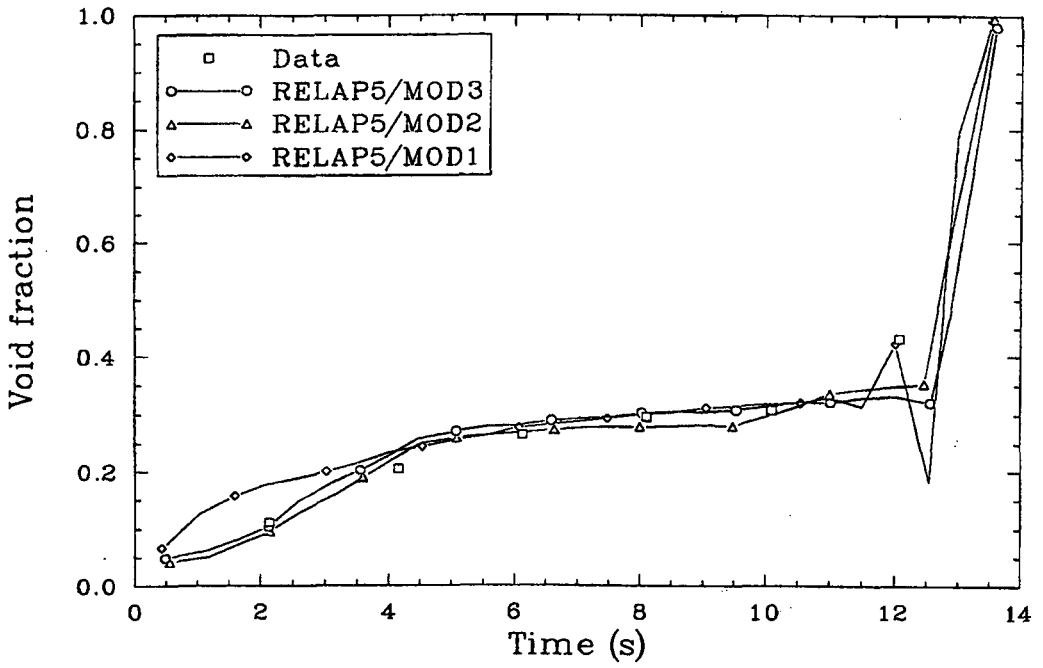

jan-r241

Figure 2.2-9. Measured and calculated (RELAP5/MOD1, MOD2, MOD3) void fraction profile in the vessel at 10 s for GE level swell Test 1004-3.

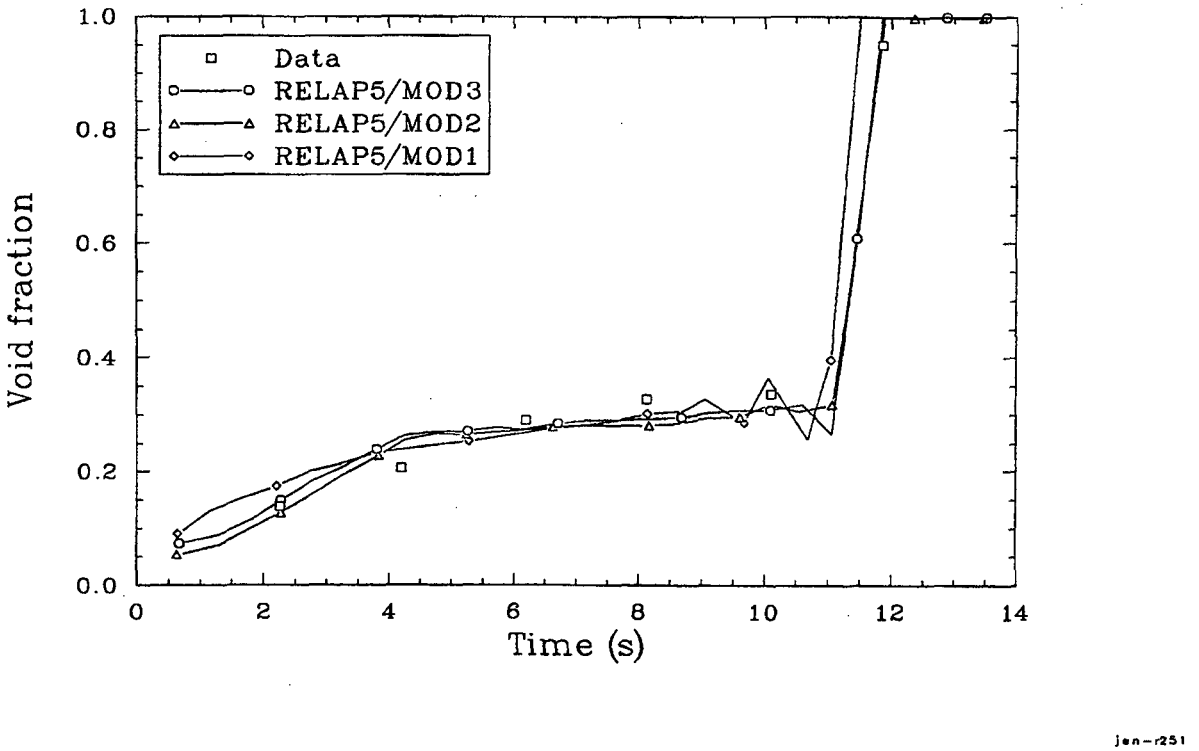

Figure 2.2-10. Measured and calculated (RELAP5/MOD1, MOD2, MOD3) void fraction profile in the vessel at 40 s for GE level swell Test 1004-3.

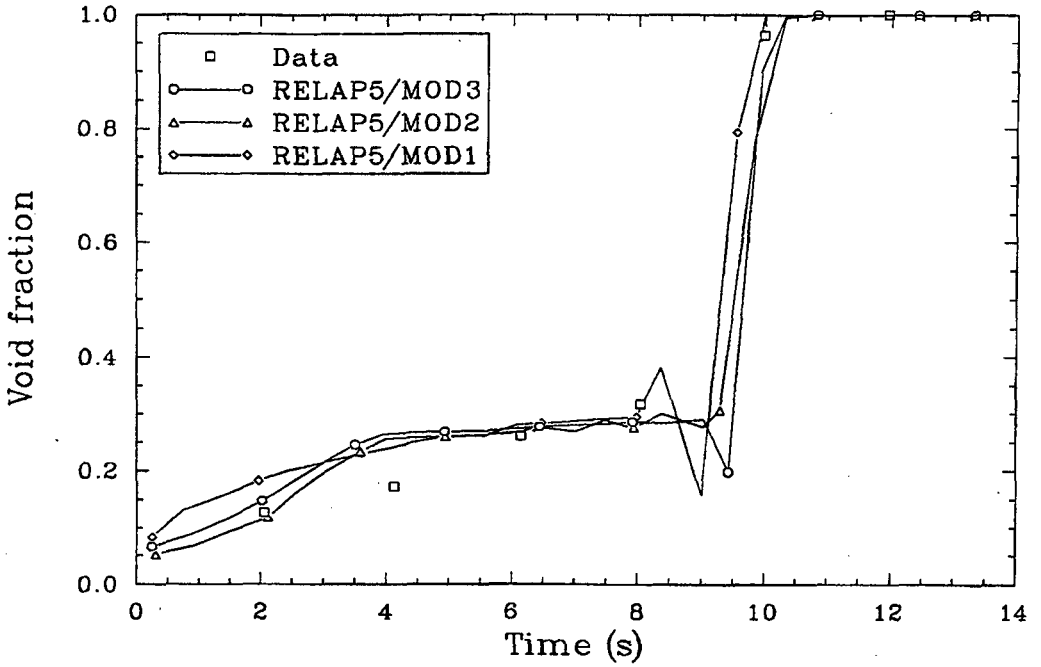

Figure 2.2-11. Measured and calculated (RELAP5/MOD1, MOD2, MOD3) void fraction profile in the vessel at 100 s for GE level swell Test 1004-3.

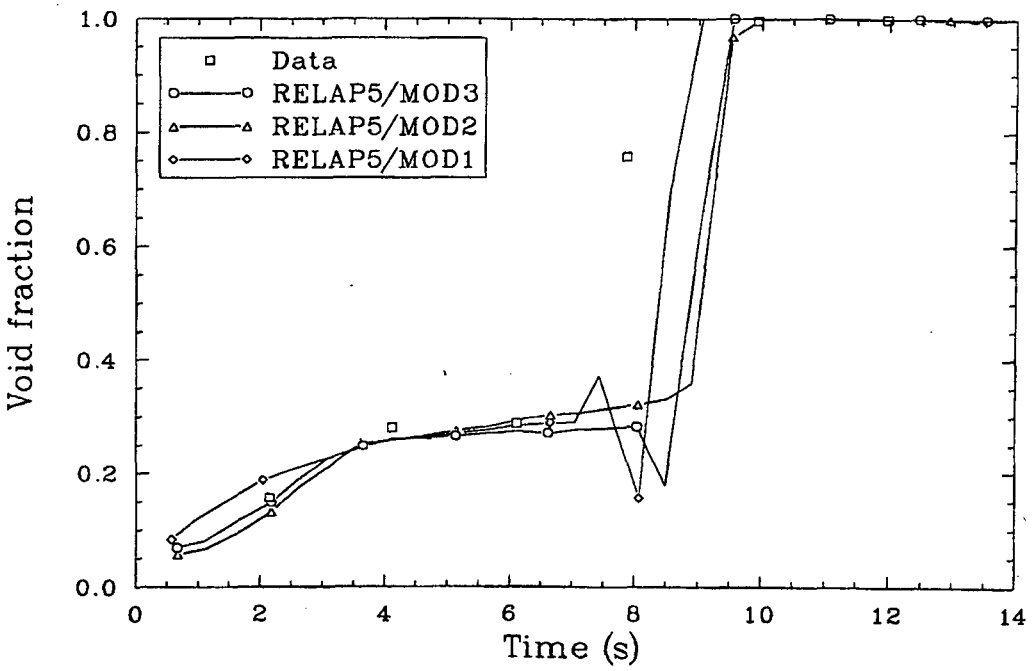

Figure 2.2-12. Measured and calculated (RELAP5/MOD1, MOD2, MOD3) void fraction profile in the vessel at 160 s for GE level swell Test 1004-3.

This pressure vessel was a 4.5-m^3 (160-ft^3) carbon steel vessel, 1.19 m (47 in.) in diameter and 4.3 m (14 ft) long. Figure 2.2-13 is a schematic drawing showing the vessel, the blowdown line, and the instrumentation locations. Both top and bottom break blowdown tests were conducted in this vessel. The blowdown flow rate and depressurization rate were varied by mounting different sized flow-limiting venturi nozzles in the horizontal portion of the blowdown line. Rupture discs were used to initiate the blowdown. Test 5801-15 is a top blowdown test. Test procedures and measurements were similar to those discussed in the previous section.

The RELAP5 model of the Four-Foot GE Test Facility is shown in Figure 2.2-14. The vessel was modeled using a 6-volume pipe, a branch, and a 20-volume pipe. From the branch, a 4-volume pipe was used to model the vertical dip tube and a 2.2-volume pipe was used to model the first part of the blowdown line. For MOD3, it was necessary to turn off vertical stratification and water packing; otherwise, the code ran slower.

Comparisons of RELAP5/MOD3 and MOD2 to pressure and void fraction measurements are shown in Figures 2.2-15 through 2.2-19. Figure 2.2-15 shows the pressure versus time in the top of the vessel, and Figures 2.2-16 through 2.2-19 show the void fraction versus length in the vessel at times 2, 5, 10, and 20 s. The pressure agrees fairly well, with the dip in pressure at the beginning being reproduced. The MOD3 pressure, however, is lower than the data and MOD2 at the end. The void fraction plots don't agree as well with the data as they do in the small vessel comparisons, although MOD3 is smoother than MOD2. The void fraction data are obtained from Δp measurements. The interpretation of Δp as indicative of void fraction is based on the assumption of quasi-steady conditions, which is inaccurate for a fast blowdown due to inertial effects. Unfortunately, the raw Δp data are not available from the report. If these data were available, more direct comparisons could be made. Since the 1.22.2-m (4-ft) vessel experiment is a fast blowdown, this may be a possible explanation.

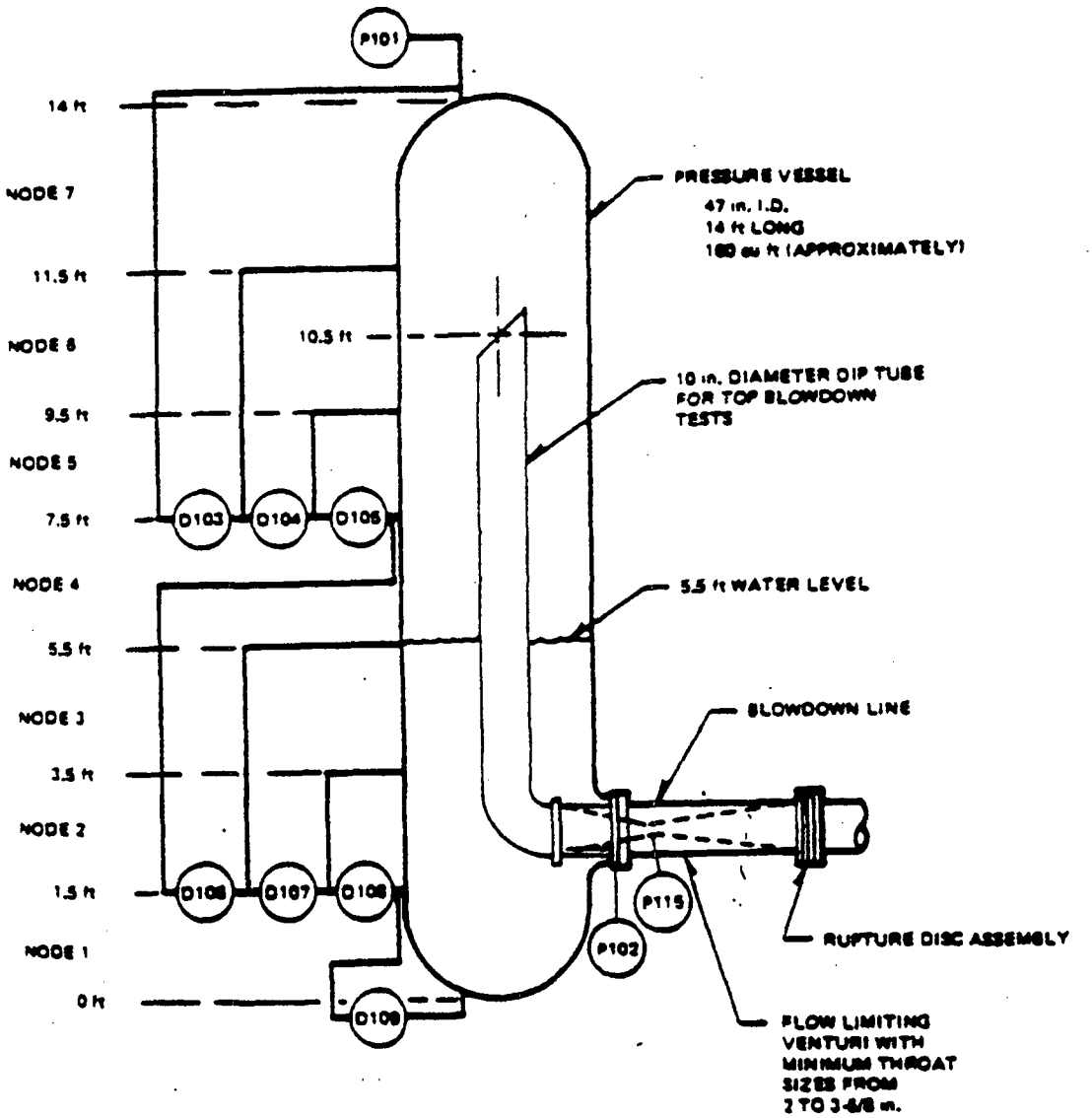

Figure 2.2-13. Schematic for GE level swell Test 5801-15.

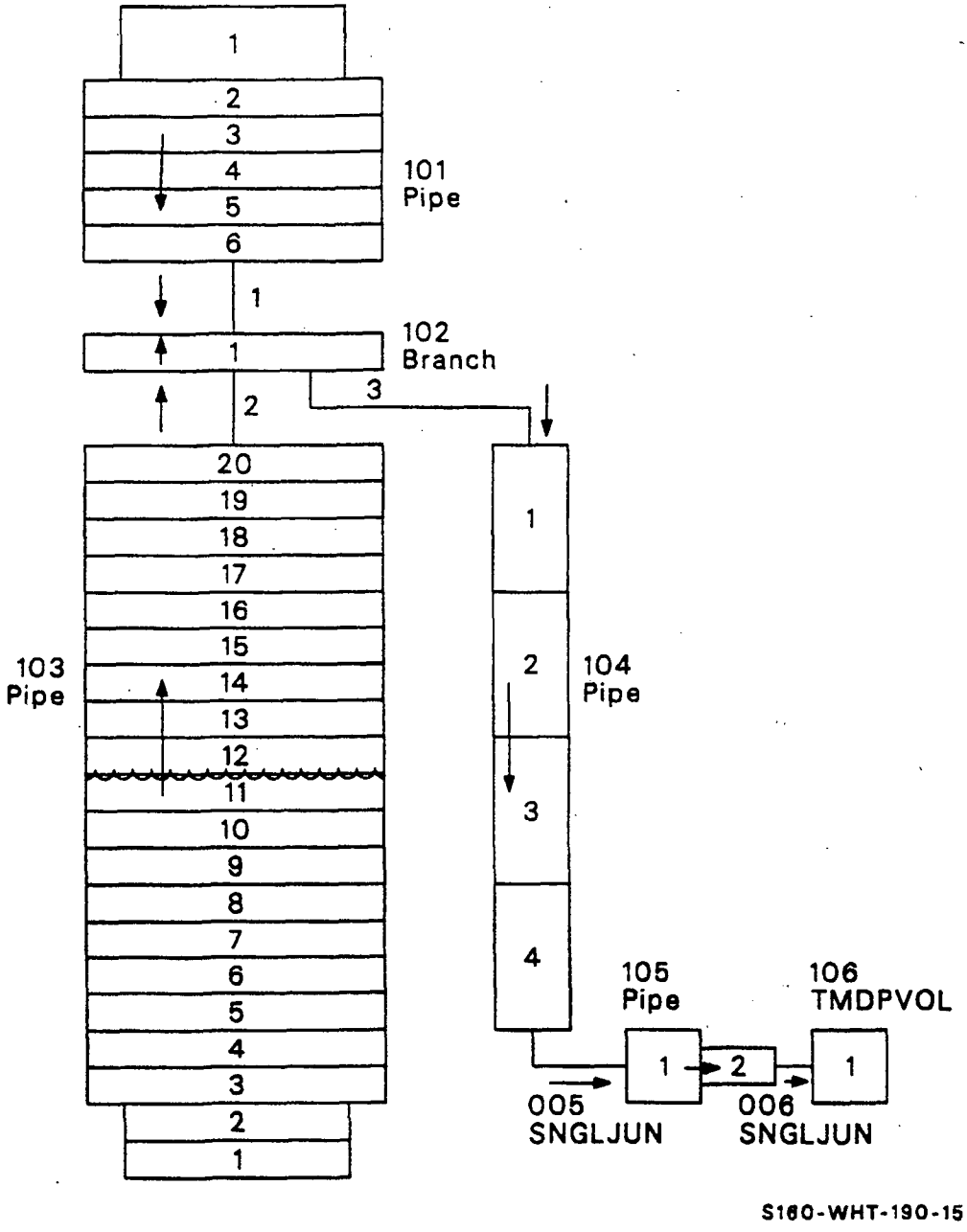

Figure 2.2-14. Nodalization for GE level swell Test 5801-15.

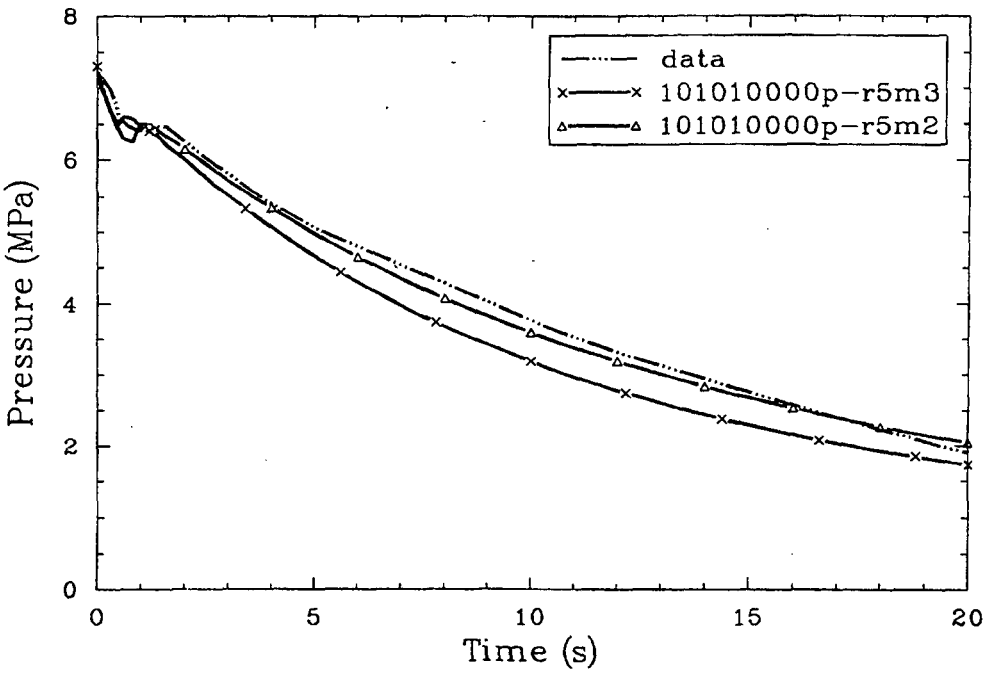

Figure 2.2-15. Measured and calculated (RELAP5/MOD1, MOD2, MOD3) pressure in the top of the vessel for GE level swell Test 5801-15.

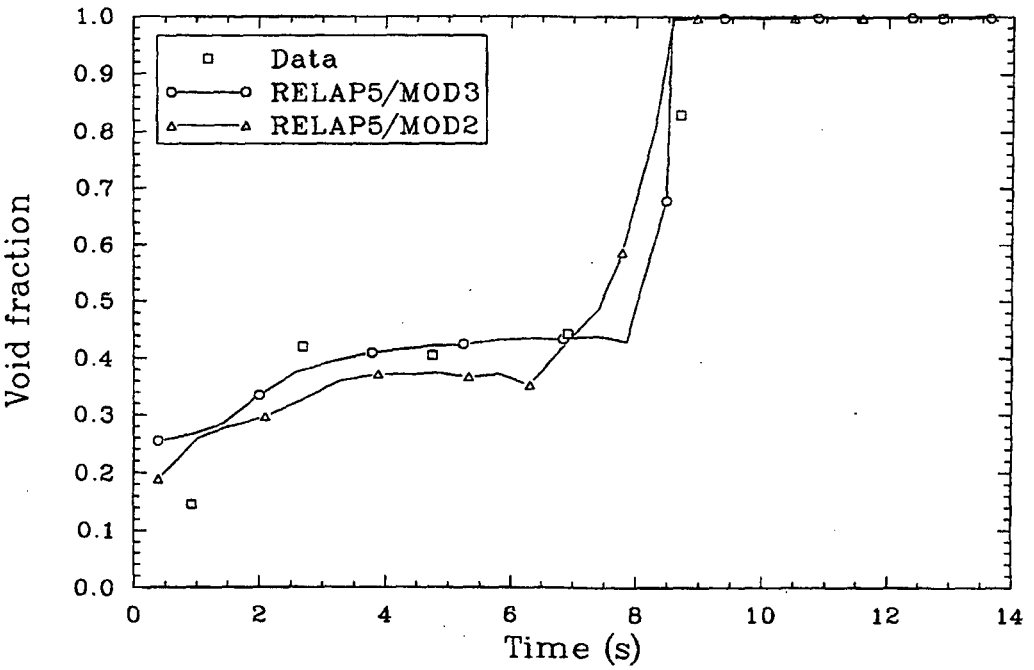

jan-r281

Figure 2.2-16. Measured and calculated (RELAP5/MOD1, MOD2, MOD3) void fraction profile in the vessel at 2 s for GE level swell Test 5801-15.

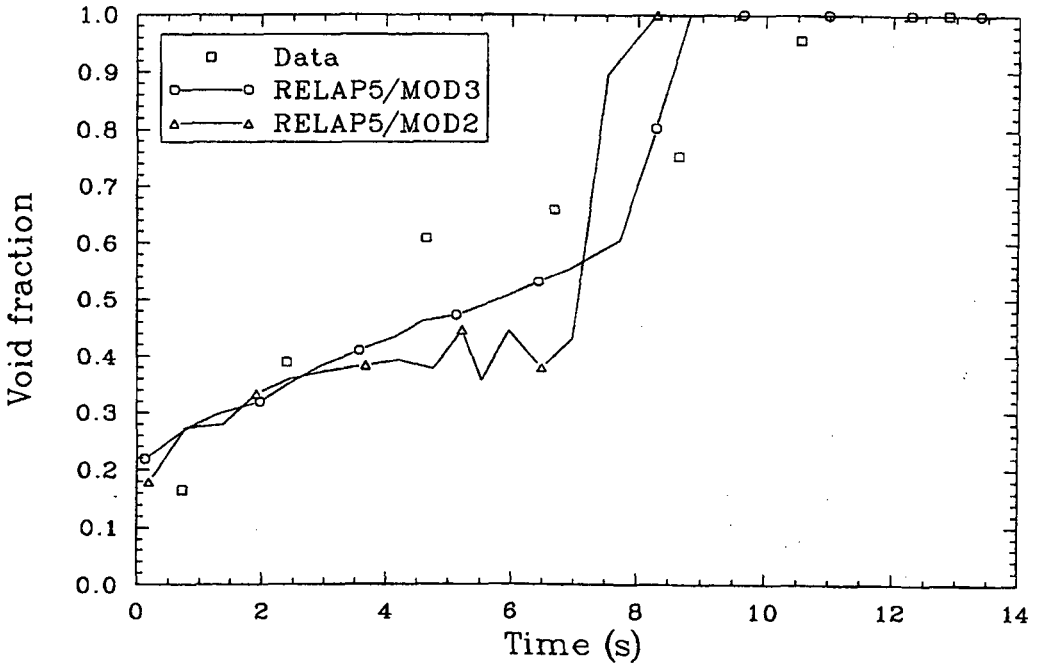

jan-r291

Figure 2.2-17. Measured and calculated (RELAP5/MOD1, MOD2, MOD3) void fraction profile in the vessel at 5 s for GE level swell Test 5801-15.

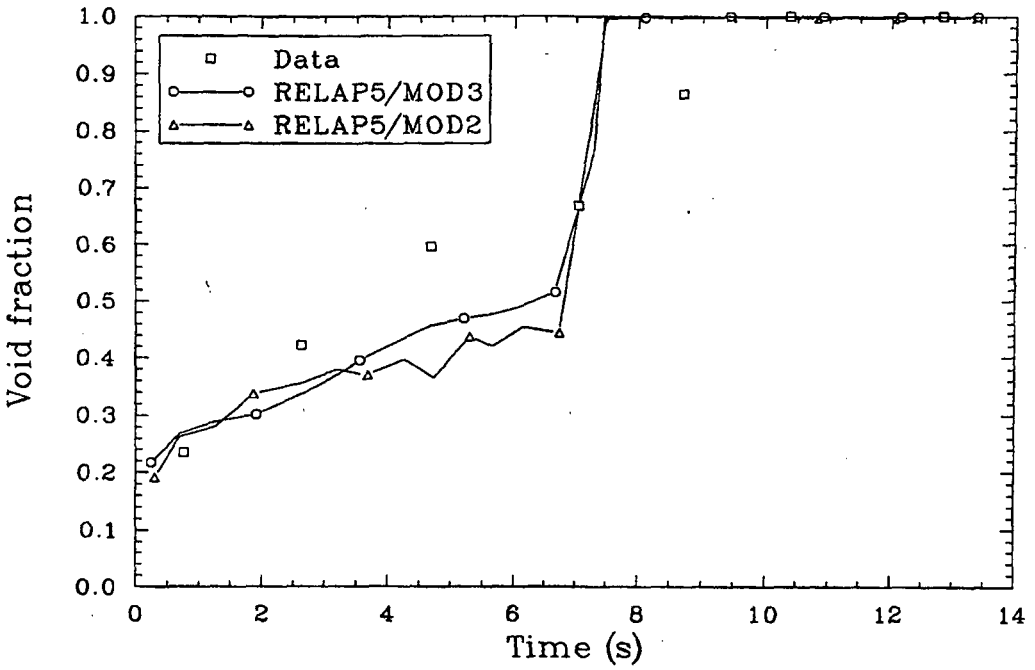

Figure 2.2-18. Measured and calculated (RELAP5/MOD1, MOD2, MOD3) void fraction profile in the vessel at 10 s for GE level swell Test 5801-15.

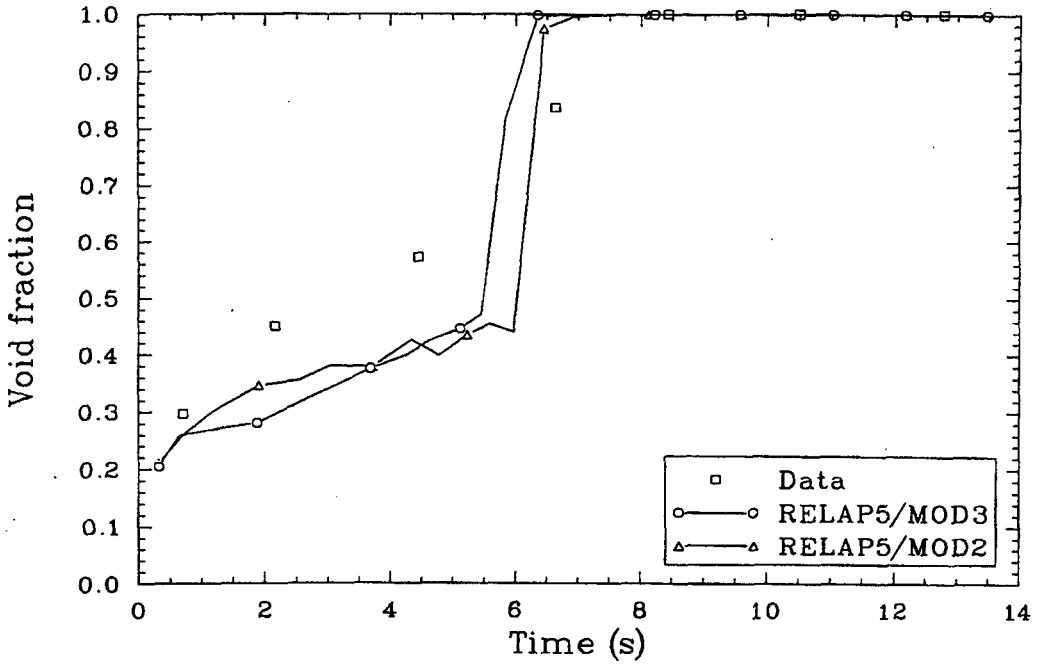

jan-r311

Figure 2.2-19. Measured and calculated (RELAP5/MOD1, MOD2, MOD3) void fraction profile in the vessel at 20 s for GE level swell Test 5801-15.

The MOD3 calculation was run to 20 s on Version 5il, using the Cray, and required 2380 attempted advancements and 38.23 cpu seconds. The MOD2 calculation was run to 20 s on Cycle 4, using the Cyber, and required 1614 attempted advancements and 59.89 cpu seconds.

2.2.4 Dukler Air-Water Flooding Tests

Dukler and Smith[2.2-5] conducted a simple flooding experiment at the University of Houston to study the interaction between a falling liquid film with an upflowing gas core. A sketch of their test loop is shown in Figure 2.2-20. The flow system consisted of a 1.52.2-m (5-ft) length of 0.05-m (2.2-in.) I.D. plexiglass pipe used as a calming section for the incoming air, a 0.305-m (1-ft) I.D. section of plexiglass pipe for both introducing the air to the test section and removing the falling liquid film, a 3.96-m (13-ft) test section consisting of 0.05-m (2.2-in.) plexiglass pipe, and an exit section for removing the air, entrainment, and the liquid film flowing up. Measurements of the pertinent flow rates, pressure gradients, and the liquid film thickness over a wide range of gas and liquid flow rates in the flooding region were taken. The liquid film upflow, downflow, and entrainment rates were determined by weighing the liquid flow for a fixed period of time (see discharge lines to weigh tanks labeled B in Figure 2.2-20). Most of the instantaneous measured parameters were oscillations once quasi-steady state conditions were met, and it was necessary to time-average these parameters. Dukler and Smith indicate that the countercurrent flow limiting (CCFL) process is basically an unstable process that is driving the oscillations.

Of particular interest is the CCFL phenomenon. The experiment was modeled using the nodalization shown in Figure 2.2-21. The equal velocity option was used at junction 10103 to prevent liquid from flowing down the bottom pipe. The drain of falling liquid film through junction 10102 was accomplished by setting appropriate form loss factors for junction 10102 and an appropriate pressure for time-dependent volume 200. A large number of steady-state runs were carried out for a variety of liquid and air injection rates. These runs correspond to all four liquid injection rates and every

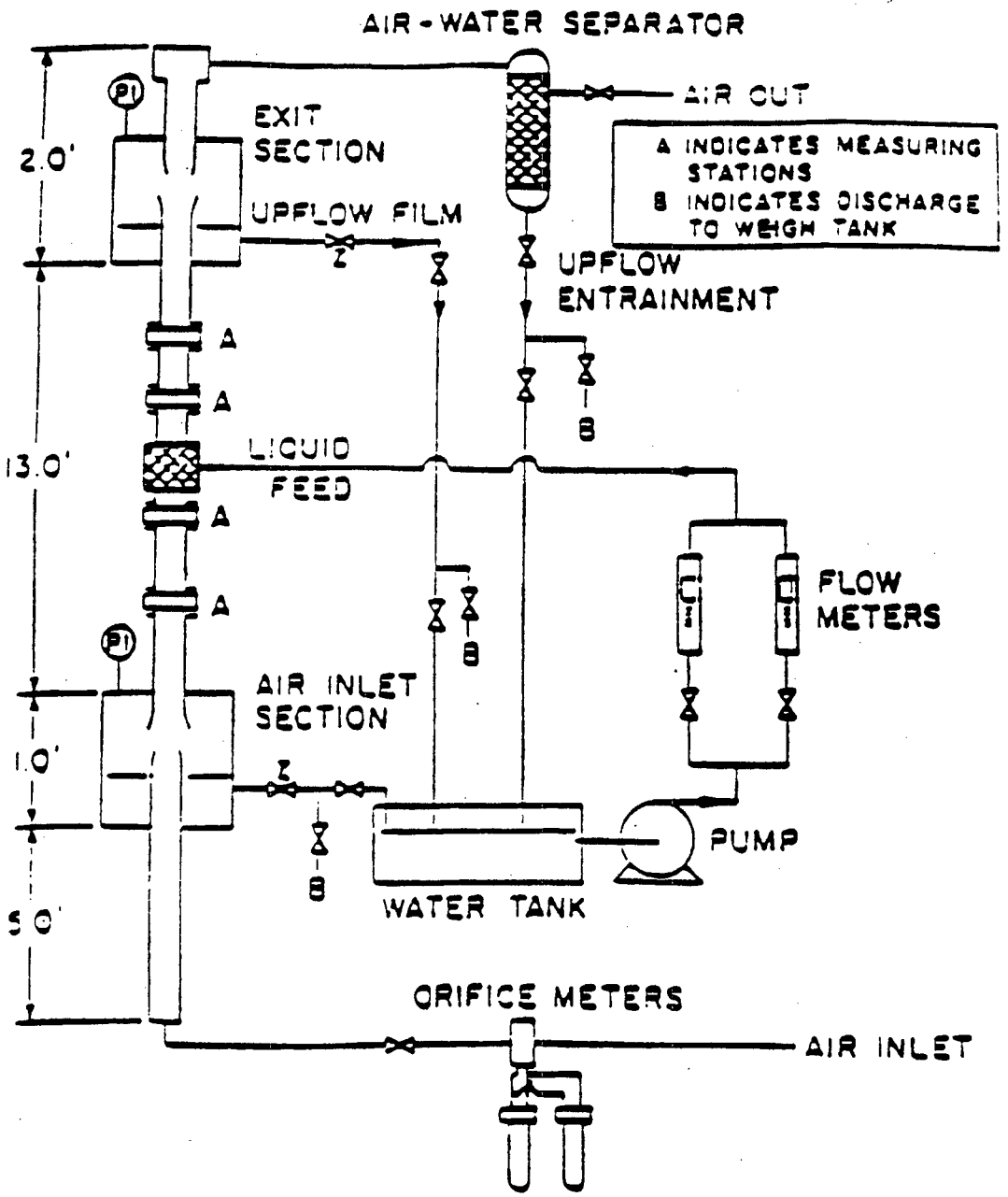

Figure 2.2-20. Flooding/upflow test loop schematic diagram.

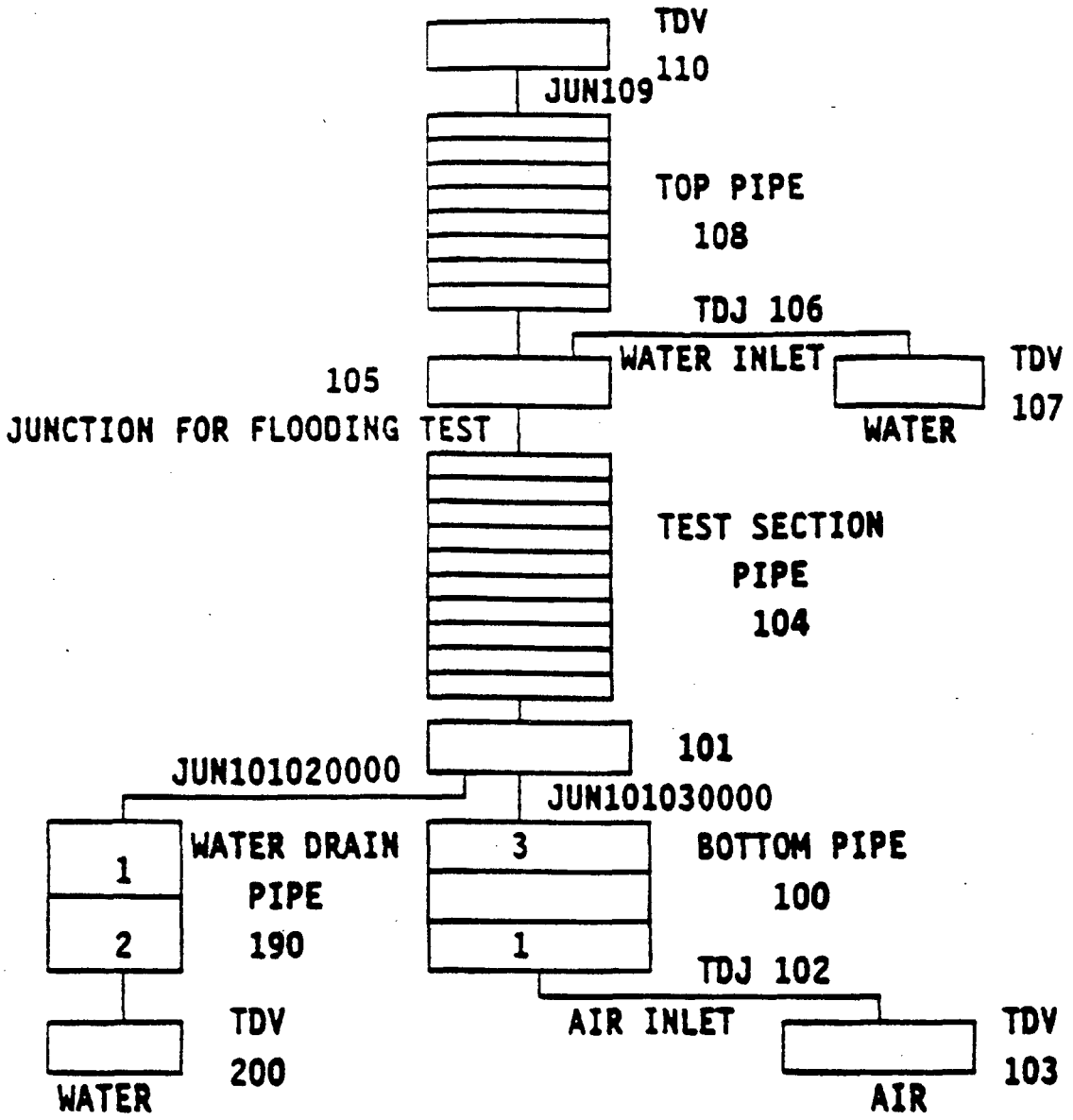

Figure 2.2-21. Nodalization for Dukler's air-water test problem.

third air injection rate. Using every third rate was done to reduce computer costs.

Figures 2.2-22 and 2.2-23 show the calculated instantaneous liquid downflow rate at junction 101020000 and the pressure in volume 104020000 for injection rates of 250 lb/h of air and 100 lb/h of liquid. As with the experiments, the results are oscillatory. Because of the oscillating nature of the results, and following the experimental method, an average liquid downflow rate was calculated using an integral controller component from 70 to 100 s on the instantaneous liquid downflow rate to obtain the mass, and then dividing by 30 s to find the average. The data and RELAP5/MOD3 calculation (without using the CCFL correlation flag) of the average liquid downflow rate are shown in Figures 2.2-24 and 2.2-25. For most of the cases, the liquid downflow is much higher than the data.

A second set of calculations were carried out with the junction between components 105 and 104 flagged as a CCFL junction and a CCFL input data card used for this junction. Dukler discussed more than one CCFL correlation, but the one that appeared to be best for his test is a Wallis form of the correlation ($\beta = 0$), with a constant m = 1 and c = 0.88. Thus, the form of Equation (???) in Volume I of this manual is

$$H_g^{1/2} + H_f^{1/2} = 0.88 \quad . \tag{2.2-1}$$

This correlation was found to be reasonable for air/water systems where standing waves appeared on the surface of the liquid film. Dukler found this to occur in his experiment. Using these on the CCFL input data card along with $D_j = 2(A_j/\pi)^{1/2}$ (where A_j is the pipe area), the steady-state calculations were rerun. The results are shown in Figure 2.2-26, which indicates that calculated liquid downflow rates are quite close to the data.

The MOD3 calculations (40 total runs, 20 without the CCFL flag on and 20 with) were run to 100 s on Version 4b1, using the Masscomp, and required

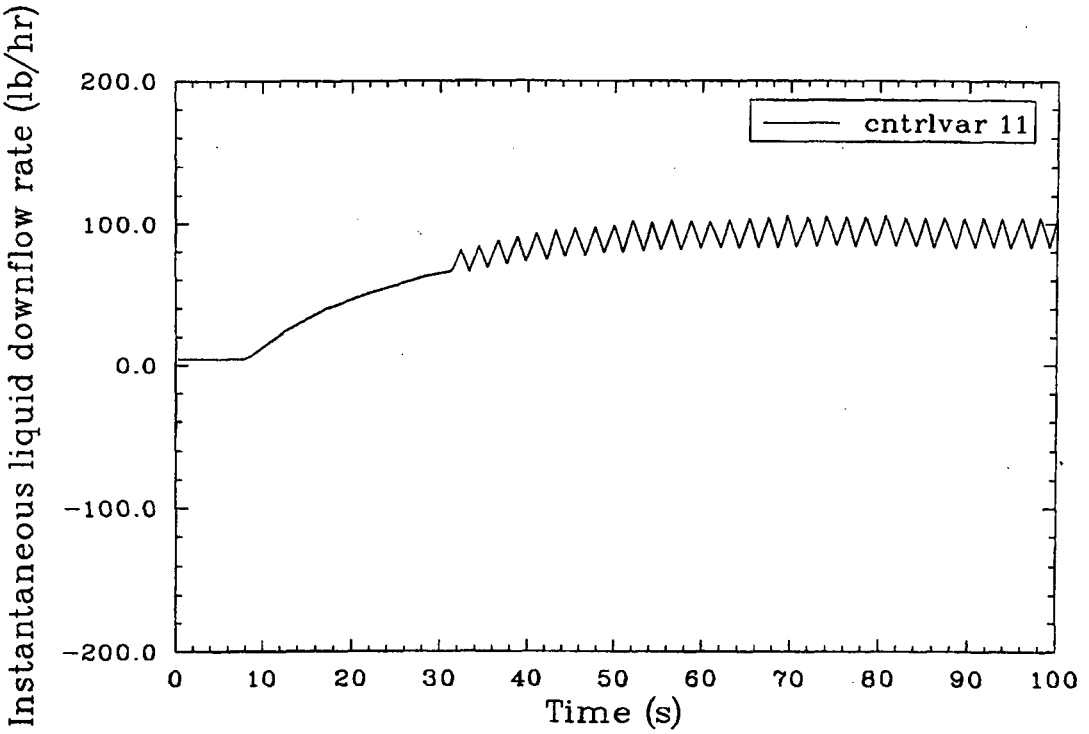

Figure 2.2-22. RELAP5/MOD3 calculation of instantaneous liquid downflow rate in junction 101020000 for Dukler's air-water problem (air injection rate = 250 lb/h; liquid injection rate = 100 lb/h).

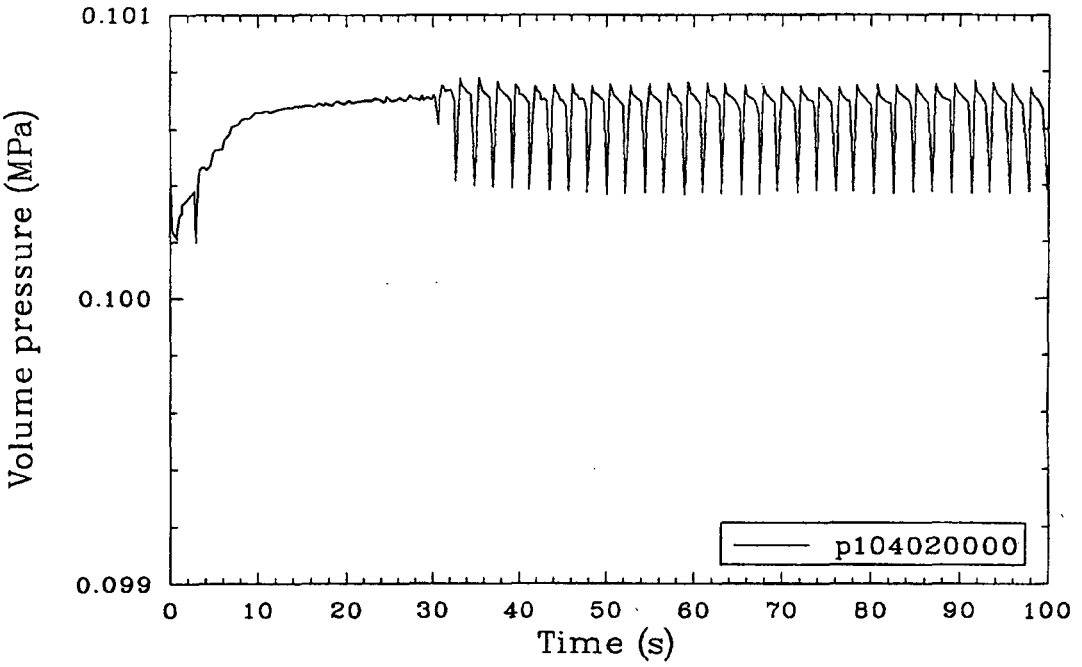

Figure 2.2-23. RELAP5/MOD3 calculation of instantaneous pressure in volume 104020000 for Dukler's air-water problem (air injection rate = 250 lb/h; liquid injection rate = 100 lb/h).

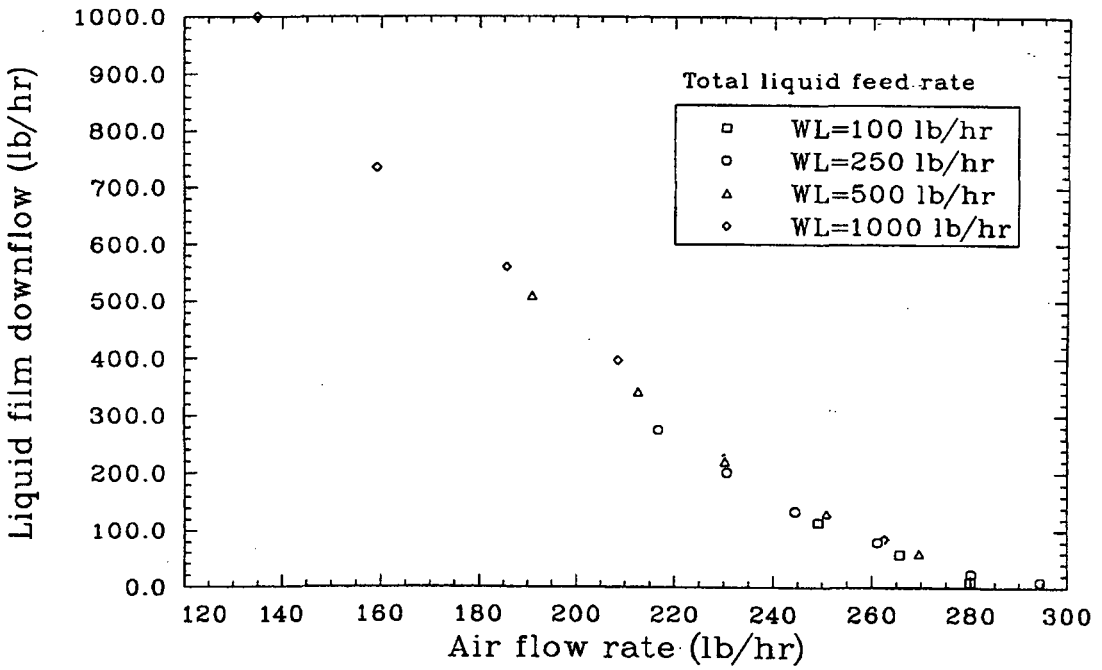

Figure 2.2-24. Data for liquid downflow rate for Dukler's air-water problem.

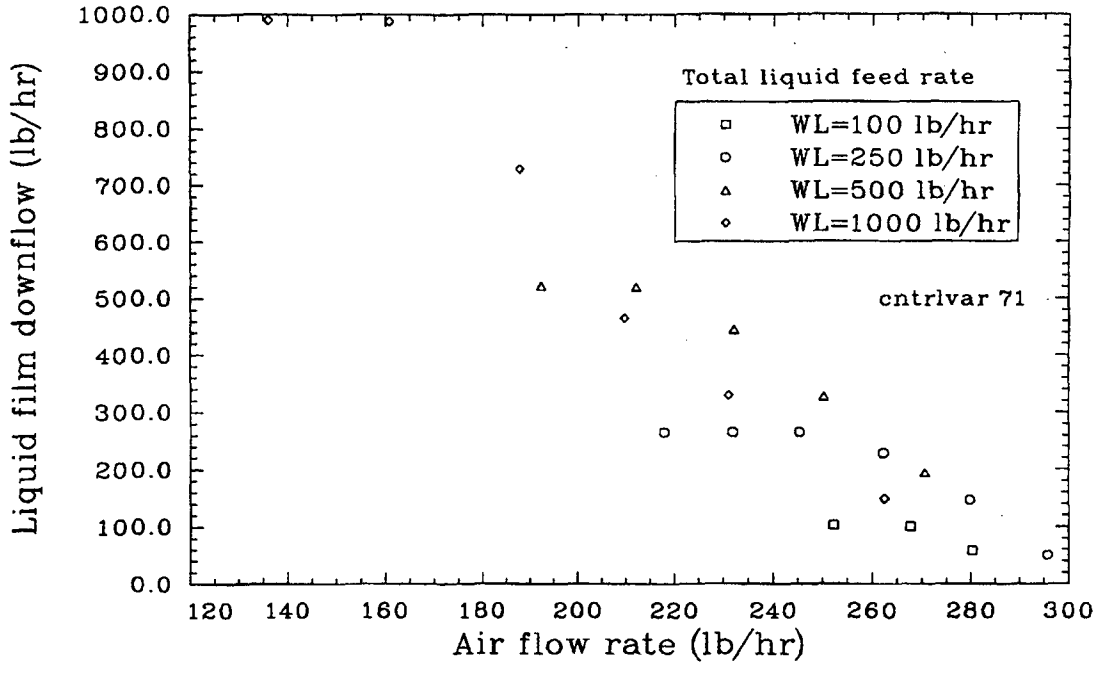

Figure 2.2-25. RELAP5/MOD3 calculation without using the CCFL correlation flag for liquid downflow rate for Dukler's air-water problem.

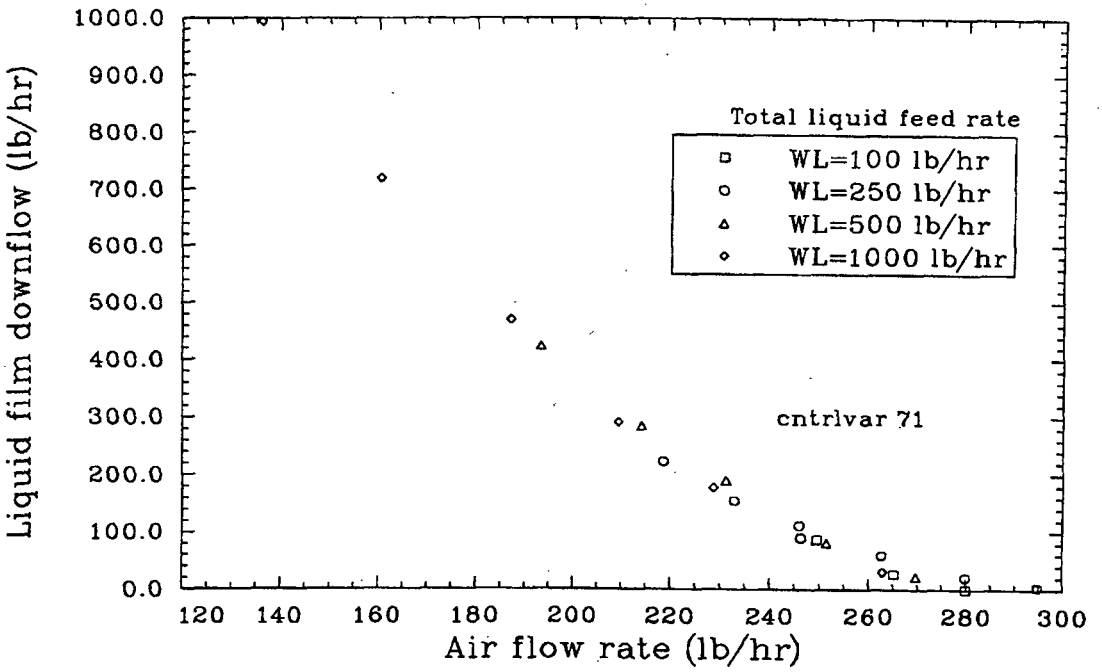

Figure 2.2-26. RELAP5/MOD3 calculation using the CCFL correlation flag for liquid downflow rate for Dukler's air-water problem.

a range of 4096 to 12147 attempted advancements and a range of 6081 to 17955 cpu seconds.

2.2.5 Marviken Test 24

Marviken III Test 24, a full-scale critical flow test, was selected to check out and evaluate the RELAP5 choked flow model. Because of the short nozzle design (L/D = 0.33) and the long duration (about 20 s) of subcooling at the break, the test is particularly well-suited for establishing the applicability of the RELAP5 subcooled choking criterion, which is based on the Alamgir-Lienhard-Jones subcooled nucleation correlation.[2.2-4]

Marviken III Test 24 is the twenty-fourth test in a series of full-scale critical flow tests performed as a multi-national project at the Marviken Power Station in Sweden.[2.2-6] The test equipment consisted of four major components: a pressure vessel, a discharge pipe, a test nozzle, and a rupture disc assembly.

The pressure vessel was originally a part of the Marviken nuclear power plant. Of the original vessel internals, only the peripheral part of the core superstructure, the cylindrical wall, and the bottom of the moderator tank remained. Gratings were installed at three levels in the lower part of the vessel to prevent the formation of vortices that might enter the discharge pipe. The vessel had an inside diameter of 5.22 m and was 24.55 m high as measured from the vessel bottom to the top of the top-cupola. The net available internal volume was 420 m^3.

The discharge pipe consisted of seven elements, including an axisymmetric inlet section, a connection piece, two pipe stools, two instrumentation rings, and an isolation ball valve. The internal diameters of the connection piece, pipe stools, and instrumentation rings were all 752 mm. The flow path through the ball valve contained fairly abrupt diameter changes of 30 mm. The axial distance from the discharge pipe entrance to the end of the discharge pipe (nozzle entrance) was 6.3 m.

The test nozzle was connected to the lower end of the discharge pipe. The nozzle consisted of a rounded entrance section, followed by a test section 500 mm in diameter, with a length-to-diameter ratio (L/D) of 0.33 for Test 24.

A rupture disc assembly was attached to the downstream end of the test nozzle. The assembly contained two identical rupture discs, and the test was initiated by overpressurizing the volume between the discs. This overpressure caused the outer disc to fail, which subsequently resulted in the failure of the inner disc. Failure of the discs was designed to occur along the entire periphery so that they were completely removed from the nozzle exit.

A schematic of the pressure vessel and discharge pipe is shown in Figure 2.2-27 (see Reference 2.2-6 for detailed drawings). The initial water level in the vessel was at an elevation of 16.7 m above the discharge pipe inlet. A warmup process was then applied to produce a temperature profile, also shown in Figure 2.2-27. From the top of the vessel down, the fluid conditions were as follows: a steam dome (above 19.88 m) saturated at 4.96 MPa, a saturated liquid region extended for about 2 m, and a transition region where the temperature dropped rapidly down to 504 K at the discharge pipe inlet. The fluid at the bottom of the vessel was about 32 K subcooled relative to the steam dome temperature. The test was initiated at the above fluid conditions by releasing the rupture disc. The ball valve started to close after 55 s and was fully closed at 65 s.

A sketch of the RELAP5 nodalization is shown in Figure 2.2-27. The vessel was represented by 39 volumes and was subdivided from the top as follows: one volume for the top-cupola, one volume for the steam dome, one volume for the two-phase interface region, 36 volumes of equal length (0.5 m) for the main portion of the vessel, and one volume for the bottom of the vessel, which takes into account the standpipe entrance. All junctions in the vessel were modeled using the smooth option. The discharge pipe was modeled by six volumes. The third and fifth junctions of the discharge pipe were modeled abrupt, while the rest were modeled smooth. The nozzle was

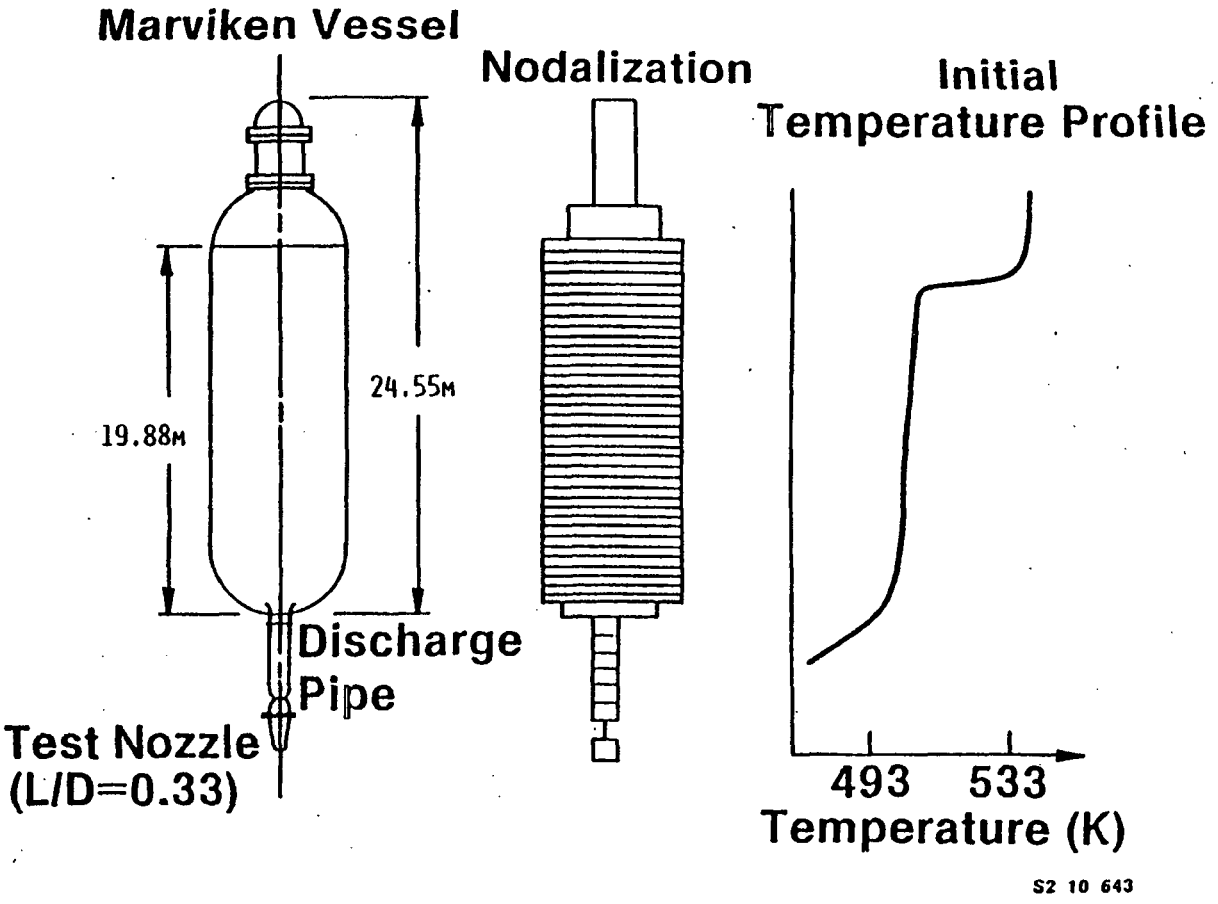

Figure 2.2-27. Schematic, nodalization, and initial temperature profile for Marviken Test 24.

modeled as a single junction with a smooth area change, and no special nodalization was used in the nozzle region. This was possible because RELAP5 includes an analytical choking criterion, which is applied at the throat of the nozzle. The time-step control cards used 0.05 s as the user-inputted maximum time step from 0 to 5 s, and 0.25 s for the remainder of the run. The small time step in the early part was used to force the code to follow the rapid acceleration phenomena in the first part of the test.

A comparison of RELAP5/MOD3 prediction to the pressure measurement in the top of the vessel is shown in Figure 2.2-28. The comparison is comparable to that obtained with RELAP5/MOD2. Figure 2.2-29 shows a comparison of RELAP5/MOD3 to the density measurement in the middle of the discharge pipe. The code calculation is lower than the data, and the result is similar to that obtained with RELAP5/MOD2. Finally, Figure 2.2-30 shows a comparison of RELAP5/MOD3 to the mass flow rate measurement at the nozzle. The result is similar to that predicted by RELAP5/MOD2, and again the calculation is below the data in the last part of the test.

The mass flow rate shown in Figure 2.2-30 in the two-phase portion of the test lies slightly below the mass flow rate computed by RELAP5/MOD2 during the same portion of this test. The decrease is due to the change in the interfacial friction model for large-diameter pipes, which results in a higher slip ratio in RELAP5/MOD3 relative to MOD2 for the same set of fluid conditions. The slip ratio implied by the interfacial friction model is used to unfold the phasic velocities from the choking condition, and a higher slip ratio reults in a lower liquid velocity and a higher vapor velocity. Since the void fraction at the choking plane remains relatively low (less than 30%) throughout the test, the lower liquid velocity computed by RELAP5/MOD3 results in a slightly lower discharge flow rate. The results of this assessment demonstrate that changes to one code model (i.e., the interfacial friction model) can affect the performance of another, completely separate model (i.e., the critical flow model).

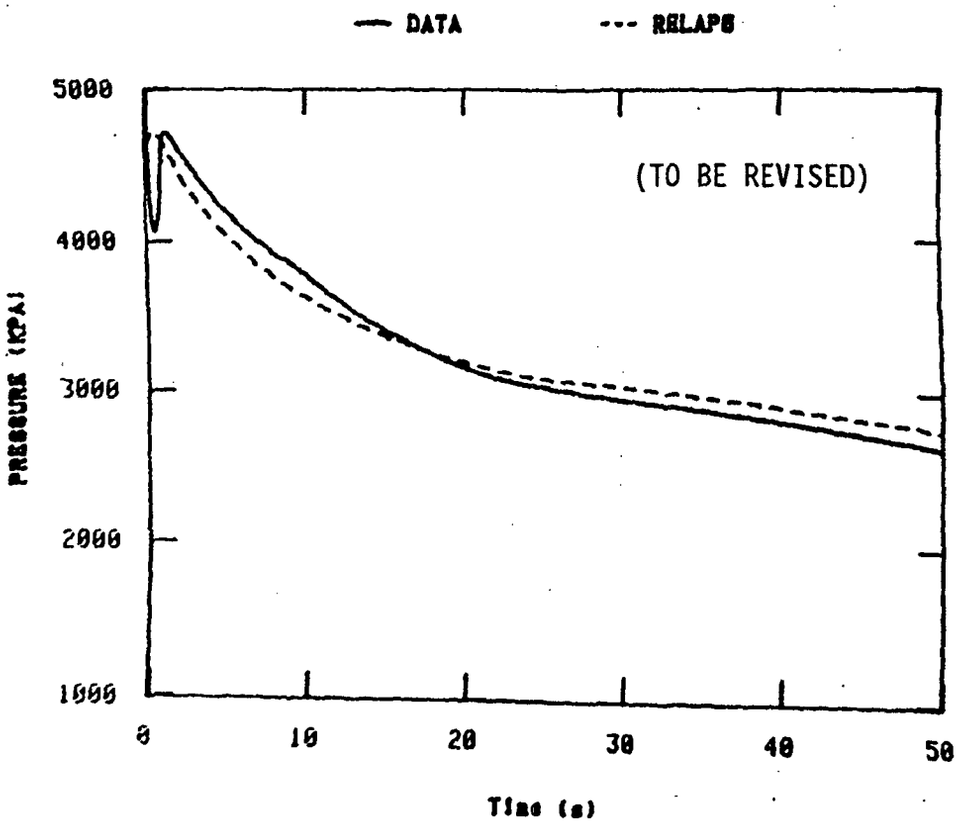

Figure 2.2-28. Measured and calculated (RELAP5/MOD2, MOD3) pressure in the top of the vessel for Marviken Test 24.

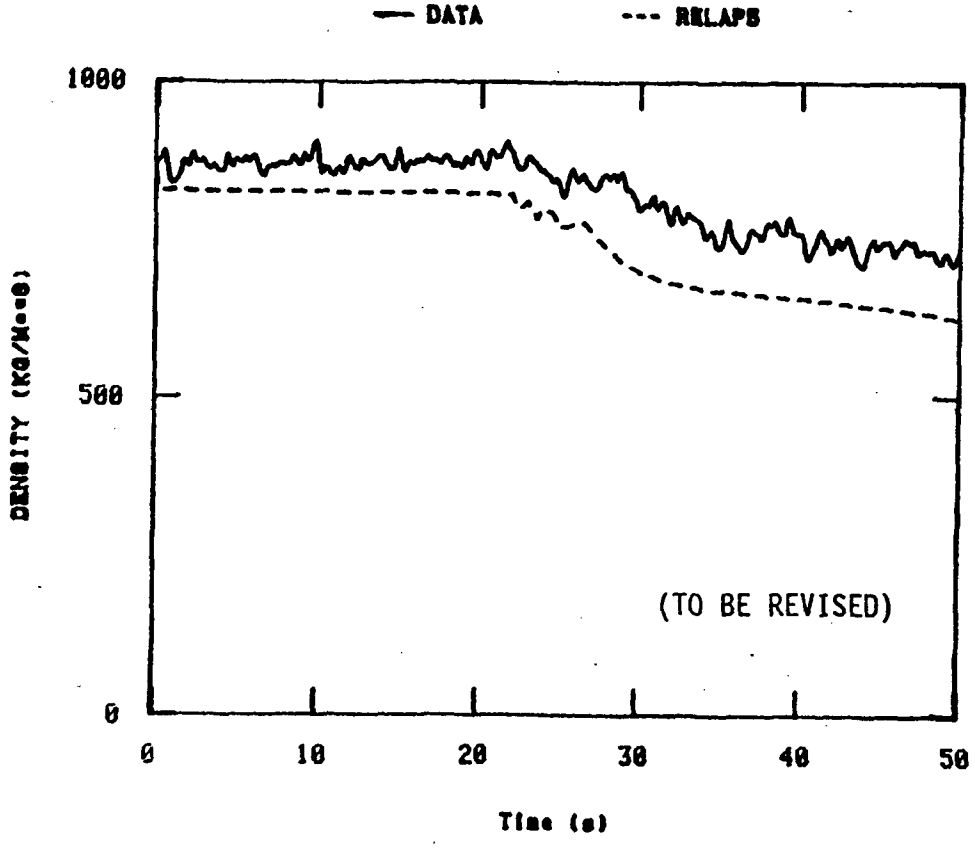

Figure 2.2-29. Measured and calculated (RELAP5/MOD2, MOD3) density in the middle of the discharge pipe for Marviken Test 24.

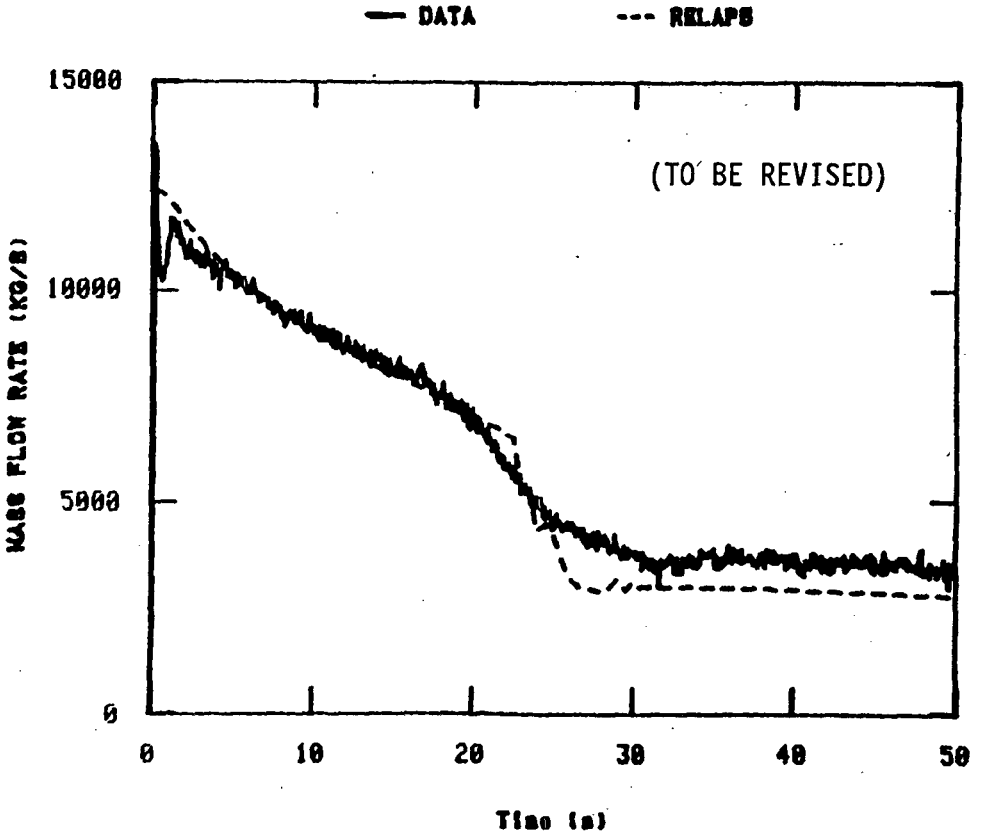

Figure 2.2-30. Measured and calculated (RELAP5/MOD2, MOD3) mass flow rate at the nozzle for Marviken Test 24.

In summary, for Marviken Test 24, RELAP5/MOD3 compares quite well to the data. The comparison is similar to that obtained in RELAP5/MOD2.

2.2.6 Marviken Test 22

Marviken III Test 22 was conducted by expelling water and steam-water mixtures from a full-size reactor vessel through a large-diameter discharge pipe that supplied the flow to a reactor pipe simulator (test nozzle). The test nozzle consisted of a rounded entrance section followed by a 500 mm, constant diameter, test section having a length-to-diameter ratio of 1.5.

The initial steam dome pressure was 4.93 MPa, and the initial subcooling at the nozzle entrance was 95 K relative to the steam dome saturation temperature. Saturation conditions were recorded in the discharge pipe from 26 to 33 s. The system needed 1.2 s to establish a stable rate of depressurization. Saturation conditions were present everywhere in the discharge pipe from 33 s until the test was terminated at 48 s with a steam dome pressure of 2.4 MPa.

A schematic of the pressure vessel and discharge pipe is shown in Figure 2.2-31 (see Reference 2.2-7 for detailed drawings). The warmup process produced the temperature profile shown in Figure 2.2-31.

A sketch of the RELAP5 nodalization is shown in Figure 2.2-31. It is the same as Test 24 except that the nozzle is modeled in Test 22 because it is longer. In addition, the choking flag was turned off in all volumes upstream in the discharge pipe. This is a common necessity when choking occurs, and it was needed for this model.

A comparison of RELAP5/MOD2 to the pressure measurement in the top of the vessel is shown in Figure 2.2-32. The comparison is somewhat similar to Test 24, low in the beginning and high at the end. Figure 2.2-33 shows a comparison of RELAP5/MOD3 to the mass flow rate measurement at the nozzle. As with Test 24, the calculation ends up below the data and the mass flow rate computer by RELAP5/MOD3 was slightly lower than that computed by

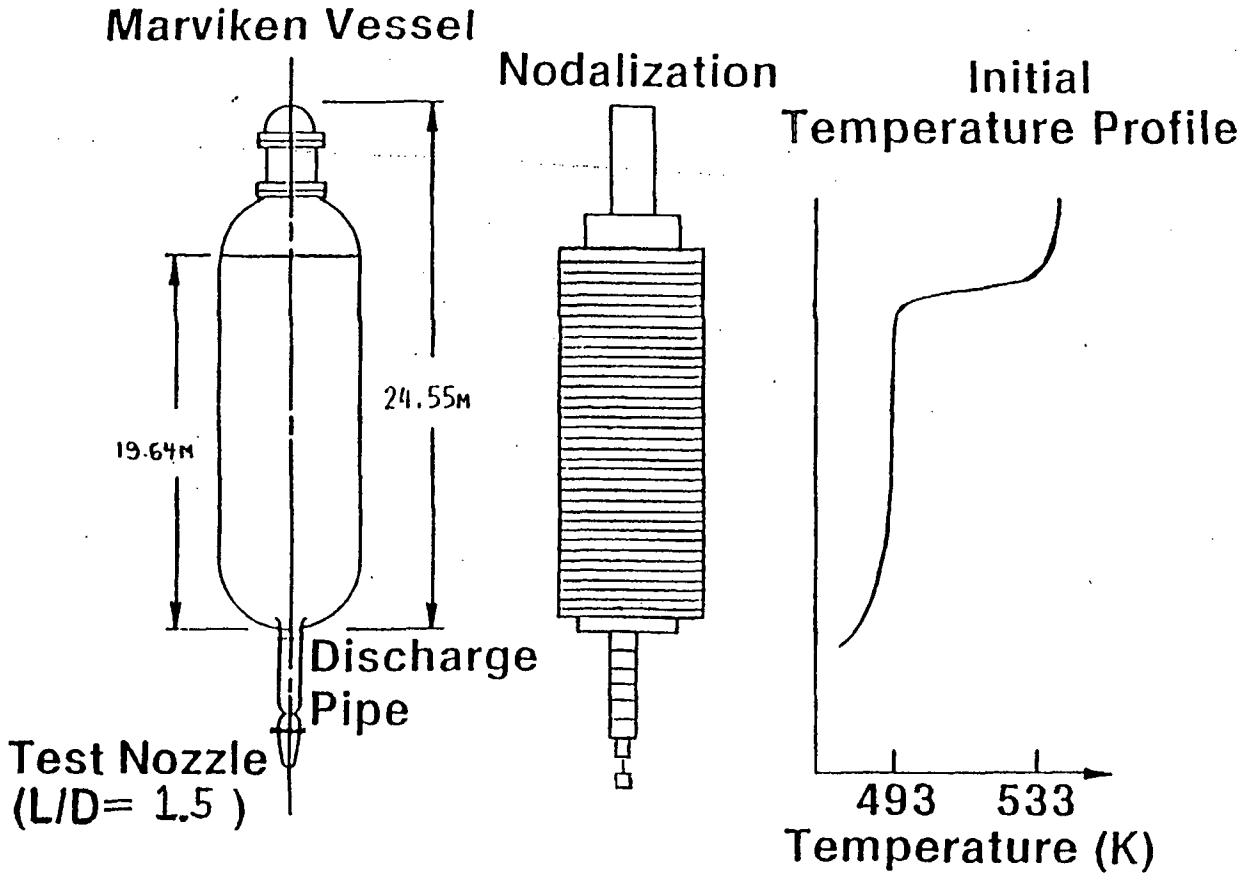

Figure 2.2-31. Schematic, nodalization, and initial temperature profile for Marviken Test 22.

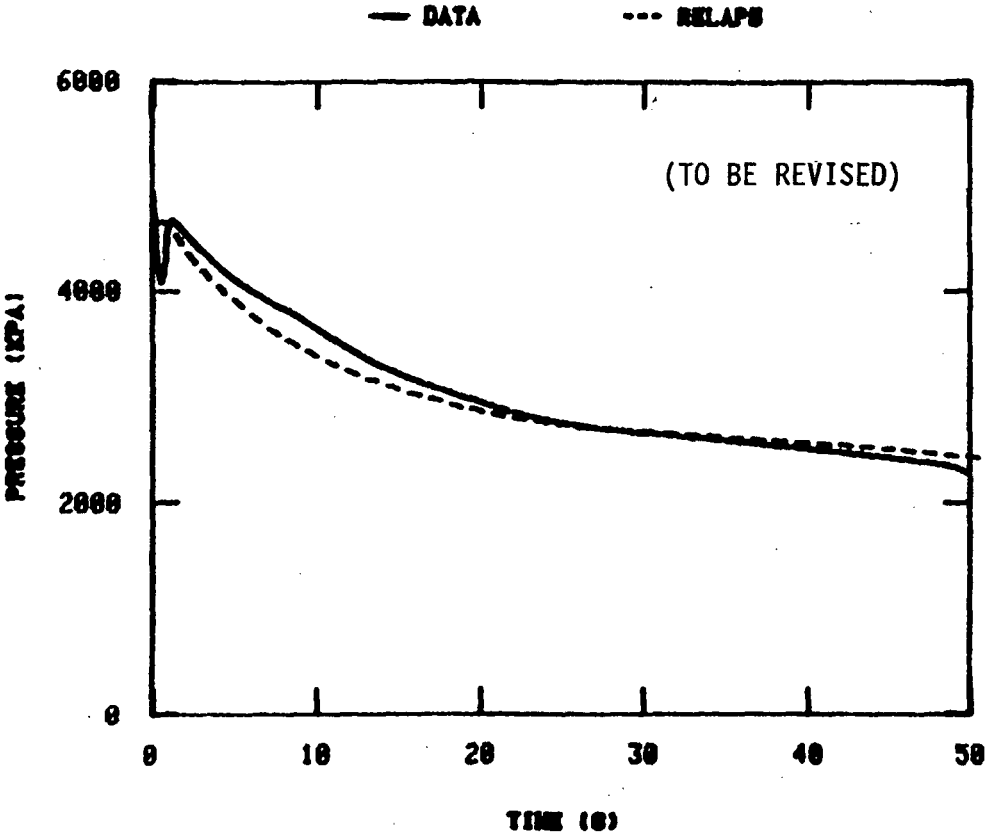

Figure 2.2-32. Measured and calculated (RELAP5/MOD2, MOD3) pressure in the top of the vessel for Marviken Test 22.

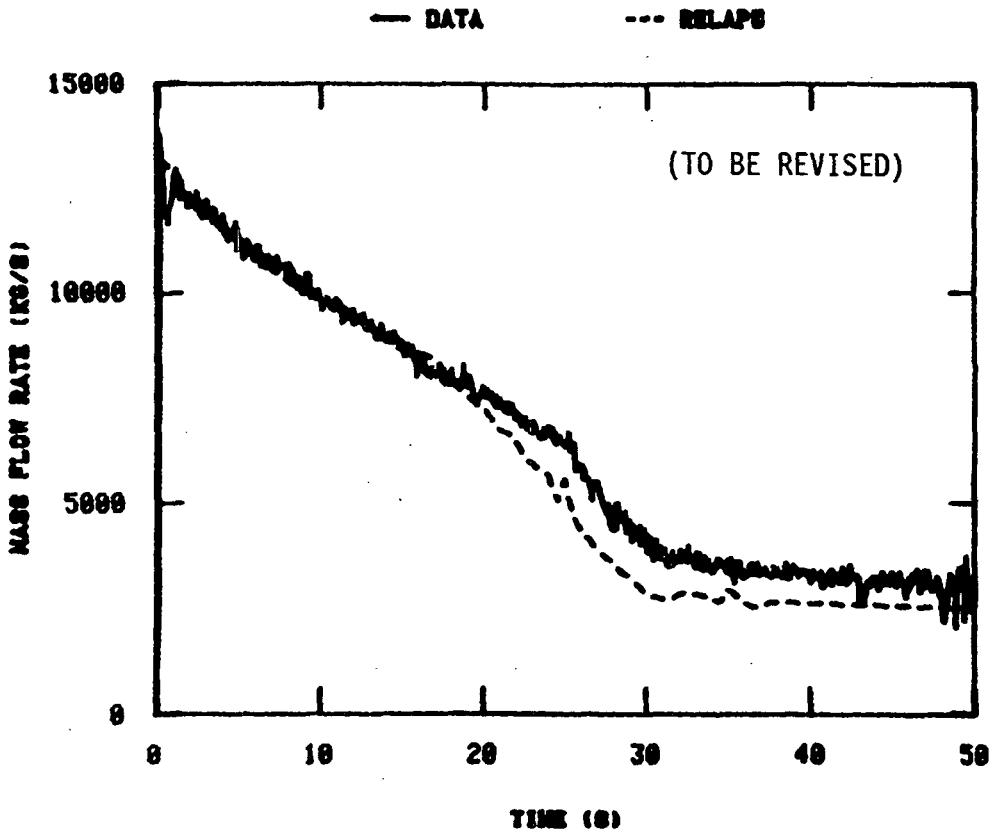

Figure 2.2-33. Measured and calculated (RELAP5/MOD2, MOD3) mass flow rate at the nozzle for Marviken Test 22.

RELAP5/MOD2. For Test 22, the deviation occurs earlier than for Test 24, because calculated two-phase conditions develop too early in the bottom of the pipe. This is probably due to the nucleation model used in the code, which is based on the Edwards pipe experiment.[2.2-8]

In summary, for Marviken Test 22, RELAP5/MOD3 results compared well with the data. To obtain these results, it was necessary to turn choking off in the upstream discharge pipe.

2.2.7 LOFT Test L3-1 Accumulator Blowdown

This problem simulates the blowdown of the LOFT Accumulator A and surge line during Test L3-1. Test L3-1 was a nuclear small-break experiment conducted at the LOFT Facility.[2.2-9] During this experiment, the LOFT PCS underwent a blowdown simulating a small break. As the pressure decreased at the intact loop cold leg emergency core cooling (ECC) injection point, it became less than the pressure in the accumulator. At this time, the accumulator also began to blow down, consequently injecting cold water into the primary system cold leg. The purpose of this problem was to demonstrate the performance of the RELAP5/MOD3 accumulator model in simulating the blowdown of the LOFT accumulator.

Figure 2.2-34 is a schematic showing the arrangement of the LOFT Accumulator A and surge line relative to the cold leg ECC injection point. The accumulator is a 1.25-m (49-in.) diameter cylindrical tank with elliptical ends. The effective volume of liquid and gas available for injection is adjustable by varying the height of a standpipe inside the tank. For Test L3-1, the standpipe height was approximately 0.76 m (30 in.), giving an effective liquid-gas volume of approximately 2.88 m^3 (103 ft^3). Attached to the standpipe exit in the surge line and for Test L3-1, the length of the combined standpipe and surge line was 2.74 m (107.7 ft), with an average flow area of 0.01 m^2 (0.147 ft^2). From the standpipe entrance to the primary system ECC injection point, there is a 2.14-m (7-ft) rise in elevation.

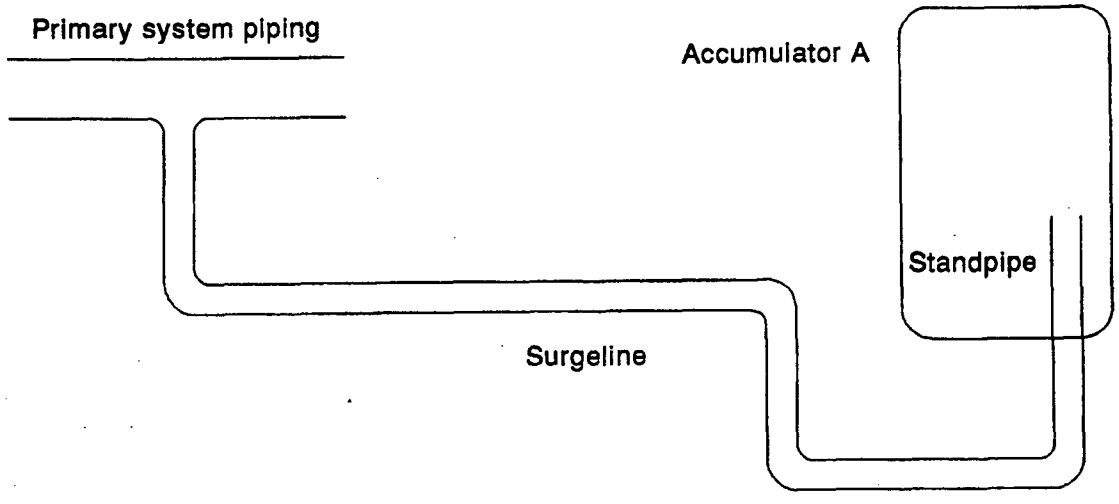

Figure 2.2-34. LOFT L3-1 Accumulator A and surgeline schematic.

Figure 2.2-35 is a schematic of the RELAP5/MOD3 model, which consists of two components. Component 1 is the accumulator component, which represents the LOFT Accumulator A and surge line. Component 4 is a time-dependent volume, which imposes the pressure history at the LOFT cold leg ECC injection point for LOFT Test L3-1. It should be pointed out that the accumulator tank volume is consistent with the accumulator standpipe height for Test L3-1. The surge line area and length are consistent with the Test L3-1 piping arrangement and include the entire surge line from its entrance in the standpipe to its injection point in the primary system cold leg. The forward and reverse loss factors represent all of the surge line orifice, bend, and contraction/expansion losses distributed over the length of the surge line.

Calculational results are shown in Figures 2.2-36 through 2.2-40, which are plots of the accumulator gas dome pressure versus volume; the gas dome pressure versus time; a comparison of the results for liquid velocity versus time at the surge line exit, as calculated by RELAP5/MOD1, MOD2, and MOD3; and the RELAP5/MOD2 and MOD3 results for combined gas dome heat and mass transfer energy rate versus time.

In Figure 2.2-36, curves for isothermal and isentropic expansion of the gas dome and the actual data from the LOFT L3-1 test are also plotted for comparison. As seen in the plot, the calculational results agree reasonably well with the data and lie between the isothermal and isentropic expansion curves, as expected.

In Figure 2.2-37, the accumulator pressure data from the LOFT L3-1 test are also plotted for comparison. The pressure data were obtained by digitizing the data points from curves plotted for the LOFT L3-1 data report.[2.2-10] As seen in Figure 2.2-37, the accumulator pressure/time response agrees well with the data.

Figure 2.2-38 is a plot of the calculated liquid velocity at the exit of the accumulator surge line. As seen in the figure, the velocities computed exhibit instabilities. However, these instabilities may possibly

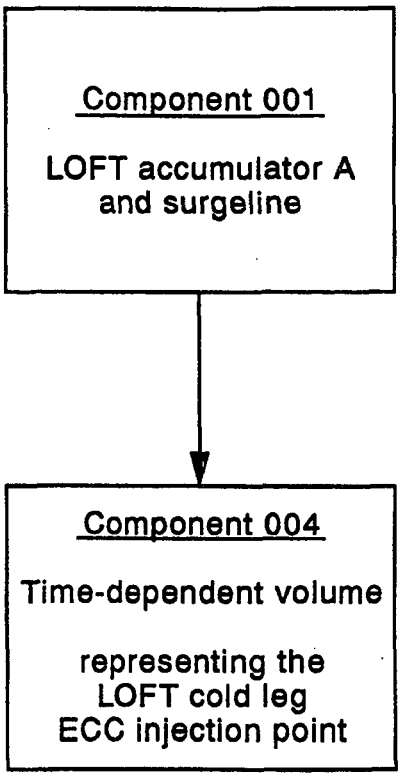

Figure 2.2-35. LOFT L3-1 accumulator model schematic.

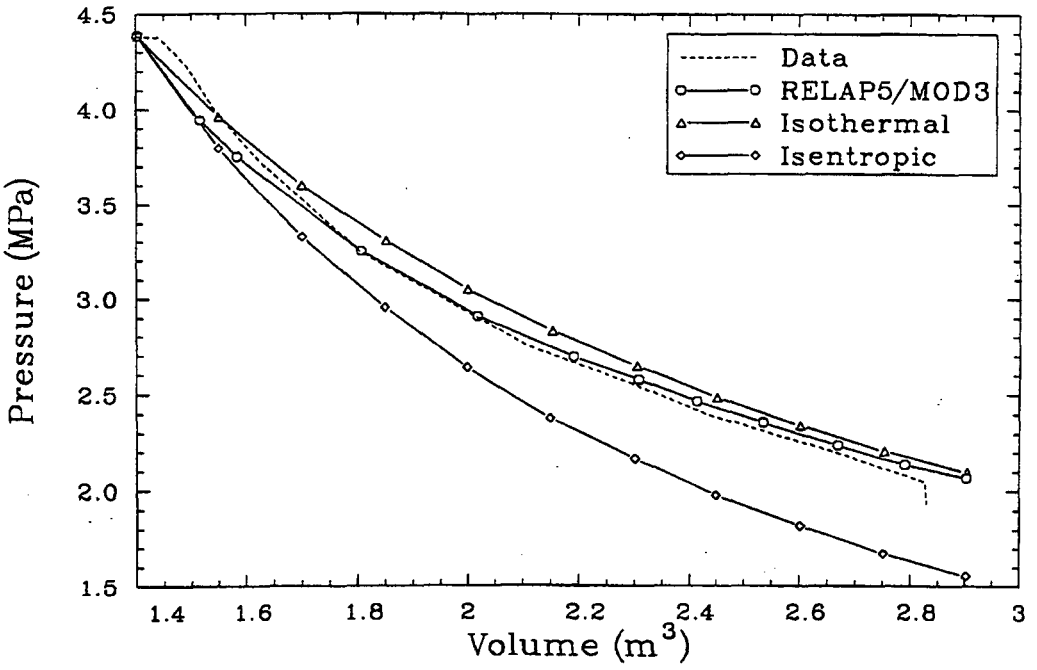

Figure 2.2-36. Calculated accumulator gas dome pressure versus volume.

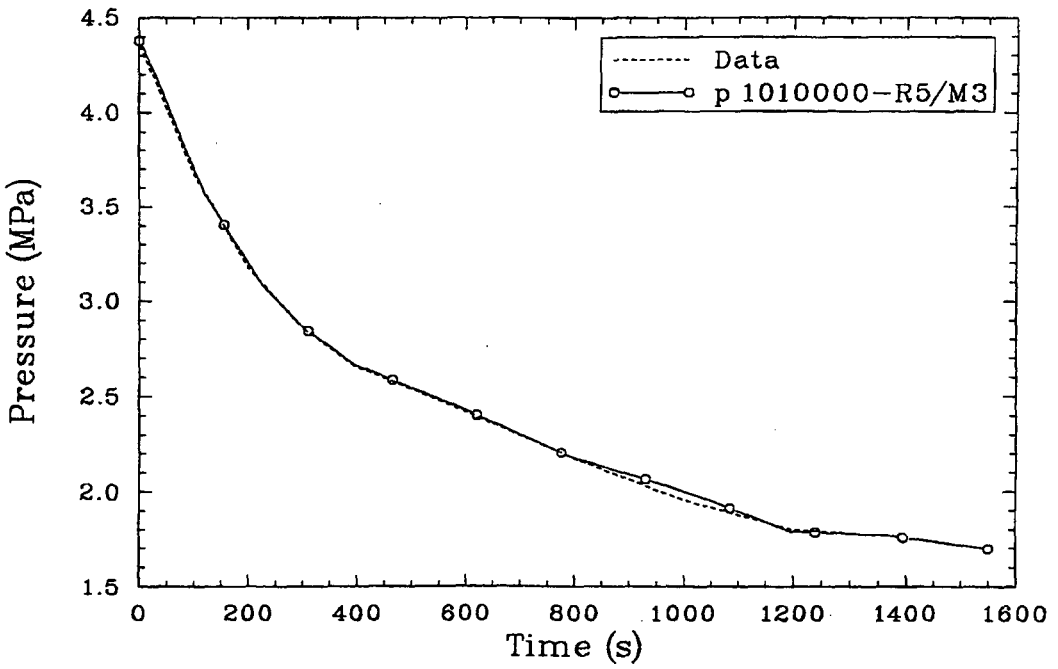

Figure 2.2-37. Calculated accumulator gas dome pressure.

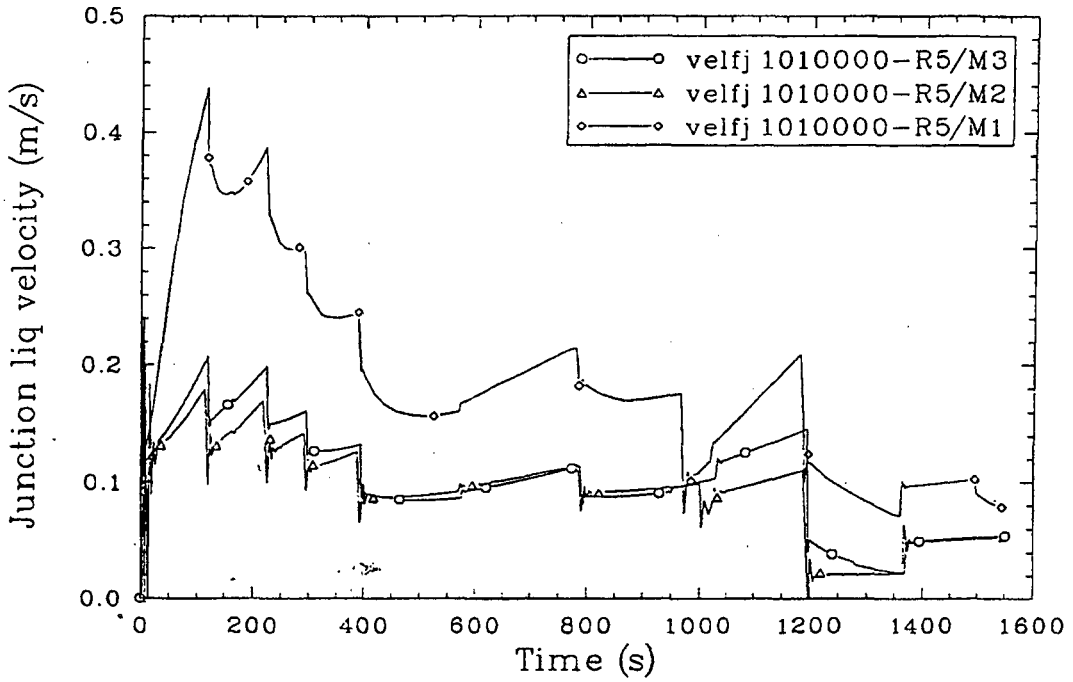

jen-sm111

Figure 2.2-38. Calculated accumulator surge line liquid velocity.

(figure deleted)

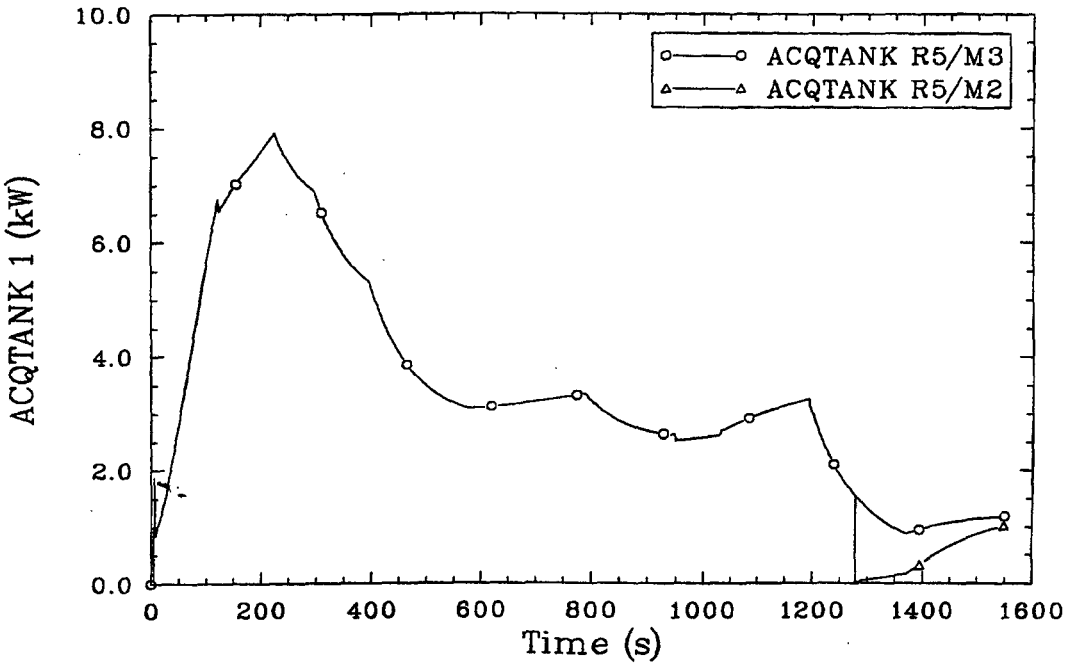

jan-cm121

Figure 2.2-40. Calculated accumulator combined heat and mass transfer energy.

be explained by considering the solution scheme. In particular, the accumulator scheme solves for the gas dome pressure at the centroid of the gas dome. Since the gas dome is expanding, the centroid is moving; and the effects of this moving mesh point should be included in the formulations. Also, in the pressure and energy solution schemes, the effects of water vapor mass and volume in the gas dome are neglected.

Figure 2.2-38 also shows the calculated liquid velocity at the exit of the accumulator surge line using RELAP5/MOD1. As seen in the figure, the abruptness of the velocity instabilities is much more pronounced than for the RELAP5/MOD2 and MOD3 results. Also, the magnitude of the velocity is lower than for the MOD3 results. In comparing the results of the three calculations, it is seen that the improved RELAP5/MOD3 accumulator model mitigates the velocity instabilities characteristic of the MOD1 model.

Figure 2.2-40 is a plot of the accumulator gas dome heat and mass transfer energy rate. The shape of this curve exhibits the same sawtooth behavior as the velocity curve of Figure 2.2-38. This is maybe due to the fact that as the velocity increases, the gas dome volume expands at a faster rate. Hence, the condensation rate increases, which, in turn, increases the rate at which the heat of formation is given up to the gas dome. An abrupt decrease in heat and mass transfer occurs at approximately 977 s, which is the time at which the gas/liquid interface leaves the tank and enters the surge line. In the accumulator model, the energy transport by mass transfer is shut off at this point. Hence, the curve at times greater than 977 s represents only the tank wall heat transfer to the gas dome. At approximately 1504 s, a small abrupt decrease in heat transfer occurs. This is the time at which liquid empties the surge line and the numerical scheme converts to that for a normal volume.

In conclusion, the results of the calculation indicate that the accumulator model in RELAP5/MOD3 reasonably approximates the behavior of an accumulator and that the instabilities exhibited by the RELAP5/MOD1 model have been mitigated. However, further development will be required to eliminate the velocity instabilities.

2.2.8 Bennett's Heated Tube Experiments

The Bennett heat tube experiments[2.2-11] were conducted using a vertical, 1.26-cm-diameter tube that was electrically heated. Water at a pressure of 6.9 MPa flowed upward in the tube. The main objectives of the experiment were to measure the dryout location [or critical heat flux (CHF) location] where liquid ceased to adhere to the inside wall and the surface temperature profiles in the region beyond the dryout point.

Three of the Bennett tests were simulated; low, intermediate, and high mass flux tests. The RELAP5/MOD3 nodalization diagram for the latter two Bennett experiments is shown in Figure 2.2-41. The figure shows a pipe having 32 vertical volumes, 31 junctions, and two time-dependent volumes to simulate the inlet and outlet boundary conditions. The heat generated by electric power in the test section was modeled using 32 heat slabs, and the initial and boundary conditions given by the test (see Table 2.2-1) were input to RELAP5/MOD3. The low mass flux case had 37 axial nodes because CHF occurred closer to the inlet and the fine mesh was extended to more accurately locate the predicted elevation.

A comparison of the calculated wall temperature and the Bennett post-CHF data for the low, intermediate, and high mass flux tests is shown in Figures 2.2-42, 2.2-43, and 2.2-44. In general, the RELAP5/MOD3-calculated wall temperature and CHF location are in very good agreement with the data for all three test cases.

2.2.9 Royal Institute of Technology Tube Test 261

The Royal Institute of Technology in Sweden obtained experimental data[2.2-12] similar to the Bennett data. The experiment used a vertical 7-m-long, 0.015-m-diameter heated tube. The RELAP5 model was as shown in Figure 2.2-41 except that 47 fluid cells were used. The boundary conditions for the model are given in Table 2.2-1.

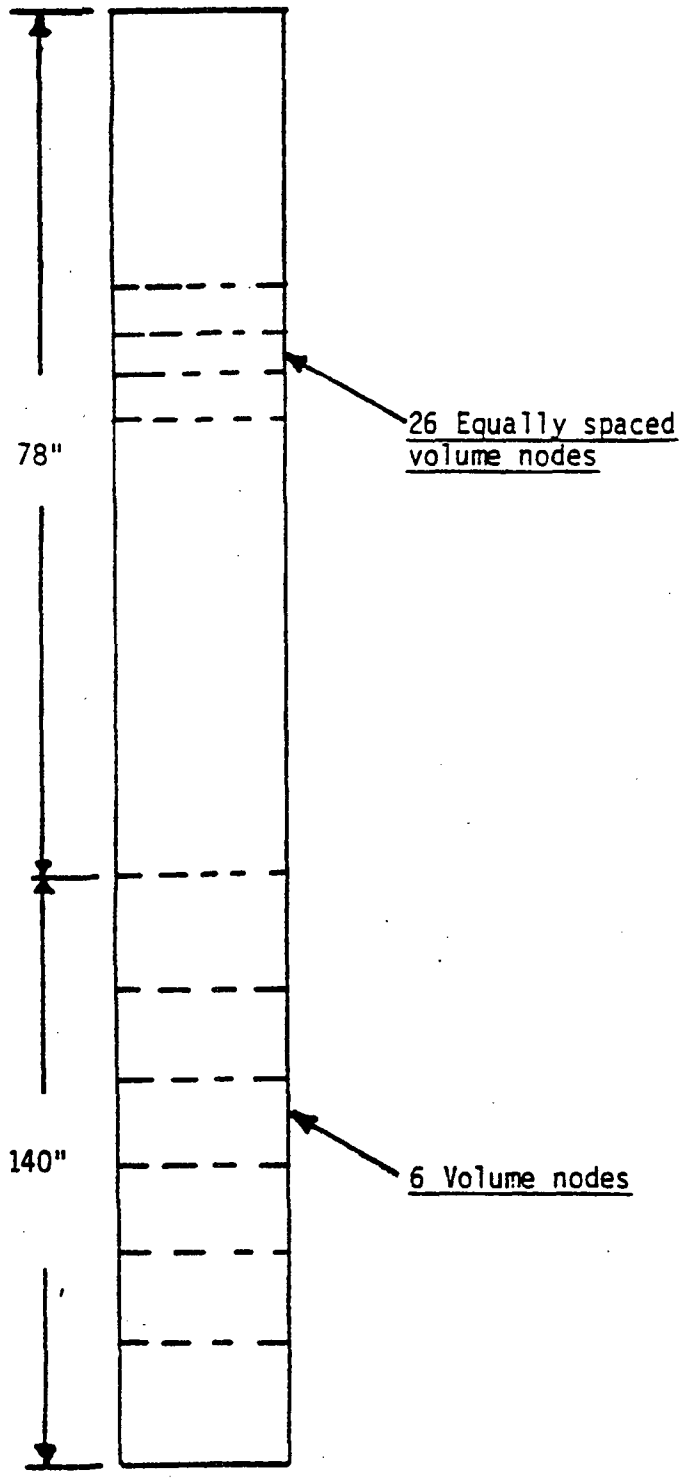

Figure 2.2-41. RELAP5 nodalization diagram for Bennett's heated tube experiment.

Table 2.2-1. RELAP5/MOD3 nonequilibrium model developmental assessment matrix

Data Source and Test Conditions	Primary Feature Assessed
Christensen Test 15 Pressure = 5.512 MPa Heat flux = 0.65 MW/m^2 Mass flux = 907.3 $kg/s-m^2$ Inlet subcooling = 12.5 K	Subcooled nucleate boiling
Bennett experiment 5358 Pressure = 6.9 MPa Heat flux = 0.512 MW/m^2 Mass flux = 380. $kg/s-m^2$ Subcooling = 34.41 K	Nonequilibrium heat transfer CHF correlation
Bennett experiment 5294 Pressure = 6.9 MPa Heat flux = 1.09 MW/m^2 Mass flux = 1953. $kg/s-m^2$ Subcooling = 18.8 K	Nonequilibrium heat transfer CHF correlation
Bennett experiment 5394 Pressure = 6.9 MPa Heat flux = 1.75 MW/m^2 Mass flux = 5181. $kg/s-m^2$ Subcooling = 13.78 K	Nonequilibrium heat transfer CHF correlation
Royal Institute of Technology Test 261 Pressure = 7.0 MPa Heat flux = 1.05 MW/m^2 Mass flux = 1988. $kg/s-m^2$ Subcooling = 10.68 K	Noneqilibrium heat transfer CHF correlation
ORNL Test 3.07.9B Pressure = 12.7 MPa Heat flux = 0.91 MW/m^2 Mass flux = 713. $kg/s-m^2$ Subcooling = 19.11 K	Noneqilibrium heat transfer CHF correlation
ORNL Test 3.07.9N Pressure = 8.52 MPa Heat flux = 0.94 MW/m^2 Mass flux = 806. $kg/s-m^2$ Subcooling = 14.29 K	Noneqilibrium heat transfer CHF correlation
ORNL Test 3.07.9W Pressure = 12.55 MPa Heat flux = 0.38 MW/m^2 Mass flux = 256. $kg/s-m^2$ Subcooling = 34.07 K	Noneqilibrium heat transfer CHF correlation

Table 2.2-1. (continued)

Data Source and Test Conditions	Primary Feature Assessed
ORNL Test 3.09.10i Pressure = 4.50 MPa Heat flux = 0.38 MW/m^2 Mass flux = 29.76 $kg/s\text{-}m^2$ Subcooling = 57.58 K	Axial void profile

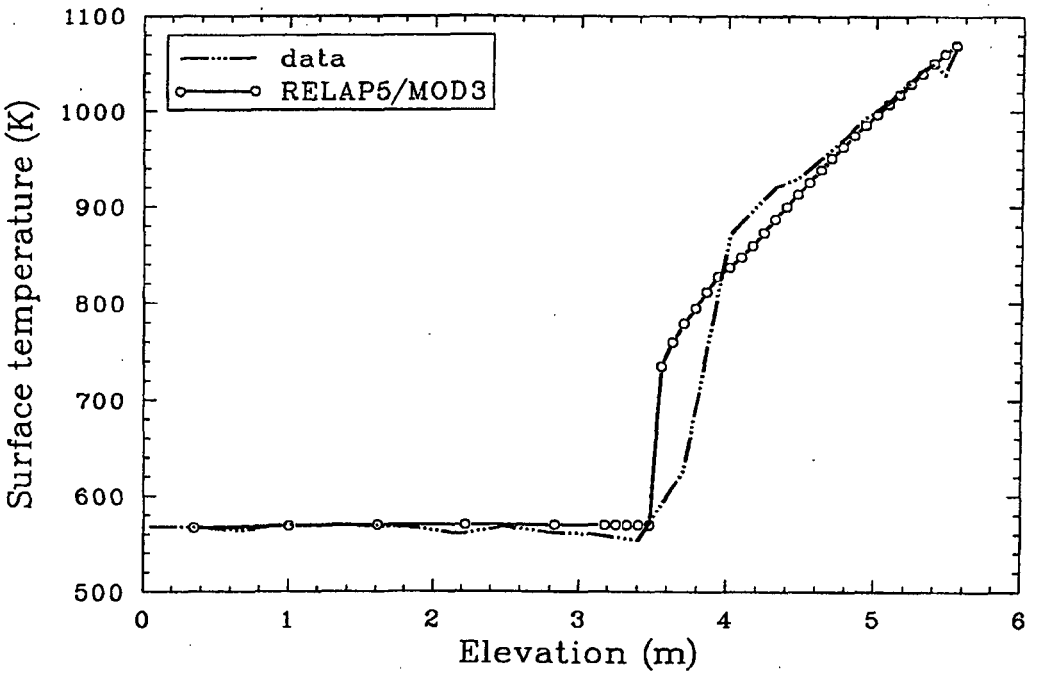

Figure 2.2-42. Measured and RELAP5/MOD3-calculated axial wall temperature profiles for Bennett's heated tube low mass flux experiment.

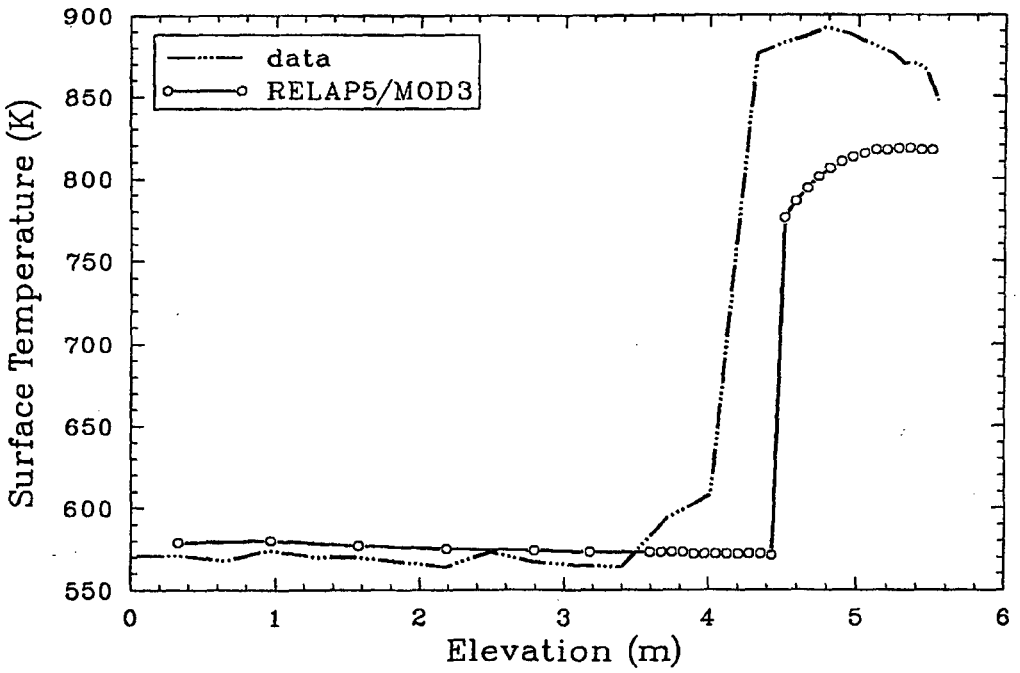

Figure 2.2-43. Measured and RELAP5/MOD3-calculated axial wall temperature profiles for Bennett's heated tube intermediate mass flux experiment.

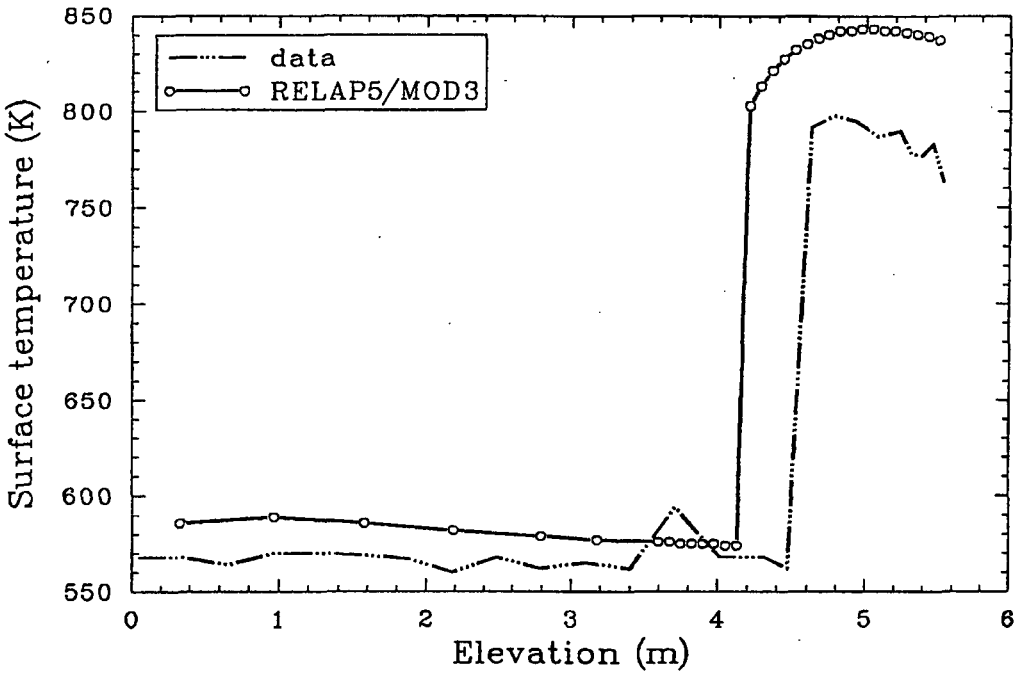

Figure 2.2-44. Measured and RELAP5/MOD3-calculated axial wall temperature profiles for Bennett's heated tube high mass flux experiment.

Reference 2.2-12 reported very poor agreement between the measured axial position of departure from nucleate boiling compared to RELAP5/MOD2, which used the Biasi CHF correlation. The measured CHF position was 4.65 m, compared to a MOD2 prediction of 6.3 m. RELAP5/MOD3 uses the AECL-UO correlation and predicts a location of 5.2 m, as shown in Figure 2.2-45. The MOD3 code underpredicts the peak wall temperature but would agree better if CHF had been predicted more accurately.

2.2.10 ORNL Bundle CHF Tests

These tests[2.2-13] were performed with an 8 x 8, full-length, electrically heated rod bundle. The rod size was the same as 17 x 17 bundles used in PWRs (0.0095 m). The tests were performed by adjusting the power until a steady-state dryout point had been established. Table 2.2-1 gives the test conditions. The model used 24 cells, each 0.15-m long.

Figures 2.2-46, 2.2-47, and 2.2-48 show the code-data comparison for these tests. The code did predict a CHF position closer to the inlet than the measured value, and the peak temperature was higher than the data.

2.2.11 ORNL Void Profile Test

ORNL tests series 3.09.10[2.2-14] is similar to the above tests; but the axial void profiles and steam temperatures are reported, as well as the rod temperatures above the CHF point. The axial position of the CHF point was not given. The rod wall temperature at a particular elevation is the average over all the rod thermocouples at that elevation. There was a dip in the average value downstream of a grid spacer, as shown in Figure 2.2-49. MOD3 has no mechanism to increase the heat transfer coefficients downstream of grids, and the calculated rod temperature shows no dip.

The steam temperature in the experiment was calculated from an energy balance and the measured bundle exit steam temperature. The MOD3 value, see Figure 2.2-50, agrees well with the reported data value.

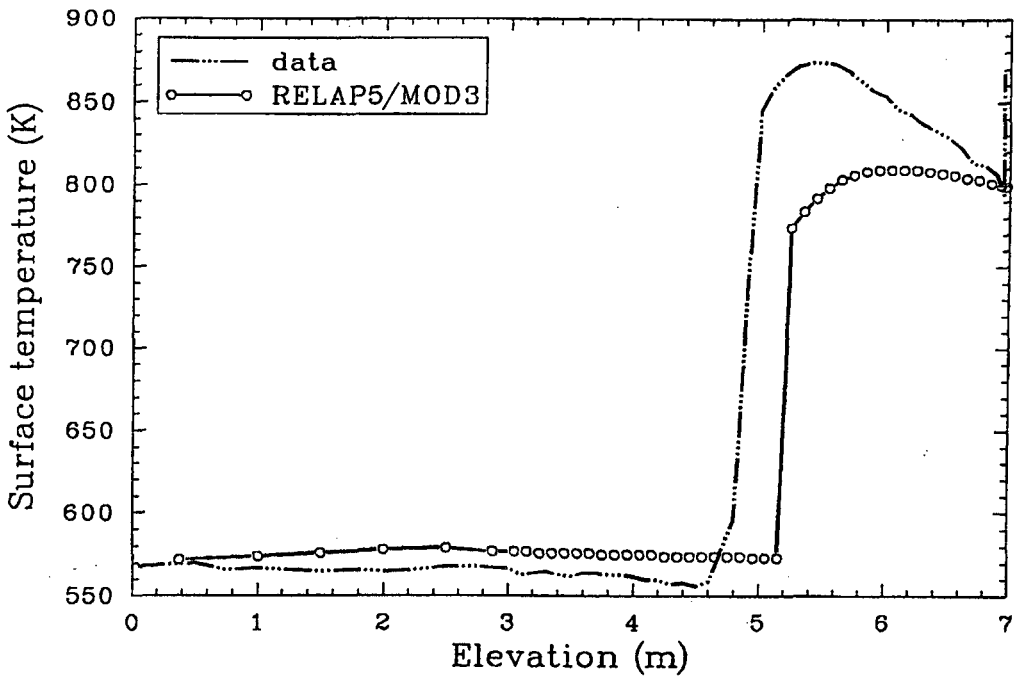

Figure 2.2-45. RELAP5/MOD3-predicted critical heat flux position.

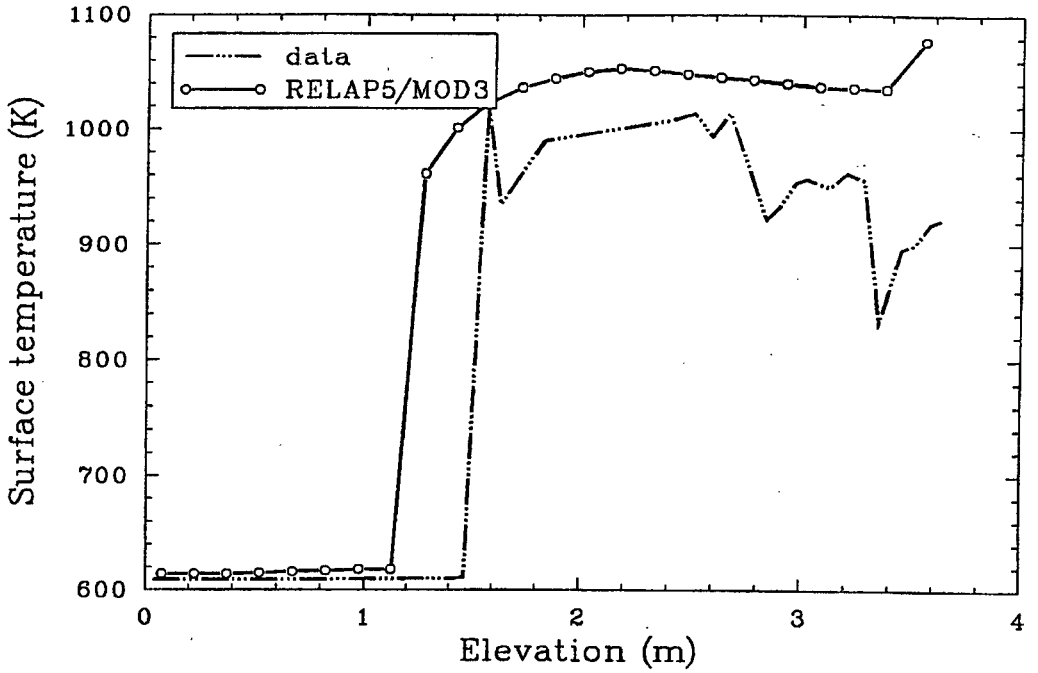

Figure 2.2-46. Measured and RELAP5/MOD3-calculated surface temperature for ORNL bundle CHF test 3.07.9B.

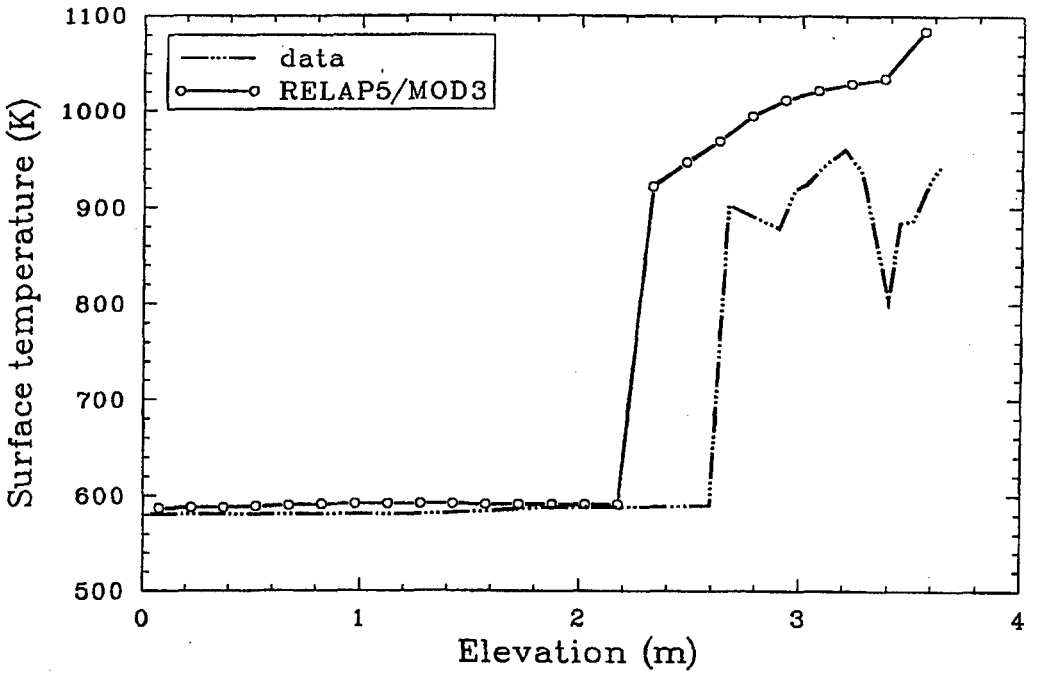

Figure 2.2-47. Measured and RELAP5/MOD3-calculated surface temperature for ORNL bundle CHF test 3.07.9N.

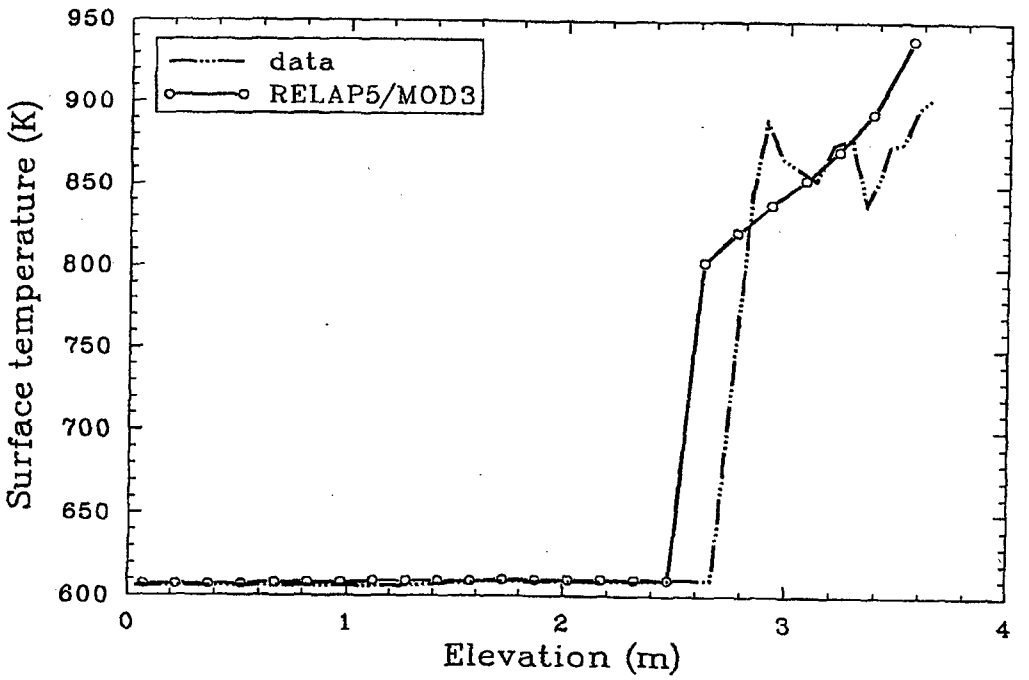

Figure 2.2-48. Measured and RELAP5/MOD3-calculated surface temperature for ORNL bundle CHF test 3.07.9W.

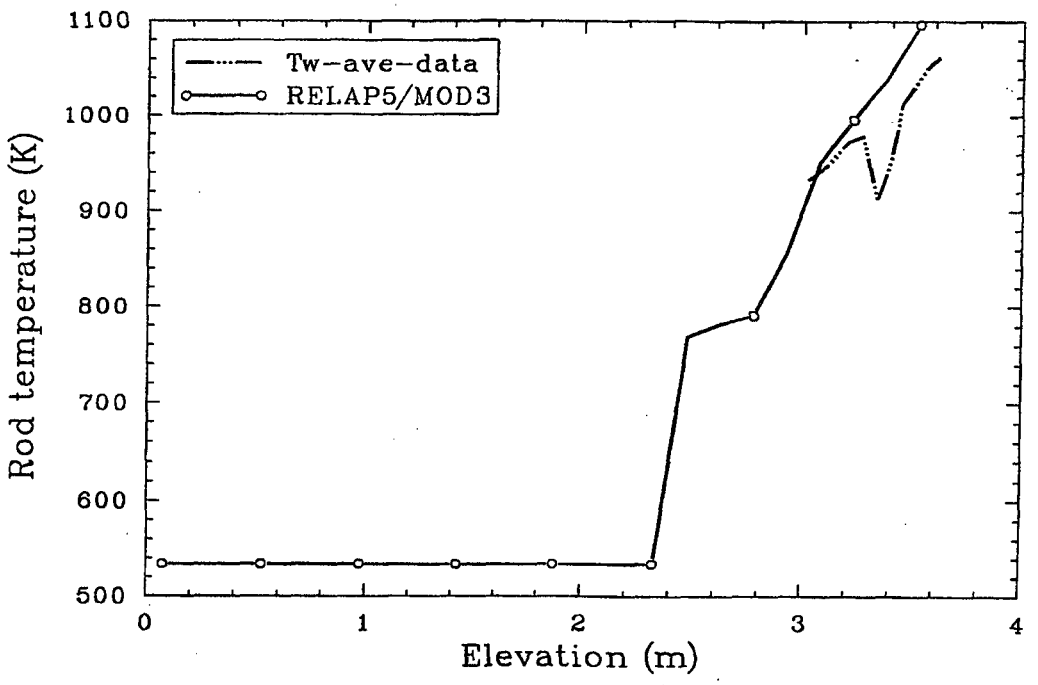

Figure 2.2-49. Measured and RELAP5/MOD3-calculated rod temperature for the ORNL void profile test.

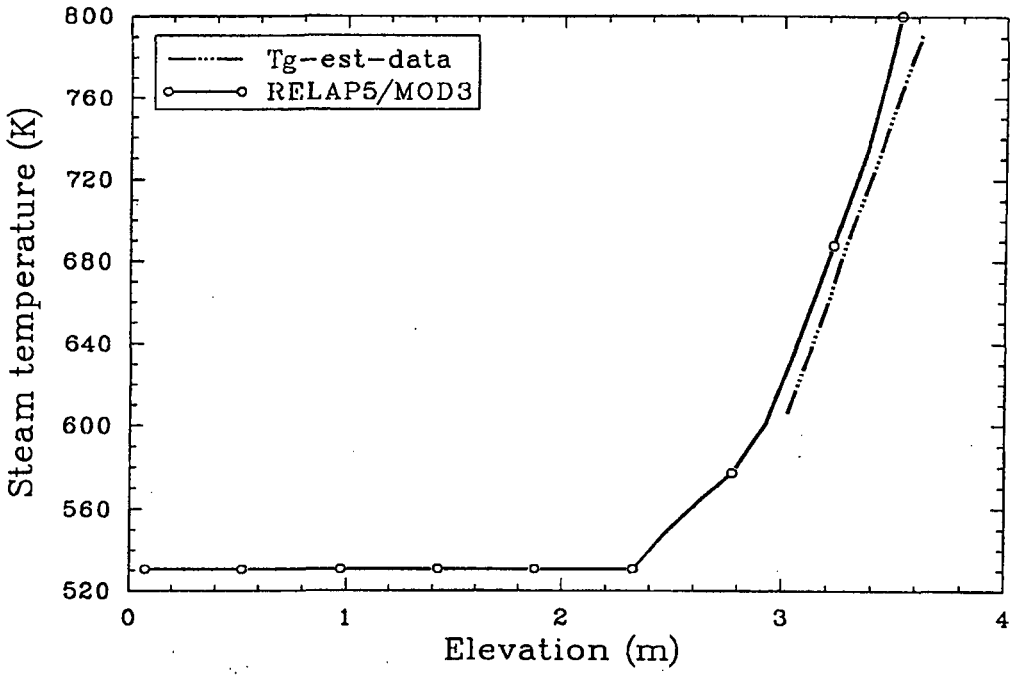

Figure 2.2-50. Measured and RELAP5/MOD3-calculated steam temperature for the ORNL void profile test.

The axial void fraction was calculated from differential pressure measurements with a reported accuracy of ± 3%. The RELAP5/MOD3 calculation is generally above the data, as shown in Figure 2.2-51.

2.2.12 Christensen Subcooled Boiling Test 15

The interphase mass transfer and wall heat flux partitioning model was assessed using the data from a separate-effects, subcooled nucleate boiling experiment conducted by Christensen[2.2-15]. The test section was a rectangular tube with 1.11 x 4.44-cm cross section and 127-cm height. The tube was heated by passing an ac current through the tube walls. The void fraction along the test tube was measured by a gamma densitometer.

The test section was simulated by RELAP5 as 20 volumes--two time-dependent volumes, 19 junctions, two time-dependent junctions, and 20 heat slabs simulating heat generated at the walls. The test conditions given in Table 2.2-1 were input to the code.

A comparison of the RELAP5/MOD3 axial void fractions with measured data from the Christensen test 15 is shown in Figure 2.2-52. The importance of the subcooled boiling model is illustrated on this test because the water was subcooled over the complete length of the test section. The calculated rate of flashing was too large compared to the condensation rate at the inlet but compares well with the data over most of the test section.

2.2.13 MIT Pressurizer Test

The Massachusetts Institute of Technology (MIT) pressurizer test ST4[2.2-16,17] involves a small-scale, low-pressure pressurizer that is initially partially filled with saturated water. The test is initiated by opening two quick-opening valves, which results in the insurge of subcooled water into the bottom of the pressurizer. The accurate calculation of data from this test depends on accurate modeling of steam condensation on the wall as well as interfacial heat transfer between the stratified liquid and the vapor above the liquid.

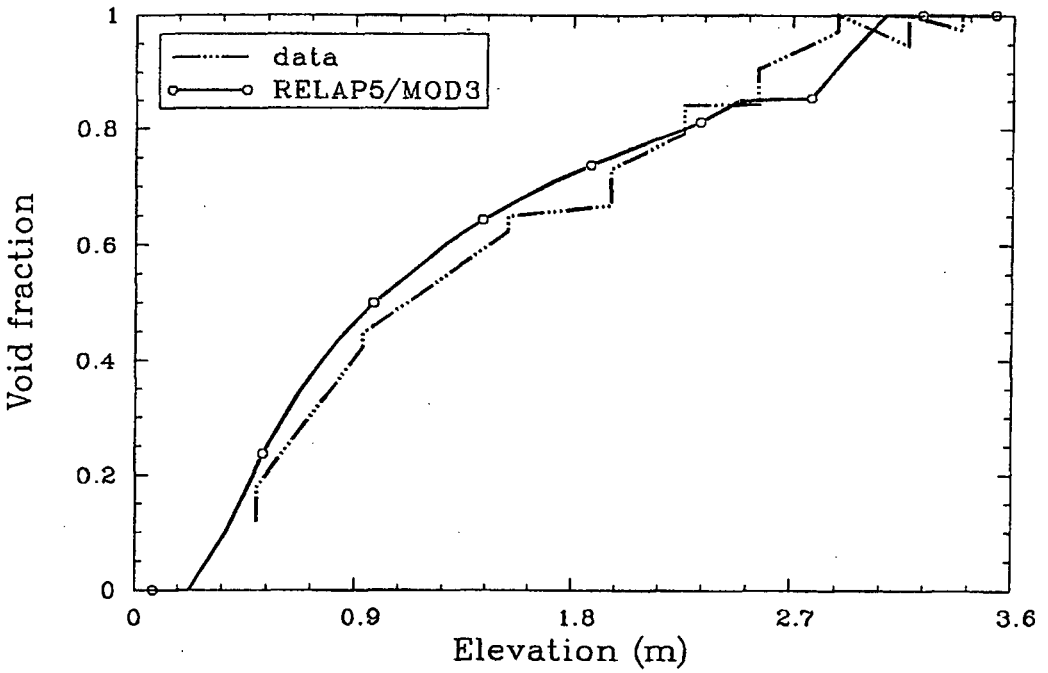

Figure 2.2-51. Measured and RELAP5/MOD3-calculated axial void fractions for the ORNL void profile test.

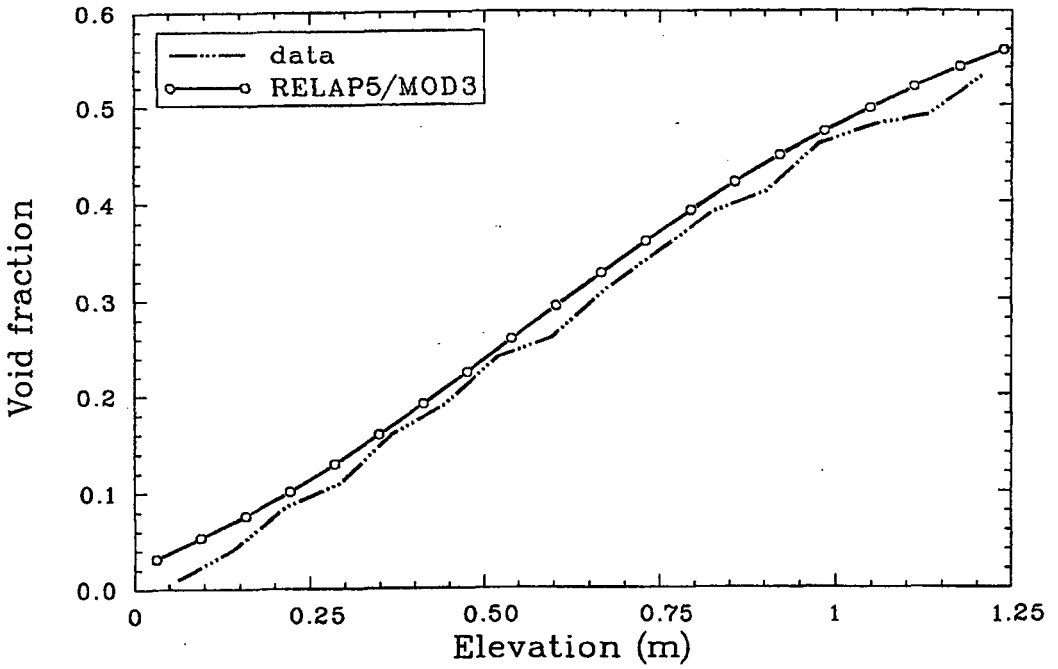

Figure 2.2-52. Measured and RELAP5/MOD3-calculated axial void fractions for the Christensen subcooled boiling test 15.

The experimental apparatus is shown schematically in Figure 2.2-53. It consists of two cylindrical steel tanks: the primary tank, 1.14 m tall and 0.203 m ID, and the storage tank. The primary tank has six windows and is equipped with six immersion heaters with a power total of 9 kW. The storage tank was pressurized with nitrogen to force the liquid into the primary tank.

Test ST4 began with the liquid level in the primary tank at 0.432 m from the bottom. The average level rise velocity was 0.0115 m/s over a 41-s time period. The primary tank was modeled in RELAP5/MOD3 with a ten-cell pipe, each with a heat slab set at the saturation temperature of the initial pressure. The water and steam in the tank were also set at the saturation value. A time-dependent junction fed water at the specified rate from a time-dependent volume to the pipe. The time-dependent volume conditions were those of the subcooled water in the storage tank. The initial subcooling as the water entered the tank was 129 K.

Figure 2.2-54 shows that the calculated rate of pressure rise is close to the measured value. Each time the level crosses a cell boundary, the calculated pressure has a dip. This is because, with no water in the cell, the energy equation is linearized around the saturation state; subcooled water enters during the time step and results in a calculated pressure reduction. Iteration would remove this problem.

Figure 2.2-55 is a snapshot of the tank fluid and inside wall temperature at 35 s into the transient. The water level is at the 0.79-m elevation. The data show that the initial 0.432 m of water was lifted with less mixing than occurred in the calculation. Since each cell in the code has only one uniform temperature, numerical mixing occurs. The trend of the data versus the calculation is excellent.

2.2.14 FLECHT-SEASET Forced Reflood Tests

In addition to data from the single-tube experiments, forced reflood test data[2.2-18] and Runs 31504 and 31701 from the 161-rod FLECHT-SEASET

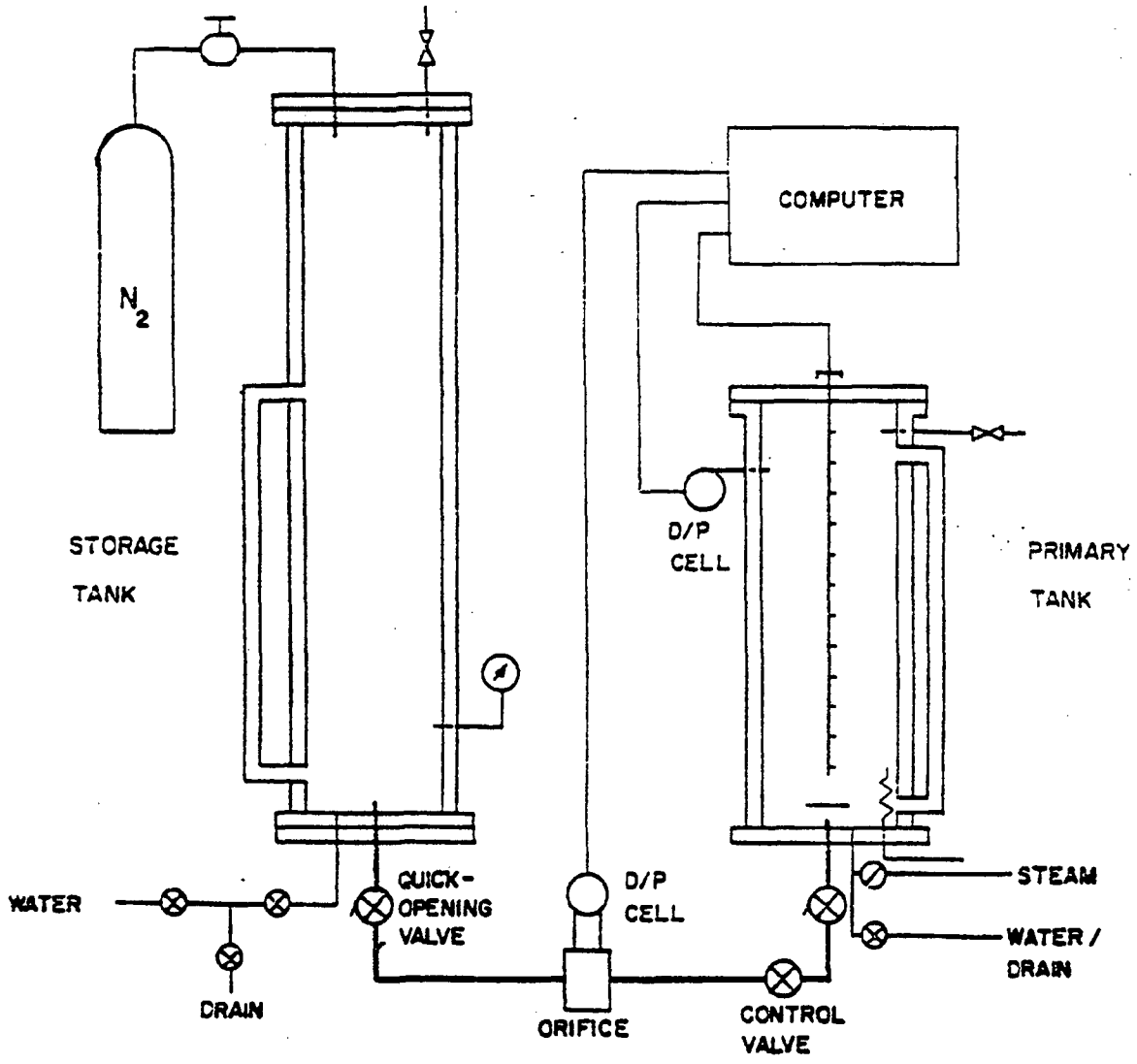

Figure 2.2-53. Schematic of the experimental apparatus for the MIT pressurizer test.

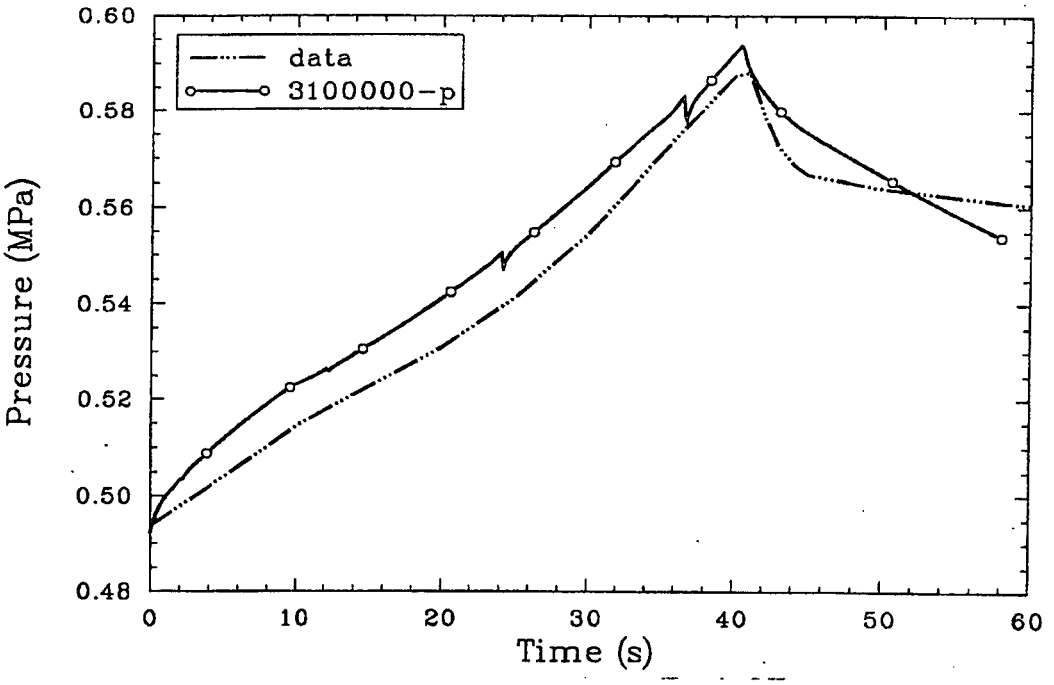

Figure 2.2-54. Measured and RELAP5/MOD3-calculated rate of pressure rise for the MIT pressurizer test.

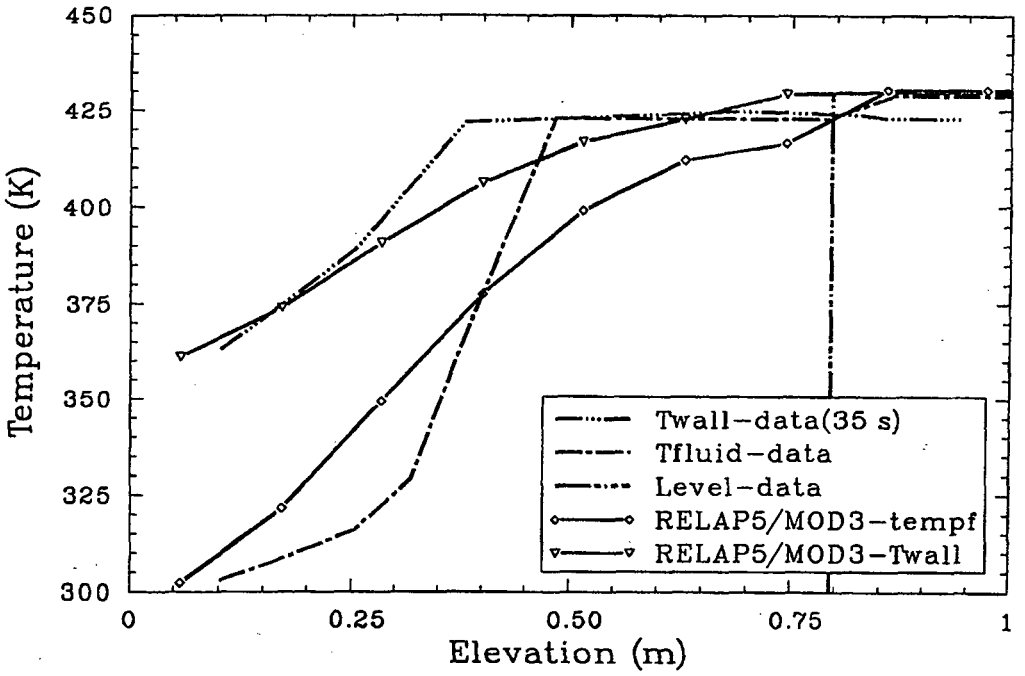

Figure 2.2-55. Tank fluid and inside wall temperature at 35 s into the transient during the MIT pressurizer test.

facility were used to assess the reflood model at low and high reflood rates. The electrically heated rod configuration was typical of a full-length Westinghouse 17 x 17 rod bundle. The rods had a uniform radial power profile and a cosine axial power profile. The primary component in the test facility was a test section that consisted of a cylindrical, low-mass housing 0.19 m (7.625 in.) inside diameter by 3.89 m (1530.0 in.) long, and attached upper and lower plenums. For the tests selected, the flooding water entered the lower plenum at a temperature of nominally 325 K (125°F), with the rods at an initial temperature of nominally 1140 K (1592°F), and an initial average power of 2.3 kW/m (0.7 kW/ft). The heated coolant exited to the upper plenum at a pressure of 0.28 MPa (40 psia).

The test section was modeled using 20 cells, as shown in Figure 2.2-56. Measured fluid conditions were used to define the conditions in the upper and lower time-dependent volumes, which represented the upper and lower plenums, respectively. The measured flow injection velocity was used to define the flow conditions at the time-dependent junction that connected the lower plenum and the pipe, which represented the low mass housing. The measured power, which decreased during the test, was used as input to the heat structures representing the rods.

On the low reflood test Run 31504, with an injection velocity of 2.46 cm/s (0.97 in./s), the code exhibited some strengths and some weaknesses. Comparisons of measured and calculated rod surface temperature histories are presented in Figures 2.2-57 through 2.2-60. The legend for the rod temperature data is the rod number followed by the elevation in inches; i. e., 7J-072 was from a thermocouple in a rod near the center of the bundle at the axial midplane [1.83 m (72 in.) from the inlet]. The measured steam temperatures at various elevations are shown in Figures 2.2-61 through 2.2-63. The legend for the calculation is the bundle component number (6) followed by the cell number (01-20). The total bundle mass inventory is compared in Figure 2.2-64. The data report shows void fractions estimated from differential pressure cells placed at 0.305-m (1-ft) intervals. The hydraulic cells in the model do not always have a midpoint in exact

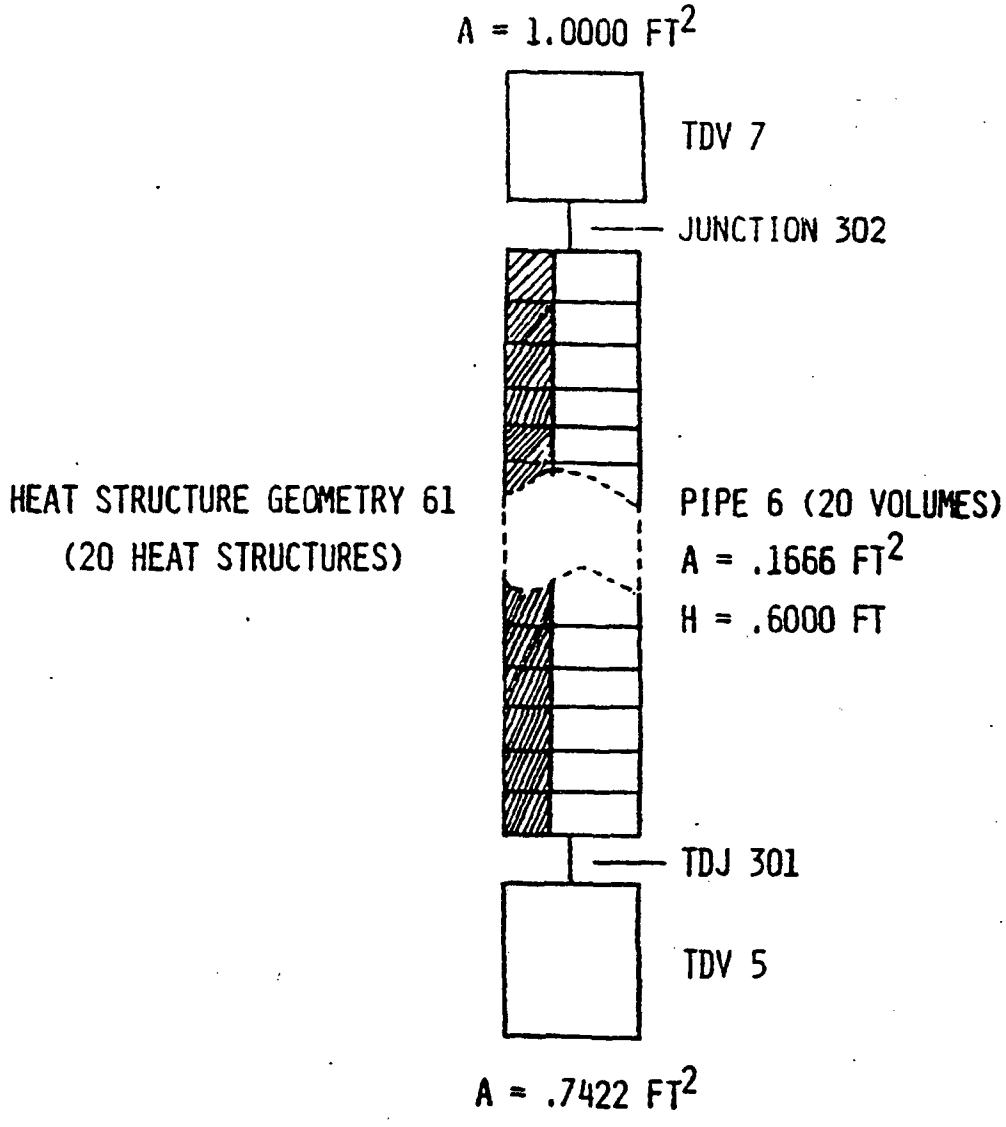

Figure 2.2-56. RELAP5 nodalization for the FLECHT-SEASET forced reflood tests.

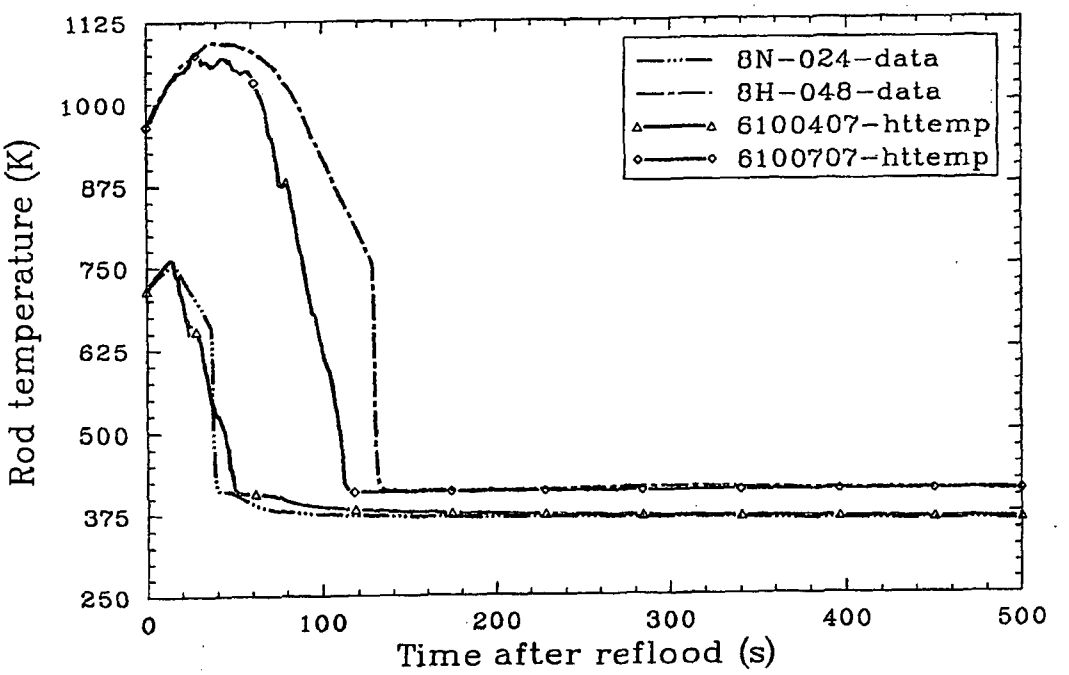

Figure 2.2-57. Measured and RELAP5/MOD3-calculated rod surface temperature histories for the FLECHT-SEASET forced reflood tests at the 0.62- (24-) and 1.23-m (48-in.) elevations.

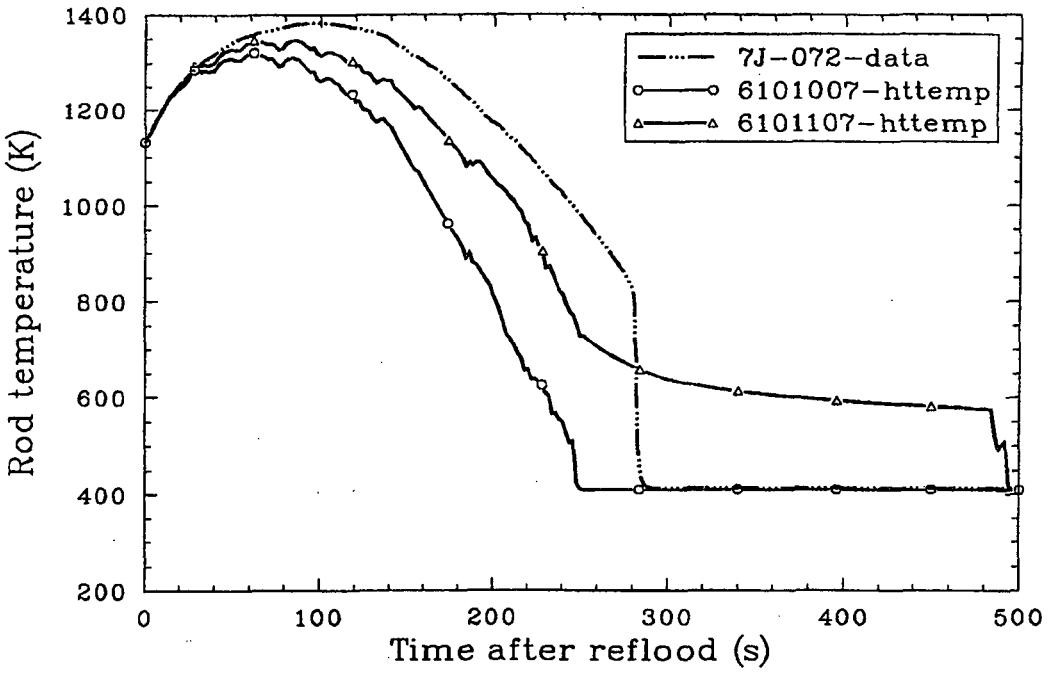

Figure 2.2-58. Measured and RELAP5/MOD3-calculated rod surface temperature histories for the FLECHT-SEASET forced reflood tests at the 1.85-m (72-in.) elevation.

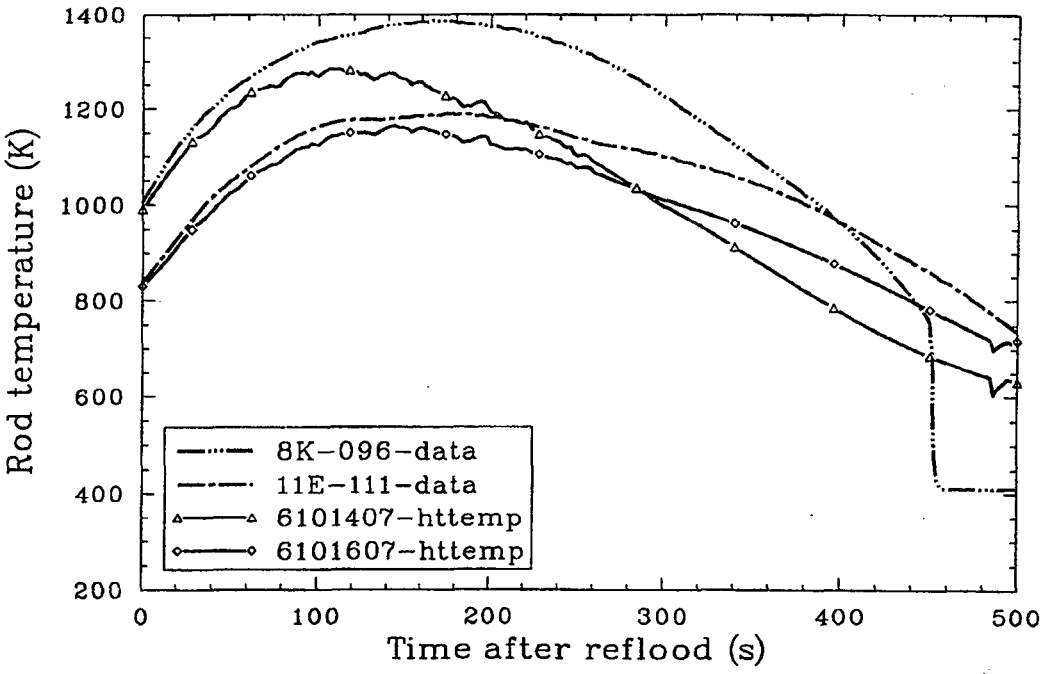

Figure 2.2-59. Measured and RELAP5/MOD3-calculated rod surface temperature histories for the FLECHT-SEASET forced reflood tests at the 2.46- (96-) and 2.85-m (111-in.) elevations.

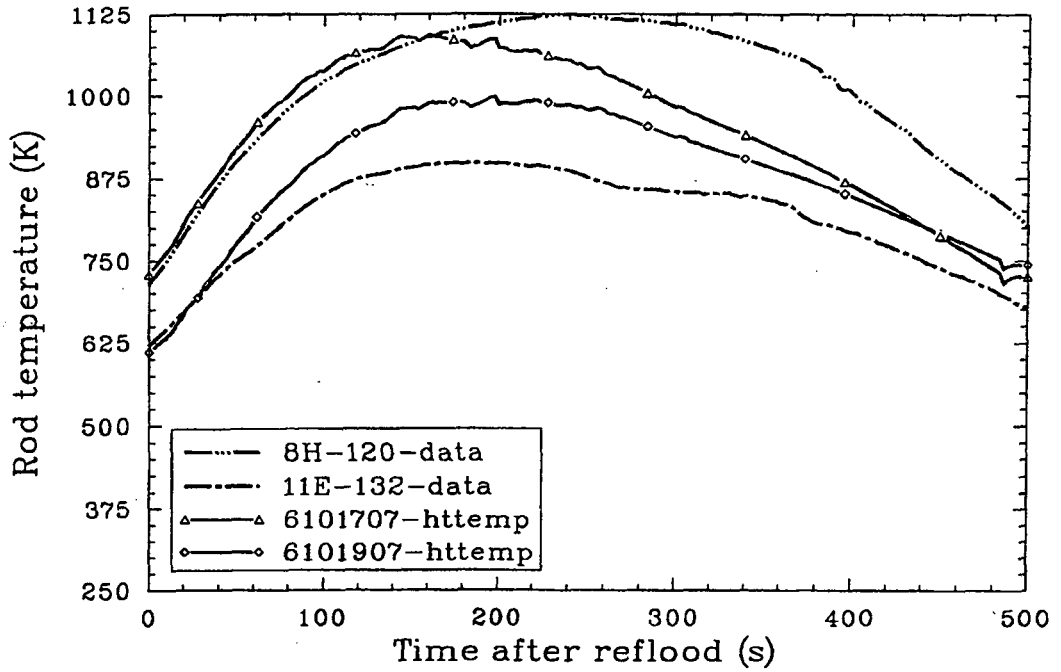

Figure 2.2-60. Measured and RELAP5/MOD3-calculated rod surface temperature histories for the FLECHT-SEASET forced reflood tests at the 3.08- (120-) and 3.38-m (132-in.) elevations.

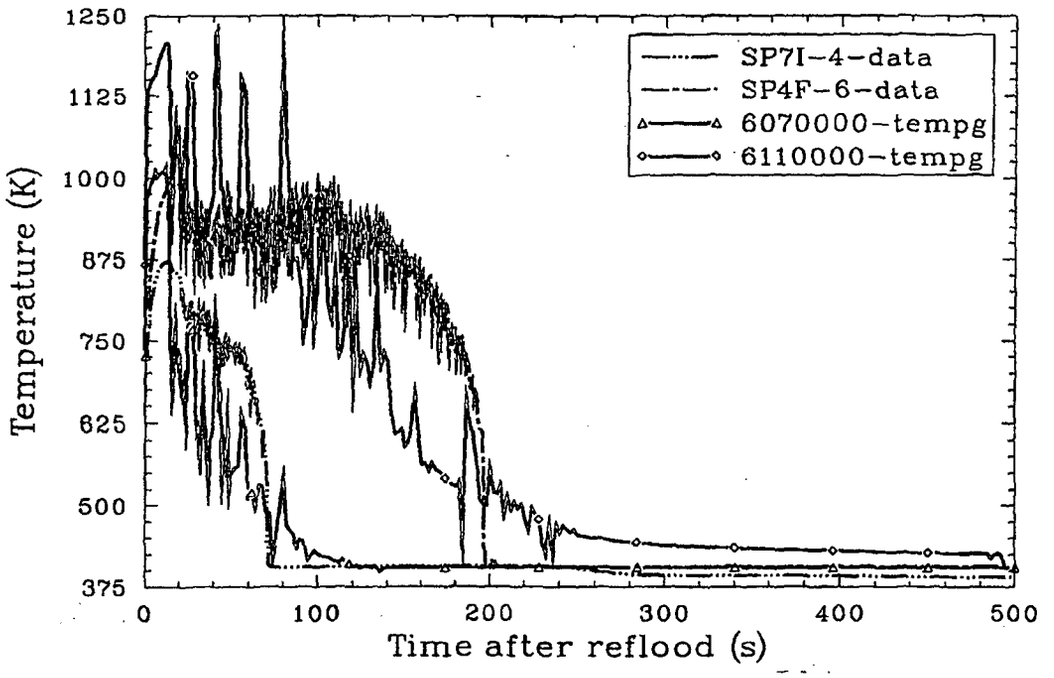

Figure 2.2-61. Measured and RELAP5/MOD3-calculated steam temperatures for the FLECHT-SEASET forced reflood tests at 1.23- (4-) and 1.85-m (6-ft) elevations.

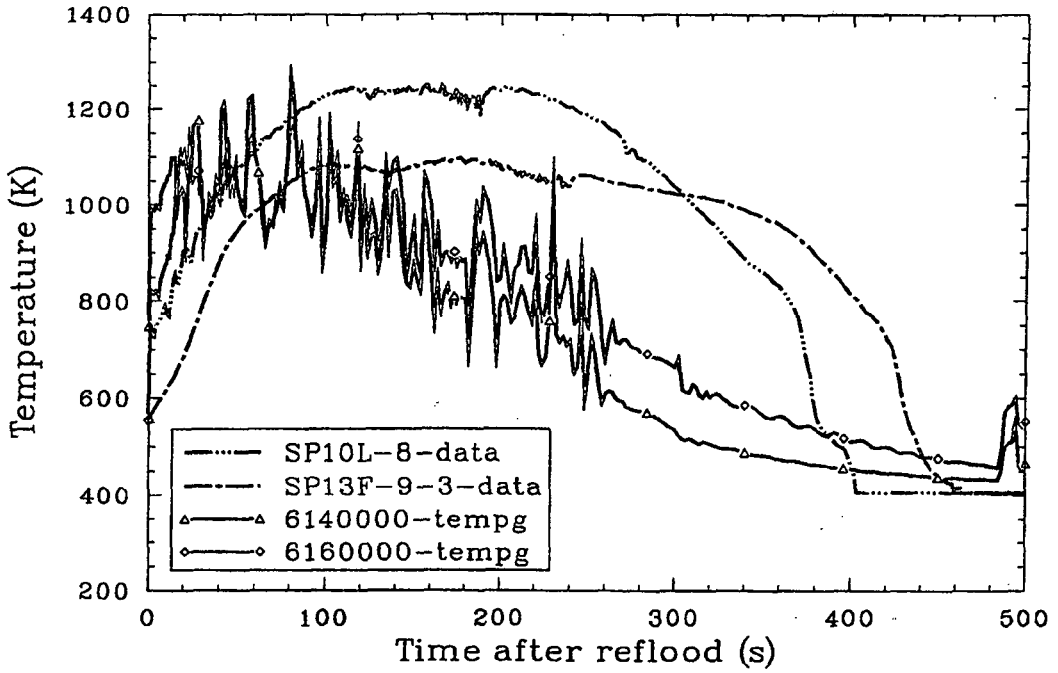

Figure 2.2-62. Measured and RELAP5/MOD3-calculated steam temperatures for the FLECHT-SEASET forced reflood tests at 2.46- (8-) and 2.85-m (9.25-ft) elevations.

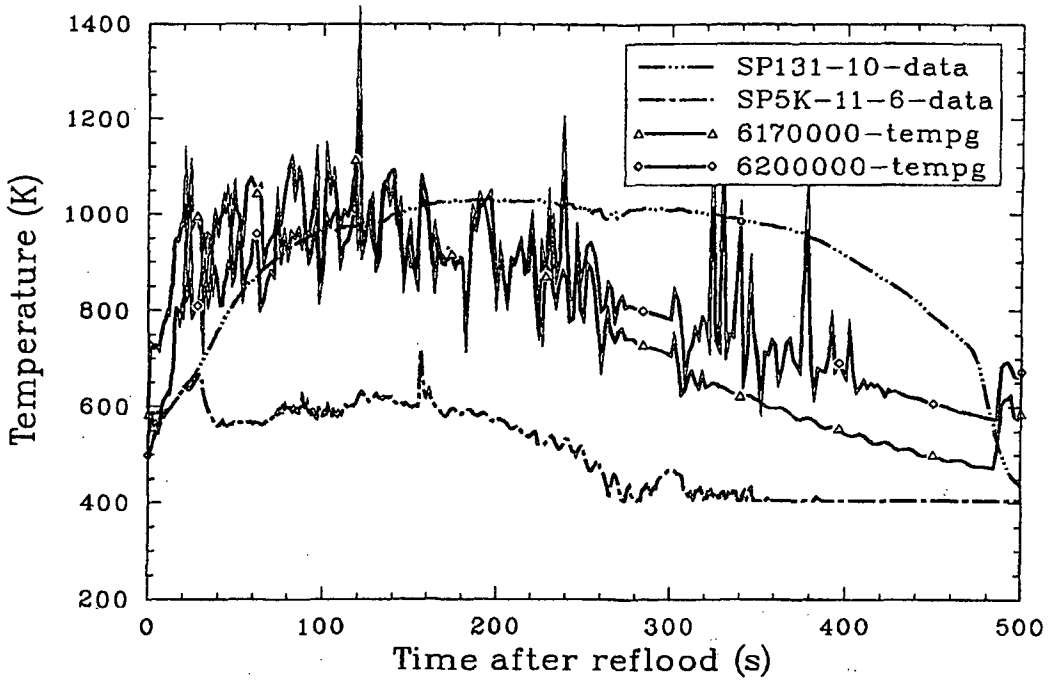

Figure 2.2-63. Measured and RELAP5/MOD3-calculated steam temperatures for the FLECHT-SEASET forced reflood tests at 3.08- (10-) and 3.54-m (11.5-ft) elevations.

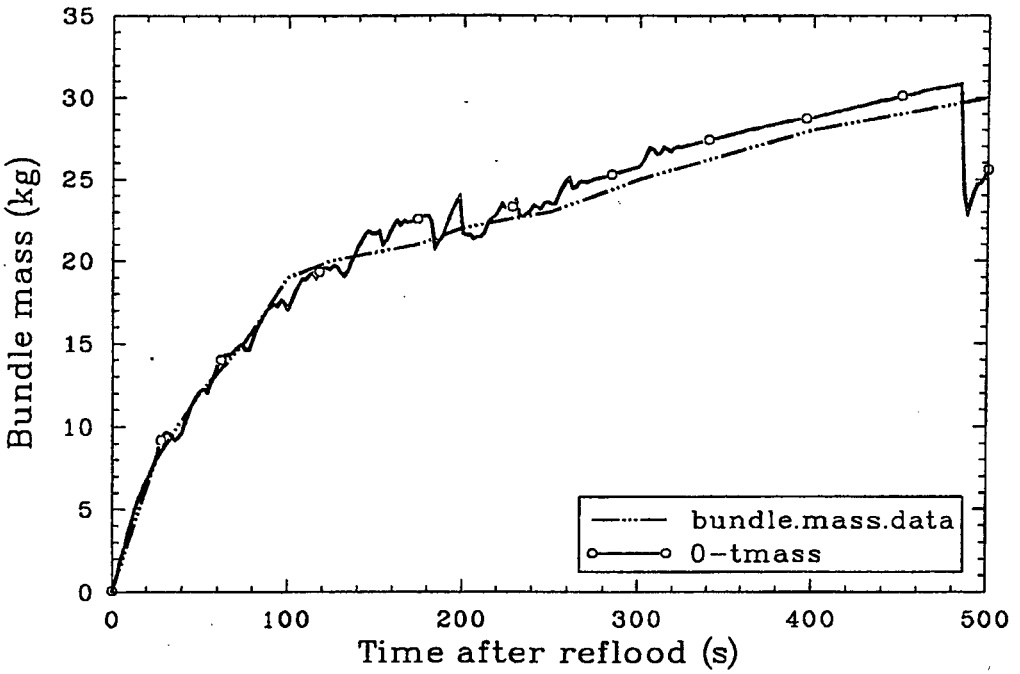

Figure 2.2-64. Measured and RELAP5/MOD3-calculated total bundle mass inventory for the FLECHT-SEASET forced reflood tests.

agreement with the midpoint of the differential pressure measurement. Therefore, two predicted void fractions are sometimes shown in Figures 2.2-65 through 2.2-69.

The predicted initial slope of the heatup rod temperature increase is accurate, but the temperature turnaround occurs too soon. The peak cladding temperature is consequently underpredicted at the midplane by about 60 K. The two calculated temperatures shown in Figure 2.2-58 are on either side of the midplane. After the midplane (cell 10) is calculated to quench at about 250 s, the predicted heat transfer rate in cell 11 decreases because high steam velocities are no longer predicted at elevation 11. This quench behavior illustrates a weakness in the reflood model. How much of the weakness can be attributed to the Chen transition boiling model compared to the interfacial drag model is unknown. The transition boiling correlation is believed to yield values that are too small. Problems with the drag model are manifested by inverted void profiles which move up the bundle as the quench front moves. Figure 2.2-70 shows the axial void profile at 300 s. The total bundle mass is predicted fairly well (as shown in Figure 2.2-64), even though the axial distribution is wrong. At about 480 s, there was a flow surge that upset even the total mass inventory. A mass redistribution also occurred at about 200 s, as shown in Figure 2.2-67; but the mass was not ejected from the bundle.

The calculated rod surface temperatures for Run 31701 are shown in Figures 2.2-71 through 2.2-73. This test uses an injection velocity of 0.16 m/s (6.1 in./s). The calculated results in the lower-to-middle elevations agree well with the data. The calculations from the upper elevations show quenching of this section around 60 s of transient time. This behavior is probably the result of using a vapor heat transfer coefficient that is too large in the transition boiling regime. This causes increased cooling of the heated walls from midplane to the top of the apparatus. This conjecture is further reinforced by the significant lack of liquid in the upper region, which should cause decreased cooling. Instead, the measured and calculated void fraction profiles, shown in Figure 2.2-74,

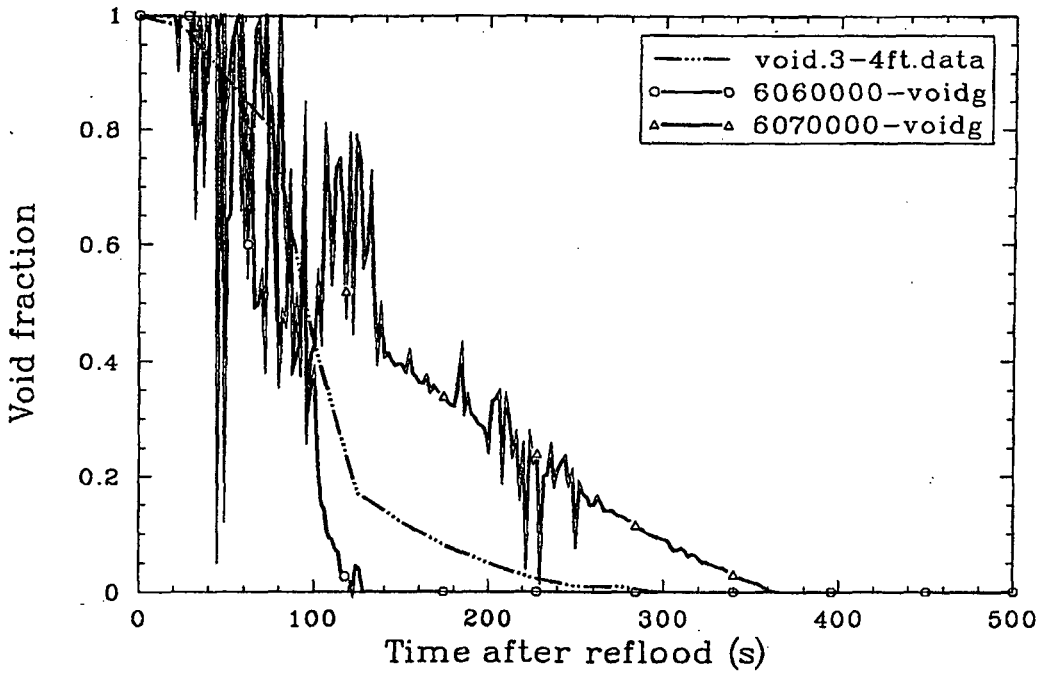

Figure 2.2-65. Measured and RELAP5/MOD3-calculated void fractions at 0.92 to 1.23 m (3 to 4 ft) for the FLECHT-SEASET forced reflood tests.

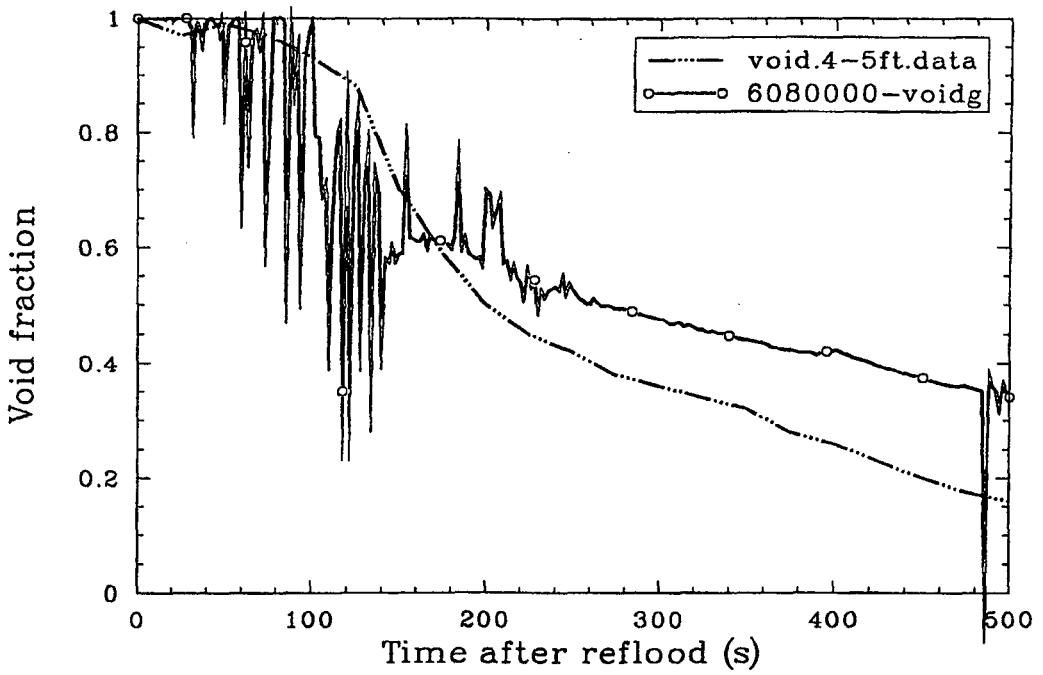

Figure 2.2-66. Measured and RELAP5/MOD3-calculated void fractions at 1.23 to 1.54 m (4 to 5 ft) for the FLECHT-SEASET forced reflood tests.

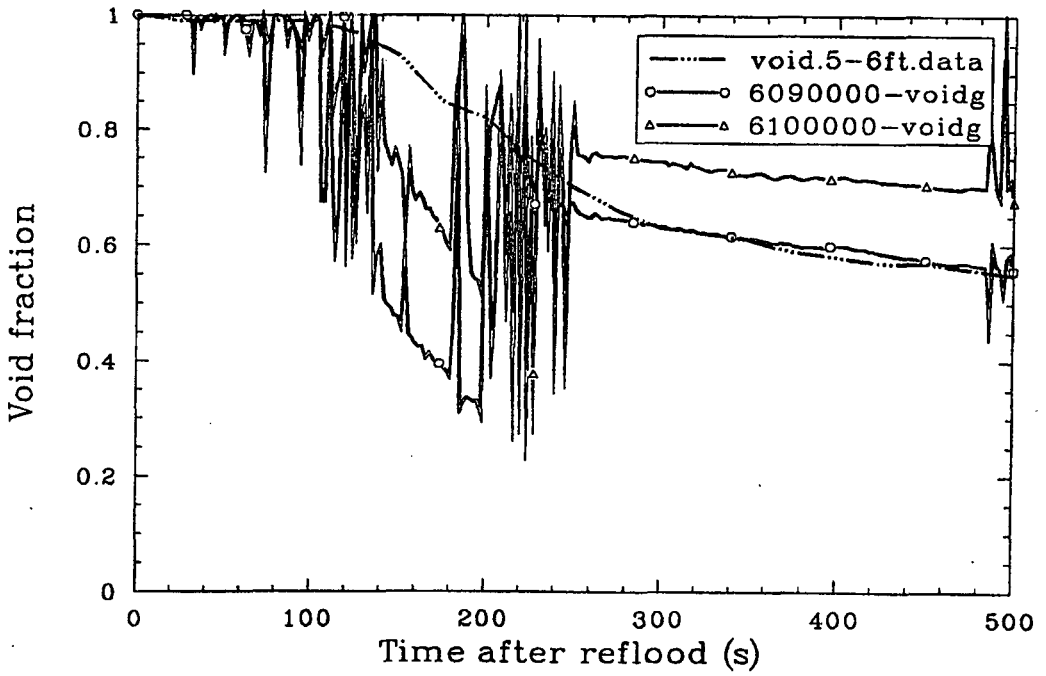

Figure 2.2-67. Measured and RELAP5/MOD3-calculated void fractions at 1.54 to 1.85 m (5 to 6 ft) for the FLECHT-SEASET forced reflood tests.

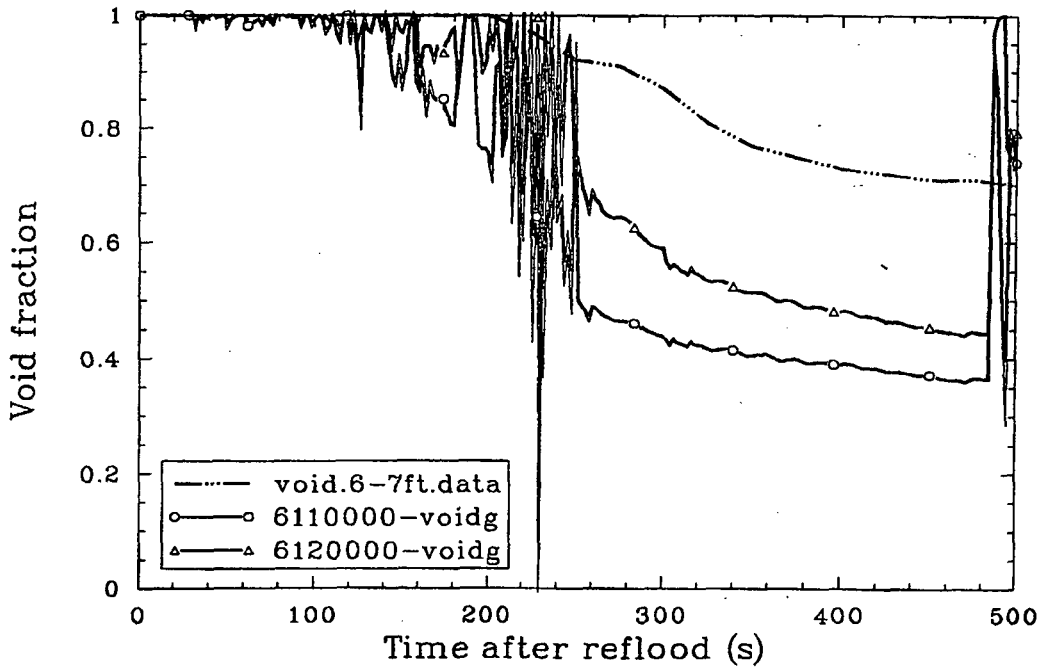

Figure 2.2-68. Measured and RELAP5/MOD3-calculated void fractions at 1.85 to 2.15 m (6 to 7 ft) for the FLECHT-SEASET forced reflood tests.

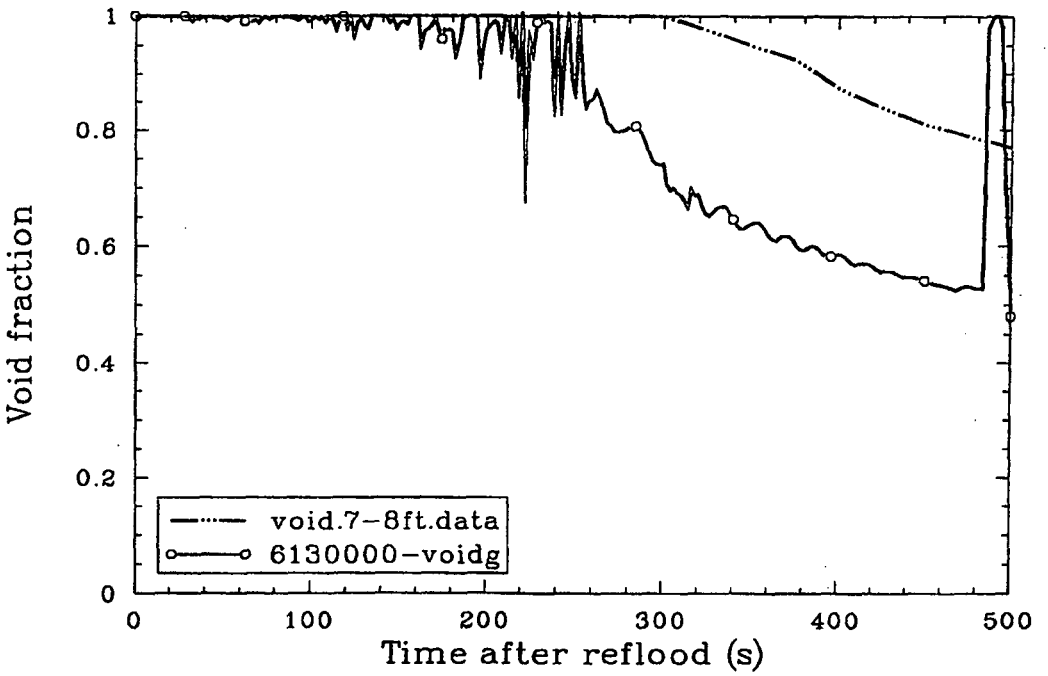

Figure 2.2-69. Measured and RELAP5/MOD3-calculated void fractions at 2.15 to 2.46 m (7 to 8 ft) for the FLECHT-SEASET forced reflood tests.

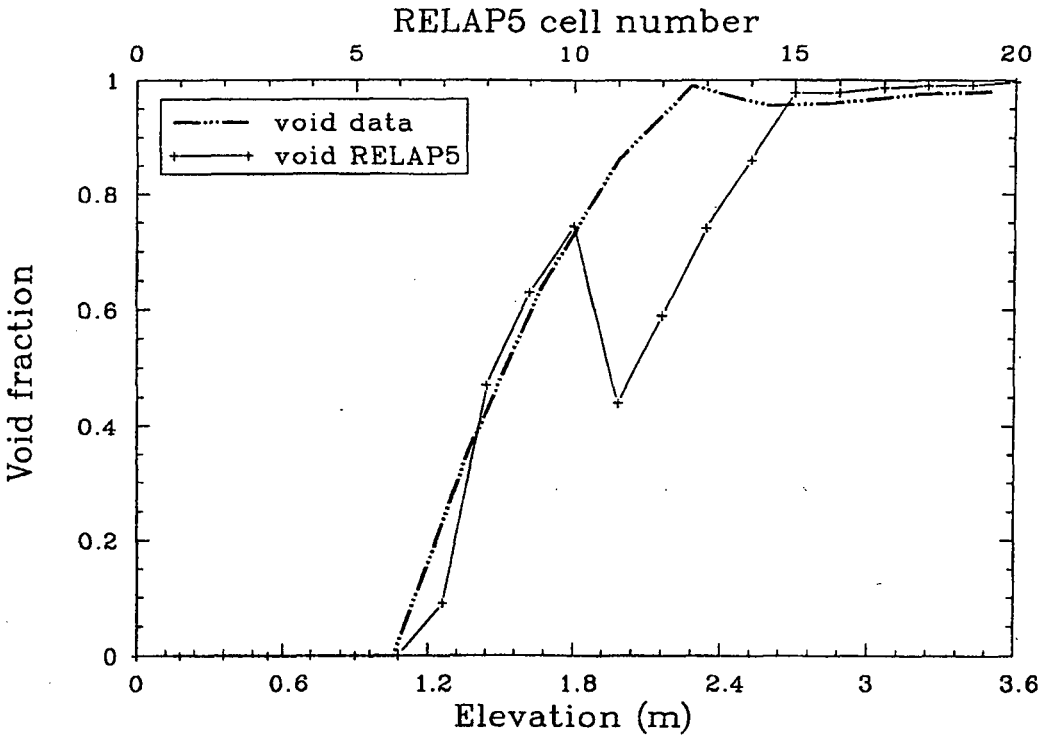

Figure 2.2-70. Measured and RELAP5/MOD3-calculated axial void profile at 300 s for the FLECHT-SEASET forced reflood tests.

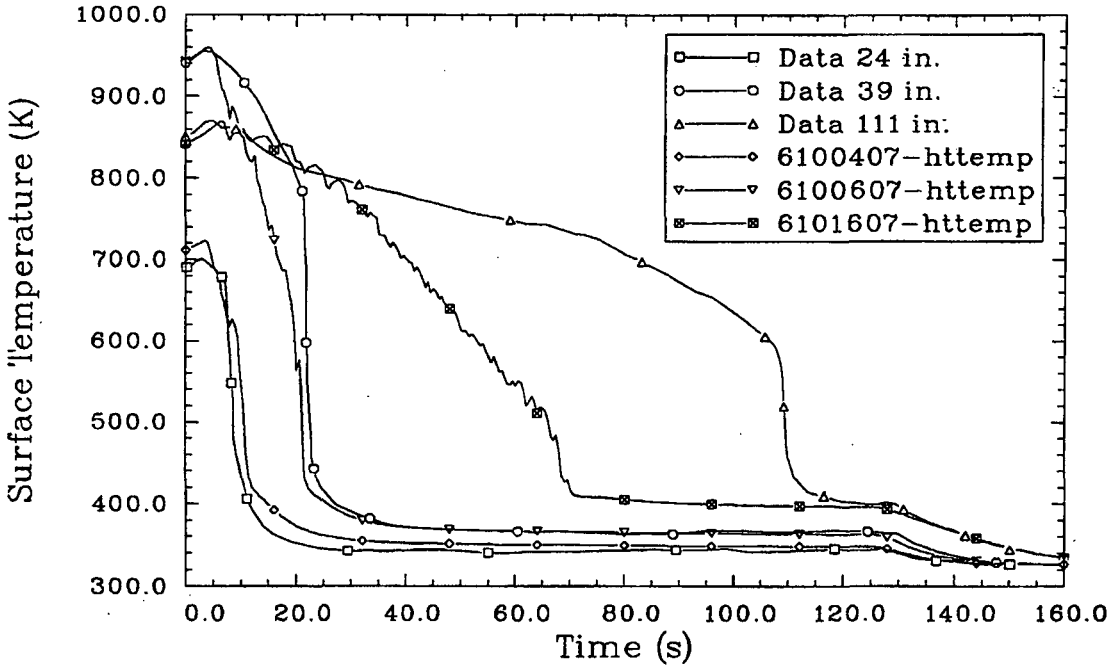

Figure 2.2-71. Measured and RELAP5/MOD3-calculated rod surface temperatures for the FLECHT-SEASET forced reflood test run 31701 at the 0.62- (24-), 1.0- (39-), and 2.85-m (111-in.) elevations.

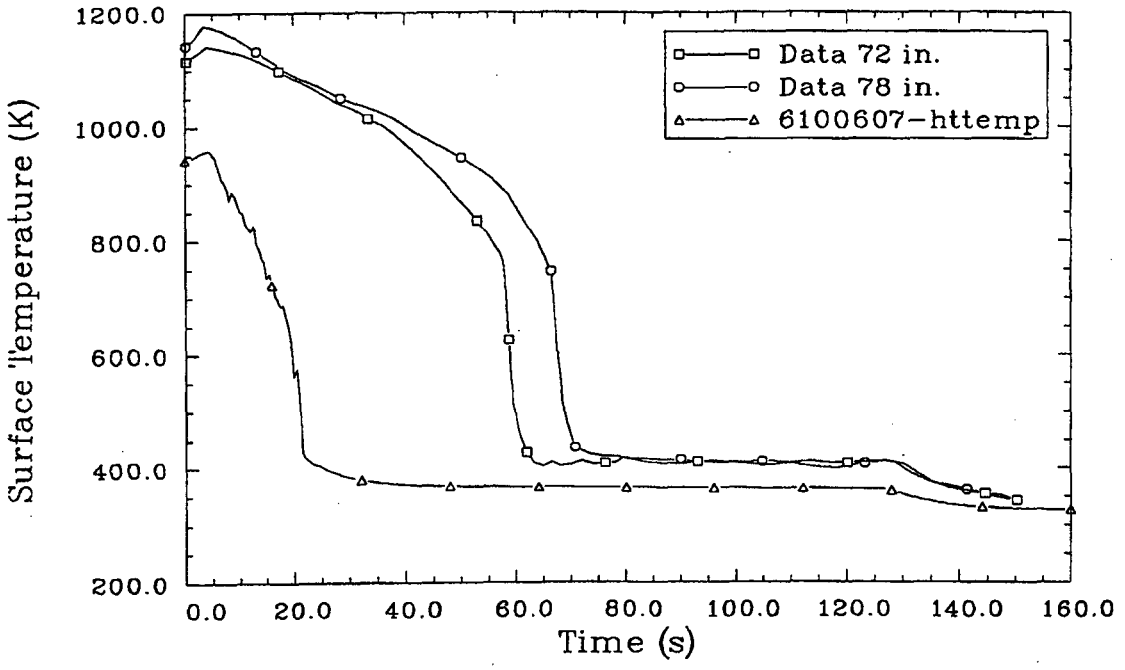

Figure 2.2-72. Measured and RELAP5/MOD3-calculated rod surface temperatures for the FLECHT-SEASET forced reflood test run 31701 at the 1.85- (72-) and 2.0-m (78-in.) elevations.

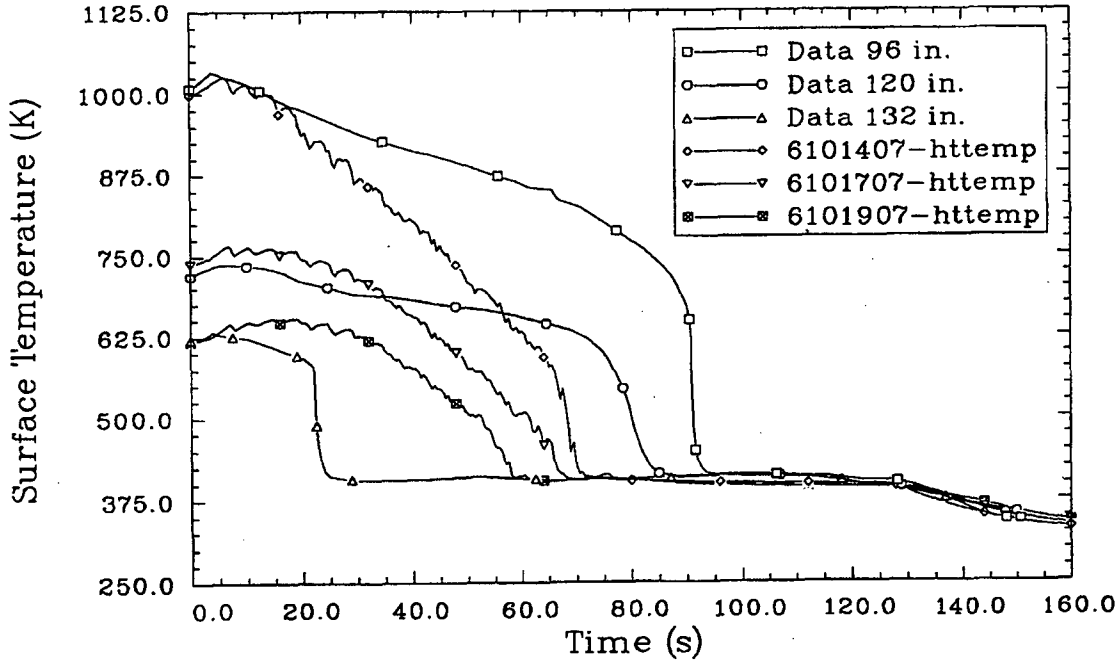

Figure 2.2-73. Measured and RELAP5/MOD3-calculated rod surface temperatures for the FLECHT-SEASET forced reflood test run 31701 at the 2.46- (96-), 3.08- (120-) and 3.38-m (132-in.) elevations.

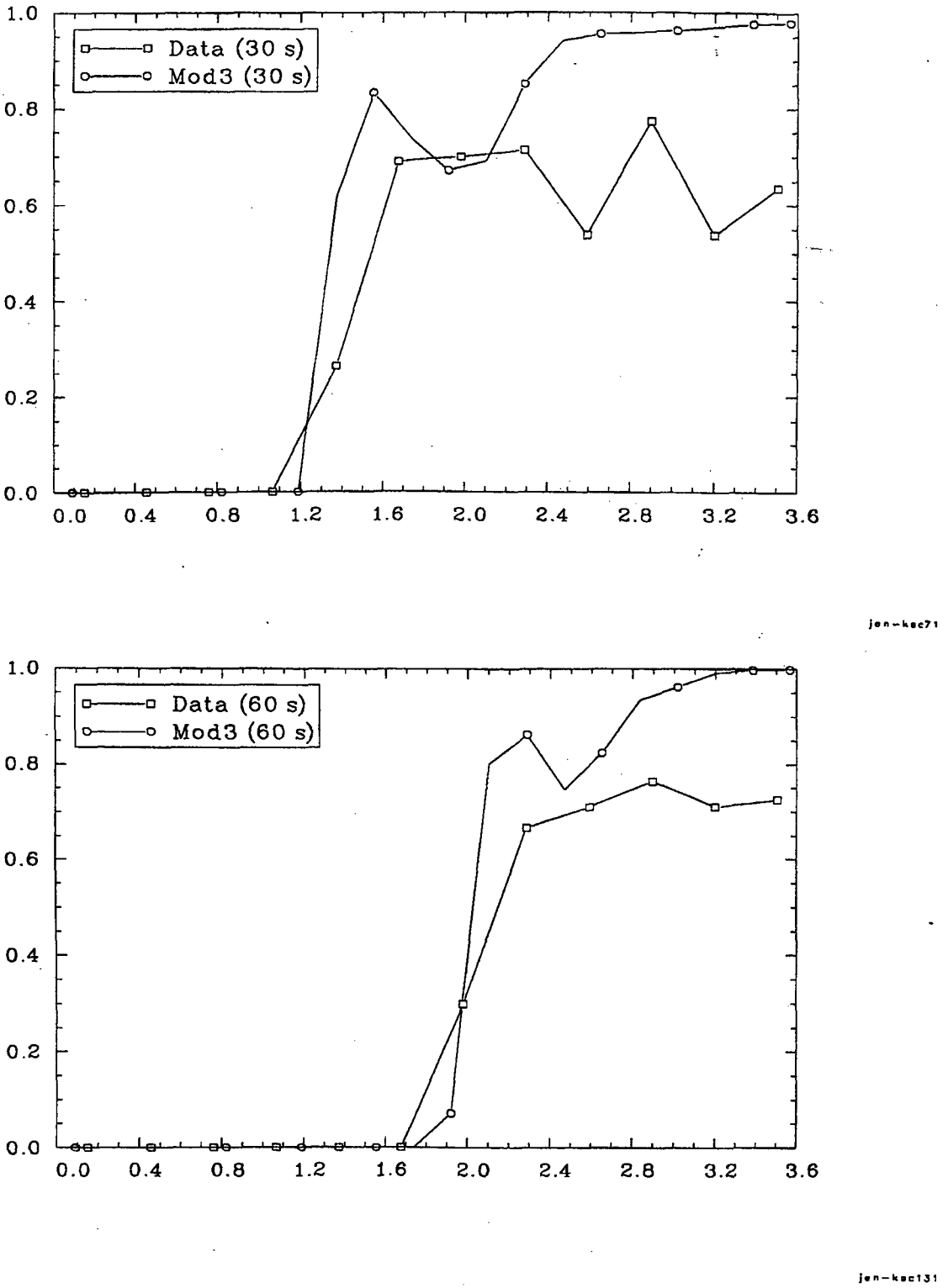

Figure 2.2-74. Measured and RELAP5/MOD3-calculated void fraction profiles for the FLECHT-SEASET forced reflood test run 31701.

clearly show the experimental apparatus containing more liquid in the upper region than the calculation.

In summary, the models in RELAP5/MOD3 that are active during reflood result in increased cooling at the upper elevations. The discrepancies between the measured and calculated cooling are a function of both incorrect void fraction profiles and incorrect vapor cooling in dispersed flow. However, the peak cladding temperature prediction on the two tests compared was not unreasonable considering the difficulty of the problem.

2.2.15 UCSB Reflux Condensation and Natural Circulation Tests 101 and 309

The University of California at Santa Barbara (UCSB) Reflux Condensation and Natural Circulation Tests 101 and 309[2.2-19] involve a closed-loop apparatus, as shown in Figure 2.2-75, which consisted of a U-tube test section (riser, U bend, and downside), cold leg, and boiler. The riser and downside were both cooled by subcooled water entering a jacket from the bottom and leaving at the top. The tests were initiated when power to the boilers were turned on. The data from these tests and other tests listed in Reference 2.2-19 are useful in understanding the mechanisms governing heat removal and liquid holdup in the primary side of steam generators in PWRs. A detailed description of the test facility is given in Reference 2.2-19.

For the two-phase situation, several flow regimes may occur. In the first, as steam generated in the boiler flows to the condensing tubes, which contains relatively cold water on their secondary sides, it condenses; and the condensate flows back countercurrent to the steam flow. This countercurrent flow of steam and water in the tubes is called reflux condensation. Under certain conditions, the steam condensate may be carried along cocurrently with the steam. This pattern is called natural circulation or, more accurately, the carryover mode, implying cocurrent flow of steam and water. The third possibility is that the flow may oscillate between reflux condensation and natural circulation. The purpose of

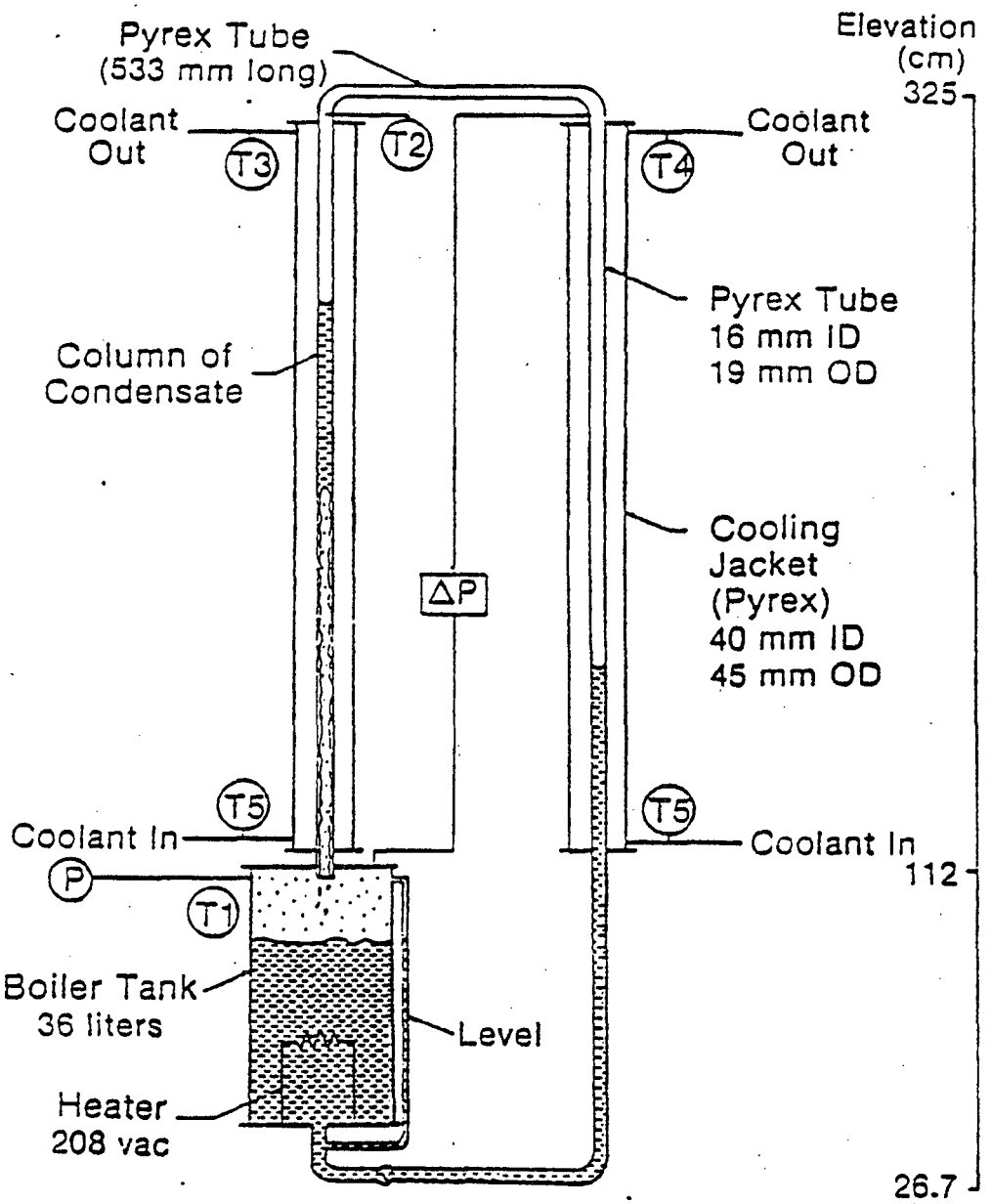

Figure 2.2-75. Schematic diagram for UCSB reflux condensation and natural circulation tests 101 and 309.

modeling these tests is to assess the ability of RELAP5/MOD3 to predict reflux condensation, natural circulation, and the oscillatory mode.

Test 101 was reported to have been carried out without noncondensable gas. Examination of the pressures and temperatures indicate that not all of the noncondensable gas was removed and that some was present during the tests, particularly in the top of the downside tube. The cooling water flow rate in each water-cooled jacket was 12.5 mL/s, and the power delivered to the boiler was 2.03 kW. The test lasted 4.9 h. Test 309 was carried out with the presence of noncondensable gas. The gas was 0.03 moles of air. For this test, the cooling water flow rate in each water-cooled jacket was 25 mL/s and the power delivered to the boiler was 2.11 kW. The test lasted 4 h.

The RELAP5 model for the UCSB test facility for Test 101 is shown in Figure 2.2-76. The U-tube test section was modeled using a 10-volume pipe for the riser portion, a 3-volume pipe for the top U bend, and a 10-volume pipe for the downside portion. The Pyrex walls in the riser and downside portions were modeled using ten heat structures, each of which had six radial mesh points. The annular water jackets in the riser and downside portions were modeled using 10-volume pipes. The inlets to the water jackets were modeled using time-dependent junctions with a velocity corresponding to a volume flow rate of 12.5 mL/s. The water entering the riser jacket came from a time-dependent volume containing subcooled water at 0.1 MPa and 297 K. A temperature gradient was inputted in the riser jacket, with the temperature in the top set to 338 K, which is the value of the first data point. It was concluded that the noncondensables were probably present in the downside part of the U tube. Thus, in order to obtain a reasonable pressure in the downside, a higher-than-measured temperature was inputted in the downside jacket. The water entering the downside jacket came from a time-dependent volume containing subcooled water at 0.1 MPa and 352 K. A temperature gradient was inputted in the downside jacket, with the temperature in the top set to 358 K.

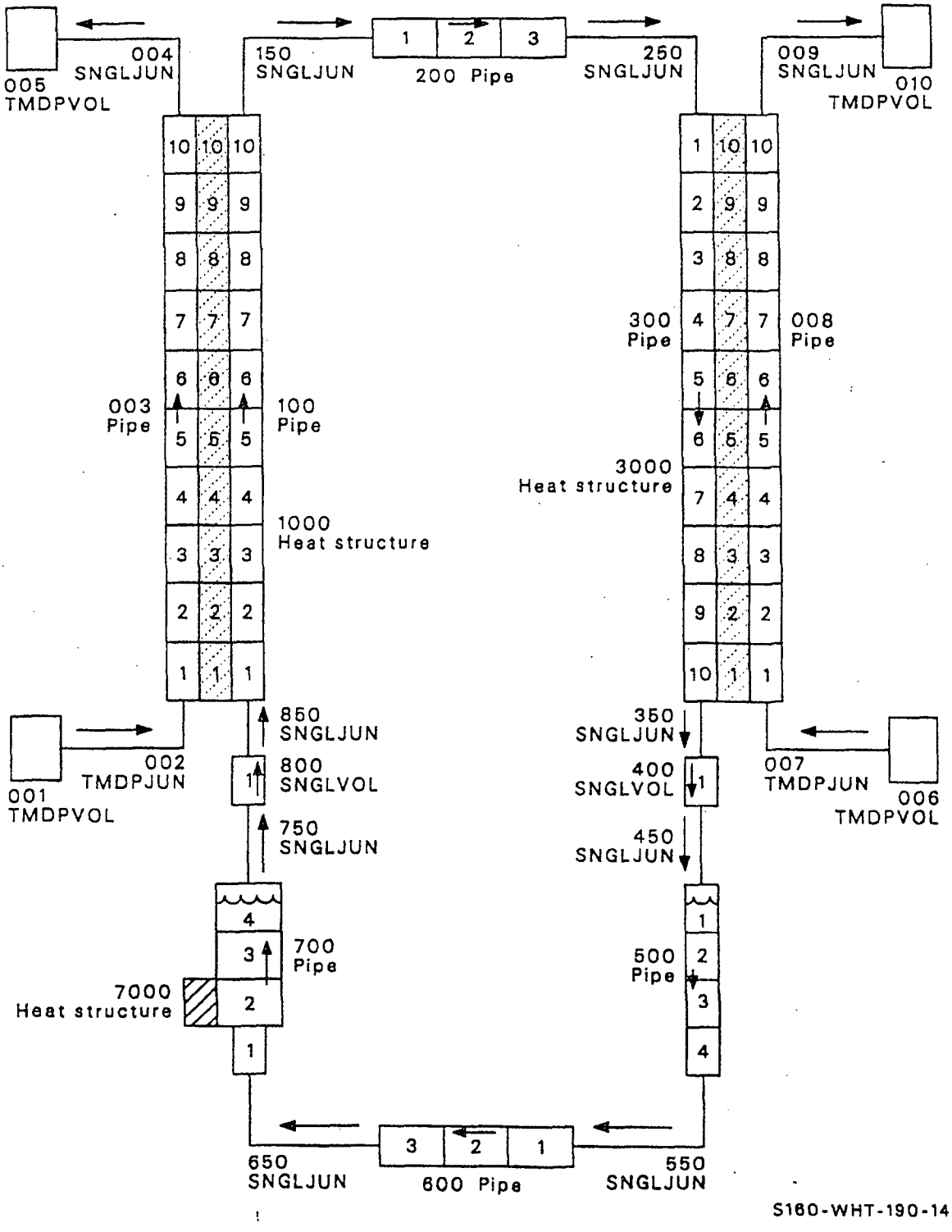

Figure 2.2-76. RELAP5 nodalization diagram for UCSB reflux condensation and natural circulation tests 101 and 309.

The boiler section was modeled using the top three volumes of a 4-volume pipe (component 700). The heating element was modeled as a single heat structure attached to the bottom volume of these three volumes. This heat structure contained three mesh points and a source corresponding to the power delivered to the boiler (2.03 kW). The cold leg was modeled using four volumes for the downside portion (component 500), three volumes for the bottom horizontal portion (component 600), and one volume for the riser portion (volume 1 of component 700). The U-tube, boiler, and cold leg sections were initialized with a pressure of 62.308 kPa, which is the value of the first data point for the boiler pressure. The temperatures were set to saturation throughout these sections. The data report[2.2-19] indicated that the boiler liquid volume was between 30 and 31 L, so it was set to 30.5 L, with liquid in cold leg up to the same level on the downside. The calculation ran very slowly with the vertical stratification and water packer models on, so both were turned off.

The RELAP5 model for the UCSB test facility for Test 309 is the same as for Test 101 except for the initial conditions. The time-dependent junctions at the inlet to water jackets had velocities corresponding to a volume flow rate of 25 mL/s. The water entering both riser and downside jackets came from time-dependent volumes containing subcooled water at 0.1 MPa and 294 K. No temperature gradient was initially input, and this pressure and temperature were input throughout the riser and downside jackets. The heat structure containing the power to the boiler had a source of 2.11 kW. As in Test 101, the U-tube, boiler, and cold leg sectors were initialized with a pressure of 62.308 kPa, and the liquid volume in the boiler was set at 30.5 L. The temperature in the vapor portion was set to 353.46 K, which is the temperature necessary for 0.03 miles of air to be present in the vapor space using the ideal gas law. Both steam and air were assumed to be present in the vapor space. The same temperature (353.46 K) was used in the liquid volumes, which turned out to be slightly subcooled (saturation temperature = 360.08 K). The calculation failed at 5 s due to a water property error with the water packer and vertical stratification models on. The calculation ran past 1000 s with both models turned off.

The simulation for Test 101 was carried out to 840 s on MOD3 and 832 s on MOD2. The MOD3 calculation was stopped at this time so that it would be comparable to MOD2. The minor edits used to derive the plots had only written out to 510 s; thus, the plots only go to 510 s. However, the remaining major edit points are indicated with an X.

Comparisons of RELAP5/MOD3, MOD2, and the data are shown in Figures 2.2-77, 2.2-78, and 2.2-79. Figure 2.2-77 shows the comparison for the pressure in the top of the boiler. The MOD3 calculation is slightly higher than the data, whereas the MOD2 calculation is slightly lower than the data; however, both increase with time. Figure 2.2-78 shows the comparison for the pressure drop between the top of the boiler and the top of the riser. Following an initial transient, the calculation settles down to a value of -9000 Pa for MOD3 and -5500 Pa for MOD2. Neither calculation increases with time. Examination of these calculations indicates that fluid is flowing counterclockwise in the loop, with no buildup of liquid occurring in the riser portion (as was seen in the data). Thus, the calculations show no change in the pressure drop, while the data show an increase. It is believed that this counterclockwise circulation is caused by the high temperature imposed in the downside water jacket to account for the leakage of noncondensable. At this time, there appears to be no way around the problem of noncondensables leaking into Test 101. Finally, Figure 2.2-79 shows the comparison for the temperature in the top of the riser water jacket. Here, both MOD3 and MOD2 calculations remain fairly constant while the data are dropping sharply with time.

The MOD3 simulation for Test 309 was carried out to 1035 s before the code failed with a singular matrix. This is considerably better than MOD2, which ended at 3 s due to a water property failure. The plots are shown to 1000 s and only show MOD3 results. Figure 2.2-80 shows the comparison for the pressure in the top of the boiler. The data increase slowly with time, whereas the calculation increases rapidly with time. Figure 2.2-81 shows the comparison for the pressure drop between the top of the boiler and the top of the riser. The calculation settles down to a value of 1200 Pa and does not rise as the data rise. Finally, Figure 2.2-82 shows the comparison

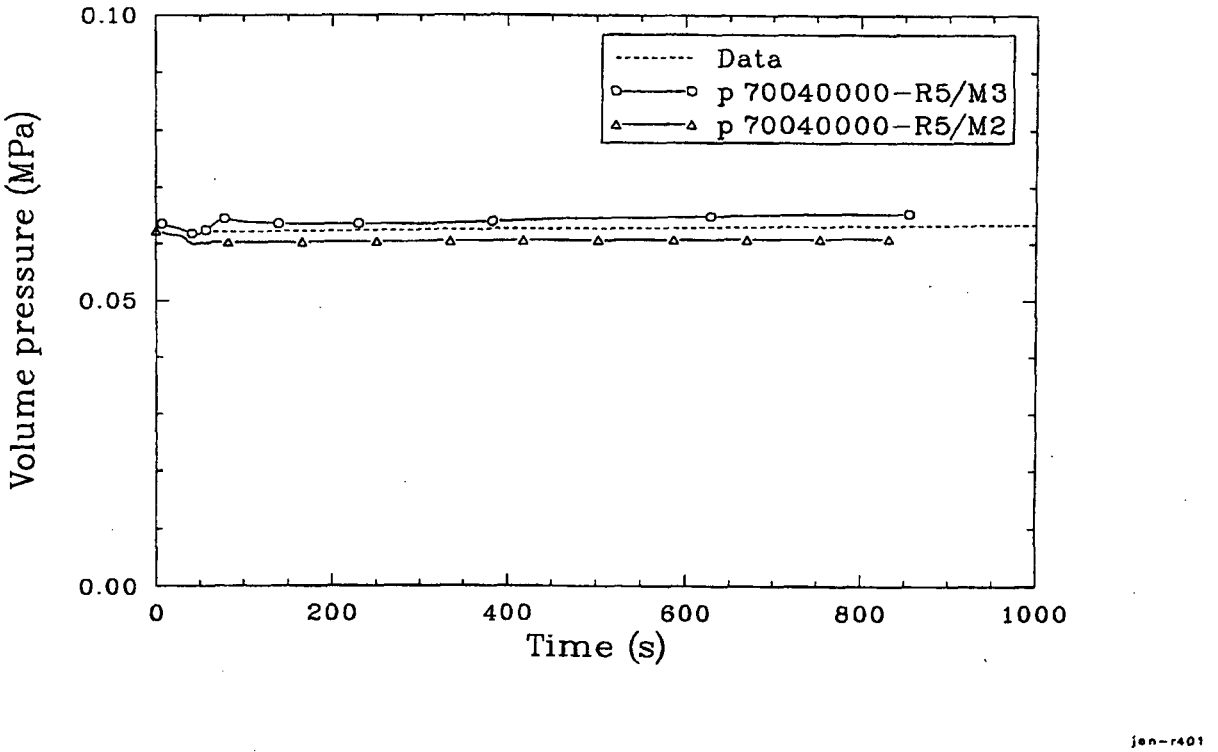

Figure 2.2-77. Measured and calculated (RELAP5/MOD2, MOD3) pressure in the top of the boiler for the UCSB reflux condensation and natural circulation test 101.

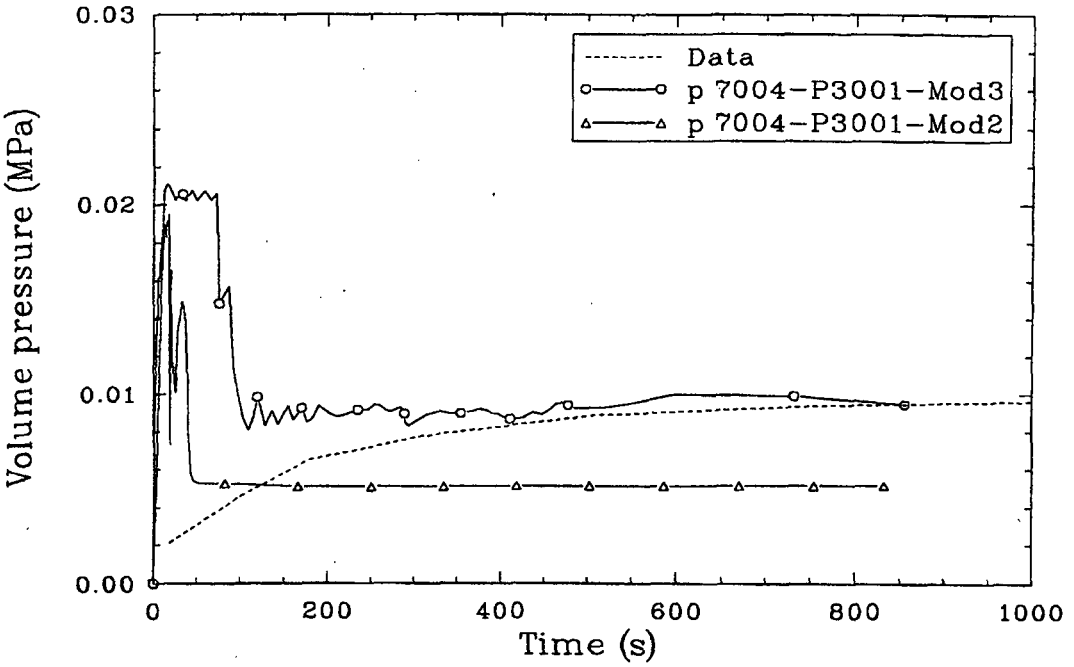

Figure 2.2-78. Measured and calculated (RELAP5/MOD2, MOD3) pressure drop between the top of the boiler and the top of the riser for the UCSB reflux condensation and natural circulation test 101.

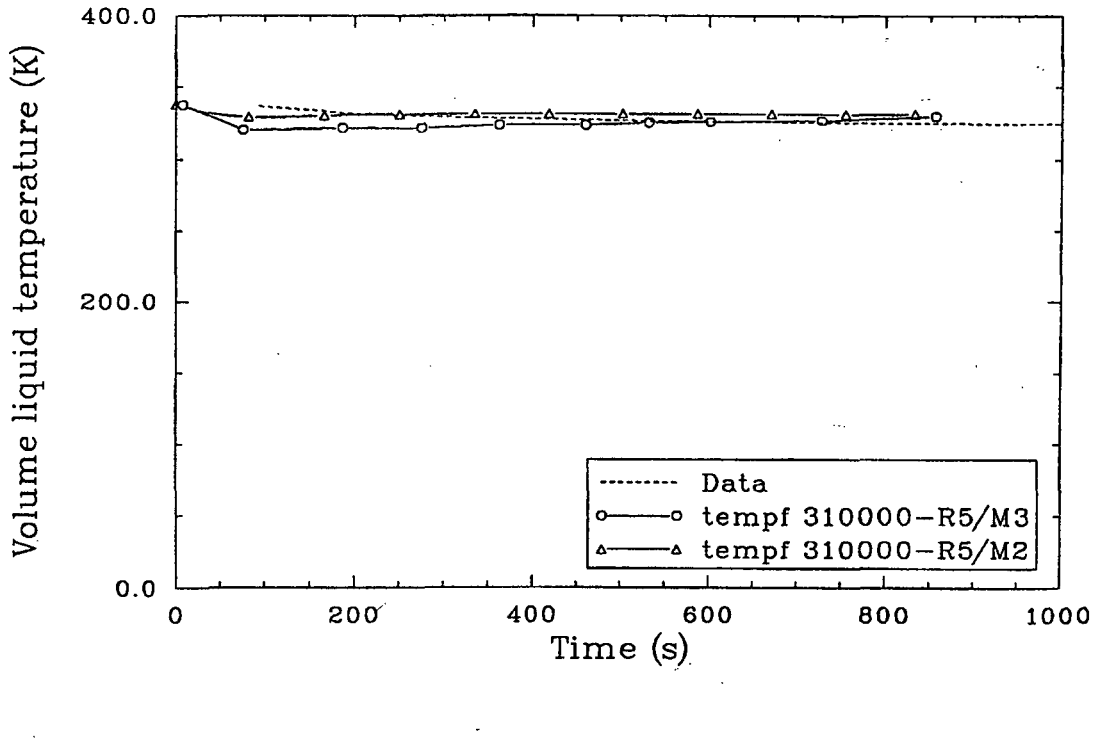

Figure 2.2-79. Measured and calculated (RELAP5/MOD2, MOD3) temperature in the top of the riser water jacket for the UCSB reflux condensation and natural circulation test 101.

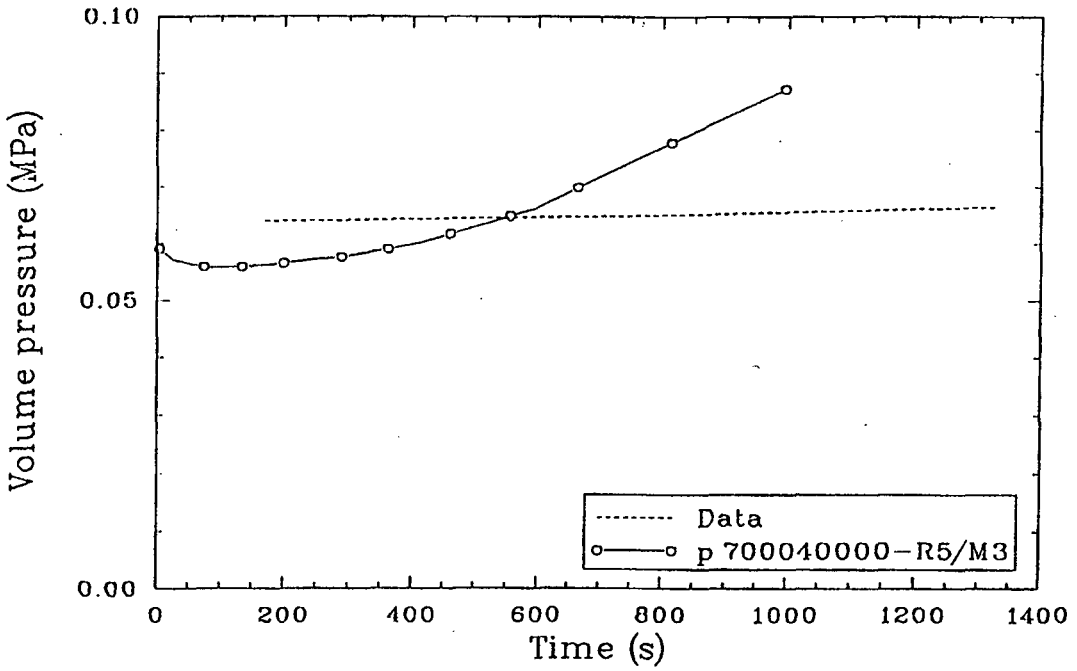

Figure 2.2-80. Measured and calculated (RELAP5/MOD2, MOD3) pressure in the top of the boiler for the UCSB reflux condensation and natural circulation test 309.

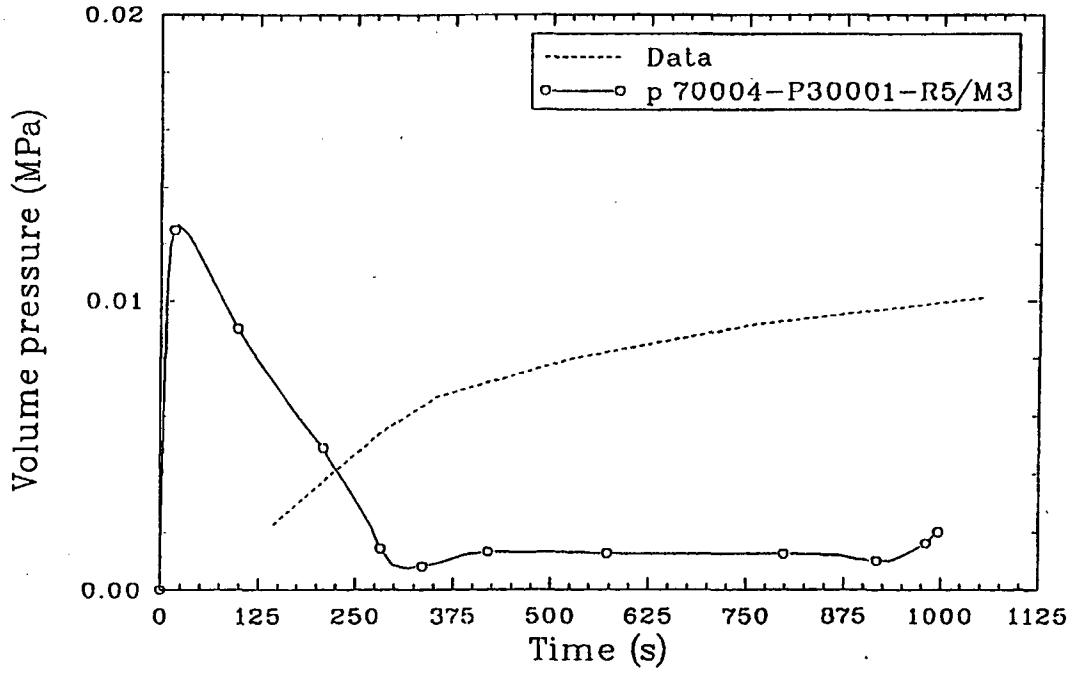

Jan-1441

Figure 2.2-81. Measured and calculated (RELAP5/MOD2, MOD3) pressure drop between the top of the boiler and the top of the riser for the UCSB reflux condensation and natural circulation test 309.

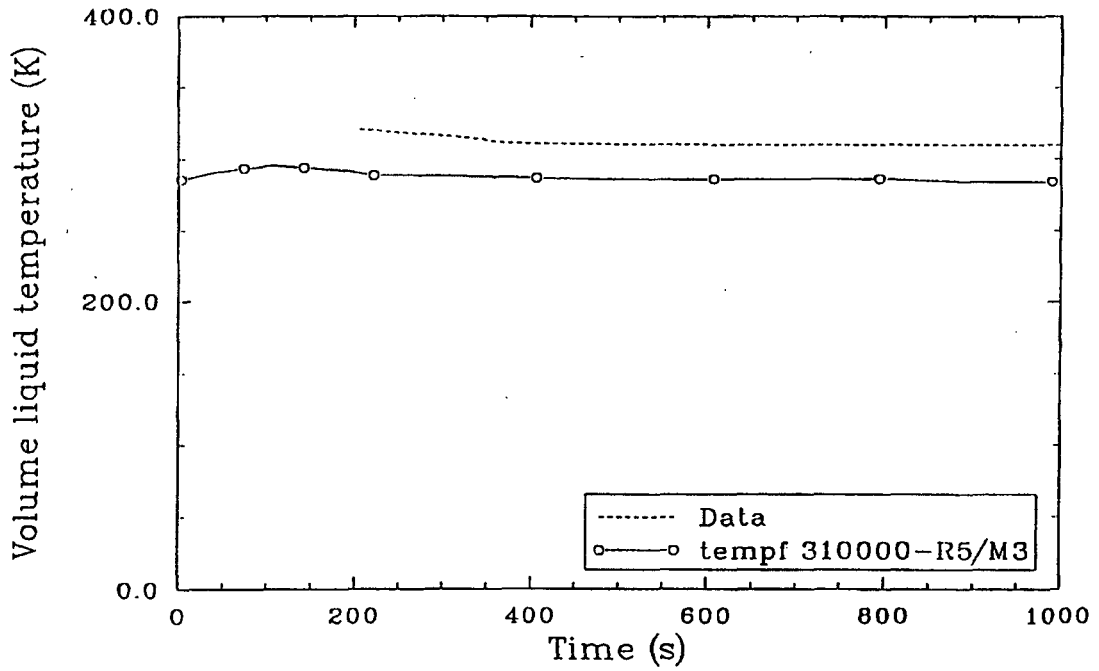

Figure 2.2-82. Measured and calculated (RELAP5/MOD2, MOD3) temperature in the top of the riser water jacket for the UCSB reflux condensation and natural circulation test 309.

for the temperature in the top of the riser water jacket. The data drop slightly with time, while the calculation needs to be rerun with temperature gradients in the riser and downside jackets.

For Test 101, the MOD3 calculation was run to 840 s on Version 461, using the Masscomp, and required 78573 attempted advancements and 159692 cpu seconds. For Test 101, the MOD2 calculation was run to 832 s on Cycle 11, using the Cyber, with an update that adds NPA refinements (RJWX011); it required 65646 attempted advancements and 4304 cpu seconds. For Test 309, the MOD3 calculation was run to 1035 s on Version 461, using the Masscomp, and required 11521 attempted advancements and 36491 cpu seconds.

2.2.16 UPTF Downcomer Countercurrent Flow Test 6

UPTF is a full-scale model of a four-loop, 1300-MWe PWR, including the reactor vessel, downcomer, lower plenum, core simulation, upper plenum, and four loops with pump and steam generator simulation. The thermal-hydraulic feedback of the containment is simulated. A schematic view of the test facility is shown in Figure 2.2-83. The test vessel, core barrel, and internals are a full-size representation of a PWR, with four full-scale hot and cold legs simulating three intact loops and one broken loop.

Test No. 6,[2.2-20] a quasi-steady-state experiment, was carried out to obtain full-scale data on downcomer/lower plenum refill behavior, which provides a counterpart to testing in scaled facilities. In this test, predetermined steam and ECC water at nearly saturated conditions were injected to determine the penetration of ECC water into the downcomer and lower plenum as a function of steam flow up the downcomer, as was done in the scaled ECC bypass facilities.

The RELAP5 nodalization used to simulate Test 6 is shown in Figure 2.2-84. A split downcomer was modeled, using components 111, 112, 121, and 122, which are annulus components (assumes no liquid drops exist when in annular mist flow). The annuli were linked using single junction 118 and multiple junction 119. The core and hot legs are lumped into one

SIEMENS

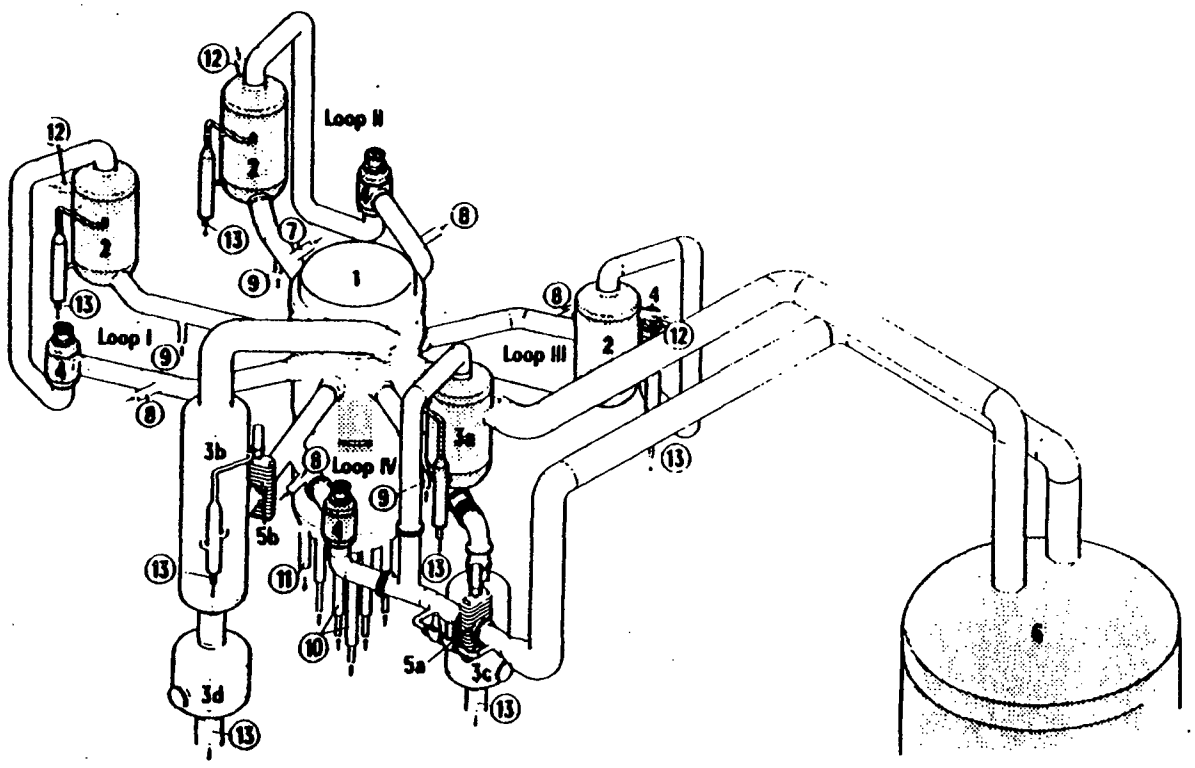

1 Test Vessel
2 Steam Generator Simulator (Intact Loop)
3a Steam Generator Simulator/ Water Separator (Broken Loop Hot Leg)
3b Water Separator (Broken Loop Cold Leg)
3c Drainage Vessel for Hot Leg
3d Drainage Vessel for Cold Leg
4 Pump Simulator
5a Break Valve (Hot Leg)
5b Break Valve (Cold Leg)
6 Containment Simulator
(7) Surgeline-Nozzle
(8) ECC-Injection Nozzles (Cold Leg)
(9) ECC-Injection Nozzles (Hot Leg)
(10) Core Simulator Injection Nozzle
(11) TV-Drainage Nozzle
(12) Steam Injection Nozzle
(13) Drainage Nozzle
Simulator

Figure 2.2-83. Schematic of the Upper Plenum Test Facility (UPTF).

.2-112 missing

This page was missing from the originally scanned document.

volume (volume 180). The four cold legs are modeled separately (components 390, 490, 500, and 690). The lower plenum was modeled using volume 150. The calculation was carried out to 30 s, using conditions of Run 133 of Test 6 (see Reference 2.2-20).

As a measure of the downcomer penetration in RELAP5/MOD3, the void fraction in the lower plenum is plotted in Figure 2.2-85. The plot labeled "ANNULUS/WALLIS" uses the recommended RELAP5/MOD3 approach; i.e., an annulus for the downcomer and the Wallis correlation for the film when in the annular mist flow regime. At 30 s, the void fraction dropped to 0.80, indicating that downcomer penetration was beginning. Next, components 111 and 121 were replaced with branch components; components 112 and 122 were replaced with pipe components; and the Bharanthan correlation was used instead of the Wallis correlation for the film when in the annular mist flow regime. The result is the plot labeled "BR/PIPE/BHARANTHAN," which is what was used for RELAP5/MOD2. At 30 s, the void fraction dropped to only 0.97, indicating no downcomer penetration.

The MOD3 calculation was run to 30 s on Version 591, using the Cray, with five updates (extra regime numbers/correct syntax errors (pclebe); correct diagnostic print (pclebf); correct interphase drag angle errors (pclebg); correct stratification smoothing (pclebh); and annular mist changes for downcomer (pcldal); it required 4061 attempted advancements and 68.14 cpu seconds.

2.2.17 References

2.2-1. J. E. Lin, G. E. Gruen, W. J. Quapp, "Critical Flow in Small Nozzles for Saturated and Subcooled Water at High Pressure," *Basic Mechanisms in Two-Phase Flow and Heat Transfer Symposium at the Winter Annual Meeting of the American Society of Mechanical Engineers, Chicago, Illinois, November 16-21, 1980*, pp.9-17.

2.2-2. R. A. Reimke, H. Chow, V. H. Ransom, *RELAP5/MOD1 Code Manual, Volume 3: Checkout Problems Summary*, EGG-NSMD-6182, February 1983.

2.2-3. J. A. Findlay and O. L. Sazzi, *BWR Refill-Reflood Program--Model Qualification Task Plan*, EPRI NP-1527, NUREG/CR-1899, GEAP-24898, October 1981.

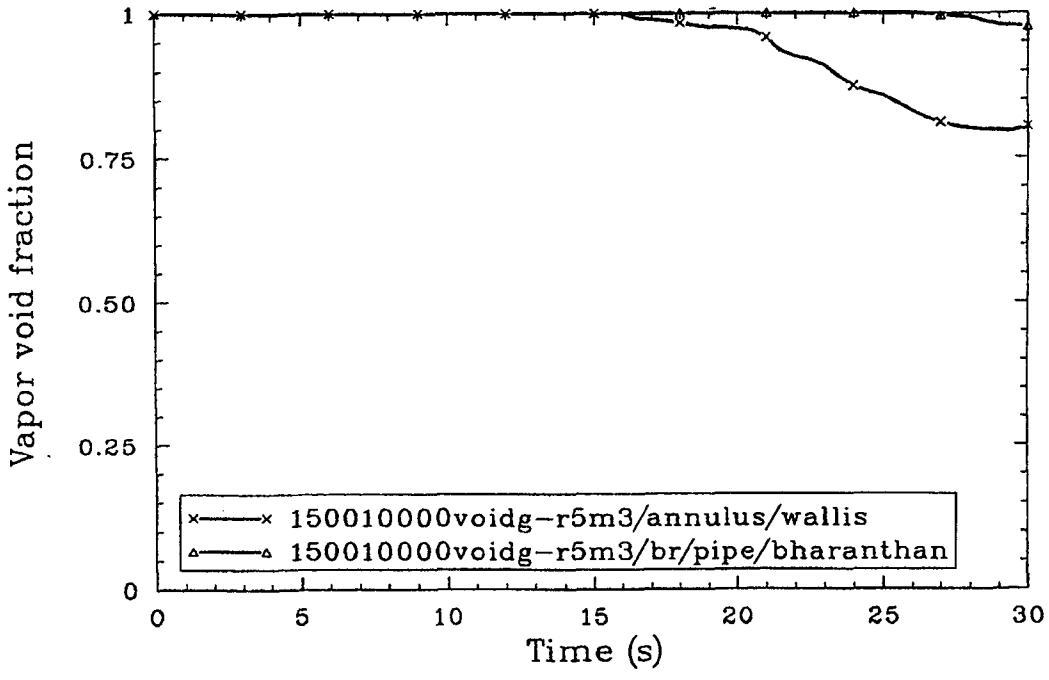

Figure 2.2-85. RELAP5/MOD3 void fraction in the lower plenum for UPTF-6.

2.2-4. N. Abauf, O. C. Jones, Jr., and B. J. C. Wu, *Critical Flashing Flow in Nozzles with Subcooled Inlet Conditions*, BNL-NUREG-27512, 1980.

2.2-5. A. E. Dukler and L. Smith, *Two Phase Interactions in Counter-Current Flow: Studies of the Flooding Mechanism*, NUREG/CR-0617, 1979.

2.2-6. L. Erickson et al., *The Marviken Full-Scale Critical Flow Tests Interim Report: Results from Test 24*, MXC224, May 1979.

2.2-7. L. Erickson et al., *The Marviken Full-Scale Critical Flow Test Interim Report: Results from Test 22*, MXC-222, March 1979.

2.2-8. A. R. Edwards and F. P. O'Brien, "Studies of Phenomena Connected with the Depressurization of Water Reactors," *Journal of the British Nuclear Energy Society, 9*, 1970, pp. 125-135.

2.2-9. D. L. Reeder, *LOFT System and Test Description (5.5 ft. Nuclear Core/LOCEs)*, NUREG/CR-0247, TREE-1208, July 1978.

2.2-10. P. D. Bayless et al., *Experiment Data Report for LOFT Nuclear Small Break Experiment L3-1*, NUREG/CR-1145, EGG-2007, January 1980.

2.2-11. A. W. Bennett et al., *Heat Transfer to Steam-Water Mixtures Flowing in Uniformly Heated Tubes in Which the Critical Heat Flux has been Exceeded*, AERE-R5373, October 1976.

2.2-12. A. Sjoberg, and D. Caraher, *Assessment of RELAP5/MOD2 Against 25 Dryout Experiments Conducted at the Royal Institute of Technology*, NUREG/IA-0009, October 1986.

2.2-13. G. L. Yoder et al., *Dispersed Flow Film Boiling in Rod Bundle Geometry-Steady State Heat Transfer Data and Corrleation Comparisons*, NUREG/CR-2435, ORNL-5822, March 1982.

2.2-14. T. M. Anklam, R. J. Miller, and M. D. White, *Experimental Investigations of Uncovered-Bundle Heat Transfer and Two-Phase Mixture-Level Swell Under High-Pressure Low Heat-Flux Conditions*, NUREG/CR-2456, ORNL-5848, March 1982.

2.2-15. H. Christensen, *Power-to-Void Transfer Function*, ANL-6385, 1961.

2.2-16. H. R. Saedi and P. Griffith, "The Pressure Response of a PWR Pressurizer During an Insurge Transient," *Transactions of ANS, 1983 Annual Meeting, Detroit, MI, June 12.2-16, 1983.*

2.2-17. H. R. Saedi, *Insurge Pressure Response and Heat Transfer for a PWR Pressureizer*, MIT ME Thesis November, 1982.

2.2-18. M. J. Loftus et al., *PWR Flecht-Seaset Unblocked Bundle, Forced and Gravity Reflood Task Data Report*, NUREG/CR-1532, EPRI NP-1459, WCAP-9699, June 1980.

2.2-19. Q. Nguyen and S. Banerjee, *Experimental Data Report on Condensation in a Single Inverted U-Tube*, EPRI NP-3471, May 1984.

2.2-20. *UPTF Test No. 6, Downcomer Counter-Current Flow Test, Siemens/KWU Quick Look Report*, UP 316/89/2, March 1989.

2.3 Integral Test Problems

2.3.1 LOFT Small-Break Test L3-7

The Loss-of-Fluid Test (LOFT) Facility[2.3-1] is a 50-MW(t), volumetrically scaled PWR system. The LOFT facility was designed to study the engineered safety features in a commercial PWR system as to their response to a postulated LOCA.

The LOFT Test L3-7[2.3-2] was performed to analyze the effects of a single-ended, offset shear break of a small [2.54-cm (1-in.) diameter)] pipe connected to the cold leg of a large, 4-loop PWR. The test was conducted at 49 MW, yielding a maximum linear heat generation rate of 52.8 kW/m.

The LOFT Test L3-7 is presented here to demonstrate the ability of RELAP5/MOD3 to calculate the important parameters in a small-break transient for a full system test.

The LOFT nuclear core is approximately 1.68 m in length and 0.61 m in diameter and is composed of nine fuel assemblies, containing 1300 fuel rods of representative PWR design. Three unbroken PWR coolant loops are simulated by using a volume/power ratio scaled by the single circulating (intact) loop in the LOFT primary system, and the postulated broken PWR loop is simulated by the scaled LOFT blowdown (broken) loop (Figure 2.3-1).

The LOFT broken loop is orificed to simulate various break sizes and contains steam generator and pump simulators to model the hydraulic resistance of these components in the broken PWR loop. Either hot-leg (reactor vessel outlet piping) or cold-leg (reactor vessel inlet piping) breaks can be simulated by relocating the steam generator and pump simulators. Quick-opening valves (with opening times adjustable from approximately 20 to 50 ms) simulate the initiation of primary coolant piping ruptures. Primary blowdown effluent is collected in a blowdown suppression tank, which can model the significant portions of the various PWR containment backpressure transients.

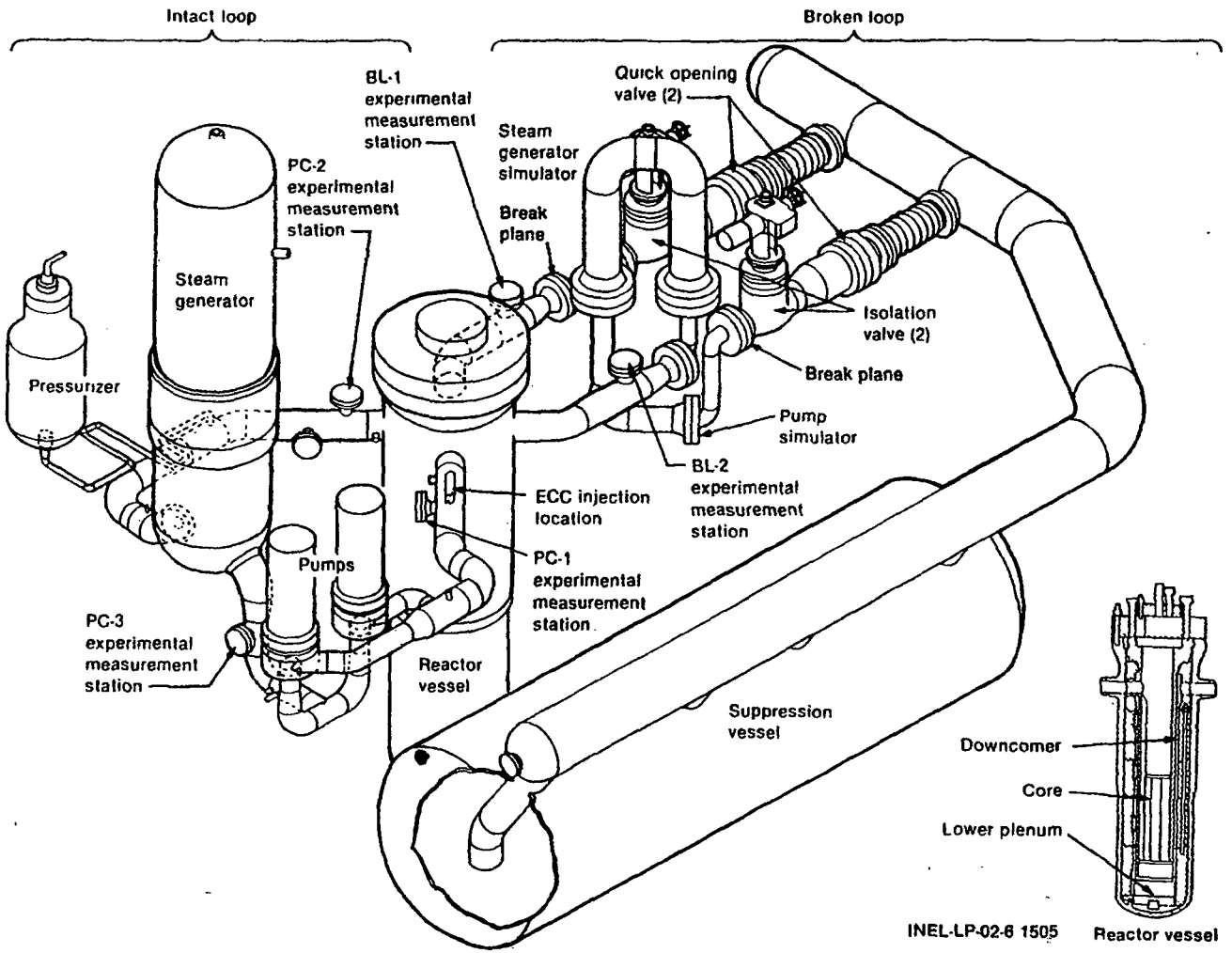

Figure 2.3-1. Schematic of LOFT test facility.

An ECC system is provided to model the loss-of-coolant engineered safety features in PWRs. The ECC is supplied by a high-pressure injection system (HPIS) centrifugal pump and a nitrogen-pressurized accumulator. Low pressure injection system (LPIS) and accumulator discharge lines are orificed as required to simulate the delivery characteristics of various PWR emergency coolant injection systems. The accumulator is equipped with an adjustable height standpipe, which allows the liquid and gas volumes to be varied. Five ECC injection points are built into the primary coolant system (PCS). These injection points are located in the intact loop hot leg, intact loop cold leg, upper plenum, lower plenum, and vessel downcomer.

Fluid pressure, temperature, velocity, and density are monitored by extensive instrumentation at key locations in the primary coolant, emergency core coolant, blowdown, and secondary coolant systems. Thermocouples monitor fuel rod cladding temperatures and support tube temperatures at 196 code locations. Four fixed nuclear detectors and a four-location traversing in-core nuclear detector system determine core power profiles and transient response.

The primary objectives of Test L3-$7^{2.3-2}$ were to establish a break flow approximately equal to HPIS flow when the primary pressure was in the range of 6.9 MPa, to establish conditions for steam generator reflux cooling, to isolate the break and stabilize the plant at cold shutdown condition, and to analyze the data obtained to investigate associated phenomena.

Prior to the break, the nuclear core was operating at a steady-state maximum heat generation rate of 52.8 $\pm$ 3.7 kW/m. Other significant initial conditions for Test L3-7 were: system pressure, 14.90 $\pm$ 0.25 MPa; core outlet temperature, 576.1 $\pm$ 0.5 K; and intact loop flow rate, 481.3 $\pm$ 6.3 kg/s. At 36 s after the break occurred, the reactor scrammed on a low system pressure signal. Within 10 s after scram verification, the pumps were manually tripped and coasted down. Pump coastdown was followed by the inception of natural loop circulation. Between 1800 (30 min) and 5974 s (1 h, 40 min), the HPIS was turned off to hasten the loss of fluid inventory

and to establish the conditions considered favorable for reflux flow in the primary loop. Starting at 3600 s (1 h), operator-controlled steam bleeding (opening the main steam bypass valve early and the main steam valve later in the transient) and steam generator feeding (using both the auxiliary and main feedwater systems) were used to decrease primary system pressure. Steam generator secondary feed and bleed maintained an effective heat sink throughout the experiment.

Later in the experiment, at 7302 s (2 h, 2 min), the blowdown isolation valve was closed, which isolated the break. System mass depletion stopped, and all decay heat energy not lost to the environment was removed by the steam generator. Primary system pressure gradually increased, causing the fluid in the system to become subcooled. Subsequently, the purification system was used to bring the reactor to a cold shutdown condition and the experiment was terminated.

The RELAP5/MOD2 model of the LOFT facility for Test L3-7 included 129 fluid control volumes and 135 flow junctions. The system nodalization is illustrated schematically in Figure 2.3-2. In the model, a total of 137 heat slabs (shown as shaded areas in Figure 2.3-2) were used to represent heat transfer in the intact loop steam generator vessel, core, primary system piping, and pressurizer. The values of the two-phase and subcooled discharge coefficients for the break used in the input deck were both 1.0.

This input deck was developed from the LOFT base deck.[2.3-3] This deck contains a filler gap (small flow path parallel to the downcomer), as this was found to be important in small breaks. This current deck has more volumes, junctions, and heat structures than the deck used in the RELAP5/MOD1 developmental assessment.[2.3-4] That particular deck had 115 volumes, 120 junctions, and 65 heat slabs.

The input deck obtained from the LOFT group for this RELAP5/MOD2 developmental assessment was modified to include crossflow junctions in four places: pressurizer, pressurizer spray, inlet annulus, and upper head. The connections between these four places and the primary system piping, as well

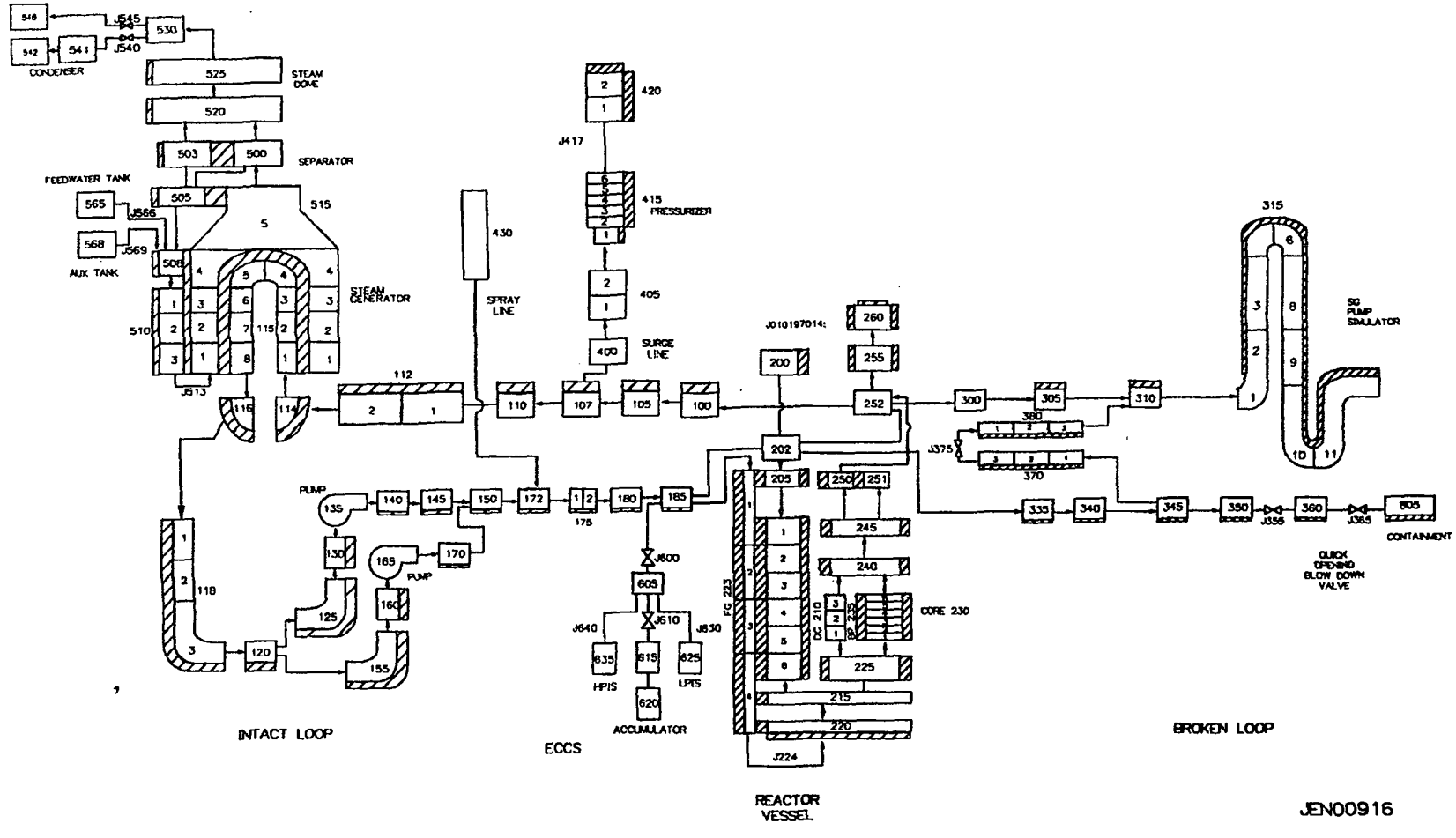

Figure 2.3-2. Nodalization for LOFT Test L3-7.

as the leak path between the inlet annulus and the upper head, were modeled as crossflow junctions.

A steady-state control system developed by the LOFT group was used in conjunction with this deck to obtain a steady state. Additional components, such as pump speed controllers, a pressurizer spray valve controller, pressurizer heaters, a pressurizer level controller using charging and letdown components, and a steam valve controller, were provided in the deck from the LOFT group.[2.3-2] The steady-state controller allows the user to specify seven set points: primary system mass flow rate, pressurizer pressure, pressurizer level, primary system cold leg temperature, steam valve relative steam position, steam generator level, and feed mass flow rate. A successful steady state was run out to 200 s, and the set points for the L3-7 test were reached. A user guideline that came to light during this process is that the choking option should be turned off in the secondary system steam valve.

The transient calculation was then carried out to 1000 s. Figure 2.3-3 shows a comparison of cpu time to simulated time for this calculation. The model ran about one to one. Figure 2.3-4 shows a comparison of the code to primary system pressure. The calculation is a little high, but not as high as the RELAP5/MOD1 calculation made using Cycle 17.[2.3-4] Figure 2.3-5 shows a comparison for the secondary system pressure. Here, the agreement is comparable to RELAP5/MOD1. To obtain this, it was necessary to adjust the leak rate out the steam valve from that used in RELAP5/MOD1. Figures 2.3-6 and 2.3-7 compare the velocities in the hot leg intact loop. They agree quite well, as did RELAP5/MOD1. Figure 2.3-8 shows the code comparison for the temperature difference across the core (upper plenum to lower plenum). Two data plots are shown because of the many possibilities for choosing a measurement site in the horizontal plane. The code calculation, for the most part, falls within the two data plots. Figure 2.3-9 compares the code to the measured mass flow rate at the break. The agreement is quite good and comparable to RELAP5/MOD1. Finally, a comparison to the hot leg intact loop density is shown in Figure 2.3-10. The code here is predicting a somewhat higher value.

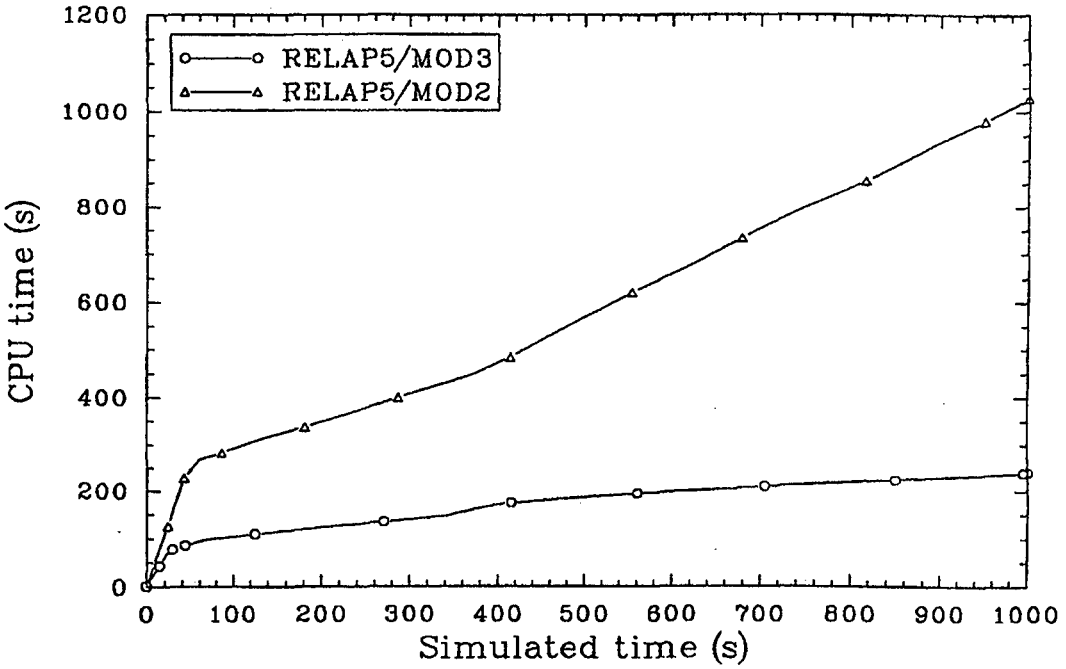

jan-cm11

Figure 2.3-3. CPU time versus simulated time for LOFT Test L3-7.

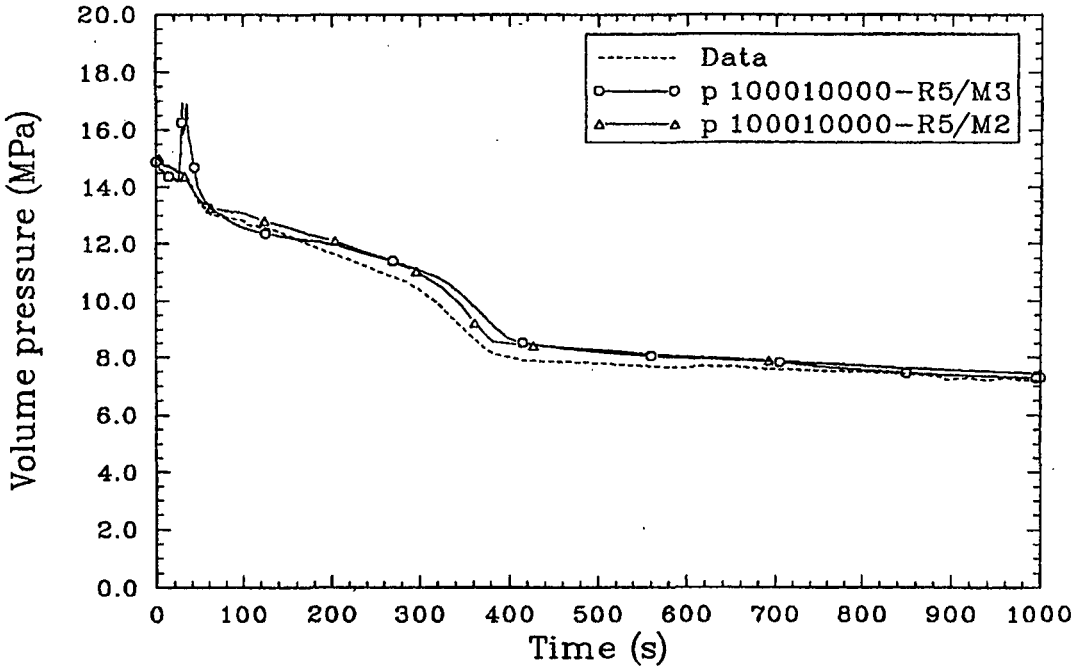

jan-cm21

Figure 2.3-4. Measured and calculated (RELAP5/MOD2, MOD3) primary system pressure for LOFT Test L3-7.

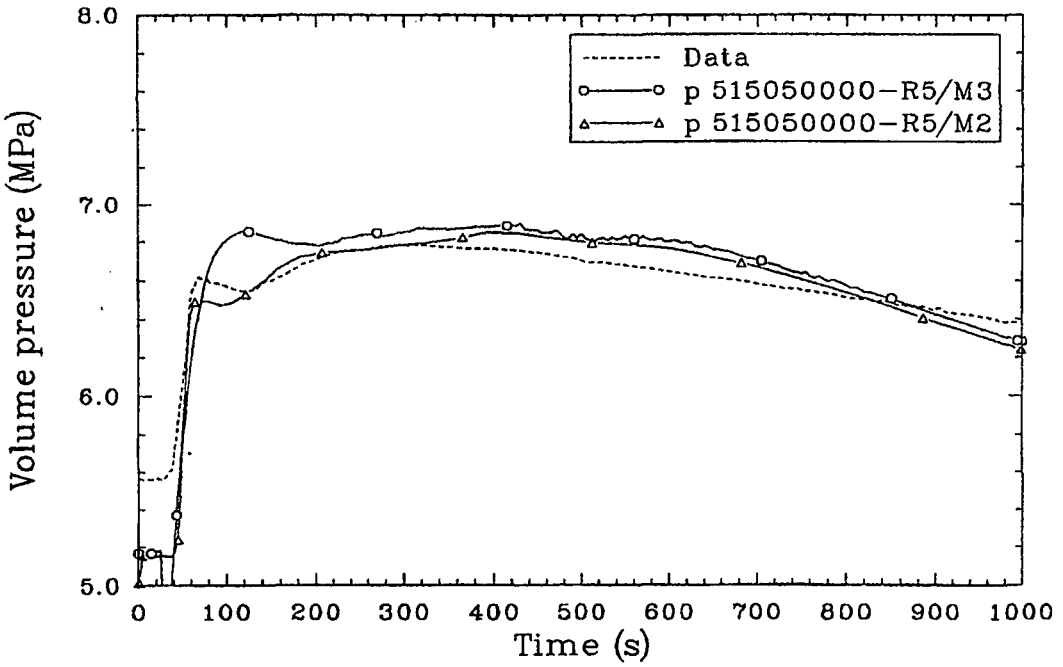

Figure 2.3-5. Measured and calculated (RELAP5/MOD2, MOD3) secondary system pressure for LOFT Test L3-7.

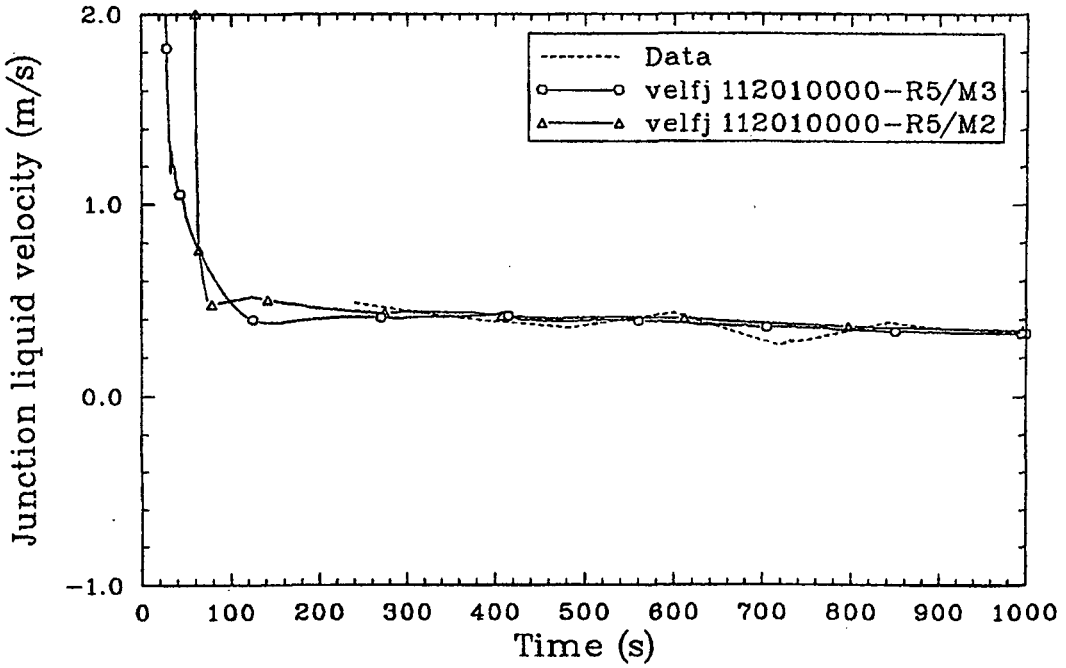

jan-cm41

Figure 2.3-6. Measured and calculated (RELAP5/MOD2, MOD3) liquid velocity in the intact loop hot leg for LOFT Test L3-7.

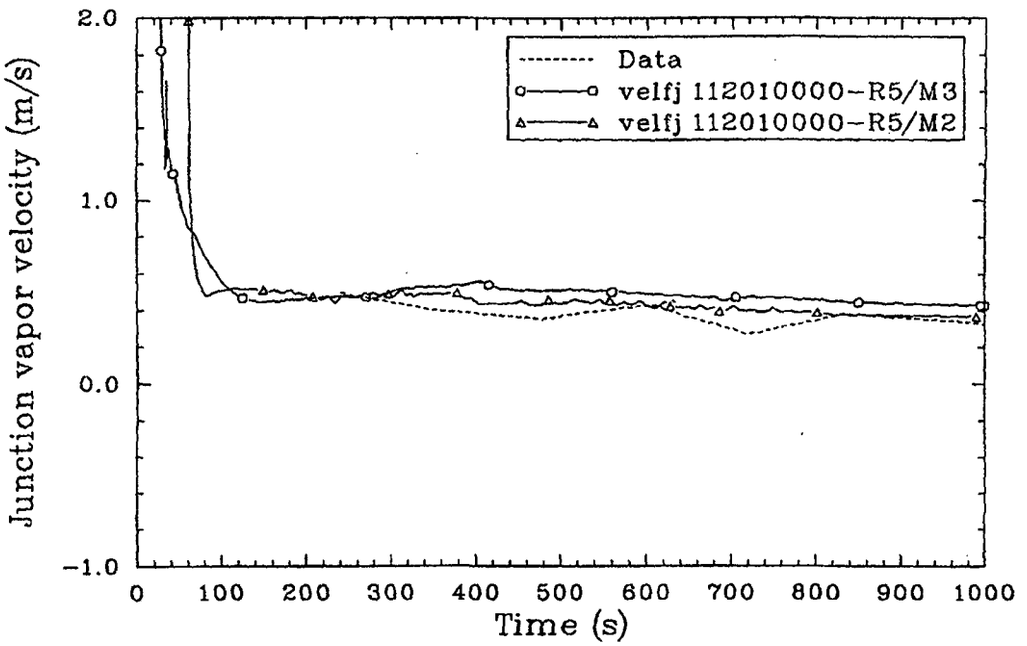

Figure 2.3-7. Measured and calculated (RELAP5/MOD2, MOD3) vapor velocity in the intact loop hot leg for LOFT Test L3-7.

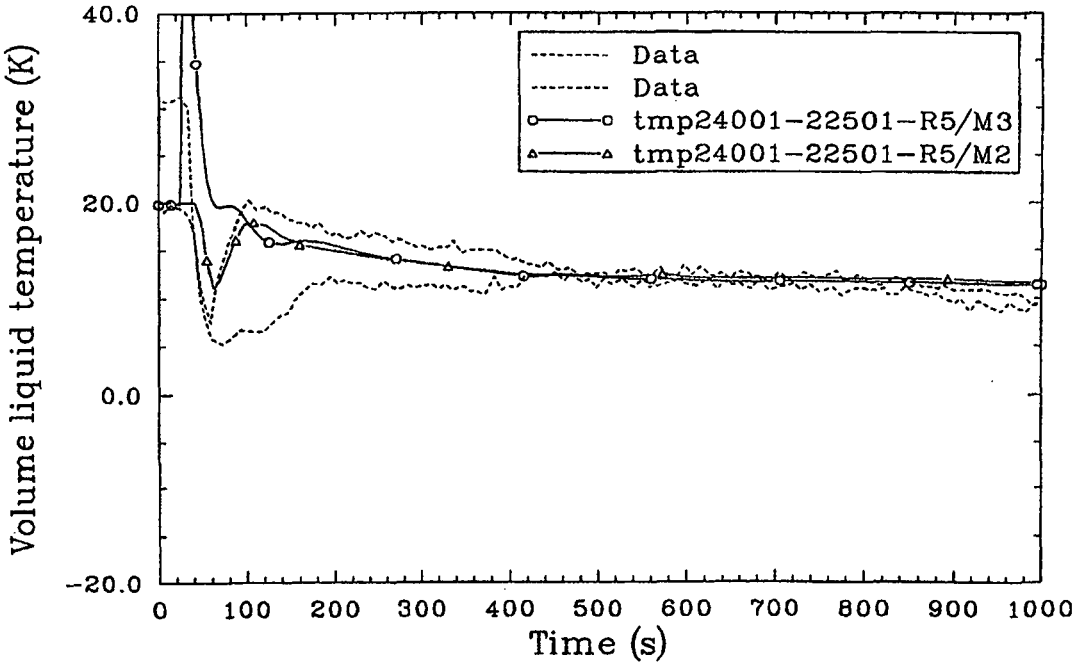

Figure 2.3-8. Measured and calculated (RELAP5/MOD2, MOD3) core temperature difference for LOFT Test L3-7.

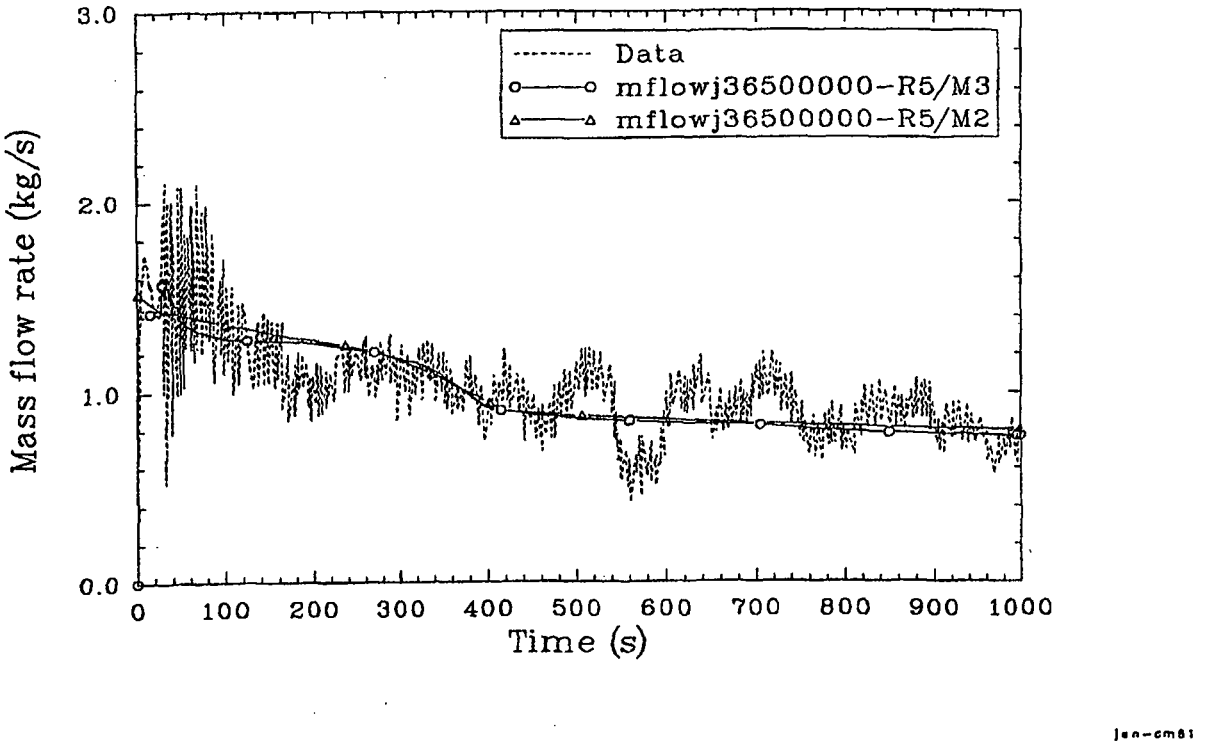

Figure 2.3-9. Measured and calculated (RELAP5/MOD2, MOD3) mass flow rate at the break for LOFT Test L3-7.

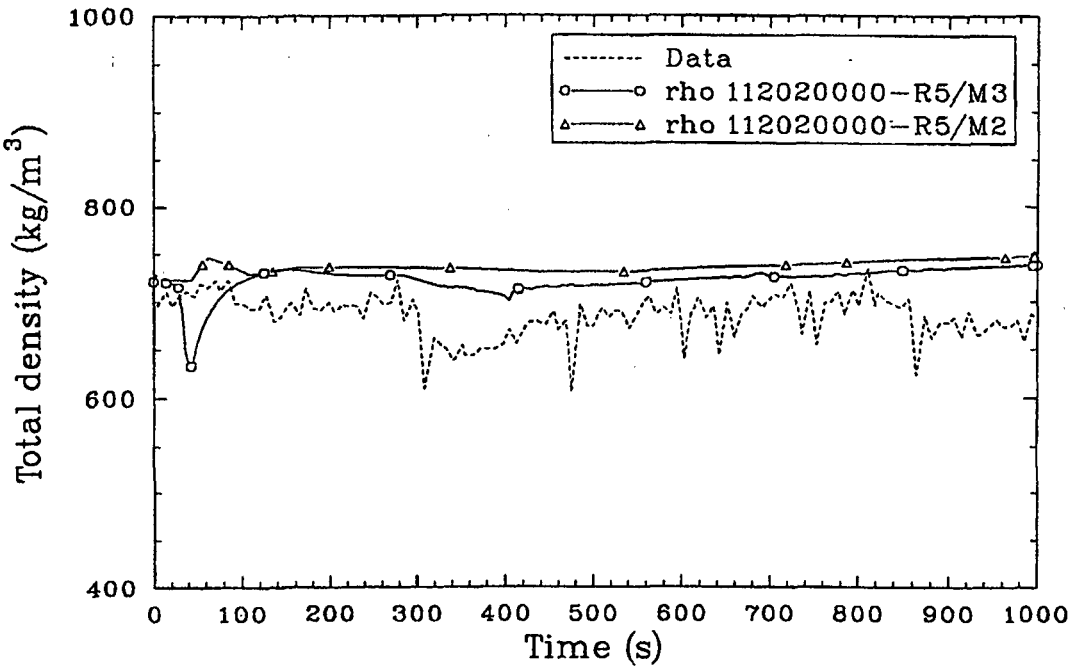

Figure 2.3-10. Measured and calculated (RELAP5/MOD2, MOD3) density in the intact loop hot leg for LOFT Test L3-7.

In summary, RELAP5/MOD2 shows good agreement with some of the key parameters of the L3-7 test when run out to 1000 s. The steam valve in the secondary side proved to be a somewhat sensitive component in running both the steady-state and the transient calculations.

2.3.2 LOFT Large-Break Test L2-5

The LOFT Test L2-5[2.3-5] was performed to analyze the effects of a 200% double-ended cold leg break with an immediate primary coolant pump trip. The test was conducted at 36 MW, yielding a maximum linear generation rate of 40.1 kW/m. The LOFT facility is described in the preceding section.

Significant initial conditions for Test L2-5 were: systems pressure, 14.94 $\pm$ 0.06 MPa; core outlet temperature 589.7 $\pm$ 1.6 K; and intact loop flow rate, 192.4 $\pm$ 7.8 kg/s.

The experiment was initiated by opening the quick-opening blowdown valves in the broken loop hot and cold legs. The reactor scrammed on low pressure at 0.24 $\pm$ 0.01 s. Following the reactor scram, the operators tripped the primary coolant pumps at 0.94 $\pm$ 0.01 s. The pumps were not connected to their flywheels during the coastdown.

A rewet of the upper portion of the center fuel assembly began at approximately 12 s and ended at approximately 23 s. Accumulator injection of ECC to the intact loop cold leg began at 16.8 $\pm$ 0.1 s. Delayed ECC injection from the HPIS and LPIS began at 23.90 $\pm$ 0.02 and 37.32 $\pm$ 0.02 s, respectively. The fuel rod peak cladding temperature of 1078 $\pm$ 13 K was attained at 28.47 $\pm$ 0.02 s. The cladding was quenched at 65 $\pm$ 2 s, following the core reflood. The LPIS injection was stopped at 107.1 $\pm$ 0.4 s, after the experiment was considered complete.

The RELAP5 model of the LOFT facility for Test L2-5 included 129 fluid control volumes and 139 flow junctions. The system nodalization is illustrated schematically in Figure 2.3-11. In the model, a total of 32 heat slabs (shown as shaded areas in the figure) were used to represent heat

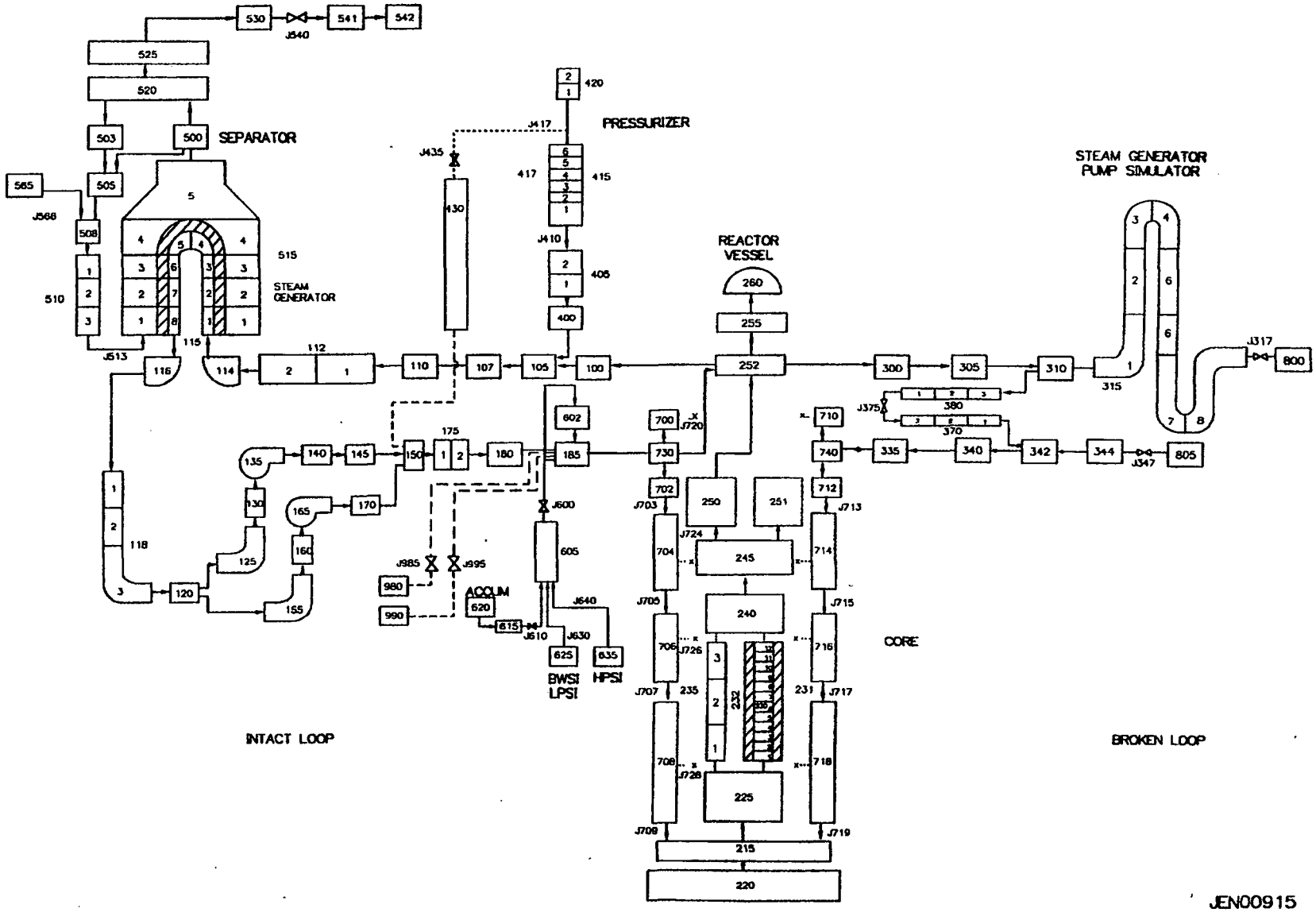

Figure 2.3-11. Nodalization for LOFT Test L2-5.

transfer in the intact loop steam generator and core. The values of the two-phase and subcooled discharge coefficients for the breaks used in the input deck were 0.93 and 0.84, respectively. As with the L3-7 deck, this input deck was obtained from the LOFT group's latest RELAP5 deck. This deck contains a split downcomer, which was found to be important in large breaks.

The input deck was modified to include crossflow junctions in the same places as the L3-7 deck. The only difference is that the L2-5 deck doesn't contain a pressurizer spray for the transient calculation (just for steady state; i.e., volume 430 and junction 435), so there is no need for a crossflow junction there. The deck was also modified to include a 12.3-volume core rather than a 6-volume core. It was felt that this final nodalization was necessary to obtain good comparison with the data.

As with L3-7, the steady-state control system was used in conjunction with this deck to obtain a good steady state. The same seven set points were used, except that the values were changed to match the L2-5 test specifications. A successful steady state was run out to 867 s.

The transient calculation was then carried out to 50 s. Comparison plots will be shown for RELAP5/MOD3, MOD2, and the data. Figures 2.3-12 and 2.3-13 show comparisons of the code to both primary and secondary system pressure. The MOD3 primary pressure is higher and closer to the data than the MOD2 primary pressure; the MOD3 secondary pressure is lower than MOD2 and the data. The agreement is good, although a little low. Figures 2.3-14, 2.3-15, 2.3-16, and 2.3-17 show comparisons to the mass flow rate in the broken loop cold leg, broken loop hot leg, intact loop cold leg, and intact loop hot leg. The increases and decreases in the calculations for the broken loop cold leg mass flow rate between 20 and 40 s occur during the time that the accumulator is on. In both the intact loop mass flow rate plots for the data, the flow direction is not indicated. This perhaps explains why the intact loop hot leg mass flow rate plots seem to be mirror images of each other about the zero mass flow rate line between 5 and 25 s. Figure 2.3-18 shows the density in the intact loop hot leg, and here the comparison seems good.

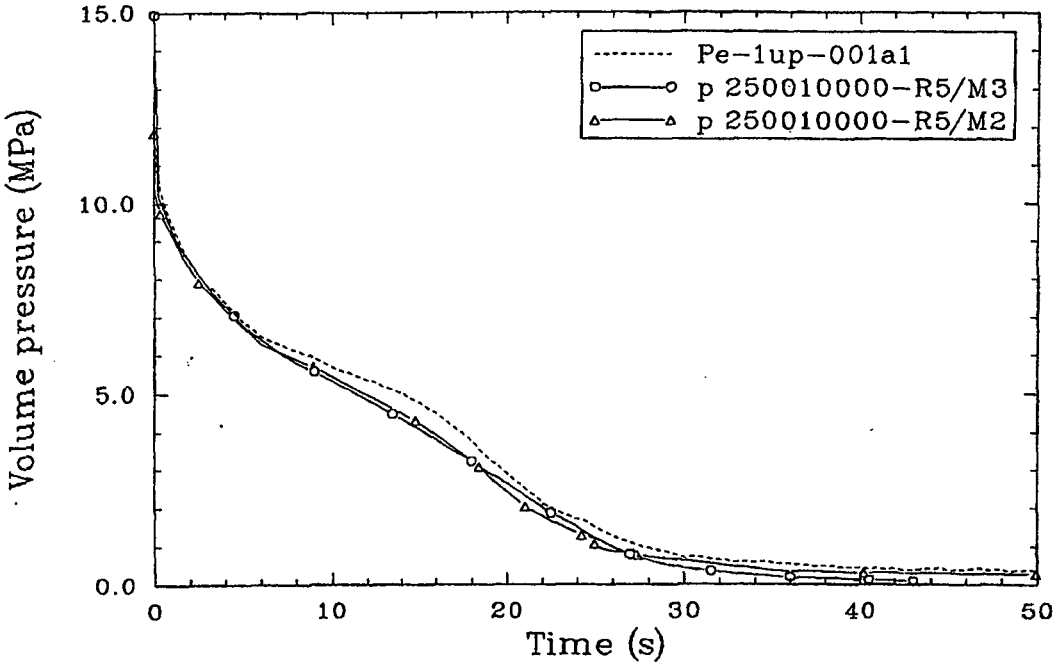

Figure 2.3-12. Measured and calculated (RELAP5/MOD2, MOD3) primary system pressure for LOFT Test L2-5.

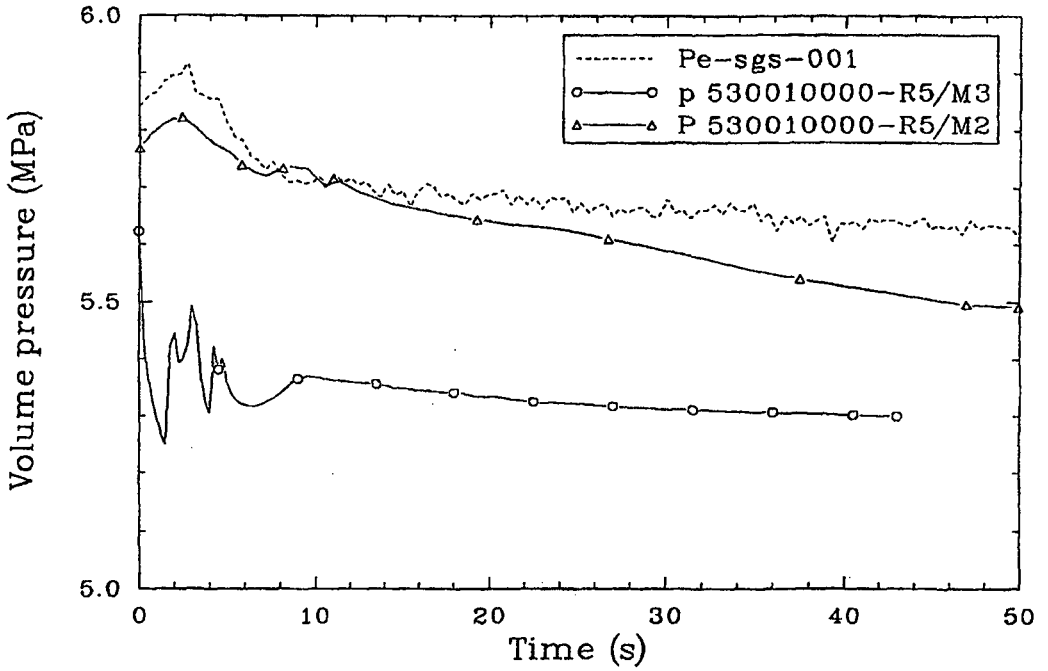

jan-r471

Figure 2.3-13. Measured and calculated (RELAP5/MOD2, MOD3) secondary system pressure for LOFT Test L2-5.

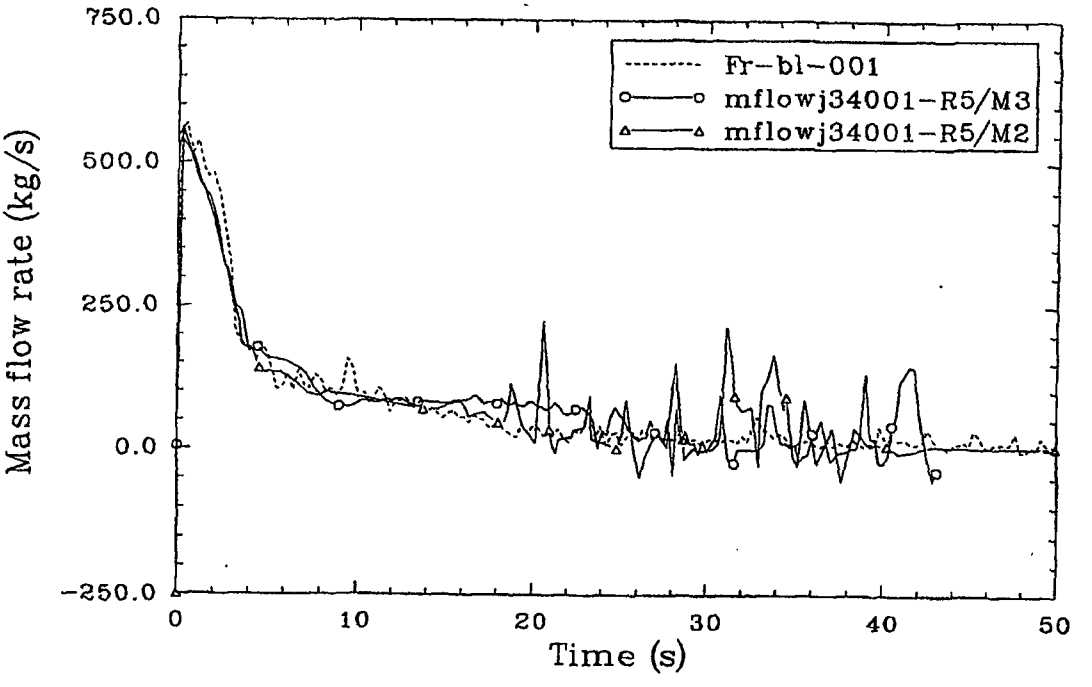

jen-r481

Figure 2.3-14. Measured and calculated (RELAP5/MOD2, MOD3) mass flow rate in the broken loop cold leg for LOFT Test L2-5.

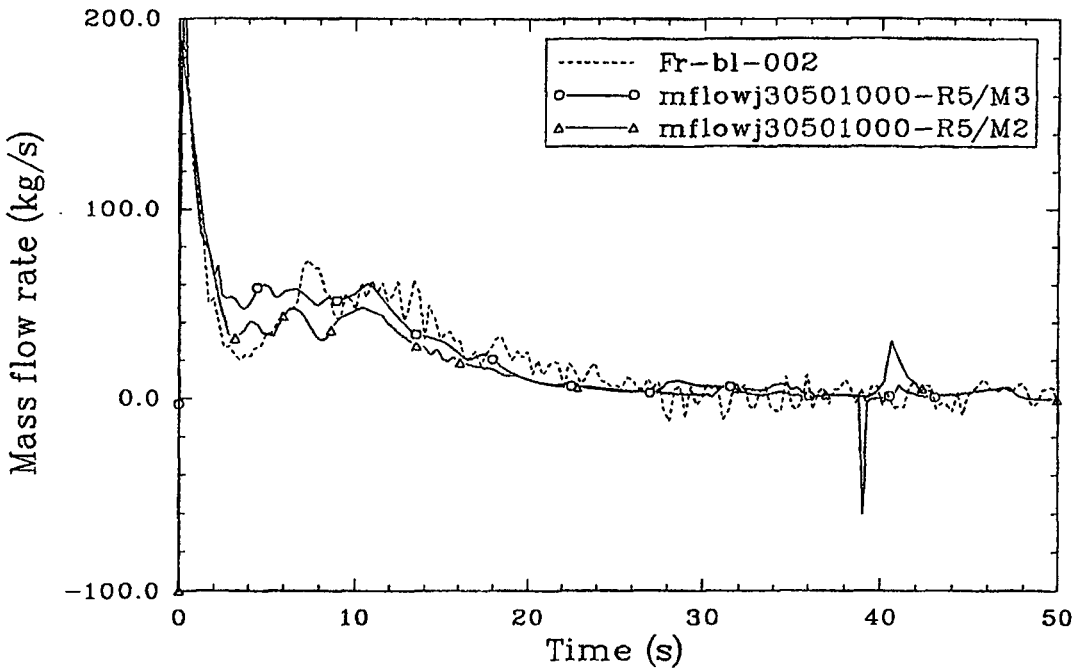

jen-r491

Figure 2.3-15. Measured and calculated (RELAP5/MOD2, MOD3) mass flow rate in the broken loop hot leg for LOFT Test L2-5.

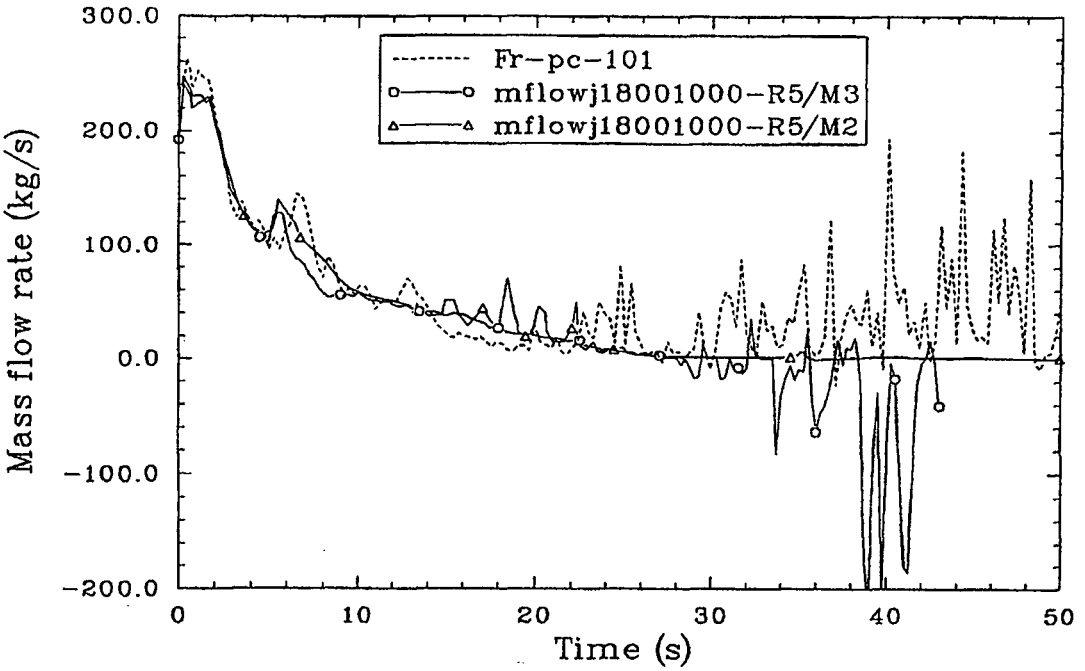

Figure 2.3-16. Measured and calculated (RELAP5/MOD2, MOD3) mass flow rate in the intact loop cold leg for LOFT Test L2-5.

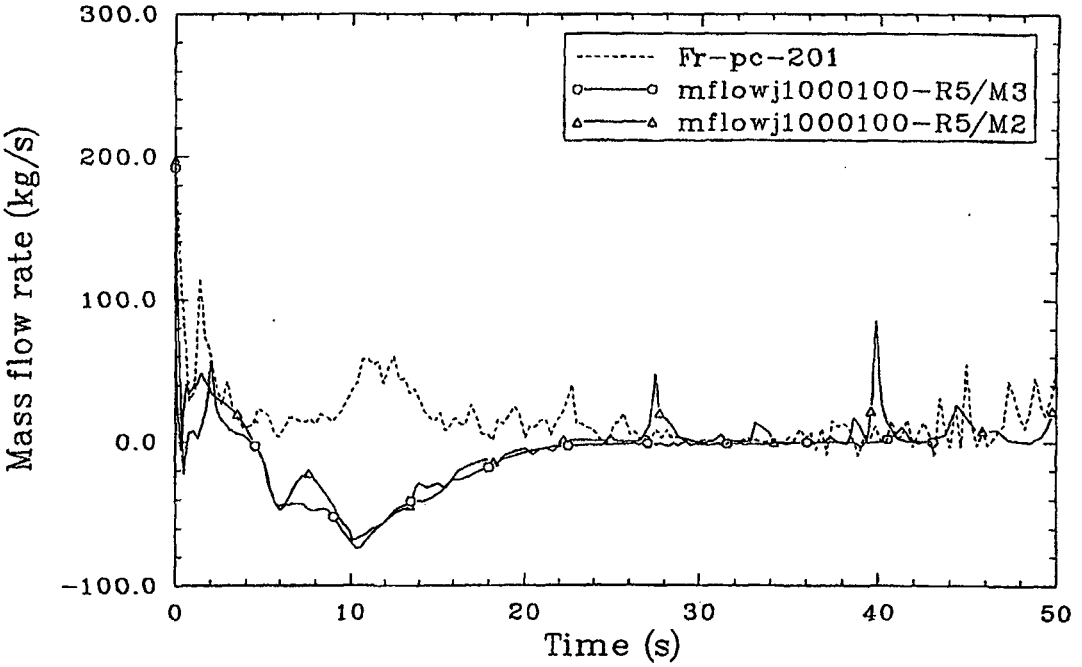

jan-r511

Figure 2.3-17. Measured and calculated (RELAP5/MOD2, MOD3) mass flow rate in the intact loop hot leg for LOFT Test L2-5.

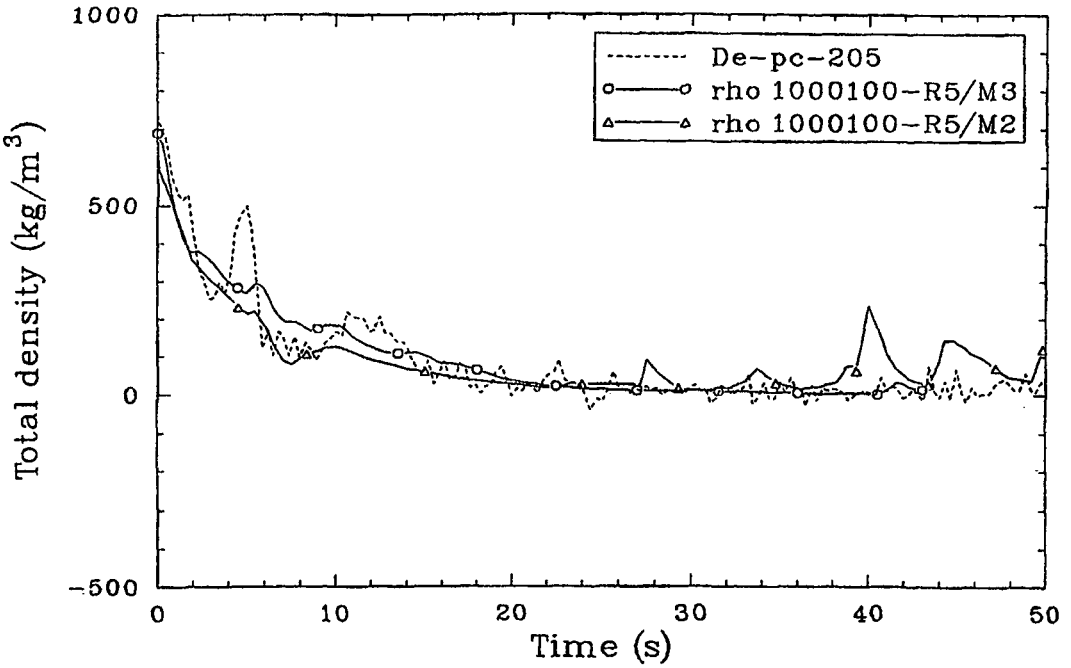

jan-r521

Figure 2.3-18. Measured and calculated (RELAP5/MOD2, MOD3) density in the intact loop hot leg for LOFT Test L2-5.

The mass flow rate from the accumulator and the accumulator level are shown in Figures 2.3-19 and 2.3-20. As the level comparison shows, the MOD3 accumulator is emptying closer to the data than MOD2. Thus, the MOD3 mass flow rate is lower than MOD2. The level plots appear to be due to the primary system pressure plots in Figure 2.3-12. In order to obtain the smooth MOD3 mass flow rates shown in Figure 2.3-19, it was necessary to make valve 600 smooth (instead of abrupt) and to include a loss factor.

The pump speed for primary coolant pump 2 (hydrodynamic volume 165) is shown in Figure 2.3-21. The agreement is quite good until 20 s, at which point the MOD3 calculation continues decreasing and the MOD2 calculation abruptly rises to about 150 rad/s. The cause of these differences is unknown at this time and will be resolved in the future. Even worse calculated excursions from the data were found in Reference 2.3-6.

The upper plenum and lower plenum temperature comparisons are shown in Figures 2.3-22 and 2.3-23. As with the primary system pressure, both the MOD3 and MOD2 calculations become lower than the data after 10 s.

A comparison for the fuel centerline temperature 0.69 m (27 in.) above the bottom of the core is shown in Figure 2.3-24. MOD3 calculations are a little higher than the data, whereas MOD2 calculations predict an earlier cooloff than actually occurs. Although not shown, the data centerline temperature begins to drop at 60 s. This early cooloff is probably the result of the high accumulator mass flow rate. Figures 2.3-25 through 2.3-30 compare the code to the measured cladding temperatures at various elevations above the bottom of the core. The MOD3 calculations at the lower elevations are higher and closer to the data than the MOD2 calculations; MOD2 calculations show an early quench, again probably due to the high accumulator mass flow rate. The MOD3 calculations at the upper elevations show some partial heatups seen in the data, whereas MOD2 does not show heatups. It appears that the MOD3 interphase drag changes have helped keep less liquid in the top of the core and thus improve the wall temperature calculations at higher elevations over what MOD2 was predicting.

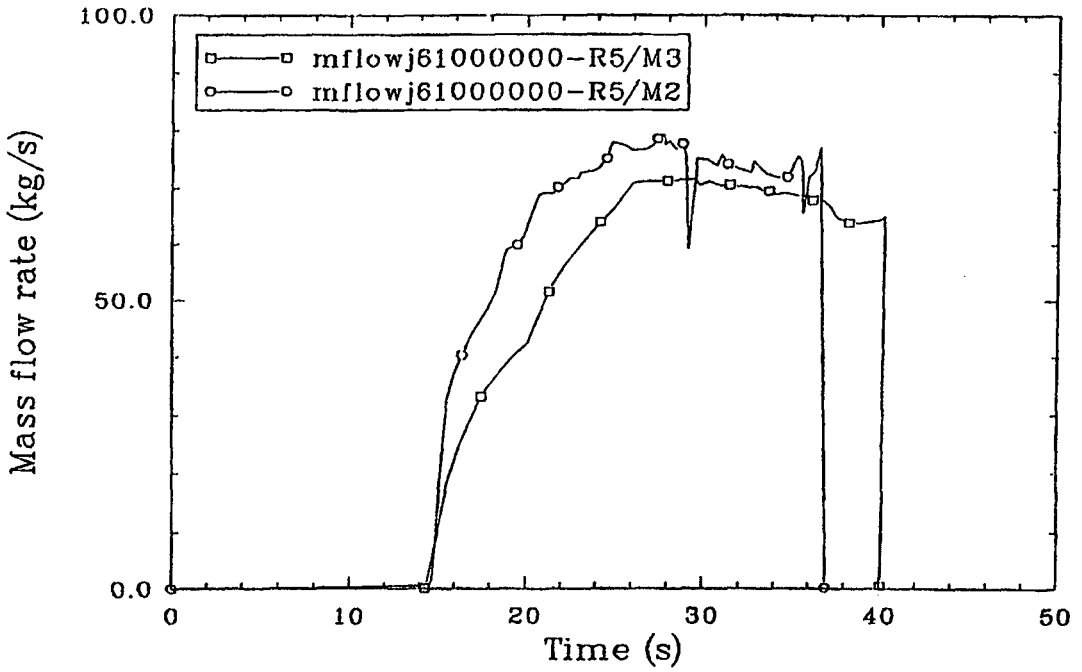

Figure 2.3-19. Measured and calculated (RELAP5/MOD2, MOD3) mass flow rate from the accumulator for LOFT Test L2-5.

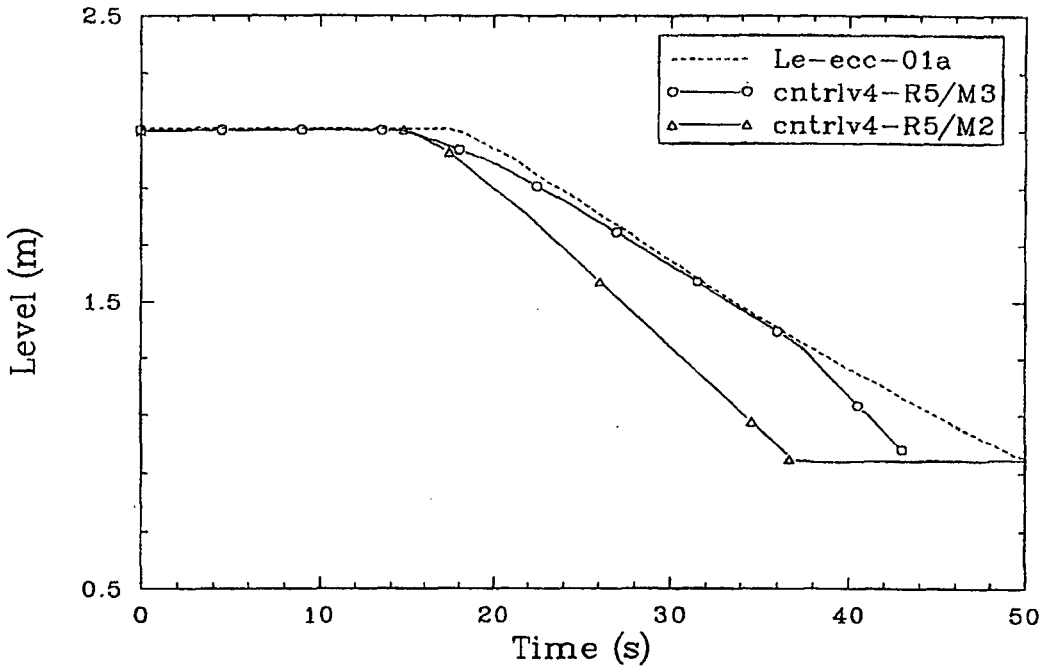

Figure 2.3-20. Measured and calculated (RELAP5/MOD2, MOD3) accumulator level for LOFT Test L2-5.

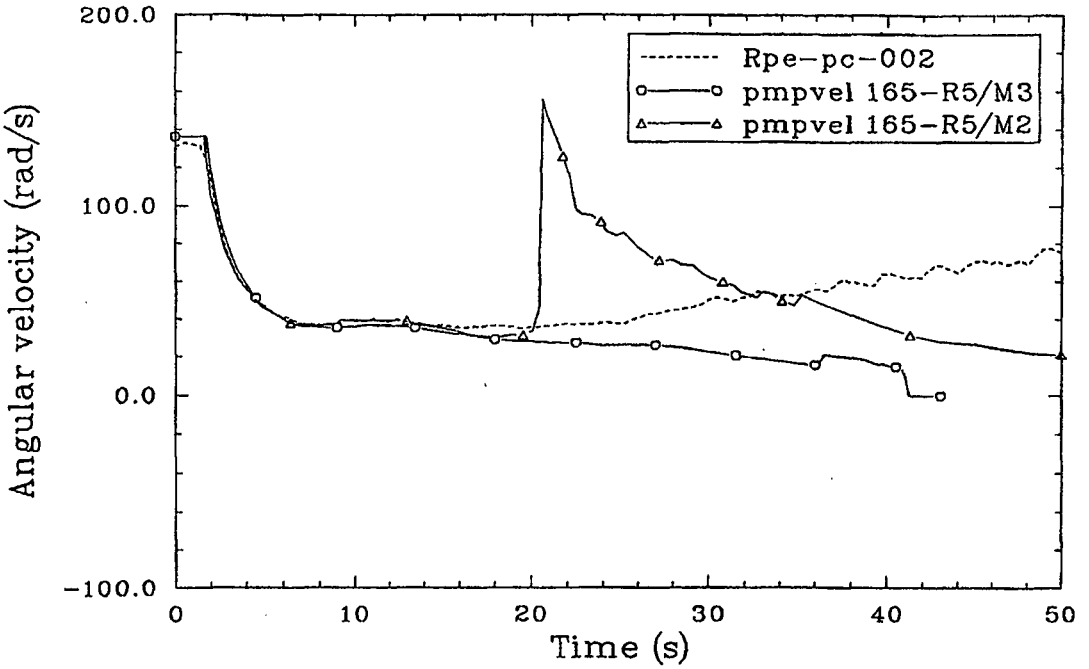

Jan-r551

Figure 2.3-21. Measured and calculated (RELAP5/MOD2, MOD3) pump speed for primary coolant pump 2 (hydrodynamic volume 165) for LOFT Test L2-5.

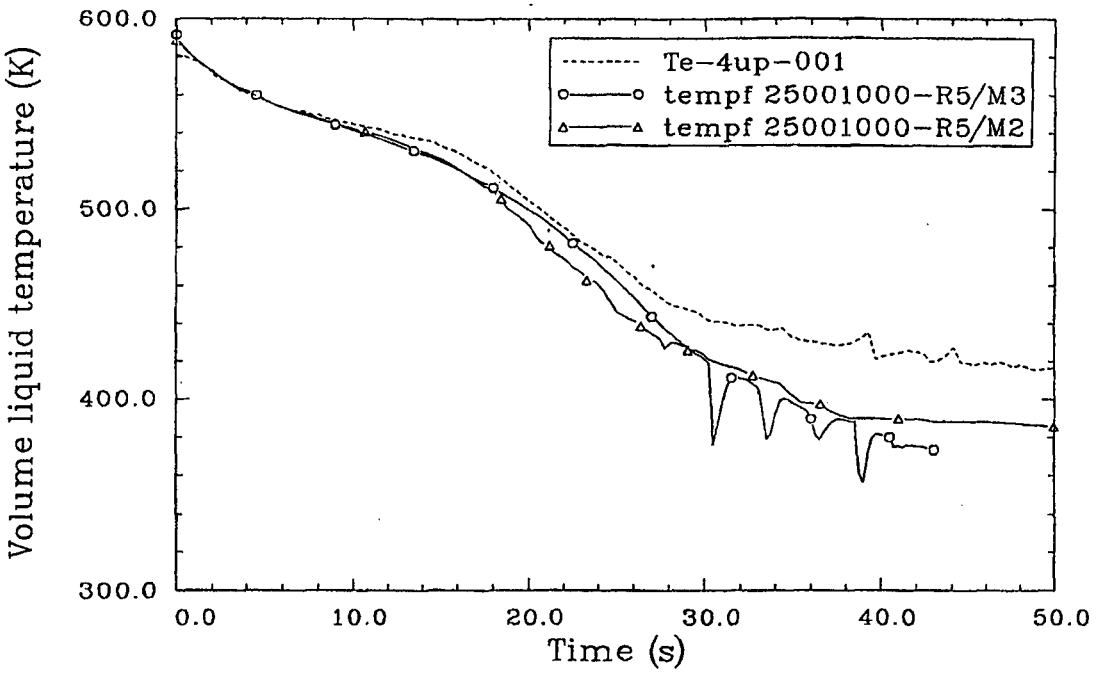

Figure 2.3-22. Measured and calculated (RELAP5/MOD2, MOD3) upper plenum temperature below the nozzle for LOFT Test L2-5.

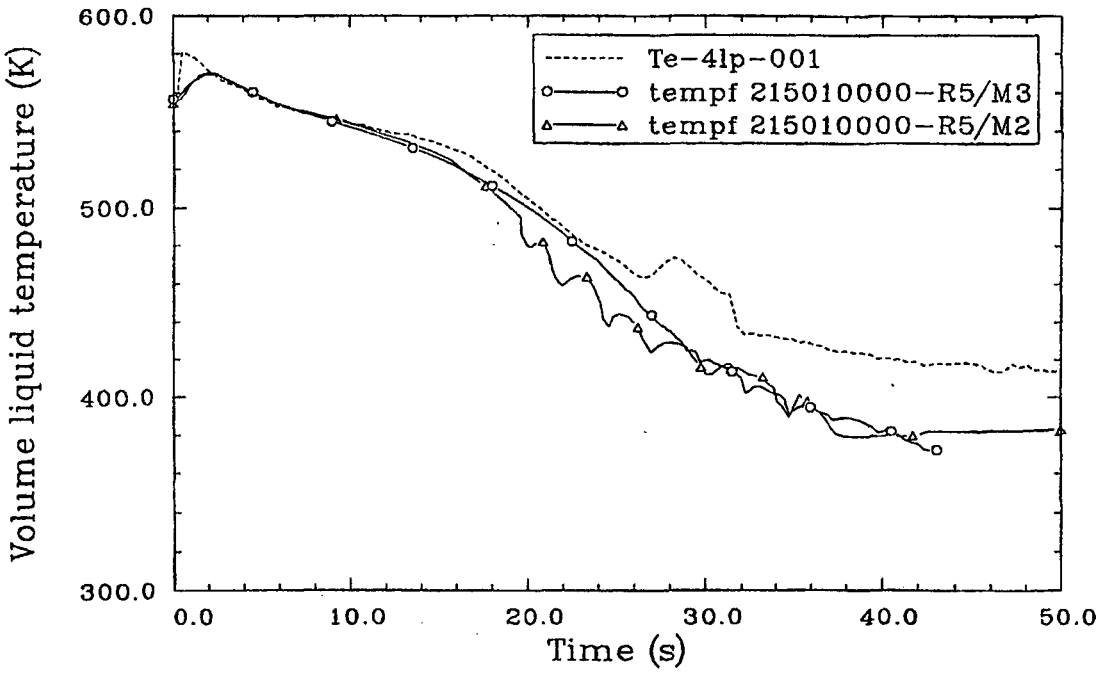

Figure 2.3-23. Measured and calculated (RELAP5/MOD2, MOD3) lower plenum temperature for LOFT Test L2-5.

.3-31 missing

This page was missing from the originally scanned document.

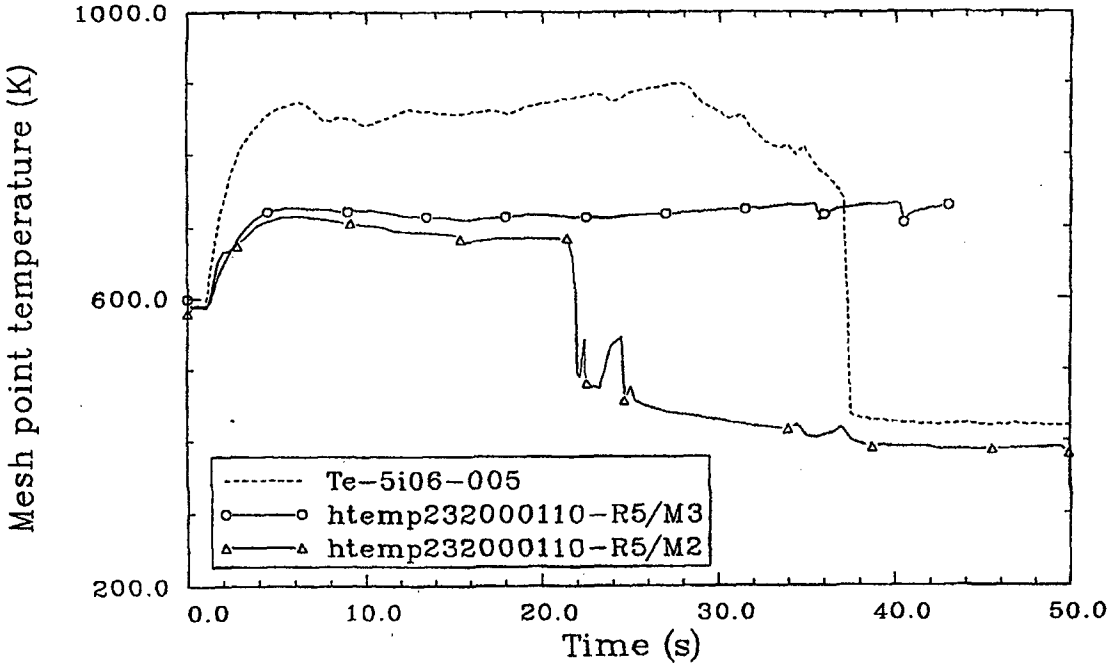

Figure 2.3-25. Measured and calculated (RELAP5/MOD2, MOD3) fuel cladding temperature 0.13 m (5 in.) above the bottom of the core for LOFT Test L2-5.

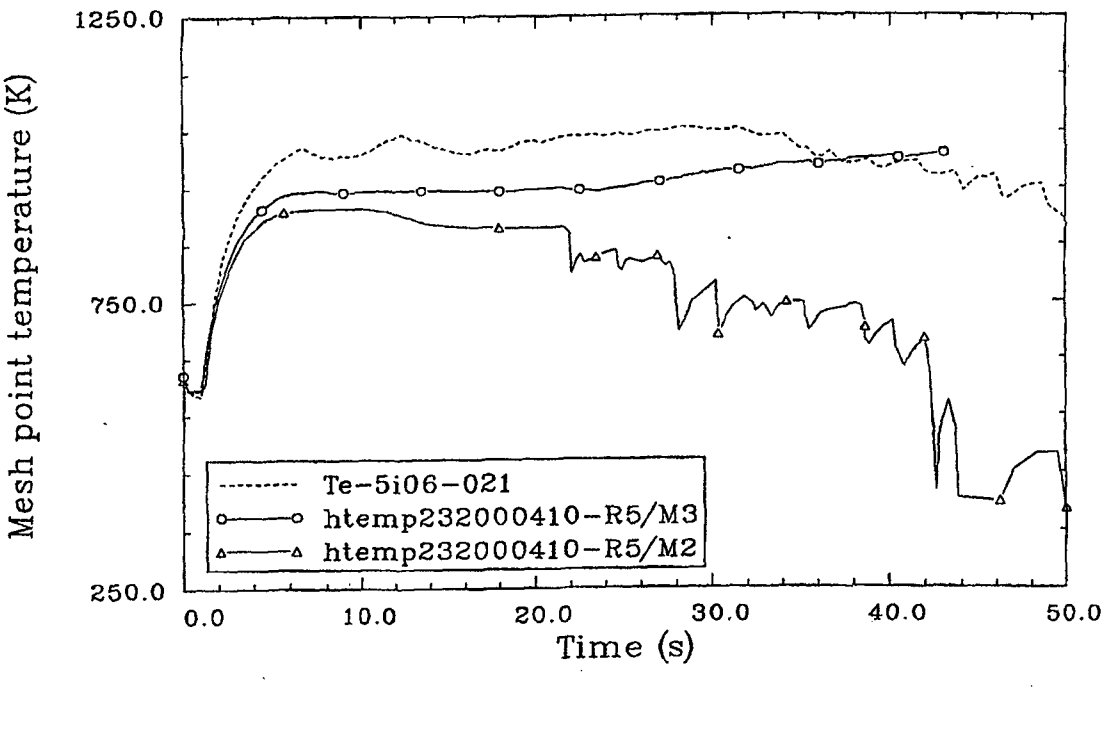

Figure 2.3-26. Measured and calculated (RELAP5/MOD2, MOD3) fuel cladding temperature 0.53 m (21 in.) above the bottom of the core for LOFT Test L2-5.

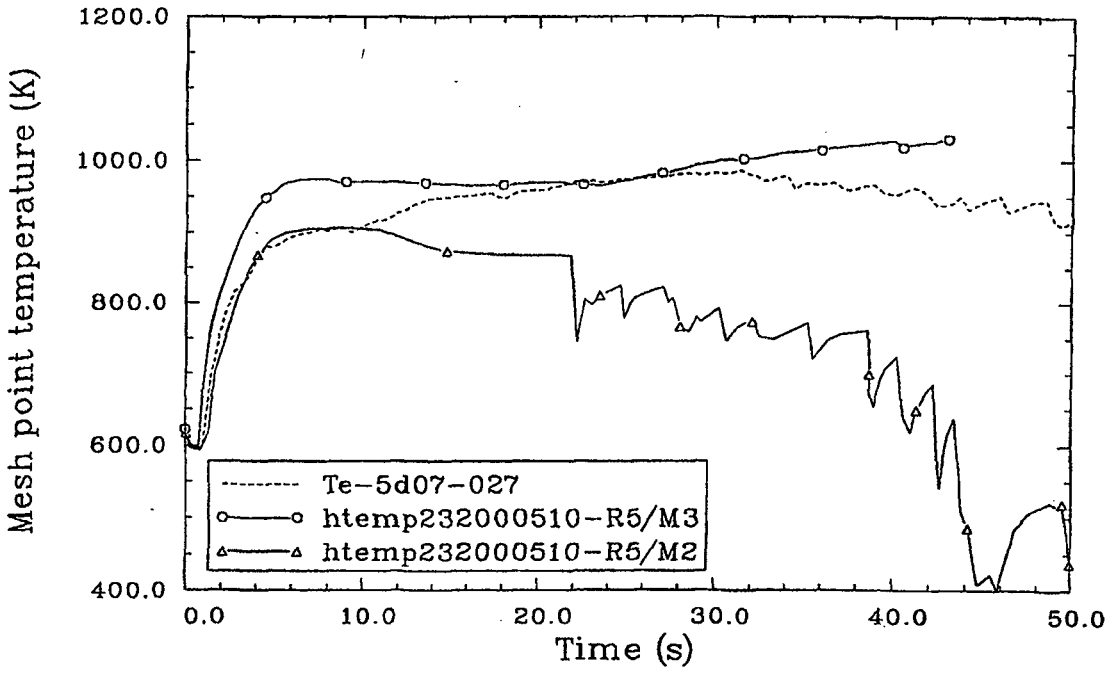

Figure 2.3-27. Measured and calculated (RELAP5/MOD2, MOD3) fuel cladding temperature 0.69 m (27 in.) above the bottom of the core for LOFT Test L2-5.

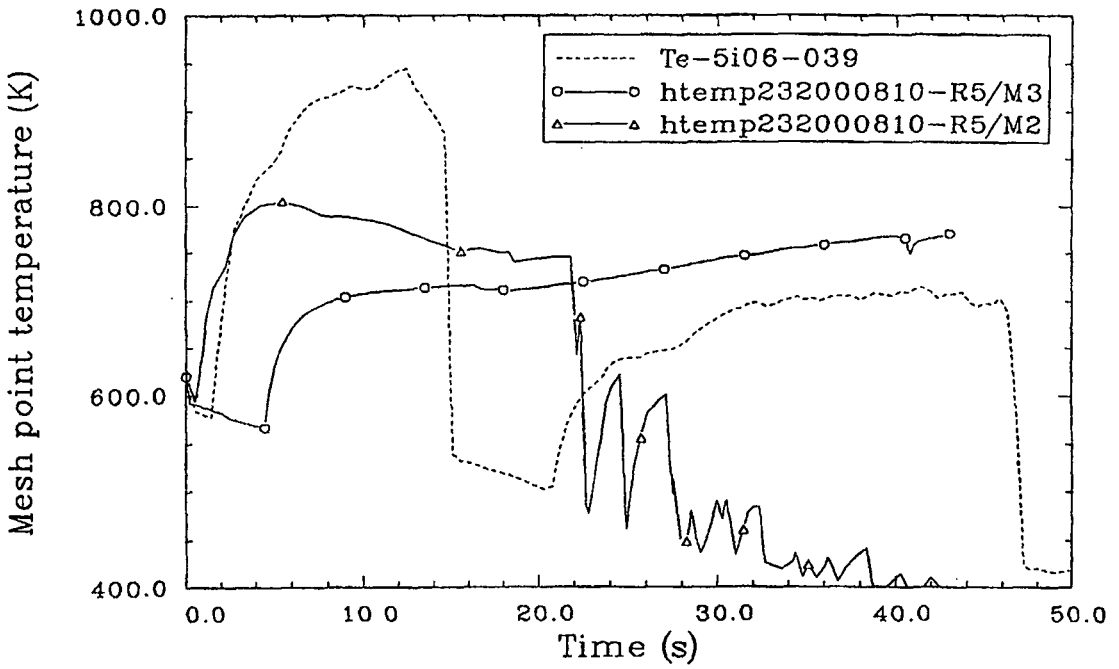

Figure 2.3-28. Measured and calculated (RELAP5/MOD2, MOD3) fuel cladding temperature 0.99 m (39 in.) above the bottom of the core for LOFT Test L2-5.

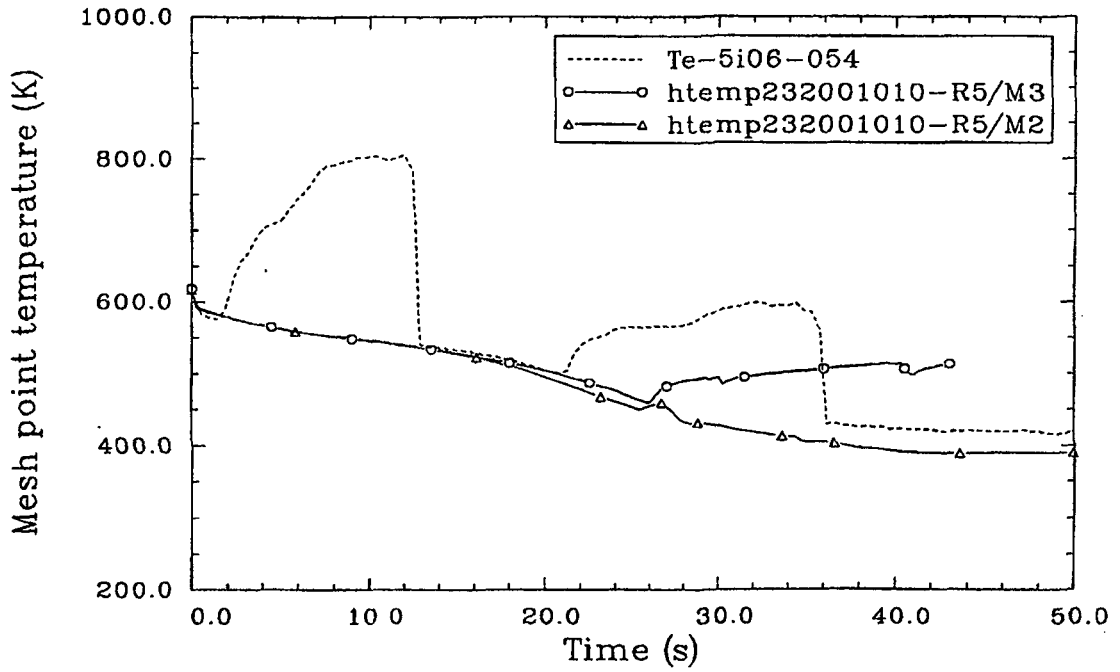

Figure 2.3-29. Measured and calculated (RELAP5/MOD2, MOD3) fuel cladding temperature 1.37 m (54 in.) above the bottom of the core for LOFT Test L2-5.

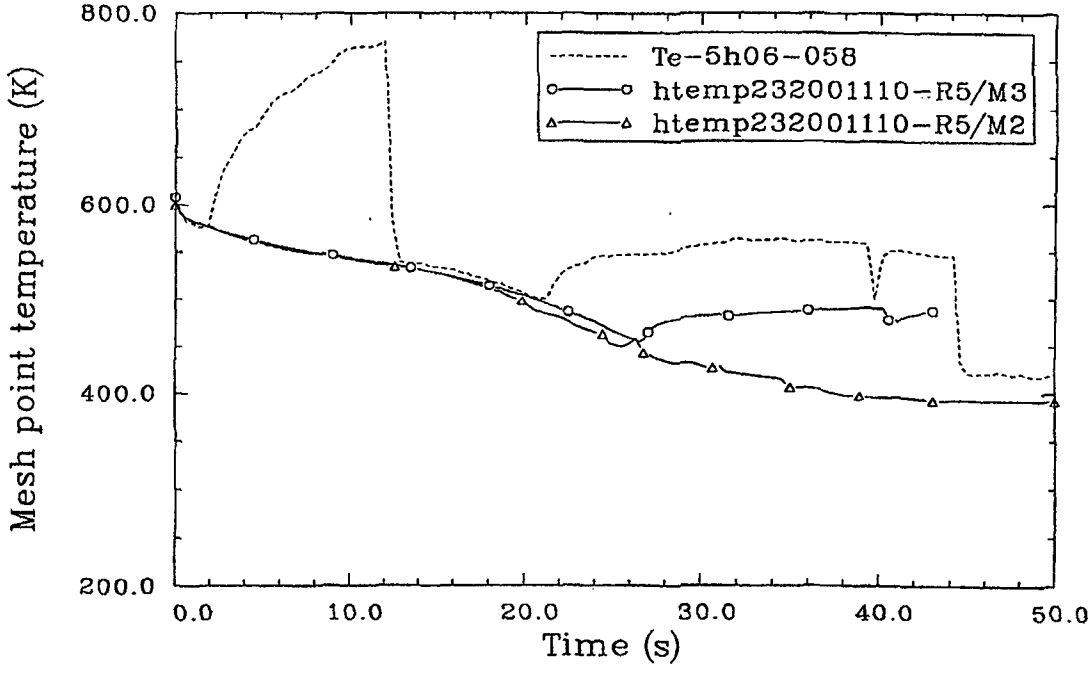

Figure 2.3-30. Measured and calculated (RELAP5/MOD2, MOD3) fuel cladding temperature 1.47 m (58 in.) above the bottom of the core for LOFT Test L2-5.

The MOD3 calculation was run to 50 s on Version 5a1, using the Cray, with an update to check on negative pressure (pcljd4); it required 8775 attempted advancements and 557 cpu seconds. The MOD2 calculation was run to 50 s on Cycle 27, using the Cyber, with four updates (use Courant time step from third group; post-CHF heat transfer fixes (TSAX017); modify interphase drag calculation for abrupt area model (HXCX017); and accumulator fixes (DMKX017). It required 4106 attempted advancements and 803 cpu seconds.

2.3.3 Semiscale Natural Circulation Tests S-NC-1, S-NC-2, S-NC-3, and S-NC-10

Natural circulation experiments were performed in the Semiscale Mod-2A test facility, a small-scale model of the primary system of a four-loop PWR nuclear power generating plant (scaling factor 1/1705). The Mod-2A system incorporates the major components of a PWR including steam generators, vessel, downcomer, pumps, pressurizer, and loop piping. Detailed descriptions of the Semiscale Mod-2A test facility and operation procedure are given in References 2.3-7 and 2.3-8.

The natural circulation experiments reported here used a single-loop configuration, including the intact loop with steam generator and vessel/downcomer, as shown in Figure 2.3-31. In the single-loop configuration, the intact loop pump was replaced with a spool piece containing an orifice that simulated the hydraulic resistance of a locked pump rotor. In addition, the vessel was modified from the normal Mod-2A configuration for all the experiments by removing the vessel upper head to ensure a uniform heatup of the entire system and to avoid condensation in upper-head structures.

The various phenomena simulated in the S-NC Test Series included: single-phase transition between modes (single-phase to two-phase to reflux); effect of secondary conditions on two-phase natural circulation; effect of secondary conditions on reflux; effect of noncondensable gas (nitrogen) on both reflux and two-phase, single, and two-loop effects; transient small break LOCAs; and ECCS effects. Only the steady-state experiments, which

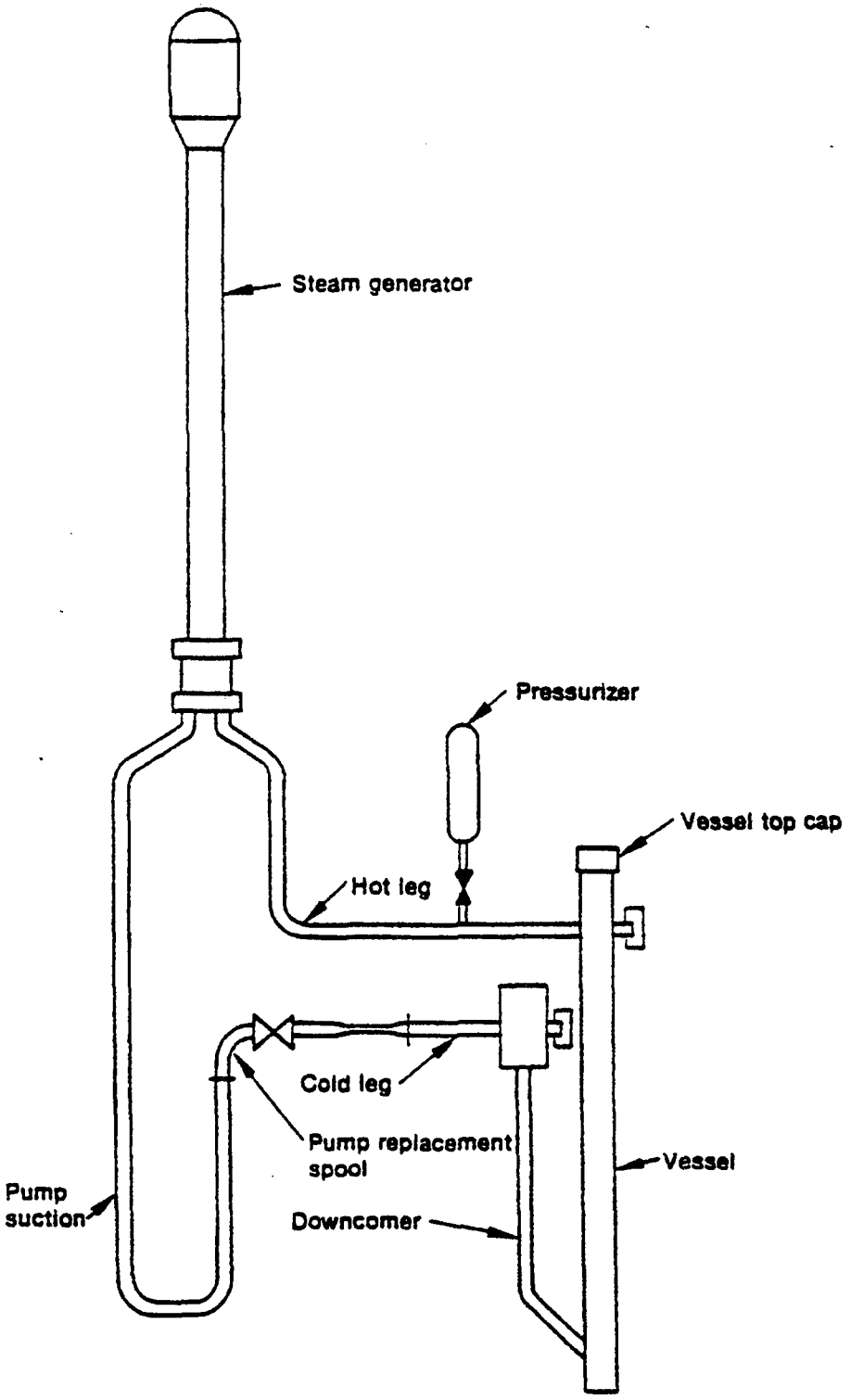

Figure 2.3-31. Semiscale Mod-2A single-loop configuration.

involved establishing various steady-state natural circulation modes by varying several key parameters, are used to assess the RELAP5/MOD3 system calculation capability during the natural circulation mode.

The RELAP5/MOD3 model used for the natural circulation study was a modified version of the standard Semiscale Mod-2A RELAP5 model representing the system configuration for the S-NC Test Series. Figure 2.3-32 shows a schematic of the model, which includes the following modifications to the standard model:

1. The broken loop piping, pump, and steam generator and the intact loop pump were removed.

2. The upper head volumes were removed.

3. The pressurizer was removed to reflect actual operating conditions for all measured conditions except a liquid-full system. Calculations for a liquid-full condition employed a time-dependent pressure boundary rather than a pressurizer.

4. The crossflow junction was utilized, connecting the primary loop piping to the vessel upper plenum, the vessel downcomer upper annulus, and the pressurizer surge line.

5. The secondary system steam separator was renodalized to represent its actual location at the top of the steam generator riser.

6. An annular bypass volume is included, which allows communication between the steam generator upper downcomer and the steam dome.

7. The steam dome was renodalized as two volumes connected by a crossflow junction. This configuration is a more precise geometrical representation of the physical steam dome in the Semiscale system.

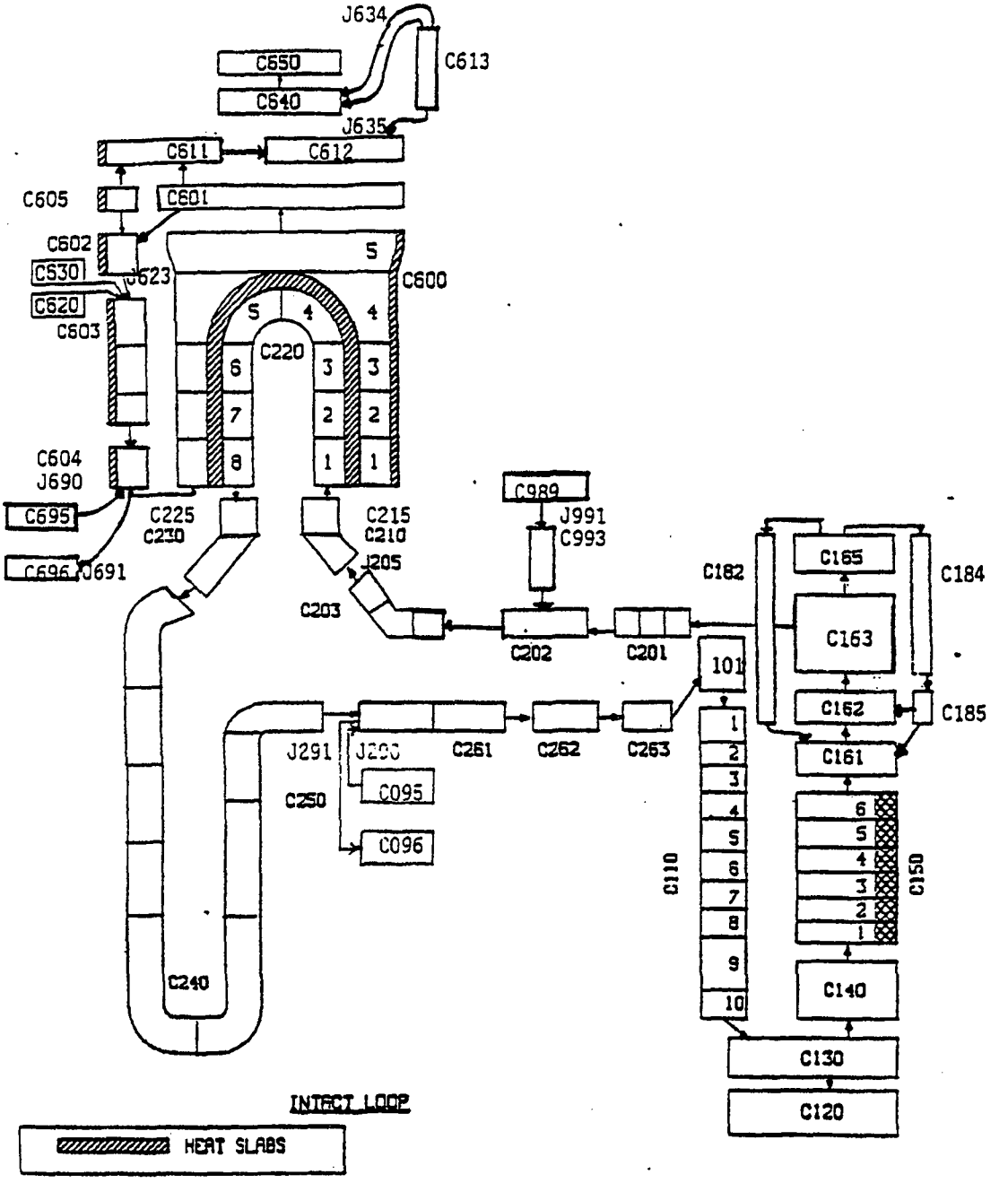

Figure 2.3-32. Schematic of RELAP5/MOD3 natural circulation test model.

8. The inside surfaces of the primary system pressure boundaries were modeled as adiabatic boundaries in lieu of modeling piping guard heaters, metal mass, and mechanistic heat loss.

The model consisted of 113 hydrodynamic volumes and 69 heat structures. All volume parameters were calculated with nonequilibrium code models. The specified core axial power profile[2.3-8] was modeled in 12 consecutive heat structures over six hydrodynamic volumes.

The RELAP5/MOD3 steady-state calculations made for the 60-kW core power tests over a range of PCS mass inventories are compared in Figures 2.3-33, 2.3-34, and 2.3-35 to the data from the S-NC Series Tests.

The data are plotted as unconnected circles in Figures 2.3-33 and show the measured PCS natural circulation mass flow rate sensitivity to the PCS mass inventory. The measured mass flow rate rose from about 0.4 kg/s (0.9 lbm/s) in a liquid-full system to about 0.82 kg/s (1.8 lbm/s) under two-phase conditions (87% PCS inventory). Further reduction in the system inventory resulted in a decrease in the mass flow rate until a condition of essentially zero mass flow was reached (50% PCS inventory). This final condition represented the reflux condition where steam and liquid were in countercurrent flow in the hot leg. This provided relatively good reflux heat transfer via condensation in the steam generator, while in the cold leg flow was nearly stagnant.

The RELAP5/MOD3 calculations were made simulating specific tests chosen to outline the overall shape of the data curve shown in Figure 2.3-33. The RELAP5/MOD3 results are plotted as squares connected by a solid line. The calculated results show the same characteristic of increased PCS flow with decreasing inventory, reaching a maximum flow at 88% inventory, then decreasing thereafter. The increasing PCS mass flow with decreasing inventory is due to boiling in the core. As a consequence of the vapor formation in the core, PCS mass flow is increased due to larger density difference between the core and the heat sink (steam generator). Reducing the PCS further causes void formation in the steam generator, thereby

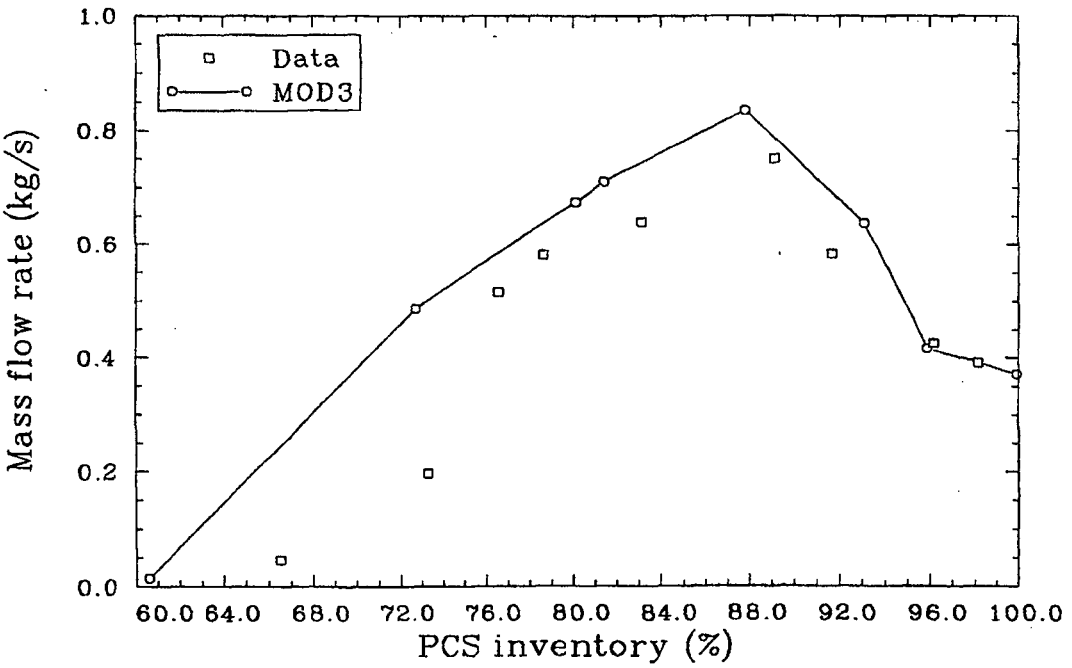

Figure 2.3-33. Measured and calculated (RELAP5/MOD3) mass flow rate at 60-kW core power for Semiscale natural circulation tests.

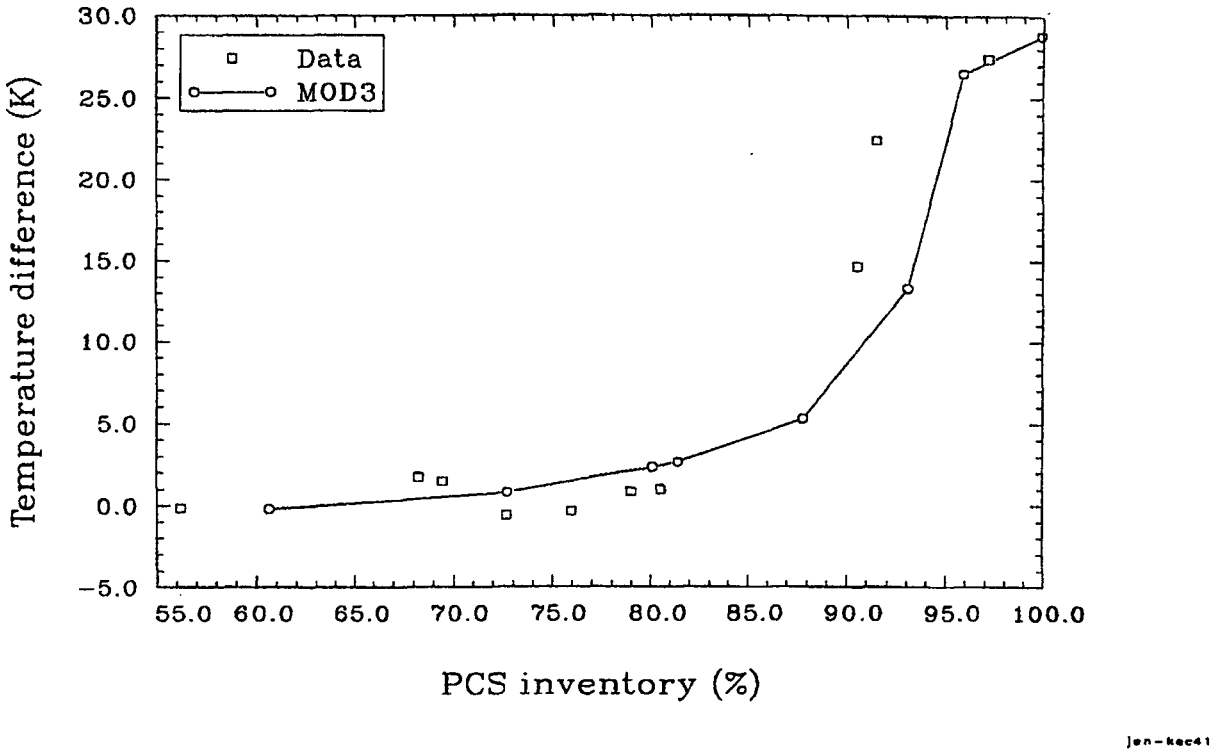

Figure 2.3-34. Measured and calculated (RELAP5/MOD3) core Δt at 60-kW core power for Semiscale natural circulation tests.

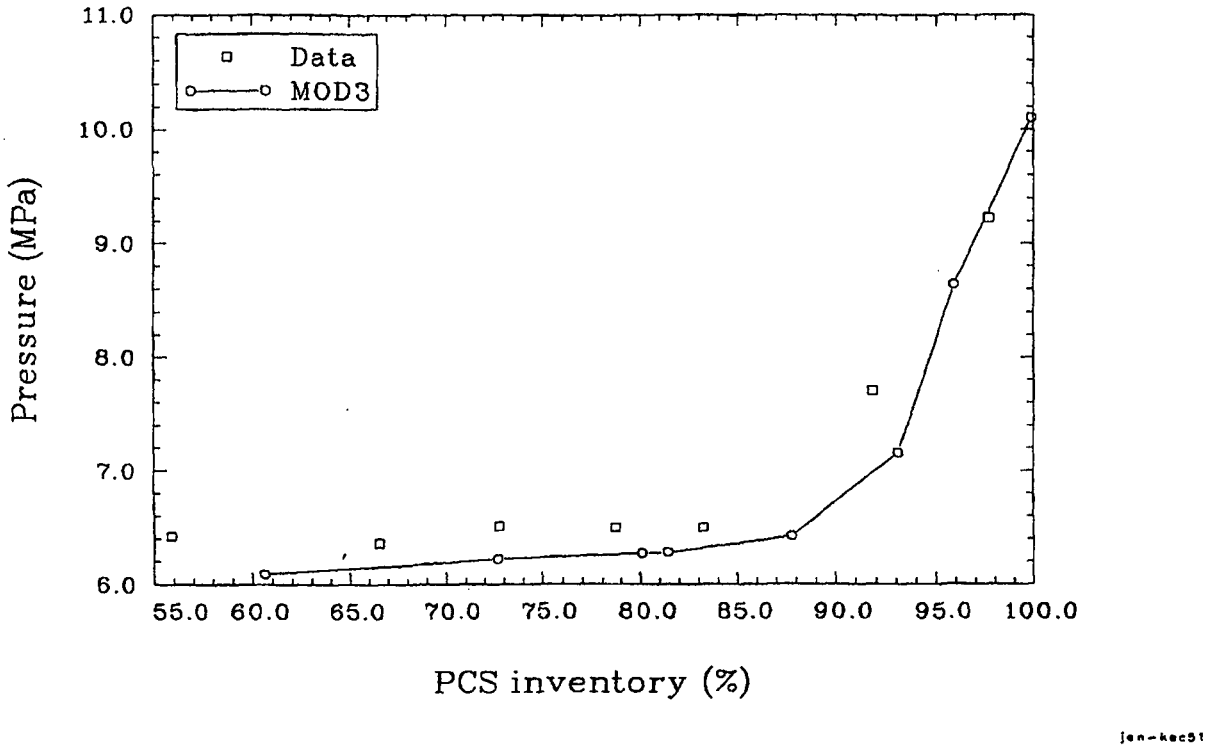

Figure 2.3-35. Measured and calculated (RELAP5/MOD3) primary pressure at 60-kW core power for Semiscale natural circulation tests.

reducing the average density difference between the heat source and heat sink. This causes a reduction in PCS mass flow as the driving potential is reduced. The calculated results show good agreement with the measured data.

As the PCS inventory was further reduced to the range of 88% to 90%, voiding also occurred in the hot leg and in the upside portion of the steam generator tubes. This resulted in decreasing the density on the upside of the steam generator, causing the net thermal driving head (NTDH) and the PCS mass flow to increase. Again, the RELAP5/MOD3 calculations show good agreement with the measurements in this regime.

As the PCS inventory was further reduced below 88%, voiding occurred in the downside of the steam generator tubes, consequently reducing the NTDH which in turn reduced the PCS mass flow rate The MOD3 calculations also show this effect.

Reflux heat transfer was evident when the system showed no cold leg mass flow with constant PCS conditions and power input. Data showed that this condition was established at about 65% PCS mass inventory. The MOD3 calculations predicted reflux heat transfer at about 61% PCS mass inventory. No calculations were made with lower PCS inventories due to excessive run times. The problem is due to void fraction oscillations occurring in the cold leg. The void fraction oscillates between 1.0 and just less than 1.0 each time step. The consequence is excessive mass error, which in turn causes reduced time step size.

Figures 2.3-34 and 2.3-35 show the core temperature difference and the PCS upper plenum pressure, respectively, for the same system inventories and core power shown in Figure 2.3-33. Both Figures 2.3-34 and 2.3-35 show excellent agreement with the data.

For the S-NC-3 calculations, in which the secondary system inventory was reduced, the results of the calculations are shown in Figure 2.3-36. In Figure 2.3-36, the measurements are plotted as unconnected circles. The measured data in the region from 15% to 45% steam generator surface area are

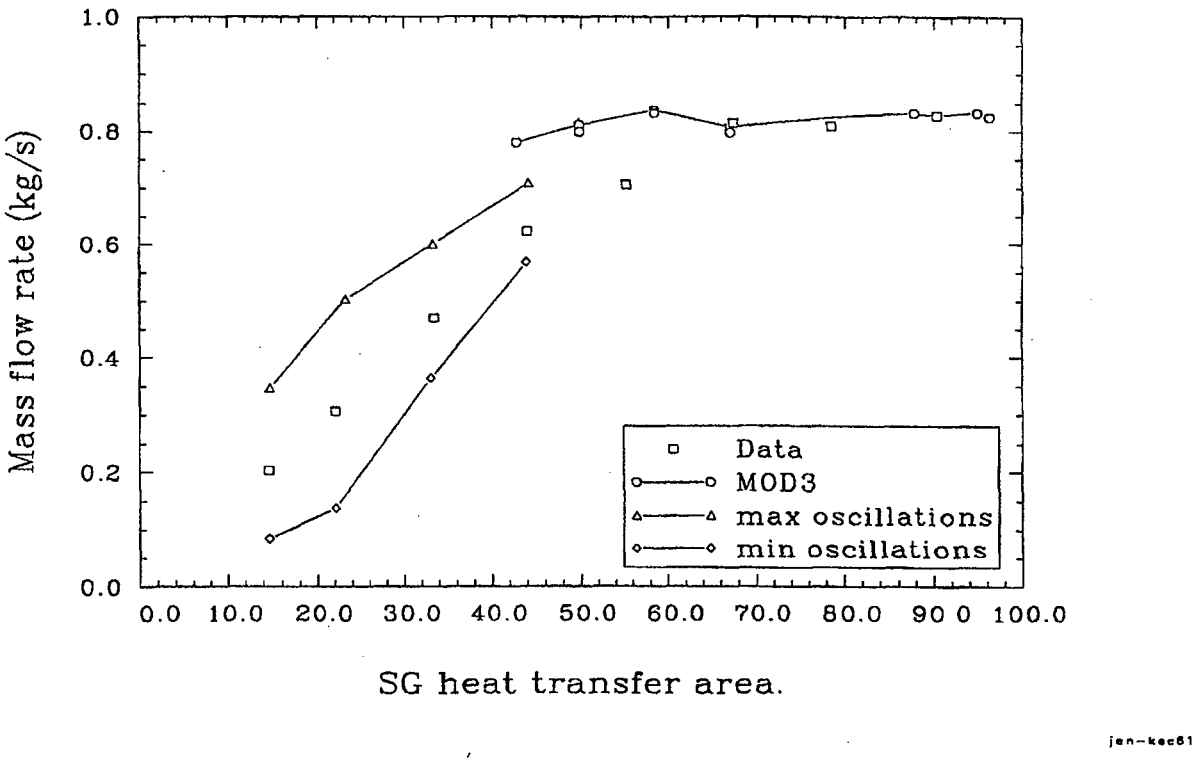

Figure 2.3-36. Measured and calculated (RELAP5/MOD3) mass flow rate versus steam generator secondary side heat transfer area for Semiscale natural circulation test S-NC-3.

the average of the minimum and maximum oscillations observed. These values are included as unconnected squares and triangles to show the range of the oscillations. The calculated results are shown with a solid line. Note that the calculations are terminated at 43% steam generator surface area. This is the point at which excessive run times were experienced with further reduction of steam generator mass.

In examining Figure 2.3-36, it is apparent that RELAP5/MOD3 results gave reasonable predictions of primary flow behavior with respect to reduced secondary system inventory. However, in the region below 55% secondary inventory, the code tended to overpredict the PCS mass flow.

In conclusion, RELAP5/MOD3 simulated the Semiscale natural circulation tests reasonably well for the higher PCS mass inventories. Also, at the higher steam generator mass inventories, the code calculations are in good agreement with the measured data. However, calculations made with extremely low mass inventory caused excessive computational time due to oscillating void fractions.

2.3.4 LOBI Large-Break Test A1-04R

The Loop Blowdown Investigations (LOBI) experiment was used to assess the RELAP5/MOD3 system calculation capability during the blowdown phase of the large-break LOCA of a PWR. The LOBI test facility, as shown in Figure 2.3-37, is located at Ispra, Italy, and supported by the EURATOM Joint Research Center.[2.3-9]

The facility was designed to supply experimental data on simulated LWR PCS response during the initial high-pressure blowdown portion of a LOCA. It is an approximately 1:700 scale model of a four-loop, 1300-MWe PWR, consisting of two primary coolant loops connected to the electrically heated reactor pressure level model. While both experimental loops are active loops containing a circulation pump and a steam generator, one (the intact loop) has three times the water volume and mass flow of the other (the single or broken loop).

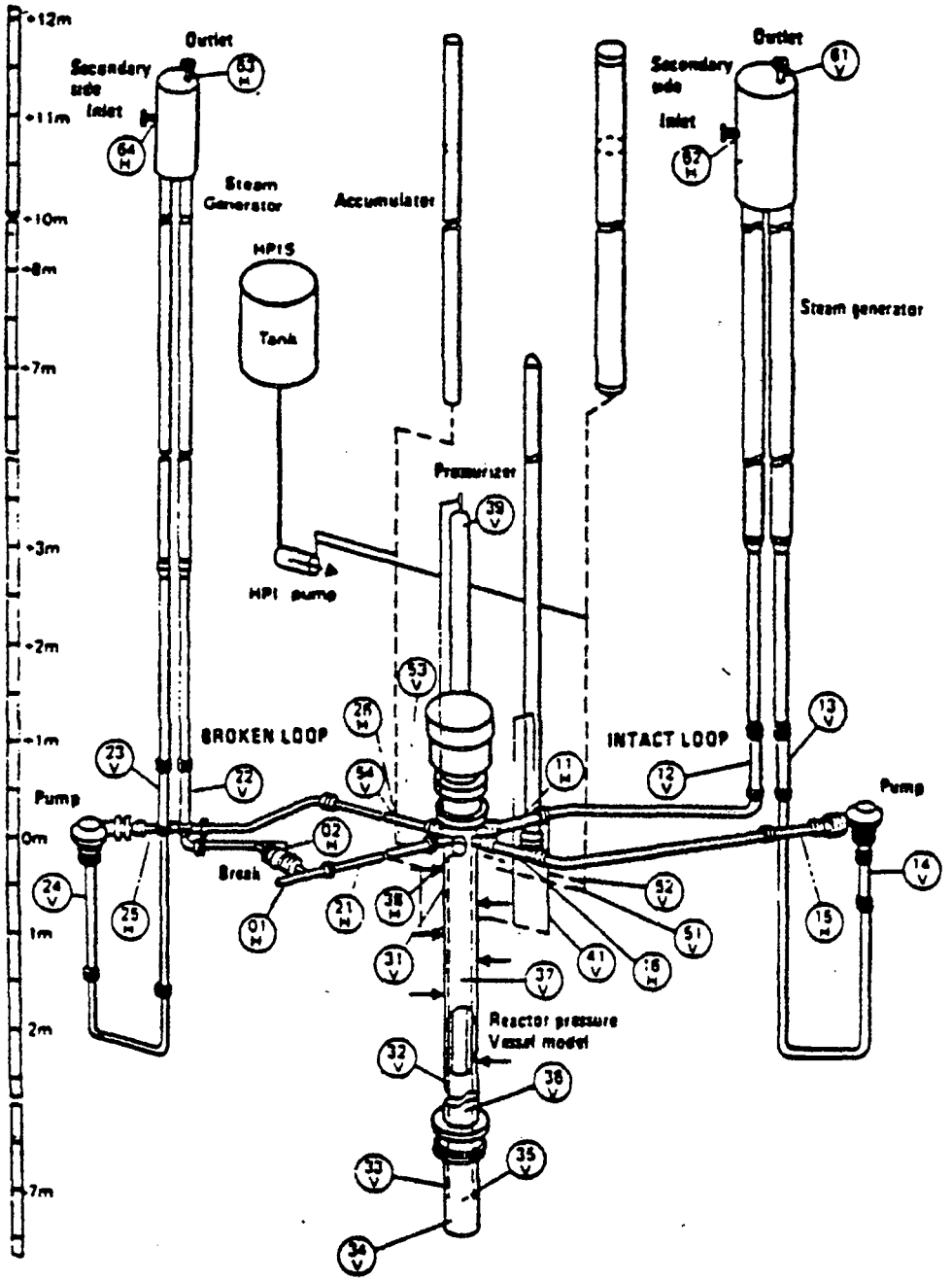

Figure 2.3-37. LOBI test facility.

The RELAP5 nodalizations developed by Sandia National Laboratories[2.3-10] for the LOBI facility, as shown in Figure 2.3-38, were used. Both loops are modeled, with the triple-capacity intact loop shown on the left, the single broken loop on the right, and the vessel in the middle.

There are a total of 186 volumes, 193 junctions, and 198 heat slabs in the A1-04R nodalization. The intact loop has 20 volumes modeling the piping and pump, while the broken loop uses 23 volumes for the piping, pump and break assembly (including a time-dependent volume repressurizing the atmosphere). Each steam generator consists of 46 volumes--13 in the primary and 33 in the secondary. (Not shown on the nodalization drawings are single-volume recirculation pipes connecting the individual hot- and cold-leg downcomers on each steam generator; also not indicated are time-dependent volumes and junctions providing the pump seal water injection and drainage.) The pressurizer and its surge line are modeled with 18 volumes, nine of which are in the pressurizer itself and three of which model the cooling pipes. (The breakup of the surge line into several components is due to the fact that the original base case nodalization modeled a branching surge line configured for both intact and broken loop hot leg injection.) The vessel itself is modeled with 31 volumes--13 in the annular downcomer, one in the lower plenum, two in the lower core support region, eight in the core heated length, three in the upper plenum, and four in the upper head and bypass line. The intact loop cold leg accumulator uses one volume. Most of the heat slabs contain five nodes, although a few have six.

The vessel nodalization is shown in Figure 2.3-39. The core region axial levels were chosen from the axial power profile, and the thermocouple locations were modeled by heat slabs. Besides the core rod heat slabs, heat slabs have been included for much of the major vessel structure--the pressure vessel itself, the core barrel, the upper closure plate, and the upper head and bypass line piping walls.

The steam generator nodalization is shown in Figure 2.3-40, together with the relative elevations of the cell boundaries. All the U-tubes in

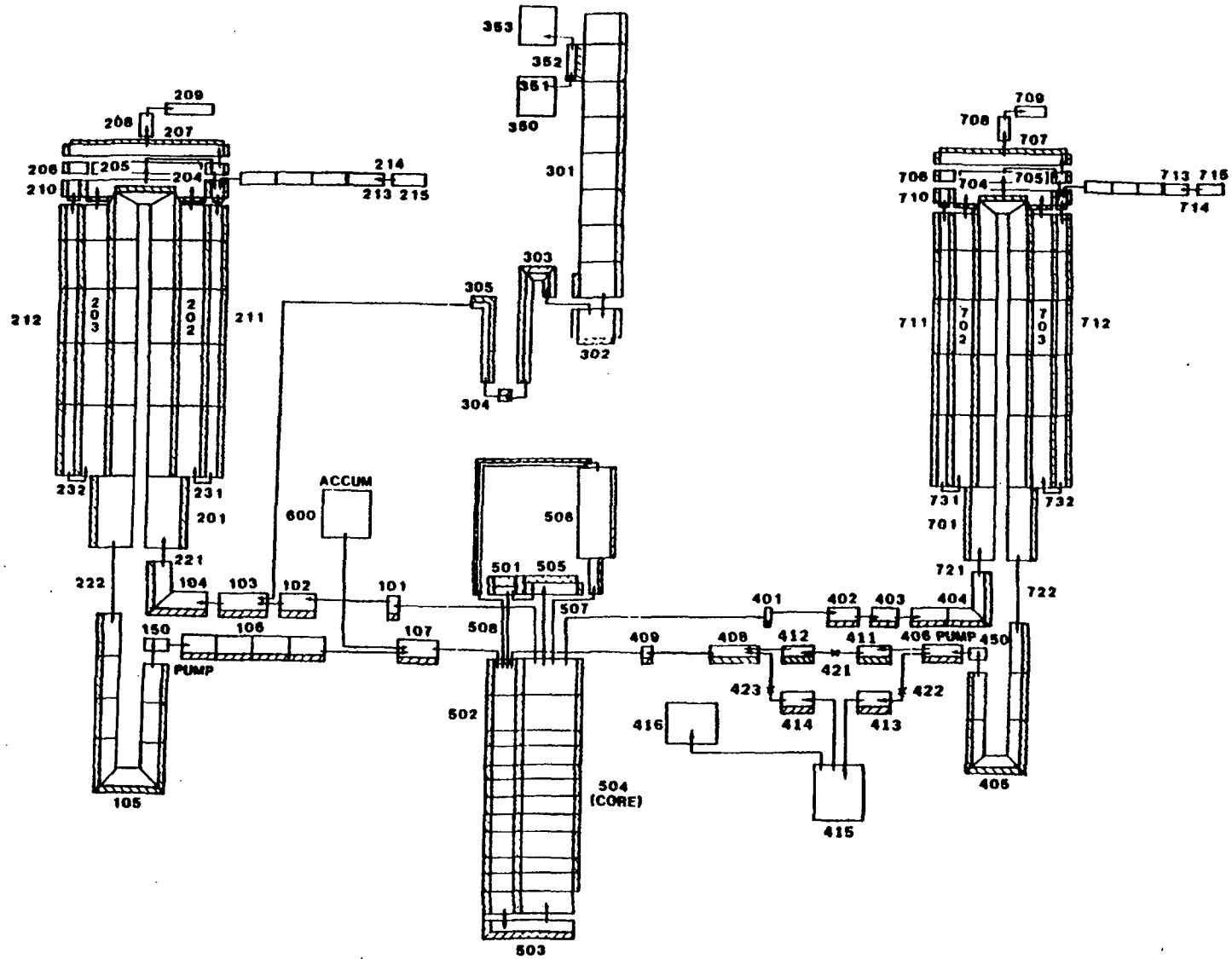

Figure 2.3-38. LOBI test facility nodalization.

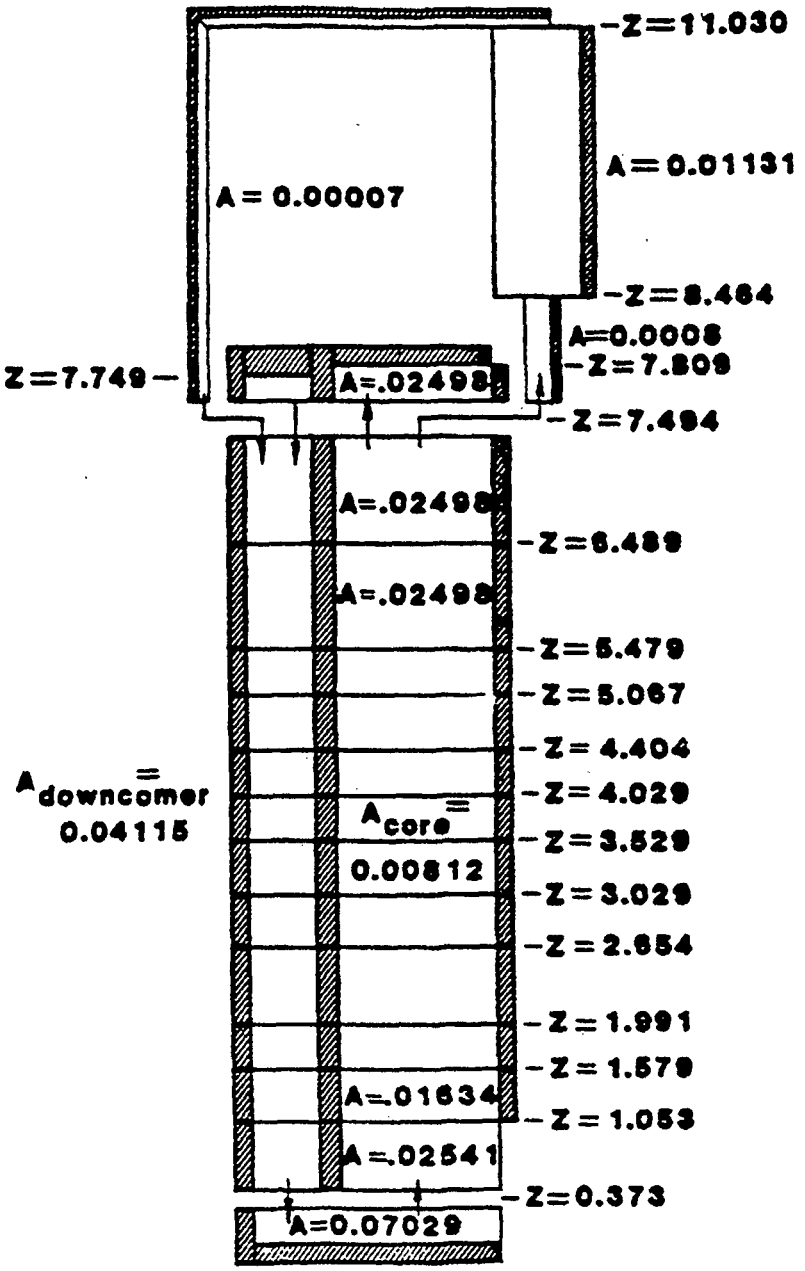

Figure 2.3-39. LOBI vessel nodalization.

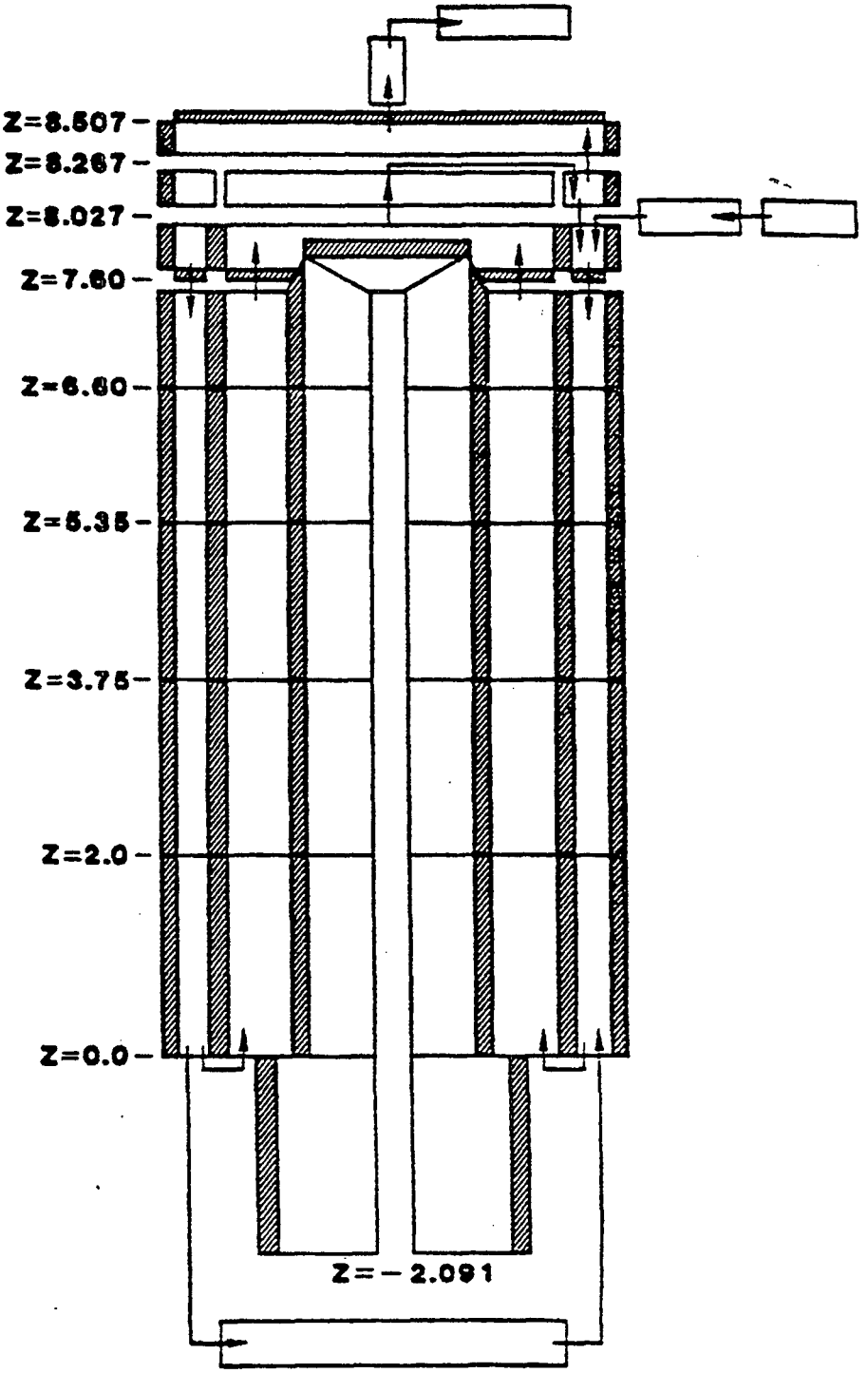

Figure 2.3-40. LOBI steam generator nodalization.

either steam generator are lumped into a single flow path. Besides the U-tubes themselves, heat slabs representing the external walls, the downcomer, and the top plate are included in the model. The recirculation pipe is indicated on this more detailed drawing.

Both the single-phase and the two-phase difference homologous head and torque curves for the two circulation pumps are taken from published LOBI pump curves.[2.3-11,12] The Semiscale two-phase head multiplier was used, since no other data were available. The homogeneous flow model was used in the analysis for the break flow calculation.

The first part of the LOBI experimental program consisted of the six large-break A1 tests. These were simulations of double-ended, offset-shear breaks in the cold leg pipe between the pump and the pressure vessel in a PWR. In this assessment, Test A1-04R was chosen. Test A1-04R was a repetition of the PREX test (and therefore performed with cold leg injection only), but with a different, multi-step, power curve. The test initial conditions are given in Table 2.3-1.

Figure 2.3-41 shows the pressure in the intact loop cold leg and in the broken loop upstream of the pump-side break. It should be noted that the experimental data from data reports[2.3-13,14] were digitized. The overall agreement between calculation and experiment is good. After initiation of blowdown, the saturation pressure in the hot legs is reached in ~100 ms. At this time, flashing in the hot leg starts and depressurization rate for the two curves decreases. Flashing in the intact loop cold leg occurs at ~3 s, which causes a further decrease in the depressurization rate. After ~24 s the accumulator injection starts. The RELAP5/MOD3 calculation stops at 60 s.

The pressure in the broken loop upstream of the pump-side break falls immediately to the saturation pressure and is then mainly governed by the break flow. The mass flows upstream of the pump-side and vessel-side breaks are shown in Figure 2.3-42. The calculated break flow on the pump side of the break is higher than the data during the first 20 s, and the calculated

Table 2.3-1. Steady-state conditions for LOBI Test A1-04R

Parameter	IL		BL	
	Data	RELAP5	Data	RELAP5
Core power (MW)	5.12	5.12	5.12	5.12
Pressurizer pressure (MPa)	15.3	16.3	15.3	16.3
Primary system:				
Mass flow (kg/s)	21.1	20.5	7.0	6.6
Hot leg temperature (K)	600	601	606	601
Cold leg temperature (K)	571	572	571	571
Secondary system:				
Feedwater flow (kg/s)	2.07	2.07	0.8	0.8
Feedwater temperature (K)	493	493	501	493
Steam temperature (K)	553	553	553	556
Pressure (MPa)	6.4	6.5	6.4	6.7
Accumulators:				
Pressure (MPa)	2.7	2.7	--	
Water temperature (K)	305	305	--	
Water volume (L)	224	229	--	
Gas volume (L)	56	56	--	

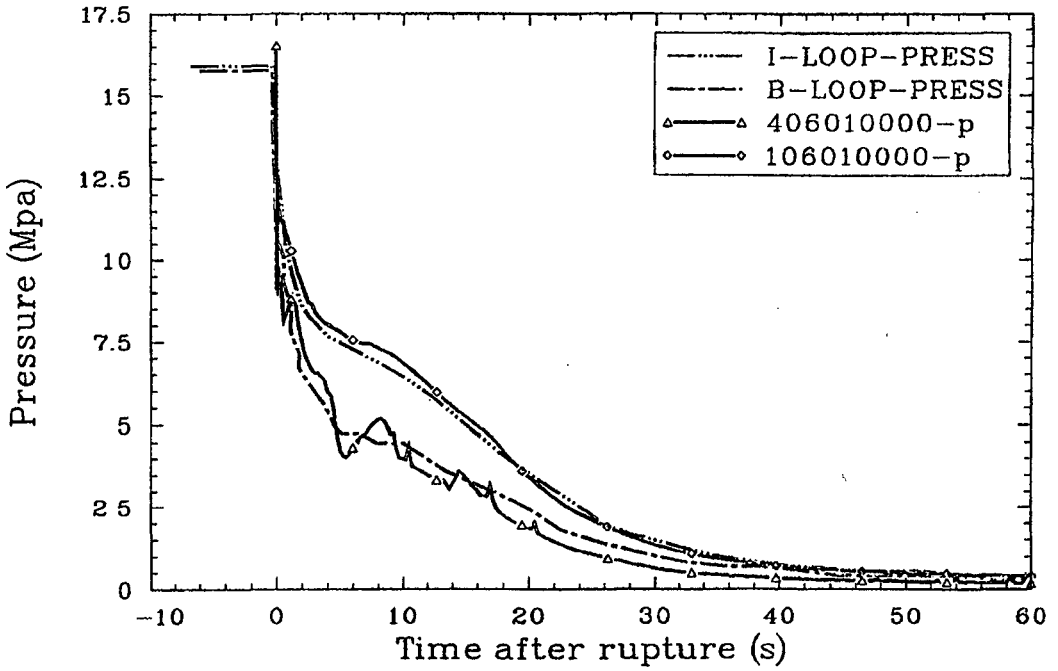

Figure 2.3-41. Measured and calculated (RELAP5/MOD3) intact and broken loop pressure for LOBI Test A1-04R.

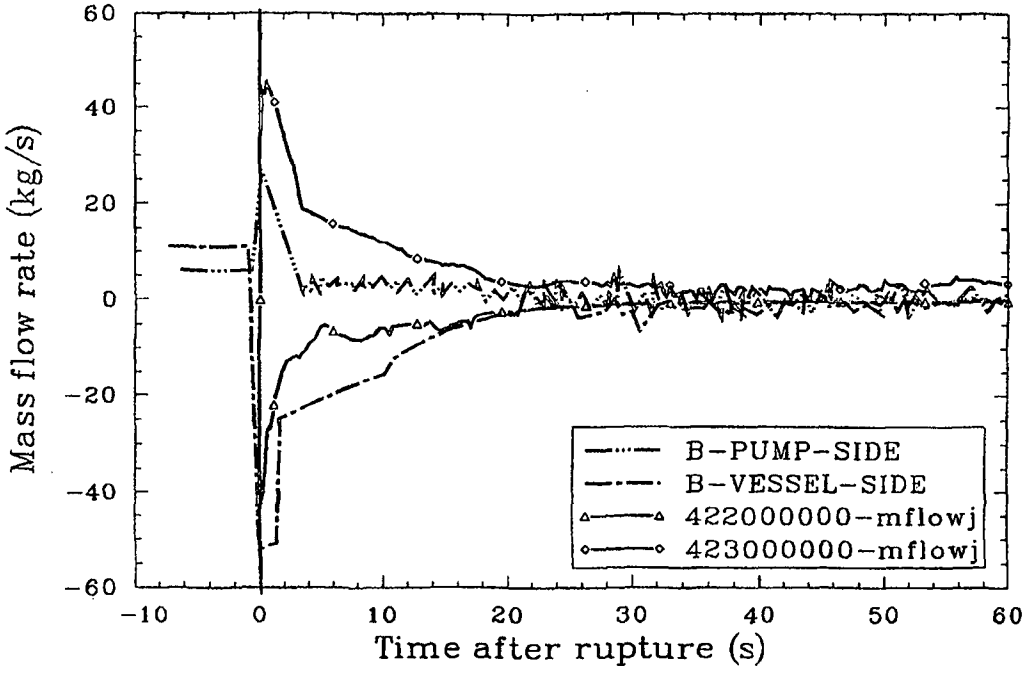

Figure 2.3-42. Measured and calculated (RELAP5/MOD3) pump-side and vessel-side break mass flow for LOBI Test A1-04.

break flow from the vessel side is smaller than the data over the same time period. The pressure histories shown on Figure 2.3-41 do not seem to be adversely impacted by the compensating flow error. Assessing the effect of this flow error on the water distribution in the core is difficult.

The calculated core differential pressure is shown in Figure 2.3-43 and exhibits the trends of the experiment data. However, the higher calculated pressure difference between 25 and 60 s could represent extra water in the core to hold down rod temperature increases to be shown later.

The injection of ECC water from the intact loop accumulator is initiated when the pressure in the intact loop cold leg falls below the accumulator activation pressure of 2.7 MPa. This occurs at ~24 s in the experiment and at ~22 s in the calculation, as shown in Figure 2.3-44; the maximum experimental injection rate is ~3.3 kg/s, but the maximum calculated injection is about 5 kg/s, which is much higher than the experiment data. The reason of this overprediction is unknown. The cold leg between the injection point and the vessel immediately filled with subcooled water in the experiment, as indicated by the steep increase of the fluid density to its subcooled value during this time period in Figure 2.3-45. In contrast, the calculation shows a slower rise and a lower maximum density. Figure 2.3-46 shows that the calculated fluid temperature in the ECC injection region is generally higher than the data after 30 s, even though the calculated injection rate was too high. Most of the injected ECC water bypasses around the downcomer and is discharged through the vessel-side break during the blowdown period.

Arithmetic mean values of measured heater rod temperatures (excluding the thermocouple signals from the outer, peripheral, bundle zone) are shown for the various instrumented levels in Figures 2.3-47 through 2.3-49. The predicted rod temperature responses match the trends of the data during the first 10 s. Heatup and quenching was widespread during this time period. The data show that there is not enough water in the core to support continued nucleate boiling and that secondary heatups occur. However, only

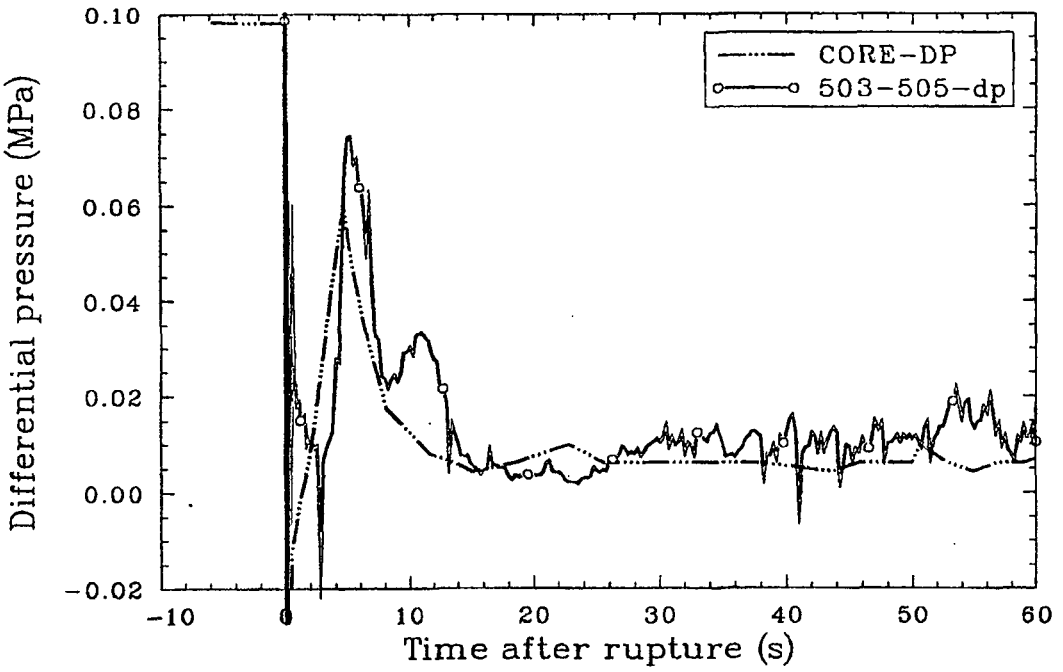

Figure 2.3-43. Measured and calculated core differential pressure for LOBI Test A1-04R.

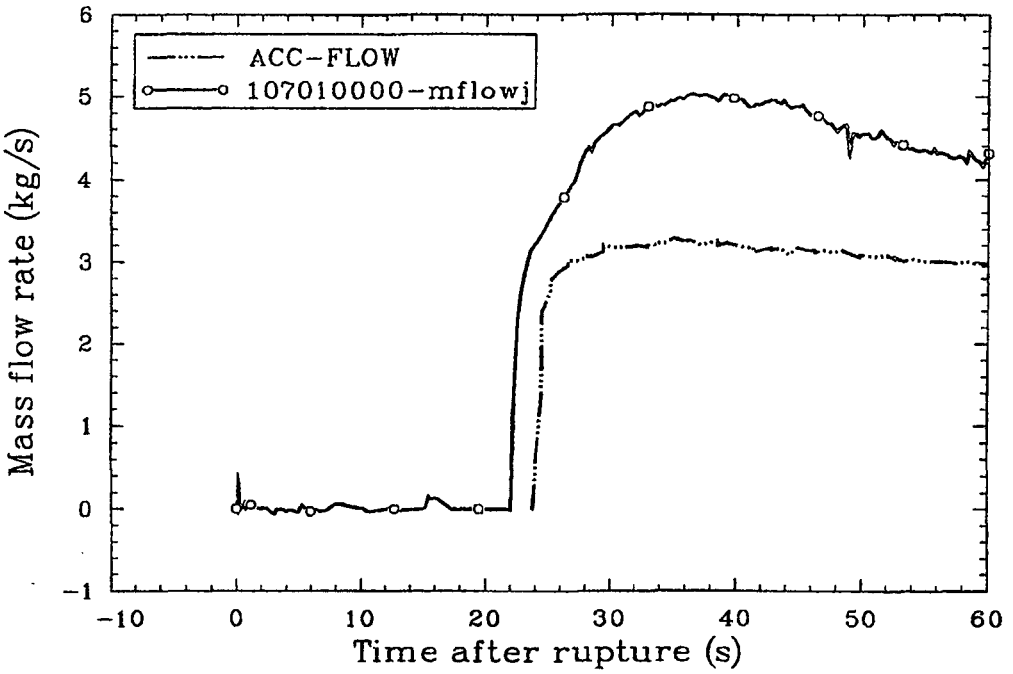

Figure 2.3-44. Measured and calculated accumulator injection flow rate for LOBI Test A1-04R.

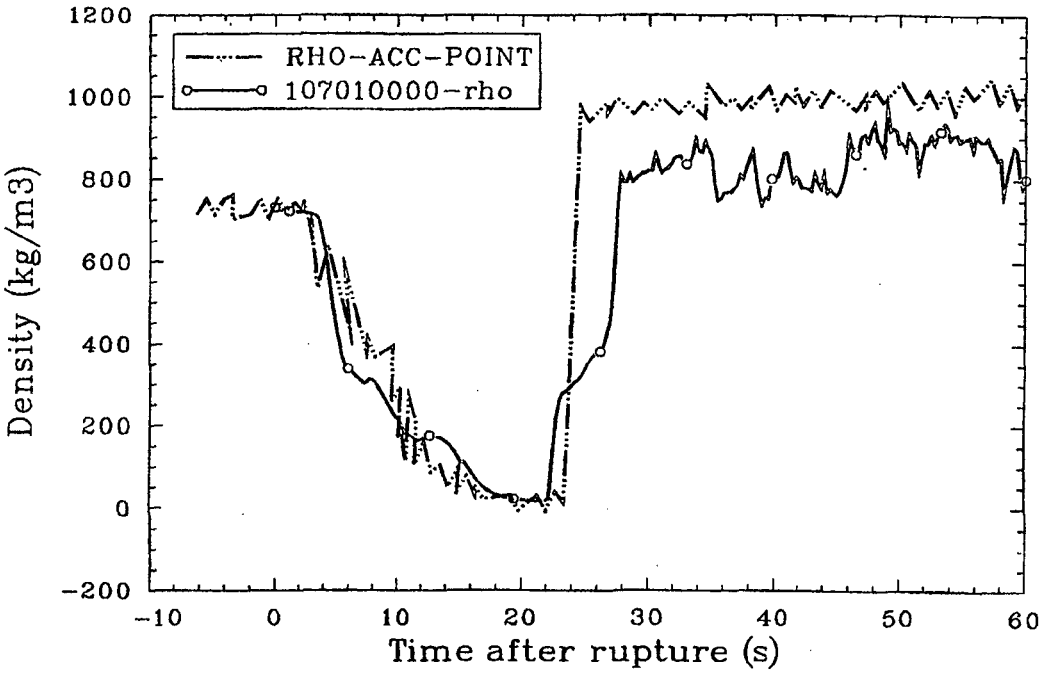

Figure 2.3-45. Measured and calculated fluid density at accumulator injection point for LOBI Test A1-04R.

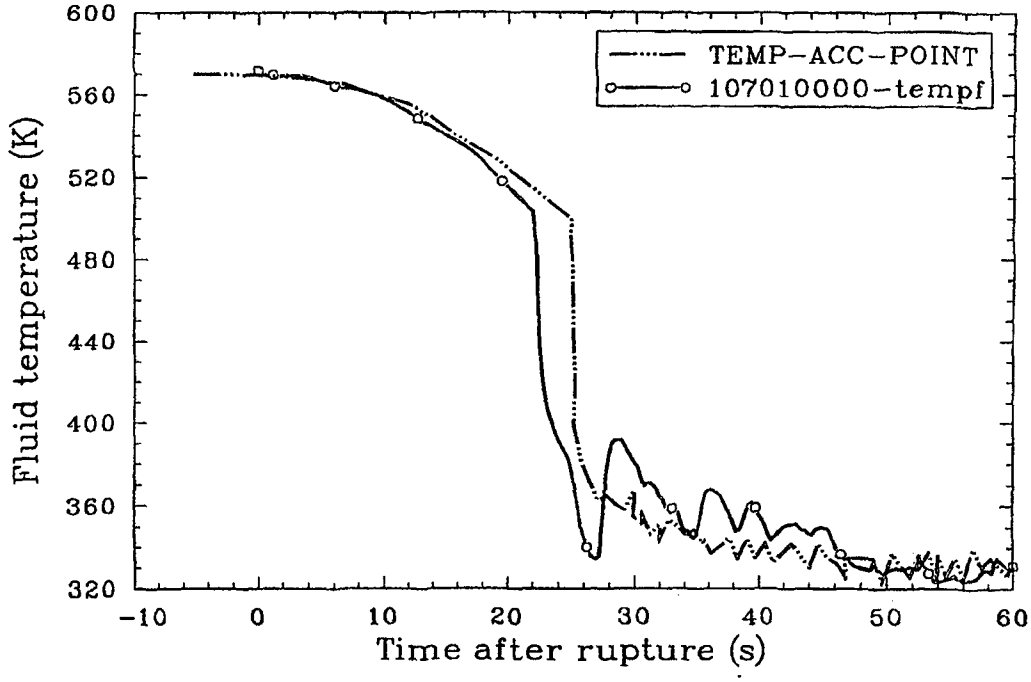

Figure 2.3-46. Measured and calculated fluid temperature at accumulator injection for LOBI Test A1-04R.

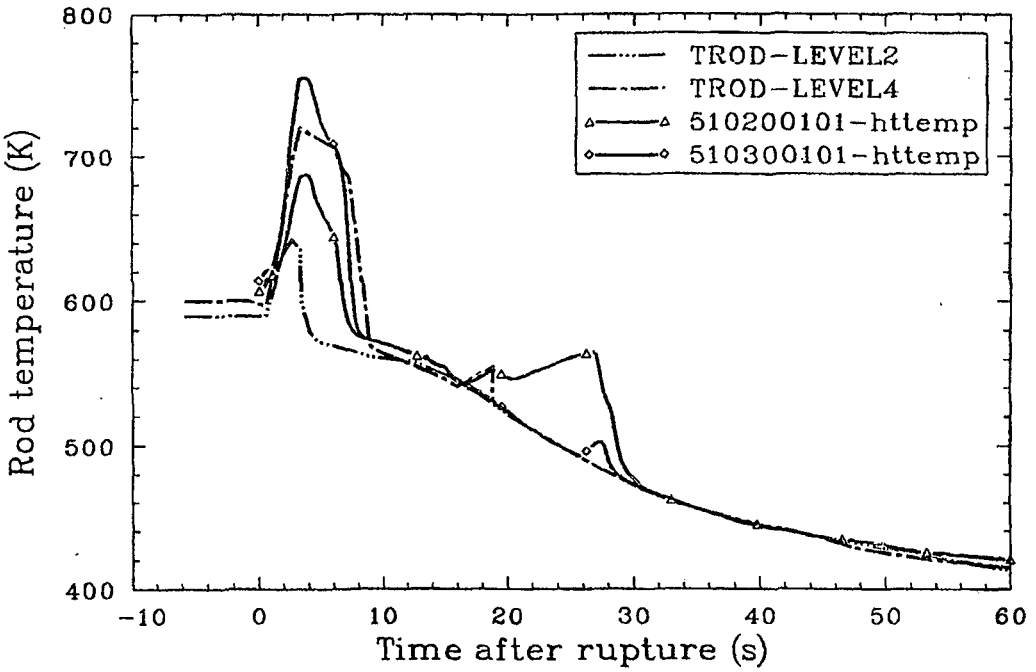

Figure 2.3-47. Measured and calculated lower core rod temperature for LOBI Test A1-04R.

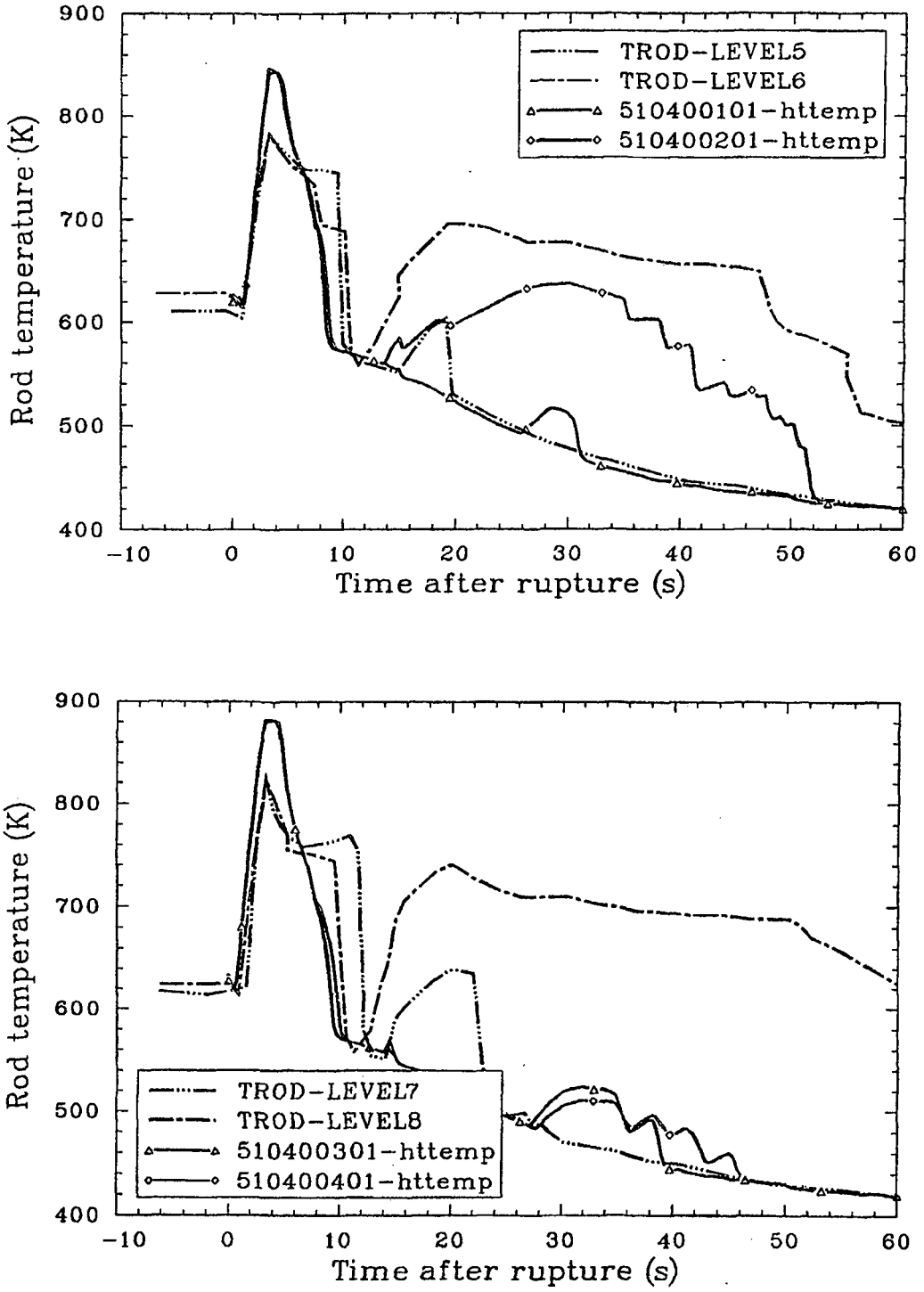

Figure 2.3-48. Measured and calculated mid-core rod temperatures for LOBI Test A1-04R.

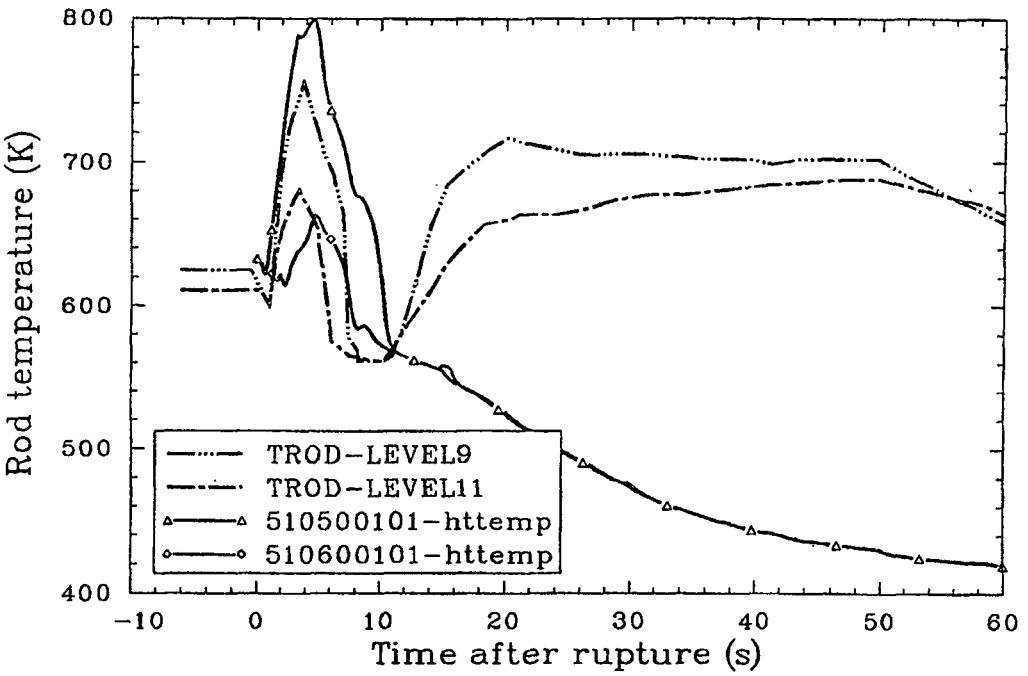

Figure 2.3-49. Measured and calculated upper core rod temperature for LOBI Test A1-04R.

a few elevations returned to film boiling in the calculation. Figure 2.3-50 shows more water at the bottom of the core in the experiment than in the calculation. One can only guess that the cause of the lower calculated rod temperatures was that the flow rate through the core was too high.

The behavior of fluid temperatures in the primary system is given in Figures 2.3-51 and 2.3-52. Both the calculated liquid (tempf) and gas (tempg) temperatures are given, since the thermocouple in the experiment could be in the steam or the water. The loop temperatures are in fair agreement with experimental measurements.

The RELAP5/MOD3 calculation is in general agreement with experimental data, but break flow and accumulator flow errors need to be removed.

2.3.5 Zion-1 PWR Small Break

The Zion-1 PWR plant is a Westinghouse 4-loop PWR, and the RELAP5 model has been used to analyze offsite power[2.3-15] and instrument tube rupture[2.3-16] scenarios. The deck has been modified to remove proprietary information and is currently being used as a quality assurance test problem that is run when new versions of RELAP5 are created at the INEL. The deck models a 2% [0.1-m (4-in.)] cold leg break. The RELAP5 nodalization diagram is shown in Figure 2.3-53. The model contains 139 volumes, 142 junctions, and 83 heat structures. Two primary coolant loops were modeled. One loop, called the broken loop, represented a single primary coolant loop. The break was modeled in the pump discharge piping of the broken loop cold leg. The other loop, called the intact loop, represented three primary coolant loops. The pressurizer was attached to the intact loop. The intact and broken loops were modeled symmetrically except for differences due to the location of the break and pressurizer. Component numbers in the intact loop loop were between 100 and 194; component numbers in the broken loop were between 200 and 294. The Zion-1 nodalization is similar to Semiscale and Loft models. Heat structures were used to represent heat transfer from fuel rods, U-tubes, pressure vessel wall, core band, core shroud, and internals in the upper head and lower and upper plena.

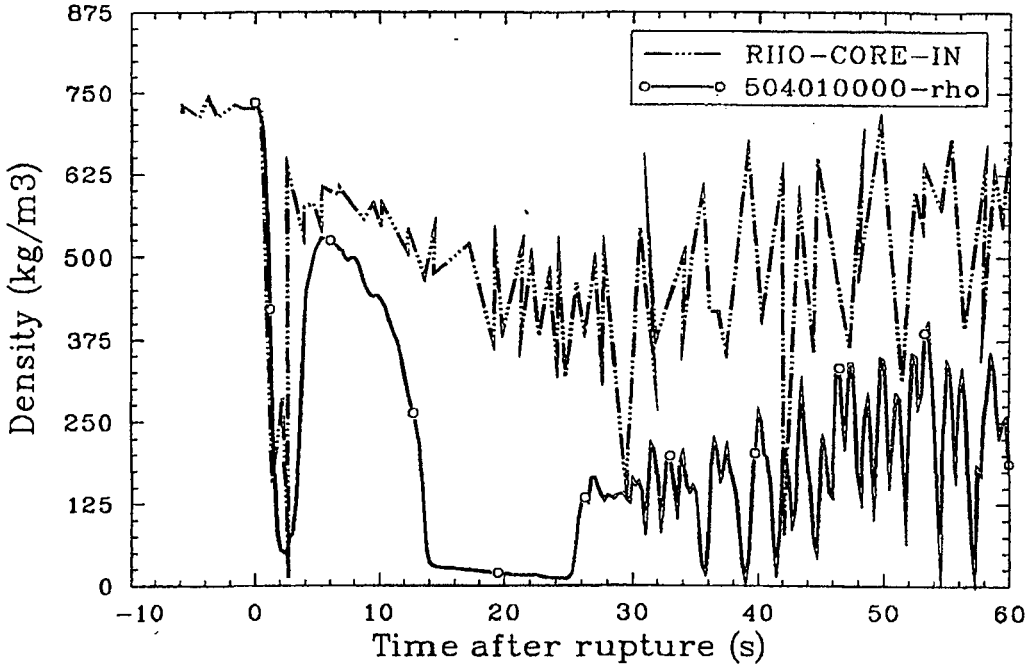

Figure 2.3-50. Measured and calculated core inlet density for LOBI Test A1-04R.

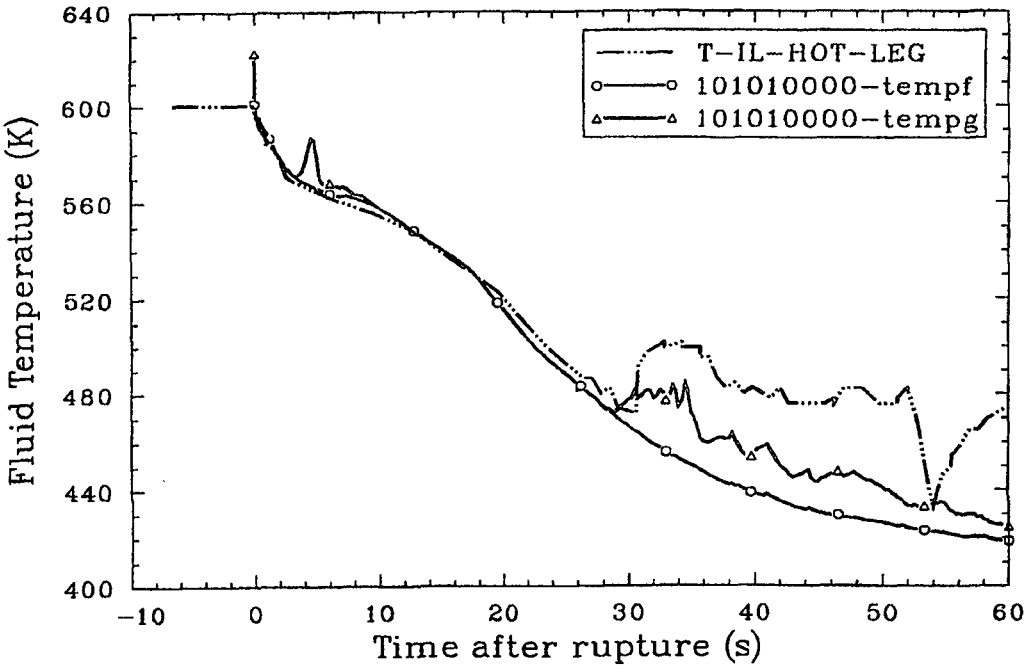

Figure 2.3-51. Measured and calculated intact loops steam generator temperature for LOBI Test A1-04R.

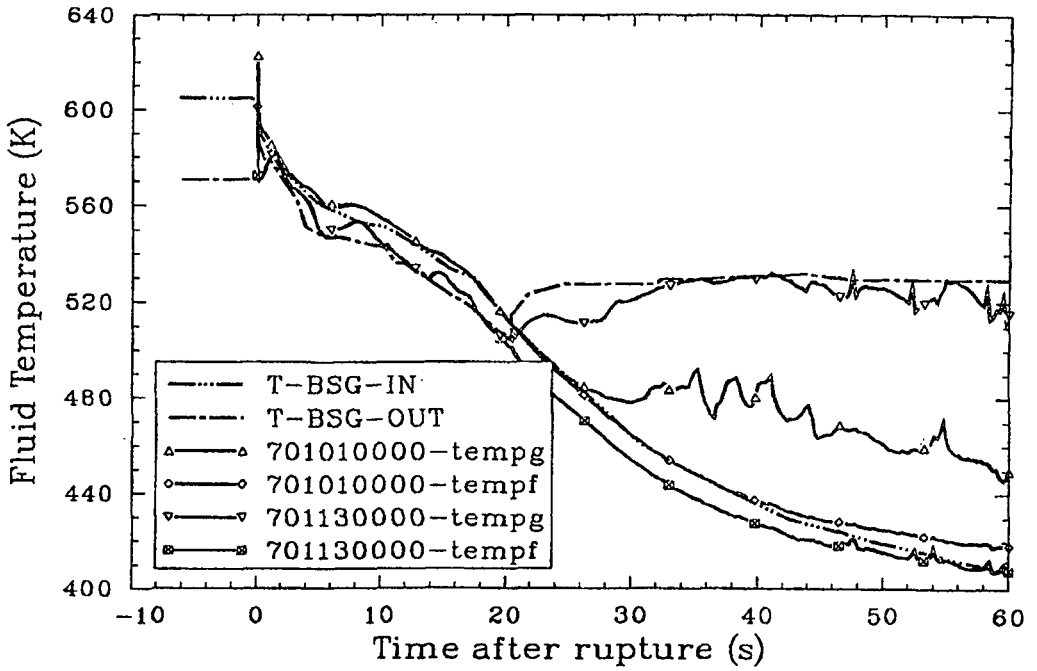

Figure 2.3-52. Measured and calculated broken loop steam generator temperature for LOBI Test A1-04R.

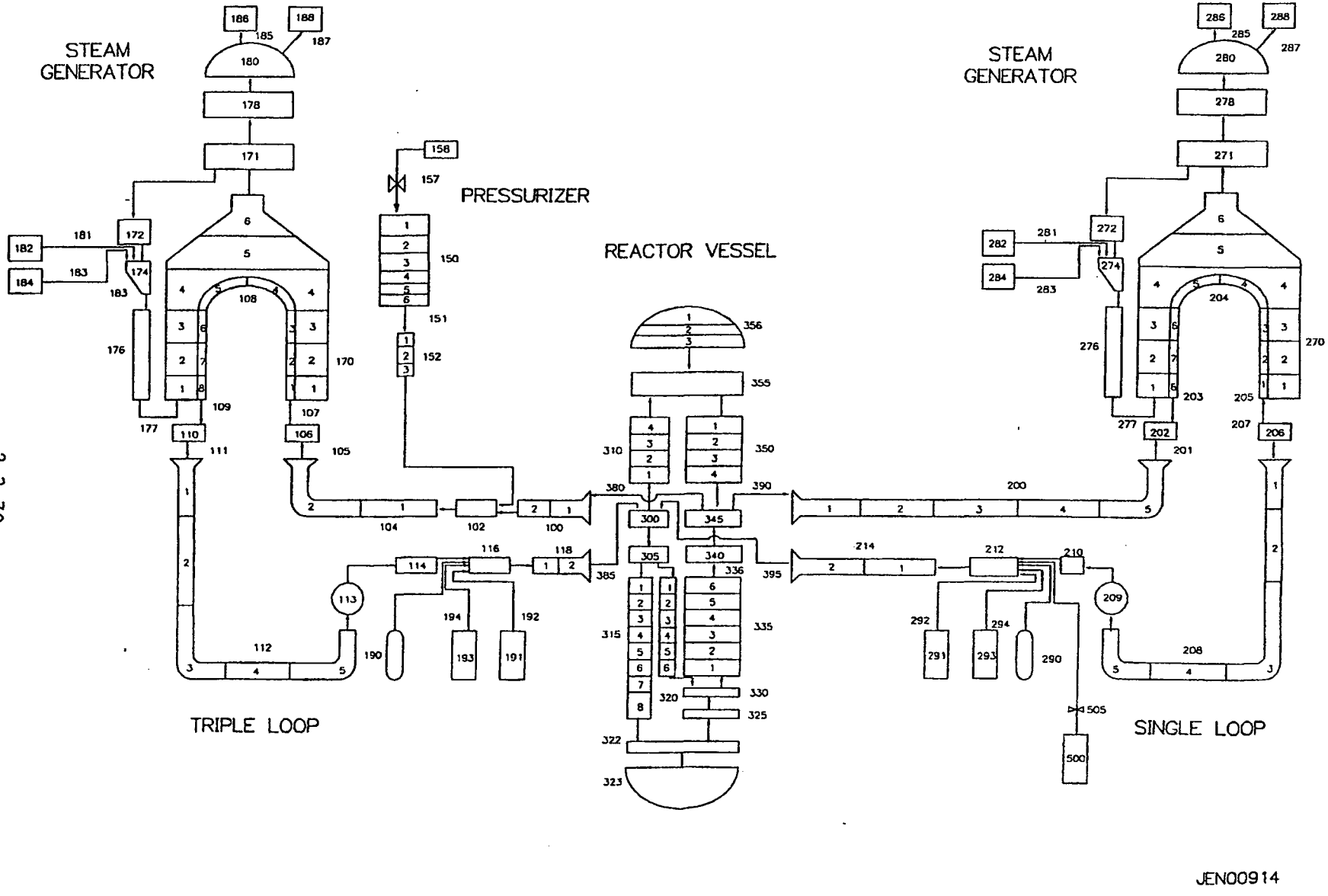

Figure 2.3-53. RELAP5 nodalization for the Zion-1 PWR.

The transient was initiated by an instantaneous opening of the break. This was accomplished by using a trip valve, which was open for times greater than 0.01 s. A scram signal was generated when the pressurizer pressure decreased to 12.82 MPa (1860 psia). Scram occurred 3 to 4 s after the scram signal was generated. The reactor coolant pumps began coasting down simultaneously with the scram signal. Valves in the steam generator feedwater and steam lines began closing simultaneously with the scram signal. The steam line and feedwater valves were linearly closed within 1 s and 10 s, respectively, of the scram signal. Safety injection and charging began 5 s after the pressurizer pressure decreased to 12.62 MPa (1830 psia). Auxiliary feedwater flow was initiated 14 s after the scram signal was generated. Automatic control of the feedwater flow based on downcomer liquid level was simulated.

Figures 2.3-54, 2.3-55, and 2.3-56 show comparisons for RELAP5/MOD3 and RELAP5/MOD2 for some selected parameters. Figure 2.3-54 shows the pressure in the upper plenum volume 345 and is representative of the primary system pressure. MOD3 is slightly below MOD2 for the first 25 s and then slightly above MOD2 for the remainder of the calculation. Figure 2.3-55 shows the pressure in the intact loop steam generator steam dome volume 180 and is representative of the intact loop secondary pressure. The MOD3 pressure increased to a higher value than MOD2 at 22 s and then settled in at a slightly lower value for the rest of the calculation. The MOD3 and MOD32 break mass flow rates in Figure 2.3-56 are very similar.

The MOD3 calculation was run to 100 s on Version 5i1, using the Cray, and required 874 attempted advancements and 64.46 cpu seconds. The MOD2 calculation was run to 100 s on Cycle 36.06, using the Cray, and required 1071 attempted advancements and 81.53 cpu seconds.

2.3.6 References

2.3-1. D. L. Reeder, *LOFT System and Test Description (5.5 ft. Nuclear Core/LOCEs)*, NUREG/CR-0247, TREE-1208, July 1978.

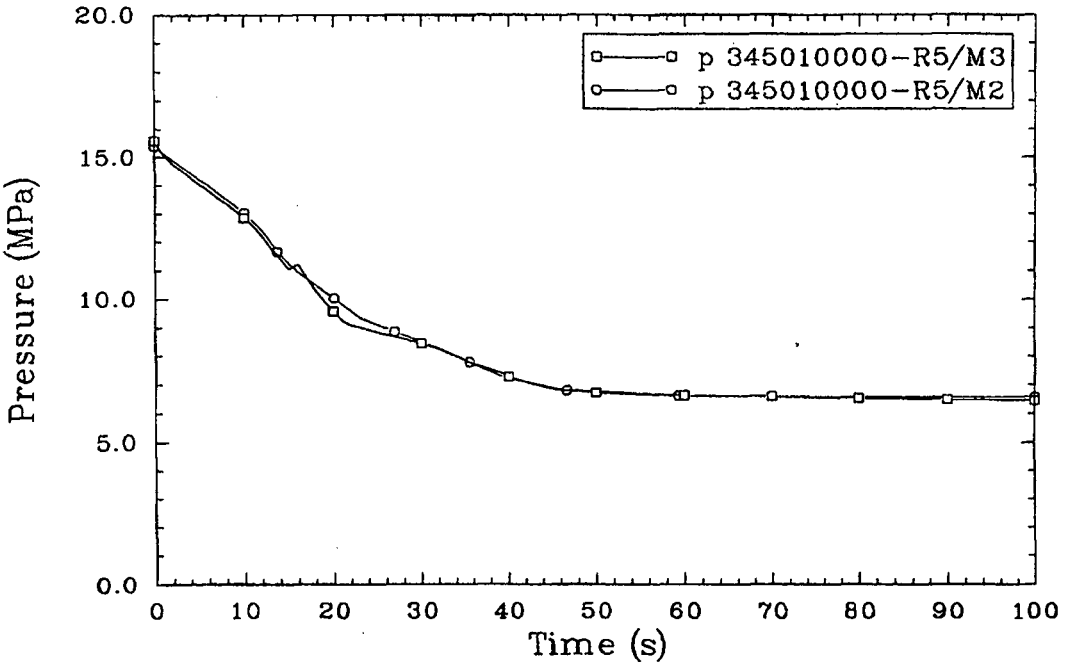

Figure 2.3-54. Calculated (RELAP5/MOD3, MOD2) primary system pressure for the Zion-1 small break.

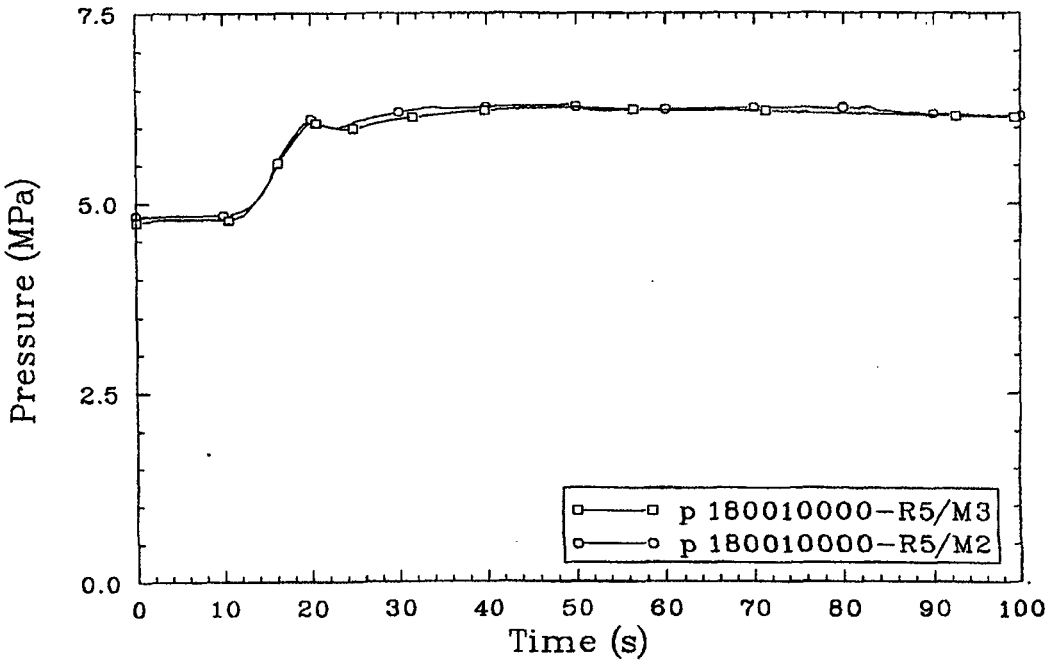

jan-r331

Figure 2.3-55. Calculated (RELAP5/MOD3, MOD2) intact loop secondary pressure for the Zion-1 small break.

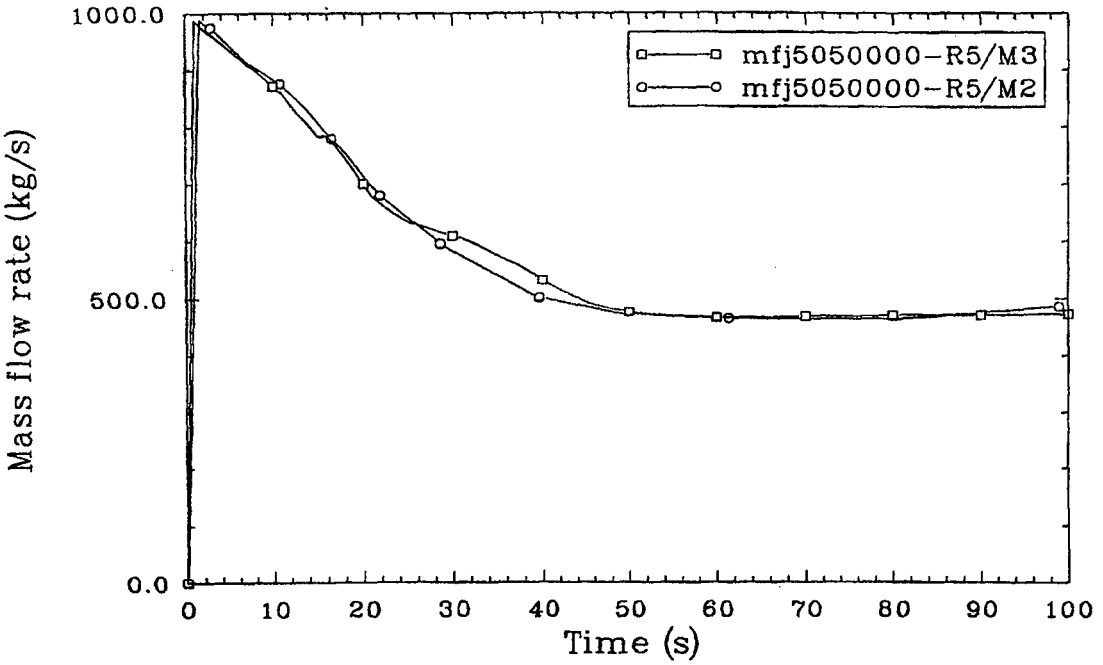

Figure 2.3-56. Calculated (RELAP5/MOD3, MOD2) break mass flow rate for the Zion-1 small break.

2.3-2. D. L. Gillas and J. M. Carpenter, *Experimental Data Report for LOFT Nuclear Small Break Experiment L3-7*, NUREG/CR-1570, EGG-2049, August 1980.

2.3-3. E. J. Kee, P. J. Schally, L. Winters, *Base Input for LOFT RELAP5 Calculation*, EGG-LOFT-5199, July 1980.

2.3-4. R. A. Reimke, H. Chow, V. H. Ransom, *RELAP5/MOD1 Code Manual, Volume 3: Checkout Problems Summary*, EGG-NSMD-6182, February 1983.

2.3-5. P. D. Bayless and J. M. Divine, *Experimental Data Report for LOFT Large Break Loss-of-Coolant Experiment L2.3-5*, NUREG/CR-2826, EGG-2210, August 1982.

2.3-6. S. L. Thompson and L. N. Kmetyk, *RELAP5 Assessment: LOFT Large Break Loss-of-Coolant Experiment L2.3-5*, NUREG/CR-3608, SAND83-2549, January 1984.

2.3-7. System Design Description for the Mod-A Semiscale System, Addendum 1, "Mod-A Phase I Addendum to Mod-3 System Design Description," EG&G Idaho, Inc., December 1980.

2.3-8. R. A. Dimenna, *RELAP5 Analysis of Semiscale Mod-A Single-Loop Single-Component Steady-State Natural Circulation Tests*, EGG-SEMI-6315, June 1983.

2.3-9. W. Riebold et al., *Specifications: LOBI Pre-Prediction Exercise, Influence of PWR Primary Loops on Blowdown (LOBI)*, Technical Note No. I.0.601.79.25, Commission of the European Communities, J.R.C.-Ispra, February 1979.

2.3-10. L. N. Kmetyk, *RELAP5 Assessment: LOBI Large-Break Transients*, NUREG/CR-1075, December 1982.

2.3-11. L. Piplies and J. Bachler, *Single-Phase Performance Characteristics of the LOBI Pump*, Technical Note No. I.07.01.79.80, Commission of the European Communities, J.R.C.-Ispra, August 1979.

2.3-12. L. Piplies and K. Kolar, *Preliminary Two-Phase Performance Characteristics of the LOBI Pump (Curves for Fully Degraded Head)*, Technical Note No I.06.01.81.13, Commission of the European Communities, J.R.C.-Ispra, February 1981.

2.3-13. L. Piplies and W. Kolar, *Quick Look Report on LOBI Test A1-04R*, Communication LEC 80-03, Commission of the European Communities, J.R.C.-Ispra, December 1980.

2.3-14. E. Ohlmer et al., *Experimental Data Report on LOBI Test A1-04R*, Communication LEC 80-03, Commission of the European Communities, J.R.C.-Ispra, December 1980.

2.3-15. C. D. Fletcher et al., *Loss of Offsite Power Scenarios for the Westinghouse Zion-1 Pressurized Water Reactor*, EGG-CAAP-5156, May 1980.

2.3-16. C. D. Fletcher and M. A. Bolander, *Analysis of Instrument Tube Ruptures in Westinghouse 4-Loop PWRs*, NUREG/CR-4672, EGG-2461, December 1986.